THE CHEMICAL PHYSICS OF INORGANIC SALTS WITH LOW MELTING POINTS.

THESIS

Submitted to

The University of London

by

John Prentice Frame BSc.

Candidate for the Degree of Doctor of Philosophy

in the Faculty of Science.

November, 1960.

ABSTRACT.

Measurements have been made of the electrical conductance of solid and molten sodium and potassium nitrites and potassium dichromate, and on molten thallium nitrate. Viscosities of these salts have also been determined. The low ratios for the activation energies E_η/E_σ for viscosity and ion conductance have been compared with other salts and some deductions as to the structure of these salts close to the freezing point, together with discussion on the possible mechanisms of these processes, have been made. Further study of the structure of molten salts has been made through an examination of the solubility of H_2O in molten sodium potassium and caesium nitrate. The role of positional holes in molten salts has been examined by this same technique and it is shown that the quasi-crystalline concept of ionic liquids can only be used with reservation.

A paper on the viscosity and conductivity measurements has been published conjointly with E. Rhodes and A. R. Ubbelohde and is presented at the end of this thesis.

ACKNOWLEDGEMENTS.

I wish to express my gratitude to Professor A. R. Ubbelohde for his able and generous guidance throughout the course of this work and also to Dr. E. Rhodes for her advice in the early stages.

J. P. Frame.

CONTENTS

	PAGE NO.
TITLE	1
ABSTRACT	2
ACKNOWLEDGEMENTS	3
CONTENTS	4-8
INTRODUCTION	9
CHAPTER 1. THE SOLID STATE	10
1.1 The Perfect Solid.	10
1.2 Ionic Crystal and Lattice Energy.	11
1.3 Ionic Radii.	14
1.4 Lattice Flaws in Solids.	15
1.4.1 Frenkel Defects.	17
1.4.2 Schottky Defects.	18
1.4.3 Lattice Defects and Melting.	20
1.5 Electrical Conductivity of Ionic Crystals.	20
CHAPTER 2. LIQUIDS	26
2.1 Theory of Liquids.	26
2.1.1 The Cell Model for Liquids.	26
2.1.2 The Hole Theory of Liquids.	27
2.2 Melting and the Structure of Molten Electrolytes.	29
2.3 Structural Changes on Melting.	31
2.3.1 Positional Randomisation.	32
2.3.2 Orientational Randomisation.	32
2.3.3 Configurational Randomisation.	33
2.3.4 Association Entropy.	33
2.3.5 Vibrational Randomisation.	33
CHAPTER 3. TRANSPORT PROCESSES IN MOLTEN SALTS.	37
3.1 Molten Salts.	37
3.2 Conductance.	37
3.3 Change in Conductivity with Melting.	41
3.4 Electrical Transport.	43
3.5 Viscosity.	45
3.6 Relating Viscosity and Conductivity.	47
3.7 Surface Tension.	49

PAGE NO.

CHAPTER 4. GAS SOLUBILITY. 53

4.1 Ideal Solutions. 53
4.2 Real Solutions. 55
4.3 Gas Solubility in Ionic Melts. 55
4.4 Molten Salts and H_2O. 62
4.5 Cryoscopy of Molten Salts. 66
4.5.1 Formation of Solid Solutions. 69
4.6 Mixed Systems. 70
4.6.1 Thermodynamic Properties of Ionic Melts. 70
4.6.2 Volume and Density of Binary Mixtures of Fused Salts. 74
4.6.3 Electrical Conductivity of Binary Systems. 76
4.6.4 Viscosity of Binary Systems. 77
4.6.5 Phase Diagrams for Some Binary Systems. 78

CHAPTER 5. GENERAL PROPERTIES OF ALKALI NITRATES, NITRITES AND POTASSIUM DICHROMATE. 87

5.1 Temperature of Fusion. 87
5.2 Crystallographic Properties. 88
5.2.1 Lithium Nitrate. 88
5.2.2 Sodium Nitrate. 89
5.2.3 Potassium Nitrate. 90
5.2.4 Rubidium Nitrate. 91
5.2.5 Caesium Nitrate. 91
5.2.6 Thallium Nitrate. 92
5.2.7 Sodium Nitrite. 93
5.2.8 Potassium Nitrite. 93
5.2.9 Potassium Dichromate 94
5.2.10 The Structure of Molten Nitrates. 94
5.3 Thermal Stability of Alkali Nitrates, Nitrites and Dichromates. 96
5.3.1 Chemical Decomposition of Nitrates 96
5.3.2 The Thermal Decomposition of Nitrites. 97
5.3.3 Thermal Decomposition of $K_2Cr_2O_7$. 98
5.4 Heats of Formation. 98
5.5 Heats of Transition. 99
5.6 Heats of Fusion. 100
5.7 The Viscosity Parameters of the Alkali Nitrates and Nitrites. 102
5.8 The Electrochemistry of Alkali Nitrates and Nitrites. 105
5.9 The Object and Scope of this Research. 105

EXPERIMENTAL 112

PAGE NO.

CHAPTER 6. PRELIMINARY EXPERIMENTAL TECHNIQUES. 113

6.1 Viscosity and Conductivity. 113
6.2 Materials. 113
6.3 Purification. 114
6.4 Drying. 115
6.5 Cleaning of Apparatus. 117
6.6 Thermostated Bath. 117
6.7 The Temperature Controller. 120
6.8 Temperature Measurement. 122
6.9 Calibration of Thermocouple. 123

CHAPTER 7. VISCOSITY MEASUREMENTS. 127

7.1 The Viscometer. 127
7.2 Constant Pressure Apparatus. 131
7.3 Calibration of Viscometers. 133
7.4 Filling the Viscometer. 136
7.5 Calculation of Results. 138
7.6 Results. 139.

CHAPTER 8. ELECTROCHEMICAL MEASUREMENTS. 150

8.1 Choice of Method. 150
8.2 The Cell. 150
8.3 The Direct Current Circuit. 152
8.4 Calibration of Conductivity Cell. 155
8.5 Results. 155
8.6 Conductivity Measurements on Ionic Melts. 163
8.7 Results. 163

CHAPTER 9. GAS SOLUBILITY IN IONIC MELTS. 175

9.1 Selection of Systems. 175
9.2 Materials. 176
9.3 Preliminary Treatments. 178
9.4 Cryoscopic Apparatus. 178
9.5 Measurement of the Freezing Point. 181
9.6 Tests on Rates of Cooling. 182
9.7 Purity of Solute and Solvent. 183
9.8 Drying of the Gas. 184
9.9 The Saturators. 185
9.10 Solid Solutes. 188
9.11 The Systematic Study of Nitrate Systems. 188
9.12 Results. 190

9.12.1 Systems Based on $CsNO_3$. 190

PAGE NO.

CHAPTER 9. (Continued..)

9.12.2 Systems Based on KNO_3. 191
9.12.3 Systems Based on $NaNO_3$. 197

9.13 Accuracy of Solubility Determinations. 203
9.14 Other Results of Interest. 203

9.14.1 The Electrical Conductivity of Solid KNO_3. 203
9.14.2 The Electrical Conductivity of Molten KNO_3. 204
9.14.3 The Specific Volume of KNO_3 - $Ba(NO_3)_2$. 205

DISCUSSION 211

CHAPTER 10. THE STRUCTURAL INTERPRETATION OF ELECTROCHEMICAL AND VISCOSITY MEASUREMENTS. 212

10.1 Electrical Conductivity of Molten Salts. 212

10.1.1 Calculation of Free Volume. 216
10.1.2 Activation Energy and Cation Radius. 217
10.1.3 Activation Energy and Free Volume. 222

10.2 Electrical Conductivity of Solid Salts. 222

10.2.1 The Relation of Electrical Conductance in Solid and Molten Salts. 224

10.3 The Viscosity of Molten Salts. 225

10.3.1 Methods of Relaxation of Shear. 229
10.3.2 Relation of Energy of Activation for Viscosity with the Cation Radius. 231

10.4 Comparison of Viscosity and Conductivity. 231

CHAPTER 11. THE STRUCTURAL SIGNIFICANCE OF H_2O SOLUBILITY IN MOLTEN SALTS. 242

11.1 The Order of Magnitude of H_2O Solubility in Molten Nitrates. 242
11.2 The Effect of Positional Holes in the Melt on Gas Solubility. 243
11.3 The Solubility of H_2O and Free Volume 247
11.4 The Form of the Solubility Curve for H_2O in Alkali Melts. 248

PAGE NO.

CHAPTER 11. (Continued...)

11.5 The Role of Positional Holes in the Sctructure of Molten Nitrates and their Influence on Physical Properties. 249

11.5.1 Positional Holes in Solid Nitrates. 249

11.5.2 The Effect of Positional Holes on the Density and Molar Volume of Mixed Nitrate Systems. 250

11.5.3 The Role of Positional Holes in the Electrical Conductivity of Molten Salts. 251

11.6 Comparison of the Results of H_2O Solubility with Some Solubility Measurements of Other Workers. 254

11.7 The Mechanism of Gas Solubility in Ionic Melts. 255

11.8 The Anomalous Behaviour of Solutions of H_2O in Molten $NaNO_3$. 267

CHAPTER 12. GENERAL CONCLUSIONS. 271

APPENDIX I Derivation of the Relation between Gas Solubility and Surface Tension. 273

APPENDIX II Calibration of Viscometers. 275

APPENDIX III Details of Solubility Results. 290

I N T R O D U C T I O N

CHAPTER 1

THE SOLID STATE

The study of liquids is closely related to the study of solids near the melting point. This is especially true of ionic solids. Thus it is necessary that at least a brief outline should be given of the theory of solids where it most directly affects liquid behaviour. Fuller accounts of solid state theory can be found in several standard texts. [1-12]

1.1 The Perfect Solid

The perfect solid can be regarded as an aggregate of atoms arranged in unbroken lattice array. Each cell of the lattice possesses an identical arrangement of the chemical constituents so that the internal structure is flawless. This system is at absolute zero of temperature and the constituent atoms are at rest except for zero point oscillation. It must be assumed that the electronic configuration of the system is in the lowest possible energy state compatible with its crystallographic arrangement.[14] This then is a definition which would fit either an insulator or a metal.

There are three principal types of insulator, namely salts, valence crystals and molecular crystals, differing primarily in the distribution of valence electrons round the atoms. In salts

there is a preferred distribution of anions about the cations arranged in a more or less spherically symmetrical manner.

1.2 Ionic Crystal and Lattice Energy

A simple ionic crystal is made up of a lattice of oppositely charged units held in equilibrium under the influence of three principal forces;

a) the electrostatic or coulomb forces between the ions which give a resultant attraction falling off with the square of the distance;

b) Van der Waal's' forces of attraction diminishing according to the seventh power of the distance;

c) interatomic repulsive forces, falling off still more rapidly with distance according to 6 - 10 inverse power laws. The resultant of these forces leads to an equilibrium position of minimum potential energy.

These forces are directly related to the lattice energy W which is defined by Born and Mayer[13] (1933) and Mott and Gurney[4] (1946) as the work necessary to separate a crystal into its gaseous ions at the absolute zero of temperature.

For an alkali halide Born and Mayer derived the following expression:

$$W = N \left\{ -\frac{\alpha e^2}{r_o} + 6w_{+-}(r) + 12w_{++}(r) + 12w_{--}(r) - \frac{c}{r^6} + \frac{9}{4} h\nu_m \right\}$$

$\frac{\alpha e^2}{r}$ is the electrostatic attractive energy per ion pair;

$6w_{+-}(r) + 12w_{++}(r) + 12w_{--}(r)$ is the overlap contribution to the expression for the energy and is of this form for the sodium chloride structure per ion pair;

$-\frac{c}{r^6}$ is the Van der Waals attractive energy between any two ions;

$\frac{9}{4} h\nu_m$ is the zero point energy per ion pair;

N is the number of ion pairs in the crystal;

α is the Madelung constant[15];

r_o is the distance between ions of unlike sign;

ν_m is the maximum frequency of the Debye frequency spectrum and c a constant.

An increase to the Van der Waals term is required when consideration is given to dipole and quadrupole interactions. In addition a contribution to the cohesive force will be given by homopolar binding. This arises when the ions become distorted due to extensive overlap of the electronic structure of adjacent negative and positive ions.

The importance of the lattice energy is in that it gives an approximate indication of thermal stability and melting point of a compound. The ions in the lattice, though in equilibrium are not rigidly held at fixed points but are free to vibrate about mean positions. With increasing temperature the amplitude of these vibrations about their mean positions increases and there is at any moment a certain departure from periodicity in the

positions of the ions. This concept affords a simple picture of the breakdown in the structure of the crystal on fusion.[16,17] Though as will be seen it is not fully in accordance with the observable facts, since such a theory suggests a complete randomisation of the ions with fusion. This, as will be pointed out later is far from being the case.

Table 1.1 records some important lattice energies of both high melting and low melting salts.

TABLE 1.1

Lattice Energies.

Low Melting Salts	a)Lattice Energy Kcal/mole	High Melting Salts	b)Lattice Energy Kcal/mole
$LiNO_3$	198.8	LiCl	199.2
$NaNO_3$	177.6	NaCl	183.1
KNO_3	162.5	KCl	165.4
$RbNO_3$	155.8	CsCl	152.2
$CsNO_3$	149.7	LiBr	188.3
$NaNO_2$	185.1	NaBr	174.6
KNO_2	166.6	KBr	159.3
$TlNO_3$	164.6	CsBr	146.3

a) Values of the lattice energy for low melting salts from Morris [18] (1958).

b) Values of the lattice energy for high melting salts taken from Partington [10] (1954).

1.3 Ionic Radii

It has been found useful in the study of ionic compounds in the crystal and the melt to relate physico-chemical properties to the relative radii of the cation and anion.[19,20] The values of ionic radii are obtained on the assumption that the ions behave as rigid spheres.[20,5,21] This is approximately true for a limited number of ions. The concept of finite ionic radii has been confirmed from the point of view of wave mechanics.[22]

However, when anions of a non-spherical nature are considered, it is only approximately true to regard them as behaving as though they have finite radii. For the purpose of comparison with more spherical ions a radius is proposed assuming the ion to be enclosed in a spherical envelope. This supposes the ion to be of the form of the sphere it would sweep out if capable of free rotation. Some evidence exists for the free rotation of NO_3^- in alkali nitrates at higher temperature. This is discussed in Chapter 5.

TABLE 1.2

Ionic Radii.

ion	r in A°	ion	r in A°
Li^+	0.60	Cl^-	1.81
Na^+	0.95	Br^-	1.95
K^+	1.33	I^-	2.16
Rb^+	1.53	CO_3^{--}	1.85
Cs^+	1.69	NO_3^-	1.89
Ag^+	1.26	CNS^-	1.95
Mg^{++}	0.65	Sr^{++}	1.13
Ca^{++}	0.99	Ba^{++}	1.35

Table 1.2 shows the magnitude of some ionic radii.

TABLE 1.3

Entropies of Fusion of Alkali Nitrates and Chlorides.

ion	radius A^o	Nitrate Entropy of fusion	Chloride Entropy of fusion
Li^+	0.60	5.8	5.6
Na^+	0.95	3.3	6.7
Ag^+	1.26	2.9	4.3
K^+	1.33	2.3	6.2
Rb^+	1.48	1.1	4.4
Cs^+	1.69	2.4	3.9

Table 1.3 compares the entropy of fusion of some alkali chlorides and nitrates together with the radius of the cation. Table 1.3 suggests that the relationship between entropy of fusion and cation radius is clearer for the nitrates than the chlorides though both NO_3^- and Cl^- are credited with similar ion radii. This comparison, however, is limited in its value in this particular case since the extent of the influence of the polarisabilities of individual ions is unknown. With this must also be considered the effect of premelting on the entropy.

Entropy of fusion is further discussed in Section 2.3.

1.4 Lattice Flaws in Solids

So far it has been assumed that the crystal is a perfectly formed three dimensional lattice with a regular array of oppositely

charged ions. However, in practice it is found that flaws exist which may affect or even determine the properties of the crystal.[1,4,9,11]

Seitz (1952)[14] lists the following primary imperfections:

(A) Phonons;

(B) Electrons and holes;

(C) Excitons;

(D) Vacant lattice sites and interstitial atoms;

(E) Foreign atoms in either interstitial or substitutional positions;

(F) Dislocations.

These imperfections may interact with imperfections of the same type or of a different type to generate imperfections of a third type; in fact the scheme of interaction can be even more complex.

Frenkel[23] (1926) first pointed out that it seemed impossible to envisage any mechanism which could account for ionic conduction through a perfect lattice. He suggested that in an actual crystal, a number of vacant sites or holes existed due to ions of the lattice migrating to interstitial positions. This basic theory has since been further extended by Frenkel (1946)[11] Wagner (1938)[24] Wagner and Schottky (1930)[25] and Jost (1933,1938).[26]

The production of vacant sites depends in general upon the existence of one of three conditions:

a) thermal agitation;

b) the presence of certain types of impurity;

c) departure from stoicheiometric proportions.

There are one or two cases where some other effect is involved. Silver iodide, for example, at room temperature is hexagonal but above 140°C exists in a high temperature modification, α- AgI, which possesses a very high ionic conductivity with a very low activation energy.[27,28] The silver ions in this structure appear to be able to move freely through the available space. Such a crystal would be expected to have a high ionic conductivity.

1.4:1 Frenkel Defects

Of the crystal imperfections three are of particular and direct importance for melting. The first is known as a Frenkel defect. This is formed when an ion leaves its normal position and moves to an interstitial position. It is assumed that the ion is so far removed from its original position that no interaction occurs between it and those ions surrounding the hole so created.

Assuming that migration of an ion in this way does not alter the volume of the crystal or affect the frequency of vibration of the ion, it can be shown [4] that the increase in the

number of defects with temperature is given by

$$n = (NN')^{\frac{1}{2}} e^{-W_f/kT} \quad \ldots\ldots\ldots\ldots (1.1)$$

n is the number of ions displaced;

N is the total number of ions;

N' is the total number of interstitial positions available;

W_f is the work required to move a single ion.

Since the above conditions are not strictly true, this expression has been modified to:

$$\frac{n}{NN'} = \gamma e^{-\frac{1}{2} W_f/kT} \quad \ldots\ldots\ldots\ldots (1.2)$$

Where γ is given by $\gamma^2 = \nu^{x+y+1} / \nu_i \nu_i'^{y} \nu'^{x}$.

ν is the vibrational frequency of an ion in a pefect crystal;

ν_i that of an interstitial ion;

ν_i' that of its y neighbours;

and ν' that of the x neighbours of the vacant lattice point.

$\nu > \nu' < \nu_i$ The value of γ may be $\gtrless 1$.

1.4:2 Schottky Defects.

Schottky defects are formed when the ions in a crystal migrate from their mean positions to the surface. Neglecting volume and frequency changes the increase in the number of defects with temperature is given by

$$\frac{n}{N-n} = e^{-W_s/kT} \quad \ldots\ldots\ldots\ldots\ldots (1.3)$$

W_s is the work of removal of an ion from its normal position to the surface of the crystal. Other symbols as before.

Again this is modified when account [4] is taken of the volume change and frequency to:

$$\frac{n}{N} = \gamma B e^{-W_o/kT} \quad \ldots\ldots\ldots\ldots (1.4)$$

W_o is the work to form a defect at absolute zero of temperature;

$B = \exp. \left\{ -\frac{\alpha V_o}{k} \frac{dW_s}{dV} \right\}$;

α is the coefficient of expansion;

V_o is the volume for which the lattice energy is a minimum;

$\gamma = \left\{ \nu/\nu' \right\}^x$

x is number of neighbours of a Schottky hole;

ν is their frequency in two directions perpendicular to the line joining the neighbours to the hole.

ν' their frequency parallel to this line.

Schottky and Frenkel defects occur simultaneously and the type with lowest activation energy will predominate. Both Schottky and Frenkel defects can group together in such a way as to form a mosaic, producing a co-operative defect in which the characteristic of both types combine with a subsequent lowering of the lattice energy. The importance of this particular type of defect is discussed by Oldham and Ubbelohde[29] (1940).

1.4:3 Lattice Defects and Melting

Lattice defects are of importance in the theories of melting particularly where it is considered as an order - disorder transition.[30,31] As yet however, there is no satisfactory quantitative formulation apart from the formal treatment by Lennard - Jones and Devonshire [32] (1939). A useful approach to the problem experimentally is in the study of electrical conductivity which enables the calculation of flaw energies and an assessment of the number and mobility of the defects to be made.

1.5 Electrical Conductivity of Ionic Crystals

Ionic [1,4,33,34] crystals possess an electrical conductivity which is small at low temperatures but much greater at high temperatures.

Joffé [35] (1931) was the first to express and establish experimentally the idea that the passage of an electric current through crystals of the rock salt type is due to the presence of dissociated positive ions which increase with temperature and which possess a marked mobility. This was extended by Frenkel [23] with his concept of moveable holes.

Over broad limits the dependence of electrical conductivity on temperature is given by:

$$\sigma = \sigma_0 e^{-E_\sigma/RT} \quad \ldots\ldots\ldots\ldots (1.5)$$

With practically constant value of the factor σ_0. E_σ is the

activation energy for the process. Frenkel[36] has derived a theoretical formula relating σ_o to T.

$$\sigma_o = \frac{e^2\delta^2 n}{\sigma T_o' kT}$$

n is the number of particles;

T is the period of free vibrations of an atom about an equilibrium position;

δ is the distance between atoms;

k and T have their usual significance.

(cf. Mott and Gurney [4] p.43 and Seitz [1] p.191)

According to this expression σ_o should be inversely proportional to the absolute temperature; this dependence is, however, masked by the more pronounced temperature dependence of the exponential term which is attributed to the thermal expansion of the lattice. In many ionic crystals a plot of log σ against $\frac{1}{T}$ reveals a break or change in slope and the temperature dependence is more suitably represented by the form

$$\sigma = \sigma_o e^{-E_\sigma/RT} + \sigma_o e^{-E'_\sigma/RT} \quad \ldots\ldots (1.6)$$

This change in the temperature dependence of σ upon T has been explained [37] in the case of the alkali halides as being due to the conduction by positive ions in the low temperature region being supplemented in the higher temperature region by a contribution from the negative ions. Measurement of transport numbers [38] has shown that at higher temperatures chloride ions make a distinct contribution to the conductivity. Mapother and

Maurer[39] (1948) however in diffusion work on NaCl have shown that both parts of the conductivity formula are necessary to represent the conduction of Na^+ ions.

Another explanation given by Smekal [40] (1925, 1927) suggests that at low temperatures the first term represents the contribution of loosely bound ions moving along internal crystal cracks, while the second term which makes the greater contribution at high temperatures is due to conduction by normal lattice ions. More elegantly Koch and Wagner[41] (1937) have demonstrated that the conductivity is dependent on the presence of vacant sites in the crystal lattice. They showed by the addition of the divalent Cd^{++} as $CdCl_2$ to AgCl the resulting increase in vacant sites produced a very large increase in the conductivity. On the basis of the results of this experiment they deduced that at higher temperatures the higher conductivity was due to thermal defects in the crystal but at lower temperatures the number of defects is small and the conductivity in this region is dependent on impurity defects being present. This demonstrates the structure sensitive nature of the conductivity in this region.

No work appears to have been done on the addition of divalent cations to univalent polyatomic salts such as the alkali nitrates, though Forland[42] (1956) has observed an increase in the electrical conductivity of solid Na_2CO_3 when additions of $CaCO_3$ are made. No details are given.

References

1. Seitz, "Modern Theory of Solids", McGraw Hill, New York,(1940).
2. Wells, "Structural Inorganic Chemistry" O.U.P. London, (1950).
3. Mott and Jones, "Theory of Metals and Alloys", O.U.P., London, (1935).
4. Mott and Gurney, "Electronic Processes in Ionic Crystals", O.U.P., London, (1940).
5. Pauling, "Nature of the Chemical Bond", O.U.P., London, (1950).
6. Wilson, "Theory of Metals", C.U.P., London, (1936).
7. Wilson, "Semi Conductors and Metals", C.U.P., London, (1939).
8. Glasstone, "Textbook of Physical Chemistry", MacMillan, London, (1948).
9. Garner, "Chemistry of the Solid State", Butterworth, London, (1955).
10. Partington, "Advanced Treatise on Physical Chemistry", Vol.3, Longmans Green, London (1954).
11. Frenkel "Kinetic Theory of Liquids", O.U.P. London, (1946).
12. Seitz and Turnbull, "Solid State Physics", Academic Press, New York, (1955).
13. Born and Mayer, "Handbuch der Physik", (1933), 24/2 726.

14. Seitz, "Imperfections in Nearly Perfect Crystals",p.3 Chapman and Hall, London, (1952).

15. Sherman, Chemical Reviews, (1932), 11, 107.

16. Lindeman, Physikal Z., (1910), 11, 609.

17. Braunbek, Z. Physik, (1926), 38, 549.

18. Morris, I. Inorg. Nuc. Chem., (1958), 6, 295.

19. Sauerwald and Schinke, Z. anorg. Chem. (1956), 287,131,313.

20. Yatsimirskii, Izvest, Sektora Fiz. Khim. Anal. Inst. Obschei i Neorg. Khim, Akad. Nauk S.S.S.R. (1949), 19, 202.

21. Goldschmidt, Z. phys.Chem., (1929), 141, 51; "Geochemistry".

22. Jensen, Gossler and Rohde, Z. Physik, (1938),110, 277.

23. Frenkel, Z. Physik, (1926), 35, 652.

24. Wagner, Trans. Far. Soc., (1938), 34, 851.

25. Wagner and Schottky, Z. phys. Chem., (1930), B11,163.

26. Jost, J. Chem.Phys., (1933), 1, 466;
Trans. Far. Soc., (1938), 34, 860.

27. Strock, Z. phys. Chem., (1934), 25B, 441;
(1936), 31B, 132.

28. Ketelaar, Trans. Far. Soc., (1938), 34, 88.

29. Oldham and Ubbelohde, Proc. Roy. Soc., (1940), 176A, 50

30. Rogers and Ubbelohde, Trans.Far.Soc. (1950), 46, 1051.

31. Davis Rogers and Ubbelohde, Proc. Roy. Soc.,(1953), 220A, 14.

32. Lennard-Jones and Devonshire, (1939), 169A, 317; 170A, 464.

33. Jacobs and Tompkins, Quart.Review, (1952).

34. Haven, Rec. Trav. Chim des Pays-Bas., (1950), 69, 1471; 1259; 1505; Phys. Soc., Defects in Crystalline Solids - Report of (1954) Bristol Conference. p.261.

35. Joffe, Physics of Crystals (1931).

36. Ref. 11, p.45.

37. Phipps, Lansing and Cooke, J.A.C.S., (1926), 48, 112.

38. Tubandt, Reinhold and Liebold, Z. anorg. allgem. Chem., (1931), 197, 225.

Tubandt, "Handbuck der Experimental Physik", Vol XII, (1932), p.397.

39. Mapother and Maurer, Phys. Rev. (1948), 73, 1260.

40. Smekal, Phys.Z., (1925), 26, 707;

Z. Elektrochem. (1927), 34, 476;

Z. Techn. Phys.(1927), 8, 561.

41. Koch and Wagner, Z physik Chem. (1937), B38, 295.

42. Forland, Office of Naval Research Tech. Report 69, Contract N6 onr. 269; task order 8NR 032-264, Pennsylvania State University (1956).

CHAPTER 2

LIQUIDS

2.1 Theory of Liquids

It is possible to consider some of the general properties of liquids as applying also to fused salts.

There are two main limiting models of liquids, one being the cell model and the other the hole model.

2.1:1 The Cell Model for Liquids

One of the earliest successful models of a liquid was due to Eyring and Hirschfelder[1] (1937) and Lennard-Jones and Devonshire[2] (1939), (see also the reviews by Prigogine[3a] (1957) Rowlinson and Curtiss[3] (1951) De Boer[4] (1952) and Rowlinson[5] (1959). The idea of these authors was based on the fact that especially near the melting point, a molecule in a liquid has not very much freedom of movement. It is surrounded by the molecules of the first co-ordination shell and though it is in continual motion due to thermal agitation, its translational motion is so inhibited by its environment that it cannot do much more than perform oscillations about a mean position, at any rate over short intervals of time. Such oscillations may be compared with those peformed by a particle in a potential well, i.e. a field of force which becomes strongly repulsive at a short distance from the centre. Again the motion might be compared to that

executed by a molecule in a crystal consisting of perpetual small oscillations about a lattice site. Kirkwood[6] (1950) has shown how it is connected with exact statistical theory.

2.1:2 The Hole Theory of Liquids.

The second approach to the structure of liquids considers the liquid to contain holes i.e. unoccupied lattice sites. This theory has been propounded in various forms by Frenkel[7], Altar[8], Furth[9], while Cernuschi and Eyring[10] (1939), Ono[11] (1947) and Peek and Hill[12] (1950) have attempted to correlate it with the cell theory. It involves as well as an increase of free volume an increase in the proportion of holes. The term "hole" as used in reference to liquid structure has a somewhat different meaning to that used in consideration of solid structures. Furth[9] has suggested that near the boiling point of a liquid they can be regarded as gas bubbles. More recently refinements have been made by Levine, Mayer and Aroeste[13] (1957), Hill[14] (1958) and McLellan[15] (1958).

Comparisons of the hole and cell theories have been made by Rowlinson and Curtiss[3] (1951) and Rowlinson[5] (1959) who criticise the hole theory as being too empirical. However, for molten salts with spherical ions of simple inert gas type, a picture of their structure based on some form of the hole theory would appear to be the most useful. A simple hole model for molten salts composed of spherical cations and anions each

behaving as an independent linear harmonic oscillator has been suggested.[16] Among the cations and anions are randomly mixed a number of holes, the total volumes of which are taken to be approximately equal to the volume change on melting. The ions remain in a cell from which they can escape by one of two methods:

i) jumping into a neighbouring hole;

ii) place exchange.

It is likely that the holes which exist in a fused ionic salt, particularly near the melting point bear a greater similarity to the holes in solid structures than the holes suggested in the above theories which have been developed with more particular reference to molecular liquids.

Application of a pure cell model to a molten salt would suggest that;

i) no decrease of co-ordination number would occur on melting;

and ii) the change in volume that occurs, in an alkali halide say, on melting should be accompanied by an increase of some 6% in the interionic distance.

A hole model on the other hand would be associated with a decrease in the mean co-ordination number. Experimental evidence shows[17,18] that a decrease in average co-ordination number occurs and further that there is a decrease in mean

interionic distance.[17, 19, 20]

For LiCl the average co-ordination number decreases[17,18] from 6 to approximately 5. Table 2.1 compares the internuclear distances in the solid and liquid states at the melting point.

TABLE 2.1

Salt	Distance Type	Co-ord. No.	Solid d Å		Liquid d Å
			25°C	MP.	MP.
LiCl	Li-Cl	6	5.14	5.29	5.15
	Cl-Cl	12	3.64	3.74	3.8
KCl	K-Cl	6	3.14	3.30	3.14
	K-K	12	4.44	4.67	4.3
CdI_2	Cd-I	6	2.99	3.06	2.90

Tempkin[21] (1946) and Forland[22] (1955) have derived thermodynamic equations on the basis of a model for ionic melts in which the anions and cations are randomly distributed over sites which are either anion or cation sites (cf. also Blander[23] 1959). This is discussed more fully in section 4.7:1.

2.2 Melting and the Structure of Molten Electrolytes.

It has been generally accepted that the structure of molten salts near their melting points is very close to that of the solid, the principal change being due to the increase in the number of holes and the loss of long range order, although short range order is maintained. Thus the picture is created of a

randomised solid. It has been pointed out by Ubbelohde[24] (1953, 1956), that the volume increase on melting of ionic crystals such as the alkali halides, is in some cases greater than 25%. Compressibility measurements show that the free volume per mole is usually of the order of 2% of the molar volume.[16] This suggests that the bulk of this volume increase with melting is due to the presence of holes. This is true of higher melting ionic salts but it is of interest to note that in the lower melting salts with non-spherical anions, such as nitrates, the volume change with fusion is small.

TABLE 2.2

Salt	$\Delta V/V_s$ %	T°C	Reference	Salt	$\Delta V/V_s$ %	T°C	Reference
a) KNO_3	1	336	25 and 25a	LiCl	26.2	613	30
$NaNO_3$	11	307	24a	LiBr	24.3	547	30
$AgNO_3$	0.7	212	24a	NaCl	25.0	801	30
$LiNO_3$	28.2	255		NaBr	22.4	755	30
NaSCN	7	287	26	KCl	17.3	776	30
KSCN	10	173.2	26	KBr	16.6	730	30
$KHSO_4$	4	210	27	NaI	18.6	651	30
b) $KCLO_3$	10.25	356	28,29	KI	15.9	723	30

a) Calculated from the crystal expansion data of Fischmeister[25] (1956) and density data of Jaeger[25a] (1917) extrapolated to the freezing point.

b) Calculated from the crystal expansion data of Ramachandran and Lonappan[29] and density data of Husband[28](1958) extrapolated to the freezing point.

Table 2.2 compares the volume change on fusion of the high melting alkali halides and the low melting salts with non-spherical anions. The difference between the values found for high melting salts and those for low melting salts has been explained[24a,26] as being due to the formation of association complexes.

Though melting may occur at a well defined point on the temperature scale it is often accompanied by the phenomenon of marked premelting.[31] The phenomenon is associated with a steep increase in specific heat and volume just before the melting point. This probably occurs in all salts to a greater or lesser degree but only in salts such as AgBr and LiF, where the strongly polarising cations can readily occupy positions other than ideal, has it been observed.

2.3 Structural Changes on Melting

Lindeman's[32] expression relating a characteristic vibration frequency to the temperature of fusion gives a simple though inadequate explanation of the phenomenon of melting:

$$T_f = Cm\nu^2 \quad V^{2/3} \quad \ldots\ldots(2.1)$$

where T_f is temperature of fusion

ν is characteristic frequency of vibration of the crystals;

V is molar volume;

m is atomic weight.

Any theory has to take into consideration the presence of two phases at the melting point.

The entropy of fusion can be expressed by the Boltzmann relation:

$$S_f = R\ln W_L/W_S$$

Where W_L and W_S are the numbers of ways of realising a liquid and solid respectively; S_f is a composite term which includes many entropy changes due to various mechanisms at work during melting. These can be written:

$$S_f = S_{vib.} + S_{orien.} + S_{pos.} + S_{config.} + S_{assoc.}$$

and may be reviewed briefly.

2.3:1 Positional Randomisation ($S_{pos.}$)

$S_{pos.}$ represents the entropy change due to positional randomisation which always occurs in the melting process, generally accompanied by an increase in volume. Various types of positional disordering exist which are assisted by Frenkel and Schottky defects as they increase towards the melting point.

2.3:2 Orientational Randomisation ($S_{orien.}$)

Where an ionic crystal is composed of non-symmetrical units the mutual orientations of the units of its structure generally become randomised on melting with respect to its crystal

lattice directions. In many cases, e.g. alkali nitrates, such randomisation has already occurred after transitions in the solid below the melting point.

2.3:3 Configurational Randomisation ($S_{config.}$)

When flexible molecules can assume more than one configuration by "free rotation" about valency bonds a further effect is introduced into the mechanism of melting in the form of a configurational entropy.

2.3:4 Association Entropy ($S_{assoc.}$)

Of some importance in inorganic salts is the contribution to the entropy of fusion of an association factor in the melt. It will be shown later that there is evidence for the presence of this in the mechanism of melting of certain low melting salts. Attention has been drawn to the existence of such an entropy contribution in salts such as KSCN, $KHSO_4$ and $AgNO_3$.[27,24a]

2.3:5 Vibrational Randomisation ($S_{vib.}$)

The contribution of a vibrational term to the entropy of melting is essential to Lindeman's hypothesis but can never be the only contribution.

References

1. Eyring, J. Chem. Phys., (1936), 4, 283

Eyring and Hirschfelder, J. Phys.Chem.(1937), 41, 249.

Hirschfelder, Curtiss and Bird, "Molecular Theory of

Gases and Liquids" Sec. 5.5 Wiley, New York, (1954).

2. Lennard-Jones and Devonshire, Proc. Roy. Soc. (1937), A163, 53; (1938), A165, 1; (1939), A169, 317; A170, 464. Lennard-Jones, Physica, 's Grav. (1937), 4, 941; Proc. Phys. Soc. (1940), 52, 729.
3. Rowlinson and Curtiss, J. Chem. Phys. (1951), 19, 1519.
4. De Boer, Proc. Roy. Soc. (1952), 215A, 4.
5. Rowlinson, "Liquids and Liquid Mixtures", Butterworths, London (1959).

5a. Prigogine "Molecular Theory of Solutions" North-Holland, Amsterdam (1957).

6. Kirkwood, J. Chem. Phys. (1950), 18, 380.
7. Frenkel, "Kinetic Theory of Liquids" O.U.P. London, (1946).
8. Altar, J. Chem. Phys. (1937), 5, 577.
9. Furth, Proc. Cam. Phil. Soc. (1941), 37, 252.
10. Cernuschi and Eyring, J. Chem. Phys. (1939), 7, 547.
11. Ono, Mem. Fac. Engng. Kyushu, (1947), Vol.10, No.4, 190.
12. Peek and Hill, J. Chem. Phys., (1950), 18, 1252.
13. Levine, Mayer and Aroeste, J. Chem. Phys. (1957), 26, 201,207. Levine, J. Chem. Phys. (1957), 27, 335
14. Hill, J. Chem. Phys. (1958), 28, 1179.
15. McLellan, Phil. Mag. (1958), 3, 707.
16. Bockris and Richards, Proc.Roy. Soc. (1957), 241A, 44.
17. Miller and Lark-Horovitz, Phys. Rev. (1937), 51, 61

18. Johnson, Agron and Bredig, J.A.C.S., (1955), 77, 2734.

19. Wood and Ritter, J.A.C.S., (1953), 75, 471.

20. Danilov and Krasnitskii, Dokl. Akad. Nauk. S.S.S.R., (1955), 101, 661

21. Tempkin, Acta physico Chim. U.R.R.S.,(1945), 20, 411.

22. Forland, O.N.R., Tech. Report No.69. Contract N6 onr. 269, Task order 8, NR. 032-264, The Pennsylvania State University. (June 1956).

Flood, Forland and Grjotheim, Z. anorg. allgem. Chem., (1954), 276, 19.

23. Blander, J. Phys. Chem., (1959), 63, 1262.

Blander, Blankenship and Newton, J. Phys. Chem.,(1959), 63, 1259.

24. Landon and Ubbelohde, Trans. Far. Soc. (1956), 52, 647.

24a. Davis, Rogers and Ubbelohde, Proc. Roy. Soc., (1953), 220A, 14.

25. Fischmeister, J. Inorg. and Nuc. Chem., (1956), 3, 182.

25a. Jaeger, Z. anorg. Chem.,(1917), 100, 61.

26. Plester, Rogers and Ubbelohde, Proc.Roy.Soc. (1956), 235A,469.

27. Rogers and Ubbelohde, Trans. Far. Soc. (1950), 46, 1051.

28. Husband, J. Sci.Instr., (1958), 35, 300.

29. Ramachandran and Lonappan, Acta Cryst. (1957), 10, 281

30. Sauerwald and Schinke, Z. anorg. Chem., (1956), 287, 131,313.

31. Ubbelohde, Trans. Far. Soc., (1938), 34, 292; Ann. Repts.

on Progress Chem., (1940), 37, 167

Quart.Revs. (Chem.Soc.), (1950), 4, 356.

32. Lindeman, Physikal Z., (1910), 11, 609.

CHAPTER 3.

TRANSPORT PROCESSES IN MOLTEN SALTS.

3.1 Molten Salts.

In the studies of the liquid structure of molten salts, many methods have been used. These include investigations of the heat and entropy of fusion, x-ray diffraction, Raman Spectra, ultra-violet spectra, molar volume, electrical conductance, viscosity, vapour pressure, cryoscopy, compressibility, refractive index, diffusion, transport number, e.m.f. of cells, surface tension, heat capacity and salt metal equilibria. Each of these methods of investigation contribute in varying degrees to a knowledge of structure. A summary of all of them will be found in the literature[1] with fuller details given in the literature cited therein.

Of particular interest in the present investigations is the influence of structure on the conductivity and viscosity and the relationship between those parameters.

3.2 Conductance

The study of electrical conductance of molten salts is of importance in determining electrovalency and covalency, extent of dissociation where mixtures of salts are being studied, inter and intra molecular forces, energies of activation, extent of deviation from ideality, nature of the conductance process and

structure of the melt. In conjunction with measurements of viscosity it assists in shedding light on the mechanism of melting [2,34] and transport properties in the melt.

For practical purposes the specific conductance is used. This is given by:

$$\sigma = \frac{C}{R} \quad \ldots\ldots\ldots\ldots (3.1)$$

where C is dependent on the dimensions of the cell[5] and R is the measured resistance. In general C is found more readily and accurately by calibrating with a conductor of known specific conductance generally by KCl [5,6,7].

σ is determined by the volume concentration; c_i, the ionic charge; Z_i, and the mobility of the ion U_i, in a uniform electric field of potential gradient of 1 volt/cm.

$$\text{i.e. } \sigma = \left(\frac{F}{1000}\right) \Sigma (C_i U_i Z_i) \quad \ldots\ldots (3.2)$$

F is Faraday's constant.

For a binary fully dissociated ionic salt this becomes

$$\sigma = \left(\frac{F}{1000}\right) CZ \Sigma U_i$$

$$\text{i.e. } \sigma = \frac{F}{1000} CZ \left(u_{anion} + u_{cation}\right) \ldots (3.3)$$

It can be shown that a parameter, the equivalent conductance Λ can be introduced such that

$$1000\sigma/CZ = \lambda_{anion} + \lambda_{cation} = \Lambda \quad \ldots\ldots (3.4)$$

where λ is the ionic conductance.

For a molten salt Bloom and Heymann[8] (1947) have derived

from the above expression

$$M_e/\rho\sigma = \Lambda \quad \ldots\ldots\ldots\ldots (3.5)$$

where M_e is the equivalent weight and ρ the density. For binary mixtures this can be replaced by M_m^1, the mean equivalent weight of the mixture such that

$$M_m = M_{e_1} f_1 + M_{e_2} f_2 \quad \ldots\ldots\ldots\ldots (3.6)$$

where f_1 and f_2 are the equivalent fractions, defined as $C_i Z_i / \Sigma C_i Z_i$.

Of some importance in any analysis of conductance results is the temperature dependence of the equivalent and specific conductances. Over short ranges of temperature these have been shown to be related by an Arrhenius type expression

$$\sigma = A_\sigma \exp\left(-\Delta E_\sigma / RT\right) \text{ Bloom and Heymann}^8 \quad (3.7)$$

$$\Lambda = A_\Lambda \exp\left(-\Delta E_\Lambda / RT\right) \text{ Bockris et al}^9 \text{ (1952)} \quad (3.8).$$

If the conditions are considered to be at constant pressure and volume, the heat of activation $\Delta H^\ddagger$ can be used instead of ΔE, the energy of activation[10], since under those conditions both are equal.

For conductance in a solid salt[11]

$$\sigma = A \exp\left\{(-W/2 + U)/ kT\right\} \text{ holds } \ldots\ldots\ldots (3.9)$$

If, however, the liquid is considered to be much more disordered and this expression changes to include on energy term only, as

$$\sigma = \left\{ A_c \exp\left(-\frac{\Delta E_c}{RT}\right)\right\} + \left\{ A_a \exp\left(-\frac{\Delta E_a}{RT}\right)\right\} \ldots\ldots (3.10)$$

(a and c denoting anion and cation respectively), and both parts of this equation are considered to be approximately equal, the relationship with temperature as represented by equation (3.7) is obtained.

Martin [12] has derived a useful connection between ΔE_σ and ΔE_Λ. This is:

$$\Delta E_\Lambda = \Delta E_\sigma + RT\alpha \quad \ldots\ldots\ldots\ldots (3.11)$$

where α is the coefficient of expansion.

It is suggested that only for relatively low temperatures, say 400°K, can E_Λ and E_σ be equated. e.g. for NaCl, E_Λ is 80% greater than E_σ. From this it is deduced that E_Λ should be chosen as the comparison function in the ratio $M = E_\eta / E_\Lambda$, rather than E_η / E_σ as suggested by Bloom and Heymann[8]. E_η is the activation of energy for viscous flow[13].

It is possible if treating conductivity as a rate process to relate the conductivity of an ion to the enthalpy and entropy by the general equation of the process[9] as,

$$\Lambda = \frac{2}{3} (Fz\, Xd^2/RT)(kT/h)\exp \Delta S^{\neq}/R \exp(-\Delta H/R) \quad \ldots\ldots\ldots (3.12)$$

F is Faraday's constant;

Z is the charge of an ion,

X is the effective potential gradient in a field of 1 volt/cm;

d is half the distance of an ion along the co-ordinate of motion.

R, k and T have their usual significance;

ΔS and ΔH are the entropy and enthalpy respectively.

Assuming [10] X = applied potential x $\frac{(D + 2)}{3}$ where D is the dielectric constant the above expression becomes:

$$\Lambda = \text{const. x } (D + 2)\ Zd^2 \exp \Delta S^{\neq}/R \exp(-\Delta H/RT) \quad \ldots(3.12)$$

$$\text{Const.} = 5.18 \times 10^{18}$$

Reference to particular measurements of electrical conductivity can be found in the review by Janz, Solomons and Gardner[4] (1958).

3.3 Change in Conductivity with Melting.

Mott[14] (1934) has used a rather simplified model of the liquid state to compute a partition function to relate the properties of the liquid and solid phases at the melting point. He assumes that both phases are dynamically similar in that the atoms in both vibrate, $\nu_s > \nu_l$ (ν_s and ν_l the vibrational frequency of solid and liquid respectively) since the liquid is less rigid. This leads to:

$$f_l = e^{-E_l/kT}\left(\frac{e^{h\nu_l/kT}}{e^{h\nu_l/kT} - 1}\right)^{3N} \quad \ldots(3.13)$$

and

$$f_s = e^{-E_s/kT}\left(\frac{e^{h\nu_s/kT}}{e^{h\nu_s/kT} - 1}\right)^{3N} \quad \ldots(3.14)$$

where E_s is the lowest energy state of the crystal;

E_l is the lowest energy state of the super cooled liquid;

N is the number of atoms.

The condition for equilibrium at the melting point Tm is:

$$\left(\frac{\nu_s}{\nu_l}\right)^3 = e^{(E_l - E_s)/RTm} \quad \ldots(3.15)$$

This becomes:

$$\left(\frac{\nu_s}{\nu_l}\right)^3 = e^{L/RTm} \quad \ldots\ldots\ldots\ldots\ldots (3.16)$$

L is the latent heat of fusion.

This ratio of the frequencies can be connected to the electrical conductivity. In simple cases

$$\frac{\sigma_l}{\sigma_s} = \frac{\nu_l^2}{\nu_s^2} \qquad \text{Seitz p.516.}$$

$$\text{i.e.} \quad \frac{\sigma_s}{\sigma_l} = e^{2L/3RTm} \quad \ldots\ldots\ldots\ldots (3.17)$$

This type of relationship holds very well for the simpler metals but fails for more complex compounds.

TABLE 3.1

Relationship between observed and calculated values for σ_s/σ_l.

	Obs σ_s/σ_l	calc.
Li	1.68	1.84
Na	1.45	1.77
K	1.55	1.75
Rb	1.61	1.76
Cs	1.66	1.75

More qualitatively it has been suggested by Bockris[15] (1948) that the ratio σ_l/σ_s distinguishes ionic from electronic conduction.

A high value for this ratio indicates that the conducting species are ions, whereas a low value less than unity is indicative of electronic conduction. It has also been suggested that the ratio σ_l/σ_s gives a measure of the crystal flaws, at any rate extensive premelting and consequently positional disordering is generally accompanied by a low value for σ_l/σ_s.

TABLE 3.2

Jump in conductivity on melting.

Substance	σ_l/σ_s	Reference
KCl	10,000	Ubbelohde[16] (1950)
KBr	7,000	"
AgCl	30	"
AgBr	20	"
$NaNO_3$	1,000	"
KNO_3	3,000	"

Table 3.2 shows the ratio σ_l/σ_s for some ionic salts. The values for AgCl and AgBr which exhibit the premelting phenomenon, are much lower than for KCl or KNO_3.

3.4 Electrical Transport.

The measurement of electrical transport in molten salts is beset with considerable difficulty, not only from the

experimental point of view but also in the interpretation of the results obtained . Schwarz [17] (1939) and Sundheim[18] (1956) have pointed out that since there can be no concentration changes in a pure molten salt there can be no measurement of transport numbers. The theory underlying transport measurements in inert solvent will be found in the standard texts.[5]

To avoid the difficulty of the term transport number Aziz and Wetmore[19] (1952) defined the 'transport fraction'. This is the number of equivalents of a given ion transported per faraday of charge passed through the melt. Laity [20] (1957) has made an approach to this problem applicable to pure salts as well as mixtures. The mobility of the ion is defined as the velocity of the ion, under unit potential gradient with respect to ions of the same kind not possessing sufficient energy to move at that particular instant, multiplied by the fraction of the ions jumping. This definition is derived from a model of the system based on the hole theory of liquid structure (see section 2.1:2) The different values obtained by various workers for transport number, measurements on the same compounds show that a careful study of technique as well as theory is necessary before any proper assessment can be made.

A review of the techniques and results of different workers has been made by Janz, Solomons and Gardner[4] (1958) and Bloom and Bockris[1] (1959). In addition to the work cited in these

reviews consult also Duke and his co-workers, Cook[21] (1958), Owens[23] (1957), Fleming[24] (1959) and Laity[25] (1959) for work on $PbCl_2$[21], NaCl and KCl[22], Li, K, $AgNO_3$[23], KCl - $PbCl_2$[24], $AgNO_3$[22], $AgNO_3$ - $NaNO_3$[26], KNO_3 - $AgNO_3$[23], and $PbCl_2$, PbBr, TlCl, $AgNO_3$[26].

3.5 Viscosity.

The viscosity of a liquid i.e. its resistance to shearing stress can be represented by an equation:

$$\eta = Ae^{E_\eta/RT} \quad \text{.....(3.18)}$$

where η is the viscosity, E_η the energy for the process and A is a constant.

General treatment of the theory of viscosity and the types of instruments used in its measurement will be found in monographs by Barr[27] (1930) and Bingham[28] (1922). Reviews of viscosity of ionic melts have been given by Harrap and Heymann[29] (1951) Trifonev[30] (1944), Usanovich[31] (1944), Volarovich[32] (1944), Frenkel[33] (1944) and Khaikin[34] (1936). Bockris[1] has included a review of viscosity studies in a general review of the physical chemistry of ionic melts.

Exponential expressions of the above type relating viscosity to temperature were first proposed by de Guzman[35] (1913) and Dunn[36] (1926) for room temperature. Theoretical treatments have been proposed by Frenkel[37] (1926), Andrade[38] (1934), Born and Green[39] (1946) and Eyring[40] (1941). Andrade deduced an

equation similar to Frenkel and Eyring in terms of a model of momentum transfer. Panchenkov [41] (1946) utilised Andrade's model to obtain an equation of viscosity of liquids, containing no empirical constants and used it to calculate the viscosities of molecular liquids with an accuracy of about 20%. However, owing to the necessity to include terms dealing with critical temperature and pressure it is quite unsuitable for use with molten salt systems where these properties are unknown. Frenkel has also obtained an expression similar to the above but with his pre-exponential term showing considerable temperature dependence. This he explains as being due to E_{vis} varying inversely with temperature. Eyring[41] derived the equation:

$$\eta = 1.09 \times 10^{-3} \frac{M^{1/2} T^{3/2}}{V^{2/3} \Delta H} e^{E_{vis}/RT} \quad \ldots\ldots (3.19)$$

where M is molecular weight;

ΔH the heat of vaporisation

V the molar volume

In this equation Ewell[43](1938) has shown the pre-exponential term to be almost temperature independent. Oldekop [44](1955) has applied the statistical theory of Born and Green [39] to the viscosity and conductance of molten salts but the temperature coefficients of the properties calculated are at considerable variance with experimental results (up to 100%). However, no

completely satisfactory calculation of the viscosities of molten salts has been found and thus the above rate equation is still the most useful. It has been shown that $\log \eta$ plotted against $^1/_T$ is linear and thus the activation energy E_{vis} is obtained.

3.6 Relating Viscosity and Conductivity.

It has been found useful to compare the energy for viscous flow E_η with that for specific conductance E_σ. These quantities are not the same but in general E_η is found to be larger than E_σ. This is explained as being due to the units involved in viscous flow being larger than those involved in the conductance process. The ratio E_η / E_σ is found useful in correlating data for different compounds.[44] It is also shown to be one of the distinguishing features between high and low melting salts. For high melting salts this ratio is in the region 2-4, whereas for low melting salts it is invariably close to 1. The significance of this will be discussed later.

Various attempts have been made to relate viscosity to conductivity. Thus if the equations for the two processes are considered

$$\sigma = A_\sigma \exp(-E_\sigma/RT) \quad \ldots\ldots\ldots (3.20)$$

and

$$\eta = A_\eta \exp(E_\eta/RT) \quad \ldots\ldots\ldots (3.21)$$

it can be seen that if

$$E_\eta/E_\sigma = M > 1$$

then $\sigma^m \eta$ = constant.

Reasonable agreement with experiment has been obtained [2,3] using this expression. A more fundamental expression has been derived by Karapachev and Stromberg [45] (1938).

$$\lambda\eta = 3.1 \left(\frac{d}{M}\right)^{1/3} \quad \ldots\ldots\ldots\ldots\ldots\ldots (3.22)$$

where λ is the molar conductance;

M is the molecular weight;

and d is the density.

Values obtained from this equation are not in good agreement with the experimental values. The values of E_η, the energy of activation, for viscosity for various molten salts are listed in the Discussion.

Again de Guzman[35] has considered the process of viscous flow to involve a similar configurational change to the process of fusion. This has led him to compare the energies required for each process. Though this relationship is no longer considered to be of importance it is of interest to note that for many salts H_f, the heat of fusion, and E_η are of the same order.

TABLE 3.3

Salt	H_f (Kcals/mole)	E_η
NaCl	7.2	9.4
KCl	6.4	7.8
$NaNO_3$	3.8	3.95
KNO_3	2.8	3.66
$LiNO_3$	6.1	4.23

The energy to form a "hole" in a liquid the same size as an ion will be of similar magnitude to the energy necessary to vaporise an ion. This has led Eyring and his co-workers[46] to connect the activation energy for viscosity with the latent heat of vaporisation. It is not necessary for the hole to be the same size as one ion but it will be a definite fraction of it. For many polar substances the value of H_{evap}/E_{η} is about 4.

3.7 Surface Tension.

Some attempt has been made to elucidate the structure of the ionic melts by measurements of surface tension[47]. However, no completely satisfactory relationship has been found. A trend has been noted in the case of the alkali halides in which γ, the surface tension, close to the freezing point decreases with increasing cation size and increasing anion size. This general trend is absent in the alkali nitrates.[48] (see Table 3.4)

TABLE 3.4

Extrapolated Values of Surface Tension at the Melting Point γ_f dynes/cm.

	Li^+	Na^+	K^+	Rb^+	Cs^+
F^-	251	201	142	133	107
Cl^-	138	114	97	98	91
Br^-	-	106	89	91	82
I^-	-	87	81	82	75
NO_3^-	117	120	113	109	110

References

1. Bloom and Bockris, "Modern Aspects of Electrochemistry" No.2. Butterworths, London (1959), p.160. Watelle-Marion, J. Chim. Phys. (1959), 56, 302.
2. Rogers and Ubbelohde, Trans. Far. Soc.,(1950), 46, 1051.
3. Davis, Rogers and Ubbelohde, Proc. Roy. Soc., (1953),220A, 14.
4. Janz, Solomons and Gardner, Chem. Rev., (1958), 58, 461.
5. Kortum and Bockris, "Text Book of Electrochemistry", Elsevier, Amsterdam,(1951).
6. Jones and Bradshaw, J. A.C.S. (1933), 55, 1780.
7. Linde, Zwolenik and Fuoss, J.A.C.S., (1959), 81, 1557
8. Bloom and Heymann, Proc. Roy. Soc. (1947), 188A, 392
9. Bockris, Kitchener, Ignatowicz and Tomlinson, Trans. Far. Soc. (1952), 48, 76.
10. Yaffe and Van Artsdalen, J. Phys. Chem., (1955), 59, 118.
11. Mott and Gurney "Electronic Processes in Ionic Crystals" O.U.P. (1948), p.48.
12. Martin, J. Chem. Soc., (1954), 3246.
13. Frenkel, "Kinetic Theory of Liquids", O.U.P. (1946).
14. Mott, Proc. Roy. Soc. (1934), 146, 465.
15. Bockris, Kitchener, Ignatowicz and Tomlinson, Disc. Far. Soc., (1948), 4, 265.
16. Ubbelohde, Quar. Rev. (Chem.Soc.), (1950), 4, 356
17. Schwarz, Z Elektro-Chem. (1939), 45, 740; (1941), 47, 144.

18. Sundheim, J. Phys. Chem., (1956), 60, 1381; (1957), 61, 116; (1957), 61, 485

19. Aziz and Wetmore, Can. J. Chem., (1952), 30, 779

20. Laity, Abstracts of Papers Presented at the 131st Meeting of the American Chem. Soc. Miami, Florida, April, 1957.

21. Duke and Cook, J. Phys. Chem. (1958), 62, 1593.

22. Duke and Cook, Iowa State Coll. J. of Sci., (1958), 33, 81; (1957), 32, 35.

23. Duke and Owens, J. Electrochem. Soc. (1958), 105, 548, 476.

24. Duke and Fleming, J. Electrochem. Soc., (1959), 106, 130. U.S. Atom. Energy Com. Isc.- 944(1957).

25. Duke and Laity, U.S. Atom. Energy Com., I.Sc - 654, (1955.

26. Duke and Laity, J. Electrochem. Soc., (1957), 104, 299; (1958), 105, 97.

27. Barr, "Monograph of Viscometry", O.U.P. (1930).

28. Bingham, "Fluidity and Plasticity", McGraw-Hill, (1922).

29. Harrap and Heymann, Chem. Rev. (1951), 48, 45.

30. Trifonev, Akad. Nauk. S.S.S.R. Conf. on Visc. of Liquids and Colloidal Solns. (1944), 2, 76.

31. Usanovich, Ibid. 85.

32. Volarovich,Ibid. 18.

33. Frenkel, Ibid. 24.

34. Khaikin, Z. Sowjetunion, (1936), 9, 504.

35. de Guzman, Anal. Fis. Quim, (1913), 9, 355.

36. Dunn, Trans. Far. Soc., (1926), 22, 401.

37. Frenkel, Z. Phys.,(1926), 35, 652.

38. Andrade, Phil. Mag., (1934), 17, 497, 698.

39. Born and Green, Proc. Roy. Soc. (1946-7), 188A, 10. Green "Molecular Theory of Fluids" North Holland, Amsterdam (1952).

40. Glasstone, Laidler and Eyring, "The Theory of Rate Processes", McGraw-Hill (1941).

41. Panchenkov, J. Phys. Chem., U.S.S.R. (1946), 20, 811; 1011.

42. Ewell, J. Appl. Phys. (1938), 9, 252.

43. Oldekop, Z. Physik, (1955), 140,181.

44. Plester, Rogers and Ubbelohde, Proc. Roy. Soc., (1956), 235A, 469.

45. Karapachev and Stromberg, J. Phys. Chem., U.S.S.R. (1938), 11, 852.

46. Eyring, J. Chem. Phys. (1936), 4, 283; Kincaid and Eyring, ibid., (1937), 5,587; (1938), 6, 620. Ewell and Eyring, ibid., (1937), 5, 726. Kauzmann and Eyring, J.A.C.S., (1940), 62,3113. Roseveare, Powell and Eyring, J. App. Phys. (1941), 12, 669. Walter and Eyring, J.Chem.Phys. (1941),9, 393. Powell and Eyring, J.A.C.S.(1943),65,648.

47. Jaeger, Z. anorg. Chem. (1917), 101,1. Drath and Sauerwald, Z. anorg. Chem. (1927), 162, 301. Dahl and Duke, U.S. Atomic Energy Comm. I.Sc. (1957), 923.

48. Frame, Rhodes and Ubbelohde, Trans. Far. Soc. (1959), 55,2039.

CHAPTER 4

GAS SOLUBILITY.

The theory of gas solubility has been fully treated in the standard texts.[1] In addition a survey of the techniques employed in the measurement of gas solubility has been given by Markham and Kobe[2] (1941). For data concerning the solubility of gases in various solvents the reference book of Seidel[3] (1941, 1950) is the most useful.

4.1 Ideal Solution.

The ideal solution can be defined as one in which for any given component i, the fugacity, f, is equal to the mole fraction, x_i, multiplied by the fugacity of the component i in the pure state in the same phase, at the same temperature.[4] For any component

$$f_i = x_i f_i^o \quad \text{.....(4.1)}$$

When the vapour phase behaves sufficiently like the ideal gas for the fugacity of the gas to be replaced by it partial pressure, the above equation assumes the form

$$p_i = x_i p_i^o \quad \text{.....(4.2)}$$

From the definition of the ideal solution it can be shown that the partial molal volume and partial molal heat contents of any component are constant for all concentrations and are equal respectively to the volume and the heat content of the given

component in the pure state in the same phase at the same temperature.[4] Thus there is no change in volume or heat content when the components are mixed to form an ideal solution in the same phase at the same temperature.

From thermodynamic considerations the following equations can be derived describing the behaviour of an ideal liquid solution of two components in equilibrium with the gaseous phase of one of them.[4] The influence of temperature in the solubility of a gas is given by an equation of the form,

$$d\ln \frac{(x_2'/x_2)}{dT} = \frac{\triangle H_v}{RT^2} \quad \ldots\ldots\ldots\ldots (4.3)$$

provided both gas and liquid solutions are ideal. In the special case in which the partial pressure of the gas, hence its mole fraction x_2' remains constant, (this condition would be approximate at total constant pressure if the vapour pressure of the solvent was negligible in comparison with the pressure of the gas) equation (4.3) becomes

$$\left(\frac{\partial \ln x_2}{\partial T}\right)_{P,p_2} = \frac{\triangle H_v}{RT^2} \quad \ldots\ldots\ldots\ldots (4.4)$$

H_v is the molar heat of vaporisation of the liquified gas at the given temperature T and total pressure P.

An analagous expression can be derived for the variation of solubility with pressure.

$$\left(\frac{\partial \ln x_2}{\partial P}\right)_T = -\frac{\triangle V}{RT^2} \quad \ldots\ldots\ldots\ldots (4.5)$$

4.2 Real Solutions.

It has been found experimentally that real solutions in the dilute range of concentration follows the relation

$$f_2 = k_2 x_2 \quad \ldots\ldots\ldots\ldots (4.6)$$

That is, in the dilute range of concentration the fugacity is proportional to its mole fraction x_2, though the proportionality factor is not necessarily the fugacity, f_2°, of the pure solute. It can be shown that for dilute solutions, the fugacity of the solvent is equal to its mole fraction multiplied by the fugacity of the pure solvent.

$$f_1 = x_i f_i^{\circ} \quad \ldots\ldots\ldots\ldots\ldots\ldots (4.7)$$

The first of these equations is substantially Henry's Law for dilute solutions, and the second Raoult's Law of the lowering of the vapour pressure of the solvent in dilute solution.

In real solutions an expression similar to (4.4) is obtained but in this ΔH, includes the heat of mixing and the heat of condensation of the gas.

4.3 Gas Solubility in Ionic Melts.

The solubility of gases in ionic melts is perhaps most closely related to studies of solubilities of gases in metals where the solubility has been found to be higher in the molten state than in the solid and increasing with temperature. This is exemplified by the studies of Johnson and Shuttleworth[5] (1959)

on the solubility of krypton in liquid lead, tin and silver. Fig. 4.1 shows the temperature relation of r the Ostwald solubility coefficient. r has been defined by Hildebrand and Scott[1] (1950) as the ratio of the number of gas atoms in unit volume of liquid to the number of gas atoms in unit volume of gas, i.e. Volume of gas dissolved in unit volume of metal. The variation of r with temperature was given by the empirical equation:

$$r = \frac{r_\infty}{\text{antilog.} T_s/T} \quad \ldots\ldots\ldots (4.8)$$

and the thermodynamic equation:

$$r = \frac{h^3}{(2\pi mkT)^{3/2}} \cdot \frac{1}{a^3} \exp.\left(\frac{S}{R}\right) \exp\left(\frac{-H}{RT}\right) \ldots\ldots (4.9)$$

where $1/a^3$ is the number of metal atoms in unit volume;

m is the mass of a gas atom (krypton);

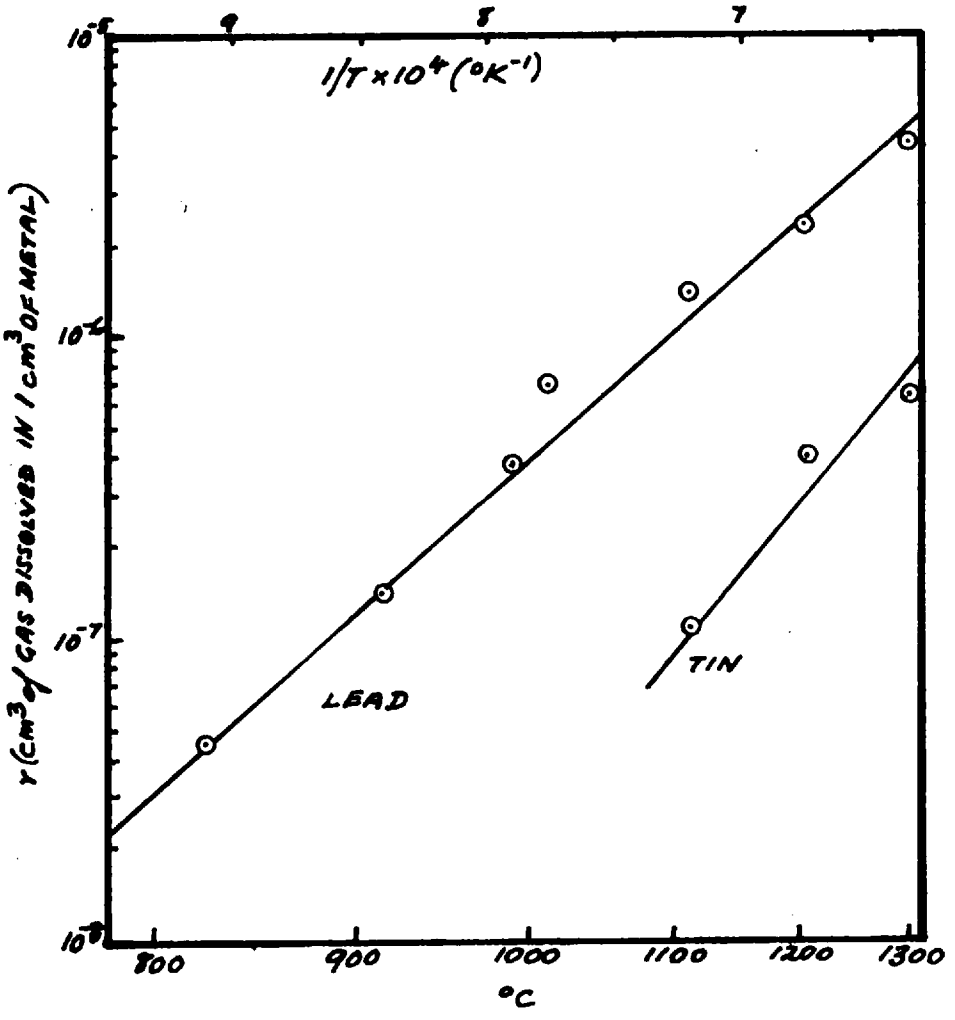
H is the energy needed to transfer an atom at rest in the gas phase into solution in the metal;

and S is the vibrational entropy of a gas atom (krypton) dissolved in the liquid metal.

Johnson and Shuttleworth have suggested that the factor determining the solubility of krypton in liquid metals is the surface energy per unit area of the liquid metal, even though the radii of the gas and metal atoms are appreciably different. This can be compared with the results of Grimes, Smith and Watson [6] (1958), Blander, Grimes Smith and Watson [7] (1959), Gerling [8] (1940), Protsenko and Bergman [9] (1950), and Bergman and Dergunov [10] (1941), for the solubilities of noble gases in molten fluoride and nitrate

FIG 4.1

THE VARIATION WITH TEMPERATURE OF THE OSTWALD SOLUBILITY COEFFICIENT γ.



mixtures. Grimes et al. and Blander et al. found that solubility increased with increasing temperature and with decreasing molecular size of the gas involved. Tables 4.1, 4.2 and 4.3 show their results for the solubility of noble gases in molten fluorides.

TABLE 4.1

Henry's law constants for He, Ne, A and Xe in Na F - Zr F_4 (53 - 47 mole %)

Kp = C/p x 10^8 (moles gas)/(cc Melt) (atm.)				
Temp ^oC	Henry's law constant x 10^8			
	He	Ne	A	Xe
600	21.6±1.0	11.3±0.3	5.06±0.15	1.94
700	29.2±0.7	18.4±0.5	8.07±0.08	3.56
800	42.0±1.3	24.7±0.7	12.0±0.6	6.32

TABLE 4.2

Henry's law constant for He, Ne and A in LiF - NaF -KF (46.5 - 11.5 - 42.0 mole %) (K as in Table 4.1)

Temp ^oC	Henry's law constant x 10^8	
	He	Xe
600	20	2.0
700	27	4.0
800	41	6.5

TABLE 4.3

Henry's law constant for He, Ne and A in LiF-NaF - KF (46.5 - 11.5 - 42.0 mole %) (K as in Table 4.1)

Temp °C	Henry's law constant x 10^8		
	He	Ne	A
600	11.3±0.7	4.36±0.2	0.90±0.04
650	13.7	-	-
700	17.5±0.2	7.51±0.22	1.80±0.04
800	23.0±0.7	11.18±0.26	3.40±0.03

The heat of solution, $\triangle H$, for these systems are listed in Table 4.4

TABLE 4.4

System	$\triangle H$ Kcal / mole			
	He	Ne	A	Xe
NaF - ZrF_4	6.2	7.8	8.2	11.1
LiF - NaF - KF	8.0	8.9	12.4	-

The solubilities of all the gases studied obeyed Henry's law. The enthalpies of solution of the gases are positive and larger, the larger the atomic weights and radii. The solubility was tested for the applicability of a mechanism first proposed by Uhlig[11] (1937) for systems wherein the gas does not react with the liquid and the free energy of solution is related to the 'surface' energy of the hole created by the gas. The derivation

of Uhlig's relation between gas solubility and the surface tension of the solvent is outlined in Appendix I.

The method employed in the above determinations involved the saturation of the melt with the gas being studied at required temperature and pressure. It was then transferred to a second compartment and a second gas used to strip the gas under examination from the solvent. The concentration of the first gas in the second gas was determined by mass spectrometry.

Protsenko and Bergman[9](1950), have studied the solubility of xenon in KNO_3 - $NaNO_3$ of eutectic composition. They found the solubility varied in the range 8×10^{-8} to 10^{-7} mole Xe/(cm^3 solvent)(atm.) between 260° and 450°C. A slight increase in solubility with temperature was reported.

Bergman and Dergunov [10](1941) examined the ternary eutectic LiF - NaF - KF for xenon solubility but were less successful since HF and SiF_4 from the glass apparatus, contaminated the recovered xenon. Solubility was estimated at 500°C to be less than 5×10^{-8} mole Xe/cm^3 atm. Gerling (1940) has examined the solubility of helium in molten KCl and gabbrodiabase. The solubilities were of the order of 1.5 - 2.5 mm^3 He/gm melt (at 0°C/760) and increasing with temperature. Shaffer, Grimes and Watson[12] (1959) have studied the solubility of HF in molten NaF - ZrF_4 and have found that it obeys Henry's law, but in contrast to their earlier work with noble gases found that the solubility decreased with increasing temperature. Tables 4.5 and 4.6 show their results

TABLE 4.5

Solubility of HF in NaF - ZrF_4 (53 mole % NaF)

Temp °C	Kx10^{5}moles HF/CCmelt(atm.)	Kx10^5 calc.
550	1.38 ± 0.02	1.45
600	1.23 ± 0.04	1.22
650	1.03 ± 0.02	1.06
700	0.93 ± 0.02	0.93
750	0.86 ± 0.02	0.83
800	0.73 ± 0.01	0.74

The temperature dependence of the Henry's law constant for the solubility of HF in NaF - ZrF_4 was given by

$$\ln K = \frac{-\Delta H}{R}\frac{1}{T} + \frac{\Delta Sp}{R} \quad \ldots\ldots (4.10)$$

Values of K calculated from this are compared with the experimental values and are listed in Table 4.5. The solubility of HF showed a marked dependence on the NaF concentration. Variations of K with NaF concentration is shown in Table 4.6 together with the constants for the equation 4.10.

TABLE 4.6

The dependence of the solubility of HF on the NaF concentration.

% NaF	K x 10^5			Const. for equation 4.9		
	600°C	700°C	800°C	- Sc	- H	- Sp
45	0.78	0.65	0.51	5.2	3.85	14.0

/Contd.

TABLE 4.6 (Continued...)

% NaF	K x 10^5			Const. for equation 4.9		
	600°C	700°C	800°C	$-\overset{\bullet\bullet}{Sc}$	- H	$-\overset{\bullet\bullet\bullet}{Sp}$
53	1.23	0.93	0.73	5.4	4.70	14.1
60	1.53	1.03	0.81	6.2	5.80	14.9
65	2.17*	1.46	1.06	6.4	6.60	15.1
80.5	12.80*	7.20*	4.43	6.5	9.70	15.2

* extrapolated from measurements at higher temperatures.

$\bullet\bullet$ for equilibrium at 1000°K.

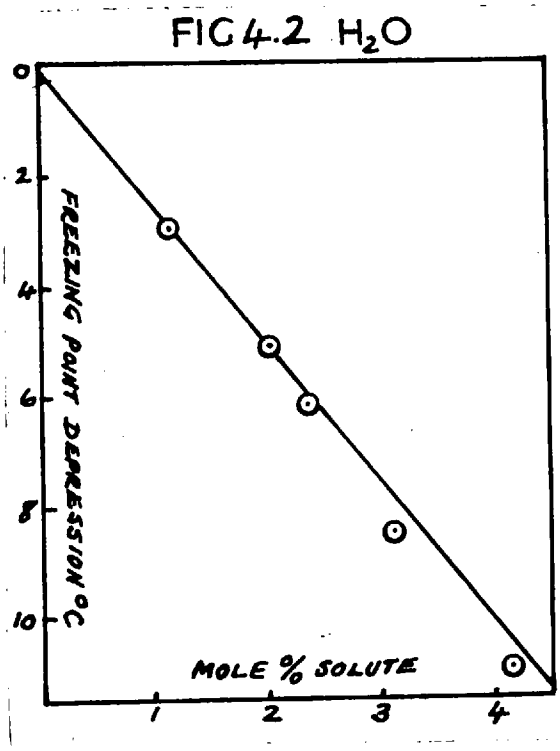
$\bullet\bullet\bullet$ for equal pressures of HF in gas and liquid.

$\triangle Sc$ and $\triangle Sp$ in entropy units.

$\triangle H$ in Kcal/mole.

4.4 Molten Salts and H_2O.

It has long been recognised that certain salts dissolve an unusual amount of water. Dantuma [13] (1928) found difficulty in keeping $LiNO_3$ dry during his viscosity studies in fused salts. However, very little quantitative work has been done on the solubility of H_2O in fused salts. Galinker and Korobkov [14] (1951) studied the interaction of water with fused alkali hydroxides and studies have been made on the hydrolysis of fused alkali halides. [15,16] More recently Laitenen [17] has discussed the problem of obtaining dry LiCl, and Keenan [18] has shown by a cryoscopic method



that H_2O dissolves in molten NH_4NO_3 without ionisation or association. Fig 4.2 shows Keenan's results. His technique involved the addition of water to NH_4NO_3 at room temperature allowing it to equilibrate for an hour, then determining the freezing point. The melt was then analysed for H_2O content. The high solubility coupled with the low vapour pressure was attributed to weak hydrogen bonding between the NO_3^- and H_2O molecule as

$$\left\{ O - N \begin{matrix} O \cdots\cdots H \\ O \cdots\cdots H \end{matrix} O \right\}$$

Further studies of H_2O fused salt systems have been carried out by Burkhard and Corbett[19] (1957) on molten mixtures of LiCl and KCl, and by Duke and Doan [20] (1958) on $NaNO_3$ - KNO_3, $LiNO_3$ - KNO_3 - $NaNO_3$ and $LiClO_4$ by following the change in pressure of H_2O vapour as it was absorbed in these melts.

Burkhard and Corbett used mixtures containing 50.0, 53.0, 60.0 and 68.6 mole % LiCl at 480°C and 50.0 and 60.0 at 390°C.

The solubilities followed Henry's law to 18 mm pressure at 480°C and to about 14 mm at 390°C. The values for the Henry's law constant found are given in Table 4.7. Fig. 4.3 shows a plot of their results.

FIG 4.3

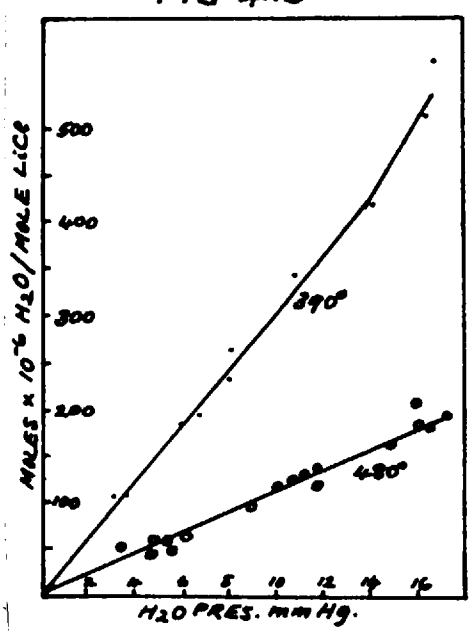


TABLE 4.7

Henry's law constant for H_2O in LiCl - KCl.

Temp °C	K (μmoles H_2O)/(mole LiCl) (mm)			
	Mole % LiCl			
	50	53	60	68.6
480	14	11.8	11.3	10.8
390	30.0	-	30.5	-

The heats of solution calculated for 50 and 60% LiCl compositions are 8 and 11 Kcal/mole respectively.

TABLE 4.8

T °C	Composition $LiNO_3$-$NaNO_3$-KNO_3 (Mole %)	Moles H_2O K(mmHg x moles Li^+) x 10^6
145	30 - 23 - 47	23.8

/Contd.

TABLE 4.8 (Continued.....)

T °C	Composition $LiNO_3$-$NaNO_3$-KNO_3 (Mole %)	Moles H_2O K(mmHg x moles Li^+) x 10^6
170	30 - 23 - 47	13.0
175	"	8.8
205	"	3.2
240	12.5 - 46.4 - 41.1	1.02
240	24.8 - 39.9 - 35.3	2.07
240	30.0 - 37.1 - 32.9	2.50
240	46.7 - 28.2 - 25.1	10.0
240	67.0 - 17.5 - 15.5	27.4
240	86.9 - 6.9 - 6.2	49.7
240	Pure $LiClO_4$	54.9
260	"	28.5
290	"	20.2

Duke and Doan state that the solubility of H_2O in $NaNO_3$ - KNO_3 was too small to be measured over their temperature range. Upon the addition of $LiNO_3$ the solubility became measurable. They found that at all compositions and all pressures the solubility of H_2O was a linear function of its pressure. Their results are listed in Table 4.8. The solubility per mole Li^+ varied approximately as the square of the Li^+ concentration. Two Li^+

are thus considered to co-operate in dissolving one H_2O molecule. This greater solubility of H_2O in Li^+ melts is qualitatively explained on the basis of an ion dipole interaction of Li^+ with the negative end of the water molecule. The most effective term of the energy of interaction is proportional to r^{-4}, where r is the distance of closest approach of the Li^+ centre of positive charge to the negative end of the dipole of the water molecule.

The heat of solution of H_2O in the 30 - 23 - 47 $LiNO_3$ - $NaNO_3$ - KNO_3 system is given as - 13 ± 4Kcal and in $LiClO_4$ as - 9 ± 3.5 Kcals. These are of a similar order of magnitude to the values for $\triangle H$ given by Burkhard and Corbett for solution of H_2O in molten LiCl - KCl (see above).

Burkhard and Corbett, and Duke and Doan found a decrease in solubility of H_2O in molten ionic systems with increase in temperature as was also found to be the case for the solubility [12] of HF in Molten ZrF_4 - NaF. This can be contrasted with the positive heat of solution found when the noble gases dissolve in molten ionic systems.[6-10] This suggests that the solution of a dipole in an ionic medium involves a different mechanism to that for the solution of an inert gas atom.

4.5 The Cryoscopy of Molten Salts.

It has been satisfactorily demonstrated that only foreign ions introduced into a solvent contribute to the depression of the freezing point. [21, 22.] This can be expressed by the equation:

$$\Delta T_f = \left\{ \frac{RT^2}{H_f} \right\} x_2 = Kx_2 \quad \ldots\ldots\ldots\ldots (4.11)$$

Where T is the freezing point of the pure solvent,

x_2, the mole fraction of the solute,

H_f, the heat of fusion of the solvent,

ΔT_f, the depression of the freezing point

and $\frac{RT^2}{H_f}$ is constant for a given solvent.

If x_2 is expressed in gm - moles, m_2, of solute per 1000 g. solvent the above expression can readily be written as $\Delta T_f = k_f m_2$ where k_f is known as the cryoscopic constant. This expression is known as the Raoult-Van't Hoff law. If more than one foreign ion is present in the solution each one will act independently of the other and the expression then applied is written $\Delta T_f = \nu k x_2$ where ν is the number of foreign ions or particles into which one molecule of the solute dissociates.

It has been shown that the lowering of the freezing point of a molten salt solvent is a linear function of the concentration of the solute, in some cases up to 7 mole % (e.g. NaCl in $NaNO_3$). Thus for molten salts the above expression holds. Knowing an accurate value for the molecular freezing point depression constant allows information to be obtained regarding the degree of dissociation of other solutes, common ion effect, and tendency to form complex ions. This has been shown by the work of Van Artsdalen [22] (1956). Using sodium nitrate as solvent

he has measured the value of the depression constant and found it to be 15.0° per mole of foreign ions per 1000 g. of solvent for NaCl, $NaBrO_3$, Na_2MoC_4 and $LiNO_3$. This can be compared with 14 .7° computed from the calorimetrically determined heat of fusion of Goodwin and Kalmus [23] (1909). This shows the effect of the presence of one foreign ion, and as would have been expected if complete dissociation took place, LiCl and $CaCl_2$ gave constants of 29.8° and 45.4° respectively. The association of ions in molten salts has also been demonstrated by Van Artsdalen.[22] He measured the freezing points of solutions of cadmium chloride in sodium nitrate in the presence of added chlorides. As the concentration of added chloride was increased, the effect of cadmium chloride on the freezing point decreased. This was interpreted as the removal of chloride ions by the cadmium, and the existence of Cd^{2+}, $CdCl_2$ and $CdCl_4^{2-}$ in the melt was postulated.

The heat and entropy of fusion for the solvent can be obtained from cryoscopic measurements. However, if premelting occurs the latent heat of fusion determined cryoscopically will be lower than that determined calorimetrically, since the latter integrates the heat content over a wide temperature range and the former only at one temperature. As a consequence the heat content of the solid separating out will be higher than expected and so the difference between the heat contents of solid and liquid will

be reduced. Following from this the entropy of fusion as given by $\frac{\Delta H_f}{T_f} = \Delta S_f$ ..... (4.12)

will also be reduced. In general, however, the values obtained for H_f compare favourably with those found by other means.

The limiting factor of the cryoscopic technique is that it leads to a knowledge of structure only near the melting point which in itself may not be sufficient indication of the structure at much higher temperatures.

Little work has been done on the cryoscopic study of molten salts where gases are the solutes, though measurements of some gas solubilities in water solvent have been determined by this method.[24] The effect of water on the freezing point of NH_4NO_3 has been studied by Keenan[18], and is discussed in Section 4.4. In treating freezing point depression studies where a gas is the solute, the same expressions as noted above and following apply.

4.5:1 Formation of Solid Solutions.

If on cooling a liquid solution the solid phase separates as a solid solution, it is necessary to make use of an equation of the form:

$$\left\{\frac{\partial \ln(x_2'/x_2)}{\partial T}\right\} = \frac{\Delta H_f}{RT^2} \quad \ldots\ldots (4.13)$$

Where H_f is the mole heat of fusion of the solvent and x_2 is the mole fraction of the solute in the solid phase. In the form given

above this becomes:

$$\Delta T_1 = \frac{RT^2}{\Delta H_f} (x_2 - x_2') \ldots\ldots\ldots (4.14)$$

This can lead to an effect where, if there is a greater proportion of solute in the solid phase than in the liquid phase, ΔT becomes negative and the freezing point of the solution is above that of the pure solvent.

4.6 Mixed Systems.

The theory and general thermodynamic treatment of mixtures will be found in the standard texts [1,28]. However, theoretical consideration of mixtures of fused salts has largely been neglected. Any concise theory of the structure is made difficult by the extensive nature of the force fields involved. This limits the application of any bi-reciprocal potential treatment such as the 6 - 12 of Lennard-Jones which only considers near neighbours.

4.6:1 Thermodynamic Properties of Ionic Melts.

Tempkin [25] (1945) and Forland [26] (1956) (cf. Blander [27] 1959) have proposed structures for ionic melts in which two types of position are assumed to exist, one for anions and one for cations - the cations being distributed randomly over the cation positions. This is considered to hold for mixtures of ionic salts where the cations are not very different in size. A deviation from ideal mixture is attributed to an energy of mixing.

Forland's is perhaps the most extensive treatment and

since it depends on the original model of Tempkin it will be dealt with more fully.

The possibility of mixtures of salts containing cations of the same size and charge and cations of different sizes led Forland [26] to postulate four possible structural models.

a) For a simple system of the type NaCl-KCl, the cations are assumed to be distributed over all cation positions.

This leads to an entropy of mixing of the form:

$$\Delta S = -R\,(n_{Na}\,\ln N_{Na} + n_K\,\ln N_K) \quad \ldots\ldots\ldots \quad (4.15)$$

where n denotes the number of moles. N_{Na} and N_K are ionic fractions:

$$\text{i.e.} \quad N_K = \frac{n_K}{n_{Na} + n_K}$$

The partial molar entropy of one component, KCl say, is $\overline{\Delta S}_{KCl} = -R\ln N_K$ cf. Tempkin [25]

Where the cations have different charges, and here Forland considers the system $Na_2CO_3 - CaCO_3$, the same expression as above is derived for the entropy of mixing.

Further $\overline{\Delta S}_{CaCO_3} = -R\ln N_{Ca}$

and $\overline{\Delta S}_{Na_2CO_3} = -2R\ln N_{Na}$

It is assumed that the number of cation sites

is determined by the number of cations and is not dependent on charge. Thus the increase in number of vacant sites by the introduction of a divalent cation to a system containing monovalent cations is neglected.

b) The presence of vacant sites is recognised in a second model. This proposes that a vacant site is adjacent to the divalent ion in a system where divalent and monovalent cations have common anions. For $Na_2CO_3 - CaCO_3$ therefore the liquid may be regarded as a mixture of Ca^{2+} + a vacant site and two Na^+ ions on adjacent sites. This leads to an entropy of mixing of the form:

$$\Delta S = - R(1/2\ n_{Na} \ln N'_{Na} + n_{Ca} \ln N'_{Ca}) \quad .....(4.16)$$

and $$\overline{\Delta S}_{CaCO_3} = - R \ln N'_{Ca}$$

and $$\overline{\Delta S}_{Na_2CO_3} = - R \ln N'_{Na}$$

N' is called an electrical equivalent fraction and

$$N'_{Na} = \frac{1/2 n_{Na}}{1/2 n_{Na} + n_{Ca}} \qquad N'_{Ca} = \frac{n_{Ca}}{1/2 n_{Na} + n_{Ca}}$$

However, it is reasonable to assume that the vacant cation site associated with a divalent cation can be at any of the sites surrounding the Ca^{2+} ion in its second co-ordination sphere.

This leads to a further model c) in which

$$\triangle S = - R \left(n_{Na} \ln N'_{Na} + n_{Ca} \ln N'_{Ca}\right) \quad \ldots\ldots(4.17)$$

From this is obtained:

$$\bar{\triangle S}_{CaCO_3} = - R \ln N'_{Ca} + RN'_{Na}$$

and $$\bar{\triangle S}_{NaNO_3} = - 2 R \ln N'_{Na} - RN'_{Ca}$$

The derivation of this expression is the same as that used by Flory [29] (1942) for a mixture of organic molecules of different sizes.

d) A fourth possible model is considered where two monovalent cations exchange positions with one divalent cation and a separate independent vacant cation site. Using this model the entropy of mixing for a system of the type $CaCO_3 - Na_2CO_3$ will be:

$$\triangle S = -R \left(N_{Na} \ln N''_{Na} + n_{Ca} \ln N''_{Ca} + n_{(c.v.)} \ln N''_{(c.v.)} - n_{Ca} \ln \frac{n_{Ca}}{n_{Ca} + n_{(c.v.)}} - n_{(c.v.)} \ln \frac{n_{(c.v.)}}{n_{Ca} + n_{(c.v.)}}\right) \ldots(4.18)$$

Here N" is the number of cations of one kind divided by the total number of cation sites. c.v. indicates a cation vacancy. If in (4.12) a cation vacancy is treated as a cation and $n_{Ca} = n_{(c.v.)}$, then the above expression becomes:

$$\Delta S = - R \left(n_{Na} \ln N'_{Na} + 2 n_{Ca} \ln N'_{Ca}\right) \quad .....(4.19)$$

and

$$\bar{\Delta S}_{CaCO_3} = - 2R \ln N'_{Ca} \quad \text{and} \quad \bar{\Delta S}_{Na_2CO_3} = - 2 R \ln N^1_{Na}$$

where N' is as defined above.

4.6:2 Volume and Density of Binary Mixtures of fused salts.

Volumes of mixtures of fused salts with a common ion are in general found to be near ideal i.e. their molar volume composition isotherms do not deviate from a linearity.

Only small changes have been found in the volumes of the $NaNO_3$ - KNO_3 mixture [30]. The systems AgBr - LiBr, AgBr - NaBr, AgBr - RbBr and AgBr - RbBr have been studied by Hildebrand and Salstom [31] (1932). Small increases were found in all cases except for LiBr - AgBr where a small decrease was found. Little deviation from additivity is found where the cations are of different charge, as was also shown by Salstrom [32] (1932) to be the case for the $PbBr_2$- AgBr system. Similarly Harrap and Heymann [33] (1955) have found marked changes in volume only where other evidence suggests complex formation and deviation from random distribution. In the system $CdCl_2$ - NaCl, $PbCl_2$ - KCl, the first shows no deviation from additivity and the second only slight deviation from a linear function. However, examination of $CdCl_2$ - KCl has shown strong positive deviation which suggests, together with data on the conductivity of these systems that this

is due to complex formation. Bloom, Knaggs, Molloy and Welch [34] (1953) have examined the systems $NaNO_3$ - $NaNO_2$, $CdCl_2$ - CdI_2, KBr - $BaBr_2$, $LiCl_2$ - $CdCl_2$, KCl - NaI, KI - NaCl, CdI_2 - KI and KNO_3 - KBr and have shown that for $NaNO_3$ - $NaNO_2$, $CdCl_2$ - CdI_2 and KI - NaCl the molar volume isotherms are approximately linear while the phase diagrams of the systems KBr - $BaBr_2$ and LiCl - $CdCl_2$ indicate the formation of congruently melting double salts.

These three systems can be contrasted with the system KCl - NaI where the phase diagram also indicates a congruently melting compound but the molar volume isotherm shows considerable positive deviation from linearity. This has been attributed to greater covalent character in this system. In CdI_2 - KI, and KNO_3 - KBr systems the phase diagrams indicate the presence of incongruently melting compounds but though the KNO_3 - KBr molar volume isotherms show little deviation from linearity those of the CdI_2 - KI system exhibit pronounced deviations.

The relating of data obtained from measurements of molar volume and density as well as the conductivity and viscosity of mixed systems to their phase diagrams can be very useful. Where conductivity and viscosity can give some indication of structural abnormalities in molten mixtures, the phase diagrams can often assist by indicating the possible compositions of some of the units involved. However, phase diagrams are not an exact guide to the behaviour of molten salts; as can be seen from the last

examples, spatial conditions existing in the solid do not necessarily have a parallel in the melt.

4.6:3 Electrical Conductivity of Binary Systems.

Ideally the electrical conductance of binary salts systems should be a linear function of the composition, however, even for simple mixtures, this is not the case. Yaffe and Van Artsdalen [35](1955) have shown that slight deviations are found in the systems KCl - LiCl, KCl - NaCl and KCl - KI, the deviations decreasing in that order. In the systems $NaNO_2$ - $NaNO_3$, $CdCl_2$ - CdI_2 and KI - NaCl slight deviations are apparent in equivalent conductance molar composition isotherms, the system $NaNO_2$ being the closest to linearity. The systems KBr - $BaBr_2$ and LiCl - $CdCl_2$ show marked negative deviations from linearity in their equivalent conductance isotherms (max. 28%), KCl - NaI exhibits negative deviation of 18%. CdI_2 - KI and KNO_3 - KBr also show negative deviations from linearity in their equivalent conductance isotherms.

For binary systems that form solid solutions, but not for those that form eutectics, Markova and Shumina [36] (1956) have suggested a relationship of the form:

$$\lambda_M = x_1^2 \lambda_1 + x_2^2 \lambda_2 + 2 x_1 x_2 \lambda_{12} \ldots\ldots\ldots (4.25)$$

to represent the ideal conductance in the melt; deviations from this are considered to be deviations from ideality.

4.6: 4 Viscosity of Binary Systems.

The viscosities of fused systemshave been reviewed [37, 26, 38]. In general it is found that the mixture of the melts of ionic salts have negative deviations from linearity for their viscosity molar composition isotherms. The systems $NaNO_3$ - KNO_3 [39] $CaSiO_3$- $MgSiO_3$ [40] K - glass - Na - glass [41], $PbCl_2$ - AgCl, $PbCl_2$ - KCl [33], all exhibit minimum points in their isothermal plots of viscosity against composition. However, the systems $MgCl_2$ - KCl [42], $TlNO_3$ - $AgNO_3$ and $AgNO_3$ - AgI [43] show sharp maxima. The occurrence of maxima in viscosity isotherms for $MgCl_2$- KCl appears to fit in with the formation of a $MgCl_4^{--}$ ion as suggested by the cryoscopic work of Flood, Forland and Leirnes (see Forland [26] 1956). Inspection of the isothermal plots of viscosity against composition for $TlNO_3$ - $AgNO_3$ and $AgNO_3$ - AgI systems suggest that their general shape describes a normal isothermal curve with a minimum if the peaks are neglected. This is demonstrated by the way in which the peak gradually disappears with rising temperature while the general form of the curve exhibits the normal negative deviation from linearity. Reference to the phase diagrams of these last two systems shows that the maxima in the viscosity isotherms coincide, with regard to composition, to points where the existence of complexes has been suggested by the phase diagrams. The gradual disappearance of these maxima at higher temperatures has been attributed to the dissociation of

these complexes.

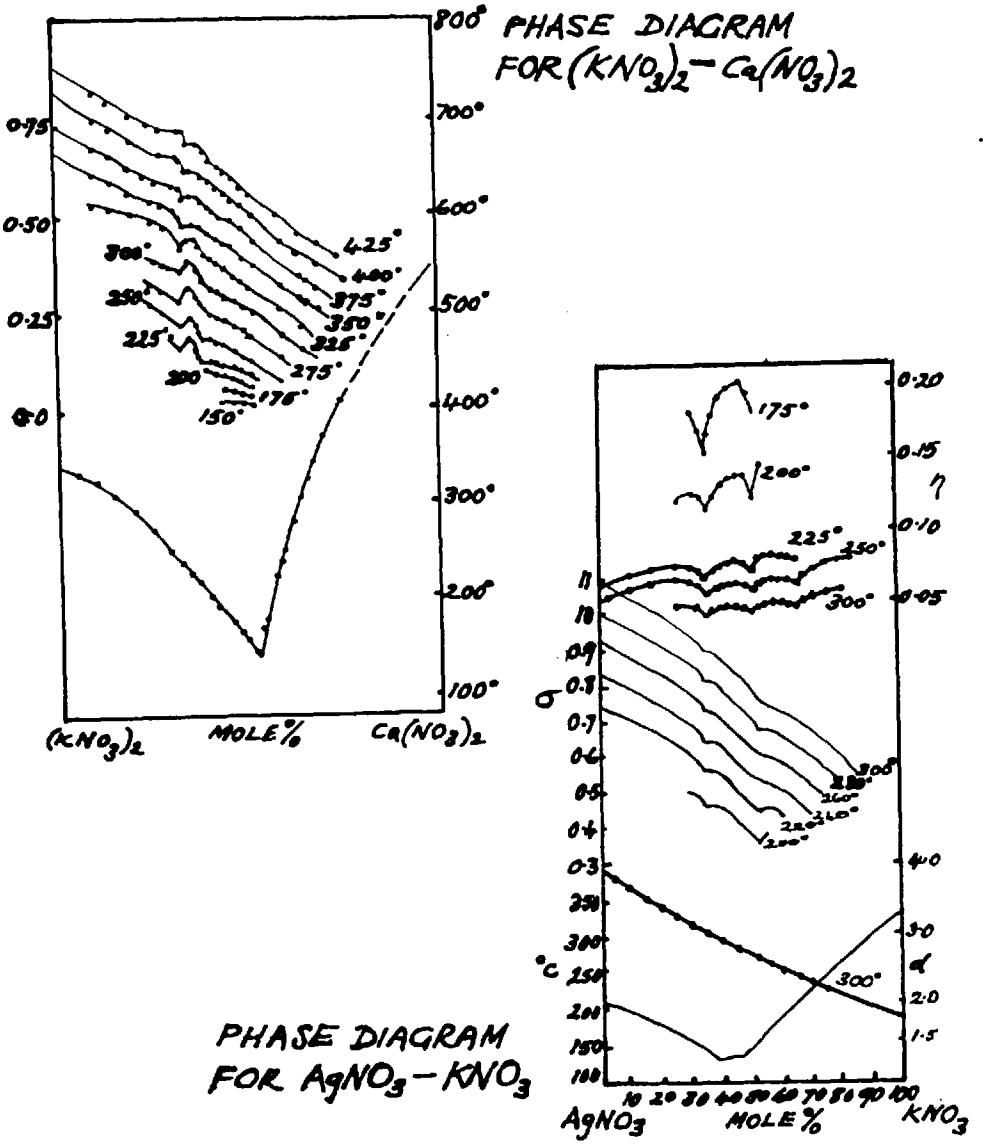
Examples of the occurence of minima on the isothermal curves for electrical conductivity and maxima on the viscosity isothermals concurrently with the indications of complex formation given by the phase diagrams and disappearing with rise in temperature are demonstrated in Fig. 4.4.

The frequency with which the formation of complexes in binary systems was accompanied by changes in the conductivity and viscosity in the melt led Bergman and Chagin [44] (1940), Luzhanaya and Vereshchetina [45] (1949), Tarasova [46] (1947) and Belyaev and Mironov [47] (1950, 1952) to consider this as the regular case and indeed, to suggest the measurement of electrical conductivity as a sensitive method of physico-chemical analysis. However, the results of Bloom, Knaggs, Molloy and Welch [34] cited above, and of Protsenko and Popovskaya [48] (1954) on the electrical conductivity of the systems $CsNO_3$ - $Cd(NO_3)_2$, $TlNO_3$ - $Cd(NO_3)_2$ and KNO_3 - $RbNO_3$ showed that no sharp changes in the molar volume isotherms were encountered, even where the phase diagrams indicated complex formation. This underlines what has been said above that phase diagram data reflect only the nature of the components at the freezing point and the same compounds will not necessarily exist in the melt above the freezing point.

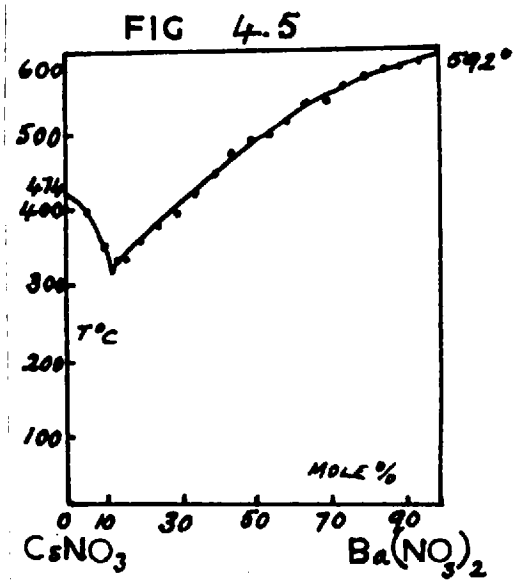
4.6:5 Phase Diagrams for some Binary Systems.

Phase diagrams of binary mixtures of molten salts are of

FIG 4.4


PHASE DIAGRAM
FOR $(KNO_3)_2 - Ca(NO_3)_2$
800°
700°
600°
500°
400°
300°
200°
100°
0·75
0·50
0·25
0·0
425°
400°
375°
350°
325°
300°
275°
250°
225°
200°
175°
150°
$(KNO_3)_2$
MOLE %
$Ca(NO_3)_2$
PHASE DIAGRAM
FOR $AgNO_3 - KNO_3$
0·20
0·15
0·10
0·05
η
175°
200°
225°
250°
300°
σ
°C
α
4·0
3·0
2·0
1·5
$AgNO_3$
MOLE %
KNO_3

some use in interpreting the information obtained from measurements of conductance, viscosity and molar volumes.



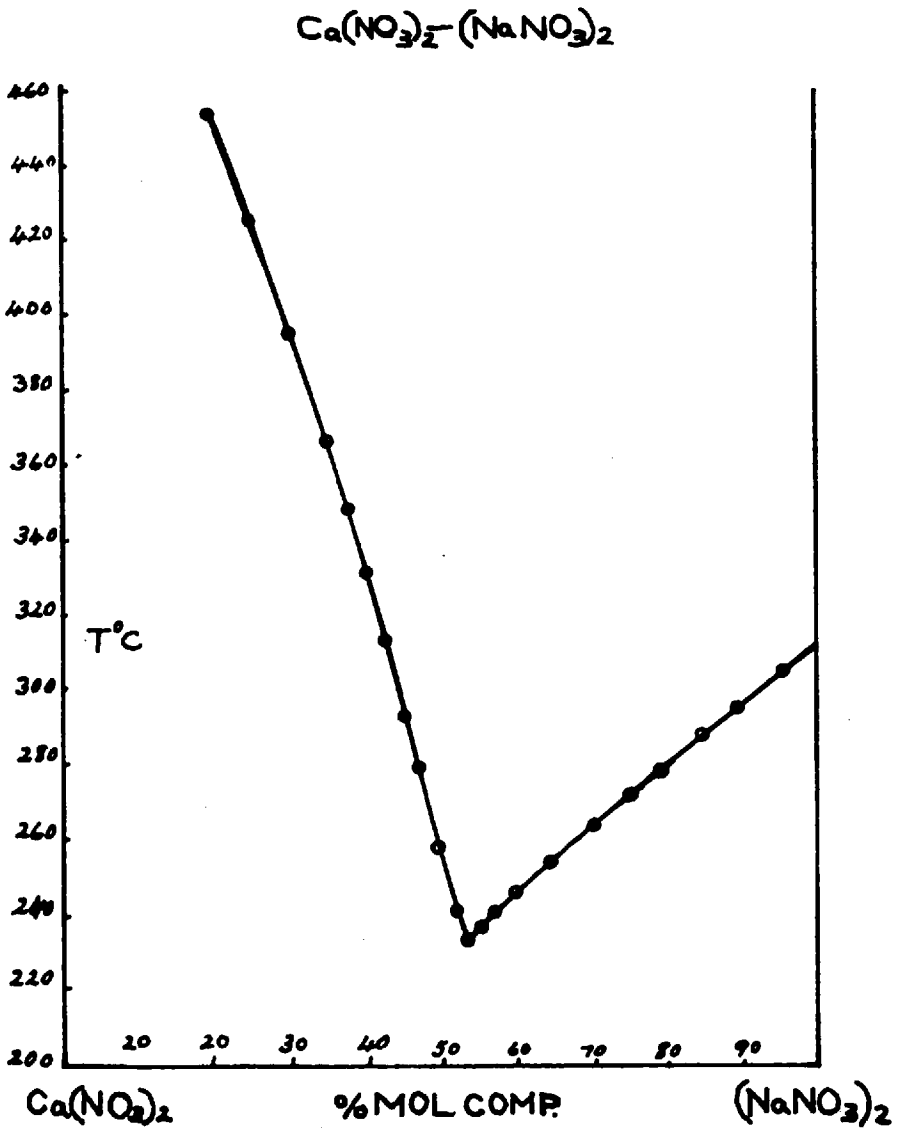
A considerable amount of work has been done recently on the phase diagrams of binary, ternary, quaternary molten salt systems. Of particular interest in the present investigations are the phase diagrams of binary mixtures of alkali nitrates and binary mixtures of alkali and alkaline earth nitrates.

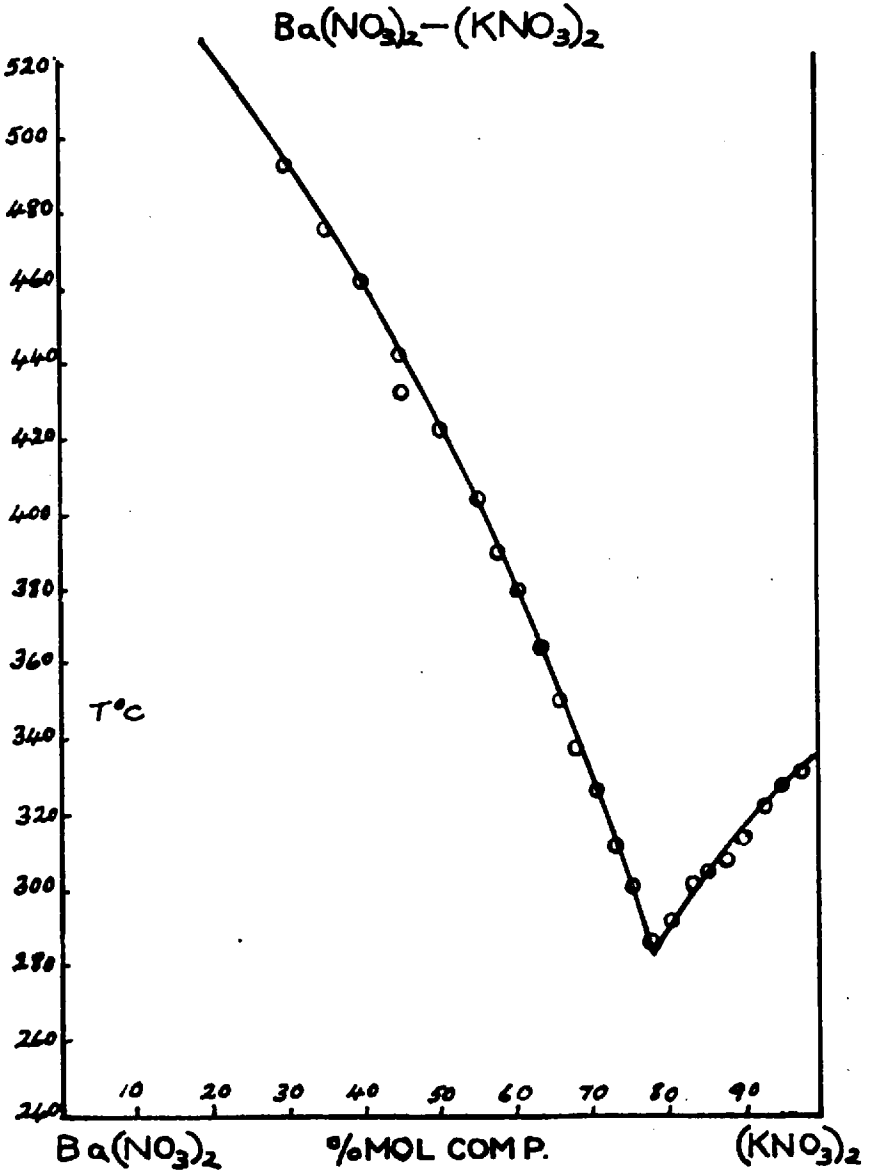
Figs. 4.5 and 4.6 show the phase diagrams for the systems KNO_3 - $Ba(NO_3)_2$ [50], $NaNO_3$ - $Ca(NO_3)_2$ and $CsNO_3$ - $Ba(NO_3)_2$ [51], These form simple eutectics with no evidence of solid solutions or intermediate compounds. Comparison with similar mixed nitrate systems show that this is generally true for those systems where the cations are of comparable size (see Table 1.2). However, where cations of markedly different cation radius are present in the same system the formation of intermediate compounds has been observed.

In certain of these mixed nitrates glass formation has been reported as for example in the system KNO_3 - $Ca(NO_3)_2$

FIG 4.6

PHASE DIAGRAMS — PROTSENKO AND BERGMAN 1948





(Rostkovsky [52] 1930), Urnes [53] (1957), Bergmann [54] (1939) and KNO_3 - $Mg(NO_3)_2$ (Stevels [55] 1952). No evidence has been reported of glass formation of the above systems. Stevels [55] and Dietzel [56] suggest that the nitrate glass formation is due to distorted NO_3^- ions. Zachariasen and Warner have been responsible for the development of the "random network" theory of glass structure. Weyl [57] however, has suggested that glass formation is a rate phenomenon and that failure to crystallise in the absence of nuclei is due to the energy barrier of nucleation being high compared with kT.

References.

1. Hildebrand, "Solubility of Nonelectrolytes" Reinhold, New York 2nd Edn. (1936).
Hildebrand and Scott, "Solubility of Nonelectrolytes" Reinhold.(New York (1950).
Prigogine and Defay, "Chemical Thermodynamics" (trans. Everett, Longmans, London (1954)).
Guggenheim, "Mixtures" Oxford, (1952).
2. Markham and Kobe, Chem. Rev., (1941), 28, 519.
3. Seidell, "Solubility", Van Nostrand (1941), Supplement,(1950).
4. Rossini, "Chemical Engineers Handbook", McGraw-Hill (1953),308.
5. Johnson and Shuttleworth, Phil. Mag., (1959), 4, No.44, 957.
Smithells, "Metals Reference Book", Butterworths, London, (1955). Rimmer and Cottrell, Phil. Mag., (1957), 2,1345.

6. Grimes, Smith and Watson, J. Phys. Chem., (1958), 62, 862.

7. Blander, Grimes, Smith and Watson, J. Phys.Chem., (1959), 63, 1164.

8. Gerling, Compt. Rend. Acad. Sci. U.S.S.R. (1940), 27, 22.

9. Protsenko and Bergman, J. Gen. Chem., S.S.S.R. (1950), 20,1365.

10. Bergman and Dergunov, Compt. Rend., Acad. Sci. U.R.S.S. (1941), 31, 754.

11. Uhlig, J. Phys. Chem., (1937), 41, 1215.

12. Shaffer, Grimes and Watson, J. Phys. Chem. (1959), 63, 1999.

13. Dantuma, Z. anorg. allgem. Chem., (1928), 175, 37.

14. Galinker and Korobkov, Doklady Akad. Nauk. S.S.S.R. (1951) 81, 407.

15. Bretsznajder, Roczniki Chem., (1930), 10, 729.

16. Fasting and Haraldsen, Tids. Kjemi, Bergvesen Met. (1945), 5, 29.

17. Laitenen, Ferguson and Osteryoung, Abst. No.146, 107th meeting The Electrochemical Society Cincinnati, Ohio, (1955). Laitenen, Ferguson and Osteryoung, J. Electrochem. Soc. (1957), 104, 516.

18. Keenan, J. Phys. Chem., (1957), 61, 780.

19. Burkhard and Corbett, J.A.C.S. (1957), 79, 6361.

20. Duke and Doan, Iowa State College J. of Sci., (1958), 32, 451.

21. Kordes, Borgman and Vogel, Z. Elektrochem., (1951), 55, 600. Kordes, Ziegler and Proeger, ibid. (1954), 58, 168.

Darmois and Rolin, Compt. rend. (1949), 229, 933.

Doucet, Le Duc and Pannetier, Compt. rend., (1953), 236, 1018.

22. Van Artsdalen, J. Tenn. Acad. Sci., (1954), 29, 122; J. Phys. Chem. (1956), 60, 172.

23. Goodwin and Kalmus, Phys. Rev., (1909), 28, 1.

24. Prytz An. Physik., (1895), 54, 130. Garelli and Falciola, Atti. Accad. Lincei, (1904), 13, 110; Gazz. chim.ital. (1904), 34, 11. Garelli, Att.Accad.Lincei (1925), 2, 120. Garelli and Monath, Atti Accad. Sci. Torino (1926), 61, 18; (1927), 62, 142.

25. Tempkin, Acta physicochim, U.R.R.S. (1945), 20, 411.

26. Forland, O.N.R. Tech. Report 69, Pennsylvania State Univ., (1956).

Flood, Forland and Grjotheim, Z.anorg.allgem. Chem. (1954), 276, 19.

27. Blander, J. Phys. Chem. (1959), 63, 1262.

28. Rowlinson, "Liquids and Liquid Mixtures", Butterworths (1959).

29. Flory, J. Chem. Phys. (1942), 10, 51.

30. Goodwin and Mailey, Phys. Rev., (1907), 25, 469.

31. Hildebrand and Salstrom, J.A.C.S. (1932), 54, 4257.

32. Salstrom, J.A.C.S. (1932), 54, 2653.

33. Harrap and Heymann, Trans.Far.Soc. (1955), 51, 268, 259.

34. Bloom, Knaggs, Molloy and Welch, Trans. Far. Soc. (1953), 49, 1458.

35. Yaffe and Van Artsdalen, J. Phys. Chem. (1955), 59, 118.

36. Markova and Shumina, Dokl, Nauk., S.S.S.R. (1956), 110, No.3, 411.

37. Harrap and Heymann, Chem. Rev., (1951), 48, 45.

38. Bockris, "Modern Aspects of Electrochemistry" No.2 Butterworths (1959), p. 160.

39. Goodwin and Mailey, Phys. Rev. (1908), 26, 28.

40. Eide, Thesis of the Norwegian Inst. of Tech., Trondheim, Norway (1952).

41. Poole, J.Am.Cer.Soc. (1949), 32, 230.

42. Karapachev and Stromberg, Z. anorg. Chem. (1935), 222, 78.

43. Bokhovkin, J. Gen. Chem., (1949), 19, 805.

44. Bergman and Chagin, Bull. Acad. Sci. U.S.S.R. Div.Chem.Sci. (1940), 5, 728.

45. Zuzhanaya and Vereshchetina, Trans. 2nd All-Union Conf. Theoret Appl. Electrochem., Acad. Sci. Ukrainian S.S.R. Press (1949).

46. Tarasova, J. Phys. Chem. U.S.S.R. (1947), 21, No.7, 826.

47. Belyaev and Mironov, Proc. Acad. Sci. U.S.S.R. (1950), 73, 1217; J. Gen.Chem. (1952), 22, 1734.

48. Protsenko and Popovskaya, J. Phys. Chem. U.S.S.R. (1954), 28, 299; J. Gen. Chem., U.S.S.R. (1954), 24, 207.

49. Consultants Bureau Inc., Chem. Coll. No.1 "Soviet Research in Fused Salts (1949 - 1955)".

50. Protsenko and Bergman, idem.

51. Plyushchev, Markina and Shklover, Dokl. Akad. Nauk., S.S.S.R. (1956), 108, 645.

52. Rostkovsky, J.R. Chem. Ges. (1930), 62, 2055.

53. Urnes, ONR. Tech. Rep. 73, Contract N6 onr 269, Task order 8, NR 032-264. (Pennsylvania State Univ. (1957)).

54. Bergman, Doklady (1939), 38, 304.

55. Stevels, Philips Techn. Rundschau (1952), 13, 35.

56. Dietzel, Congresso Internazionale Del Vetro Venezia (1953), 219.

57. Weyl, "A new approach to the Chemistry of the Solid State and its application to the Problems in the Field of Silicate Industries" quoted in ref. 53.

CHAPTER 5.

GENERAL PROPERTIES OF ALKALI NITRATES, NITRITES AND POTASSIUM DICHROMATE.

The general properties of the alkali nitrates have been described in a number of reviews[1].

5.1 Temperature of Fusion.

The alkali nitrates and nitrites investigated in the present work are typified by a definite ionic character which is accompanied by low melting point. It is found that this property of low temperature of fusion is common among salts with non spherical univalent anions and some alkali salts of non spherical divalent anions. Table 5.1 shows the low melting points of some of these salts and compares them with those of the alkali halides which have more spherical anions.

TABLE 5.1

Salt	M.P. ^{o}C	References
$LiNO_3$	251.4	Lehrmann and Breslow [3] (1938).
	252	Briscoe, Evans and Robinson [4] (1932)
$NaNO_3$	305.5	Lehrmann and Breslow [2] (1938)
	306.8	Stern [5] (1909).
	310	Kelley [6] (1934) and Nat.Bur.Stand[2](1952)

/Contd.

TABLE 5.1 (Continued...)

Salt	M.P.°C	References
KNO_3	337	Nat. Bur. Stand. Circ.[2] (1952).
	333	Briscoe and Madgin [7] (1923)
$RbNO_3$	310	Nat. Bur. Stand. Circ.[1] (1952).
$CsNO_3$	417	" " " "
	405.5	Mustajoki [8] (1957).
$NaNO_2$	271	Int.Crit. Tables 9.
	283	Bloom, Knaggs, Molloy and Welch[10] (1953)
KNO_2	441	Bureau (1935) [11a] and Dode [11b] (1936).
	424	Meneghini [12] (1912).
	387	Ettinger [13] (1932)
	419	Lengyel [14] (1933).
$K_2Cr_2O_7$	398	Nat. Bur. Stand Circ. [2] (1952).
LiCl	610	" " " " "
NaCl	808	" " " " "
NaBr	750	" " " " "
KCl	772	" " " " "
KBr	735	" " " " "
CsCl	645	" " " " "

5.2 Crystallographic Properties.

5.2:1 Lithium Nitrate

Lithium nitrate is rhombohedral (trigonal system) and has

been suggested by Retgers [15] (1889) to be isomorphous with $NaNO_3$. The unit cell contains two molecules. Crystallographic evidence does not show a transition point [16], though evidence of a solid-solid transition at 173°C has been found by Rhodes and Ubbelohde (1959) [16a], using an ultra violet spectroscopic technique

5.2:2 Sodium Nitrate.

Sodium nitrate is ismorphous with certain carbonates and borates and is described by Wyckoff [17] as a NaCl like arrangement of Na^+ and NO_3^- distorted by the spatial requirements of the complex NO_3^- anion. The symmetry is rhombohedral (trigonal system) as for $LiNO_3$. The NO_3 group is planar with the N atom the centre of an equilateral triangle of O atoms. The N - O distance [18,19,20] is 1.22 Å and the length of the unit rhombohedron 6.065 Å. The unit cell contains 2 $NaNO_3$ molecules. The crystals show a pronounced rhombohedral cleavage.

$NaNO_3$ has a second order transition [21,22,23]. Siegel [24] (1949) has suggested that above 275°C each disordered NO_3^- has an aragonite rather than a calcite co-ordination with neighbouring sodium atoms, although the packing scheme remains the same. According to Tahvonen [19] (1947) and Ketelaar and Strijk [20] (1945) above 275°C the O atoms are rotating around the trigonal axis. Tahvonen has further suggested that this rotation is accompanied by oscillations in the direction of the threefold axis (amplitude 0.2 - 0.3 Å). Siegels x-ray data suggests that free rotation of

NO_3^- is not possible, as do the infra red spectral studies of Hexter [25] (1958).

Crystallographic methods have been used to measure the thermal expansion of this salt. Saini and Mercier [26] (1934) found that the coefficient of expansion remained constant up to 200°C whereas Austin and Pierce [27] (1933), using interferometry, found it began to change at 150°C.

5.2:3 Potassium Nitrate.

The stable low temperature modification of KNO_3 is orthorhombic [28]. From the results of Edwards [28] K - N distance is 3.32 Å and K - O is 2.85 Å. The O - O distance for oxygens in the same group is 2.10 Å and for oxygens not in the same group 3.45 - 3.88 Å.

A transition occurs at 128°C. Tahvonen [18] reports this structure to be rhombohedral isotypic with the high temperature modification of $NaNO_3$. The N - O distance is 1.22 Å. The O atoms rotate in a plane perpendicular to the threefold axis and oscillate in the direction of that axis with an amplitude of 0.4 Å. In one rotation there are three oscillations caused by the position of the K atoms which prevent free rotation. A third metastable modification has been reported [29] to occur on cooling the high temperature modification. The dependence of the course of this transition on the moisture present has been pointed out by Kennedy, Ubbelohde and Woodward [30] (1953).

The thermal expansion data have been given by Lonappan[31] (1955) and Fischmeister (1956).

5.2:4 Rubidium Nitrate.

$RbNO_3$ was originally thought to have a distorted NaCl grouping of ions, and that the diffraction data were approximately those of a tetramolecular rhombohedron [32] having a = 7.36 and α = 109 28'. It is now known, however, to be a large orthorhombic unit containing 18 molecules. The crystal is pseudo hexagonal containing 9 molecules in the unit. Above a transition point the structure of $CsNO_3$ has been reported as cubic having a = 4.37 Å. More recent study [33] has suggested that the unit cell is larger having a = 8.74 Å and containing 8 molecules. The temperature of this transition has been given by Korhonen [38] as 190°C. Above 220°C a rhombohedral modification with structure similar to the high pressure modification of KNO_3 has been reported [17]. In such a case the NaCl and CsCl structures merge imperceptibly into one another. The high pressure form of KNO_3 is a bimolecular rhombohedral a = 4.365, α = 76°56'. Oxygen displaces layers of NO_3^- from the layers midway between the layers of K atoms [17]

5.2:5 Caesium Nitrate.

The hexagonal unit which has been ascribed to $CsNO_3$ contains 9 molecules. Above the transition temperature[8] of

151.5°C it appears to have a cubic modification. Finbak and Hassel [32] (1936, 1937), have given its dimensions as a = 4.49 Å. However, a larger cubic modification containing 8 molecules has been assigned to this salt by Korhonen [34] (1953) who has given as its dimensions a = 8.980 Å. A high temperature rhombohedral modification [9] similar to that of $RbNO_3$ has been reported. Ferrari Sabatini and Orioli [35] (1957) noted both cubic and trigonal structures. It has been suggested that the NO_3 group rotates at higher temperatures [9]. This has been supported by evidence from the specific heat measurements of Sato [36] (1954). He places the temperature of the onset of rotation as being between 143 and 161°C.

5.2:6 Thallium Nitrate.

Thallium Nitrate is reported by Rivoir and Abbad [37] (1943) to have an orthorhombic structure. The interatomic distances are given as N - O = 1.21 Å, O - O = 2.10 Å in the nitrate group and O - O = 2.64 Å, Tl - O = (2.75 - 2.83) Å between groups. The structure is built up from Tl^+ and NO_3^- ions arranged in a distorted CsCl structure with four different orientations of the NO_3^-. Above 142°C, NO_3^- ions rotate and a cubic CsCl structure is formed.[38] Ferrari, Cavalco and Tonelli [39] (1950) report the structure of $TlNO_3$ as rhombic. The onset of free rotation of NO_3^- in $TlNO_3$ in the temperature ranges 0-72°C has been noted by Sato.[36] Solid-solid transformations take place at 75°C and 145°C. At 170°C the

the structure is cubic [32].

5.2;7 Sodium Nitrite.

The alkali nitrites have NaCl like structures whose low symmetry is dictated by the spatial requirements of their V-shaped NO_2^- ions. $NaNO_2$ is orthorhombic with 2 molecules. The N - O distance is 1.13 Å the angle of the O - N - O = 132°. Eacn Na atom has about it four oxygen atoms at a distance of 2.46 Å, and two more 2.54 Å away. Between 160 - 166 °C there is a gradual loss in the piezoelectric property exhibited by $NaNO_2$ at low temperatures. This slow transition corresponds to an increase in symmetry but not to a radical alteration in its crystal arrangement. At 205°C a change in structure corresponding to the development of oscillations along the b axis occurs. This leads to an NO_2^- with N - O distance 1.31 Å and O - N - O angle of 114°, O - O distance is 2.22 Å, Na - O 2.54 Å (twice) and 2.48 Å (four times).

5.2:8 Potassium Nitrite.

KNO_2 is monoclinic [42] but it atomic distribution resembles $NaNO_2$. Bimolecular like $NaNO_2$, it has the shortest metallic contacts with oxygen; each K^+ is surrounded by four oxygen atoms of four different NO_2 groups (K-O = 2.75 Å) and two more oxygen atoms belonging to the same group (K - O distance is 3.01 Å). A transition has been reported at - 13°C by Ray and Ogg [43] (1956) who have suggested an order disorder of the NO_2^- ions.

5.2:9 Potassium Dichromate.

Two forms of $K_2Cr_2O_7$ exist $K_2Cr_2O_7\alpha$ and $K_2Cr_2O_7/\beta$. $K_2Cr_2O_7\alpha$ is triclinic with two CrO_4 ions forming tetrahedra having a common corner. Cr – O separations are 1.55, 1.57, 1.78, 1.91 Å for four O atoms. The Cr - 40' - Cr angle is 115°. $K_2Cr_2O_7/\beta$ is triclinic.

The lattice dimensions of these salts are collected in Table 5.2.

5.2:10. The Structure of Molten Nitrates.

Kunitomi [44] (1944, 1949) has conducted x-ray studies on $LiNO_3$, $NaNO_3$ and KNO_3, showing for $NaNO_3$ that each ion does not move at random but that the evidence of ordering in the melt near the freezing point of 310°C exists, and is still present at 380°C. $LiNO_3$ and KNO_3 are similar to $NaNO_3$, and equimolar mixtures of $LiNO_3$ and KNO_3 give x-ray patterns almost identical with the pure salts. The average spaces for $NaNO_3$ derived from Bragg's Law are 3.25 kX (318°C), 3.27 kX (344°C), 3.28 kX (360°C) cf.d (211) = 3.101 kX (280°C) by Kracek [22] and 3.033 kX (25°C) Wyckoff [17]. (kX = Å).

TABLE 5.2

Salt	Crystal form T°C	a	b	c	α	β	γ
$LiNO_3$	Hexagonal 20°C	4.692	-	15.206	-	-	-
	Rhombohedral "	5.74	-	-	48°3'	-	-

/Continued..

TABLE 5.2 (Continued...)

Salt	Crystal form	T°C	a	b	c			
	Prim.Rhombo hedral	20°C	3.71	-	-	78°27'	-	-
$NaNO_3$ II	Hexagonal	18°C	5.060	-	16.784	-	-	-
	Rhombohedral	"	6.313	-	-	47°15'	-	-
	Prim.Rhombo-hedral	"	4.04	-	-	77°27'	-	-
$NaNO_3$ I	Hexagonal	275°C	5.075	-	17.52	-	-	-
	Rhombohedral	"	6.535	-	-	45°42'	-	-
	Prim.Rhombo-hedral	"	4.134	-	-	75°40'	-	-
KNO_3 II	Orthorhombic	Low temp.	5.43	9.17	6.42	-	-	-
KNO_3 I	Hexagonal	128°C	5.423	-	19.277	-	-	-
	Rhombohedral	"	7.148	-	-	44°35'	-	-
	Prim.Rhombo-hedral	"	4.468	-	-	74°22'	-	-
$RbNO_3$	Orthorhombic	Low Temp.	18.08	10.45	7.38	-	-	-
	Cubic	190	8.74	-	-	-	-	-
	Hexagonal	250°C	5.48	-	21.41	-	-	-
	Rhombohedral	"	7.80	-	-	41°7'	-	-
	Prim.Rhombo-hedral		4.77	-	-	70°10'	-	-

/Continued..

TABLE 5.2 (Continued...)

Salt	Crystal form	T°C	a	b	c			
$CsNO_3$	Hexagonal	Low Temp.	10.74	-	7.68	-	-	-
	Cubic		4.46	-	-	-	-	-
	Cubic	161°C	8.98	-	-	-	-	-
$TlNO_3$	Orthorhombic	Low	6.18	12.29	3.99	-	-	-
	Rhombic		6.25	12.46	7.96	-	-	-
	Cubic	High	4.313	-	-	-	-	-
$NaNO_2$	Orthorhombic	25°	3.55	5.56	5.38	-	-	-
	"	205°	3.69	5.68	5.33	-	-	-
KNO_2	Monoclinic		4.45	4.99	7.31	-	114°50'	-
$K_2Cr_2O_7$	Triclinic		7.521	7.40	13.42	82°0'	9°13'	90°51'
	Monoclinic	241.6	12.99	7.36	7.48	-	91°55'	-

5.3 Thermal Stability of Alkali Nitrates, Nitrites and Dichromates.

5.3:1 Chemical Decomposition of Nitrates.

There is substantial agreement that thermal decomposition of nitrates may be represented by one of the following equations,

depending on temperature:

$$2\ MNO_3 \rightleftharpoons 2\ MNO_2 + O_2 \quad \ldots\ldots\ldots (5.1)$$

$$2\ MNO_3 \rightleftharpoons M_2O_2 + 2NO_2 \quad \ldots\ldots\ldots (5.2)$$

$$4\ MNO_3 \rightleftharpoons 2M_2O + 4NO_2 + O_2 \quad \ldots\ldots (5.3)$$

$$2\ MNO_3 \rightleftharpoons 2M + 2NO_2 + O_2 \quad \ldots\ldots\ldots (5.4)$$

Equations 5.1, 5.2, and 5.3 apply to the alkali nitrates [45-53]. In the decomposition of $NaNO_3$ according to 5.3 a little peroxide is formed; large amounts were obtained only when the salt is heated rapidly at a high temperature.[51] In the case of potassium the peroxide yield is greater.

$AgNO_3$ decomposes in accordance with reaction 5.4, but reaction 5.1 has been postulated as an intermediate.

The starting temperature [44] of the reaction 5.1 has been given as 255°C for $NaNO_3$ and 286°C for KNO_3, for reaction 5.2 as 750°C and 850°C for $NaNO_3$ and KNO_3 respectively and for reaction 5.3 as greater than 800°C for $NaNO_3$ and ca. 1000°C for KNO_3.

The thermal decomposition of $TlNO_3$ is similar to that of the alkali nitrates. It has been reported to give oxygen nitrogen, nitrogen oxides and thallous oxides as its decomposition products.

5.3:2 <u>The Thermal Decomposition of Nitrites</u>.

Early workers on the decomposition of KNO_2 report onset of decomposition at 350°C [54,55]. The equation for the reaction

has been postulated as [56]

$$3KNO_2 \rightarrow K_2O + KNO_3 + 2\,NO$$

or $$4KNO_2 \rightarrow 2K_2O_3 + NO + N$$

It would seem, however, that the temperature of onset of decomposition as suggested above is an incorrect [57] one especially when compared with the more recent studies on $NaNO_2$ where the temperature of onset of decomposition is given[52] as 550°C. It can be noted also that the melting point of 297°C given with the above investigations is well below the more generally accepted value of $>$ 400°C. (see table 5.1). It may well be that the above equations are indicative not of the decomposition of KNO_2 but of KNO_3 present as an impurity. The decomposition of $NaNO_2$ in the absence of oxygen follows the equation [52]

$$2NaNO_2 \rightarrow Na_2O + 2NO + \tfrac{1}{2}O_2$$

It would seem likely that the decomposition of KNO_2 follows a similar scheme.

5.3:3 Thermal Decomposition of $K_2Cr_2O_7$.

The thermal decomposition of $K_2Cr_2O_7$ has been said to take place at 500°C according to [58, 59, 60].

$$4K_2Cr_2O_7 \rightleftharpoons 3O_2 + 2\,(Cr_2O_3 \,?\, K_2CrO_4)$$

5.4 Heats of Formation.

The heats of formation for the alkali nitrates at 25°C are

approximately the same. Table 5.3 compares the heats of formation of the alkali nitrates and nitrites and potassium dichromate.

TABLE 5.3

Salt	Heat of formation Kcal/mole at 25°C	Reference
$LiNO_3$	115.279	Nat. Bur. Stand.[2]
$NaNO_3$	111.54	" " "
KNO_3	117.76	" " "
$TlNO_3$	58.01	" " "
$NaNO_2$	85.9	" " "
KNO_2	88.5	" " "
$Na_2Cr_2O_7$	463.4	" " "
K_2Cr_2O7	485.9	" " "
$CsNO_3$ II	118.11	" " "

5.5 Heats of Transition.

Heats of solid-solid transition are given in Table 5.4.

TABLE 5.4

Salt	Form	Temp°C	Heat Kcal/mole	Entropy cal/deg. mole
$LiNO_3$		None known.		
[a] $NaNO_3$	II I	275	0.944	1.26

/Continued...

TABLE 5.4 (Continued...)

Salt	Form	Temp°C	Heat Kcal/mole	Entropy cal/deg mole
KNO_3	IV → III	21.3	- 0.512	- 1.74
	IV → II	21.3	- 0.381	- 1.29
	III → II	21.3	0.131	0.445 ≠
	III → II	128.02	- 0.502	- 1.25 ≠
	III → I	128.02	0.558	1.39
	II → I	128.02	1.060	2.64 ≠
	II → I	127.7	1.3	3.2 ≠
a) $CsNO_3$	II → I	151.5	0.893	2.10
$TlNO_3$	III → II	61.0	0.24	0.72
	II → I	143.5	0.76	1.82
$NaNO_2$	II → I	162°	-	-
b) KNO_2	II → I	- 13	1.2	-
$K_2Cr_2O_7$	II → I	241.6	-	-

These values are mainly taken from the National Bureau of Standards[2] Circular 500.

a) = Mustajoki [8] (1957), b) = Ray and Ogg [61] (1956).

≠ The data marked appear to be in conflict.

5.6 Heats of Fusion.

Table 5.5 lists some values for the heats of fusion togethe
r

with the entropies of fusion.

TABLE 5.5

Salt	Temp °C	ΔH_f Kcal/mole	ΔS_f cal/m cal/deg.mole	Reference
$LiNO_3$	250	6.10	11.66	Goodwin & Kalmus[7] (1909)
	250	6.06	11.59	Kelley [6] (1934rev.)
$NaNO_3$	310	3.76	6.45	Kelley [6]
	310.5	5.355	9.18	Person[63](1847-9)
	308	3.69	6.63	Goodwin & Kalmus[62]
	306.2	3.49	6.03	Mustajoki[8](1957)
	310	3.8	6.5	Nat.Bur.Stand [2] (1950)
KNO_3	333	2.57	4.25	Goodwin & Kalmus[62]
	334.5	4.79	7.88	Stern [64] (1909)
	339.0	4.79	7.82	Person[63]
	337	2.8	4.6	Nat.Bur.Stand [2]
$CsNO_3$	417	3.25	4.71	Nat.Bur.Stand [2]
	405.5	3.37	4.97	Mustajoki [8]
$TlNO_3$	206.5	2.29	4.77	Nat.Bur.Stand [2]
$NaNO_2$	281	-	-	
KNO_2	440	-	-	Nat.Bur.Stand [2]
$K_2Cr_2O_7$	398	8.5	13	Nat.Bur.Stand [2]

5.7 The Viscosity Parameters of the Alkali Nitrates and Nitrites.

The viscosities of molten alkali nitrates have been studied by several workers. Fig. 5.1 shows the log η against $1/T$ plots for the alkali nitrates. A change in the slope is noticeable in the plots of $LiNO_3$ and $NaNO_3$. From a consideration of the Arrhenius expression $\eta = \eta_0 \exp E_\eta / RT$ it can be seen that this is equivalent to a decrease in the energy of activation for the process near the freezing point. Table 5.6 lists values for E_η and η_0 .

TABLE 5.6

Activation Energy for Viscous Flow in Nitrate Melts.

Melt	M.P°C	Well above F.P.			Just above F.P.			
		Temp. range°C	E_η Kcal/mole	$\eta_0 \times 10^4$	Temp. range°C	E_η Kcal/mole	$\eta_0 \times 10^4$	Ref.
$LiNO_3$	250	259-344	4.92	5.30	259-344	4.92	5.30	65
		354-429	6.91	1.30	260-354	4.23	11.90	66
$NaNO_3$	306	398-418	3.84	10.96	308-328	3.22	17.96	67
		337-495	3.85	10.60	337-495	3.85	10.60	65
		316-398	3.95	9.87	316-398	3.95	9.87	66
KNO_3	333	393-413	4.48	7.49	333-353	3.66	14.12	67
		347-506	4.41	7.73	347-506	4.41	7.73	65
		348-542	4.41	7.73	348-542	4.41	7.73	66

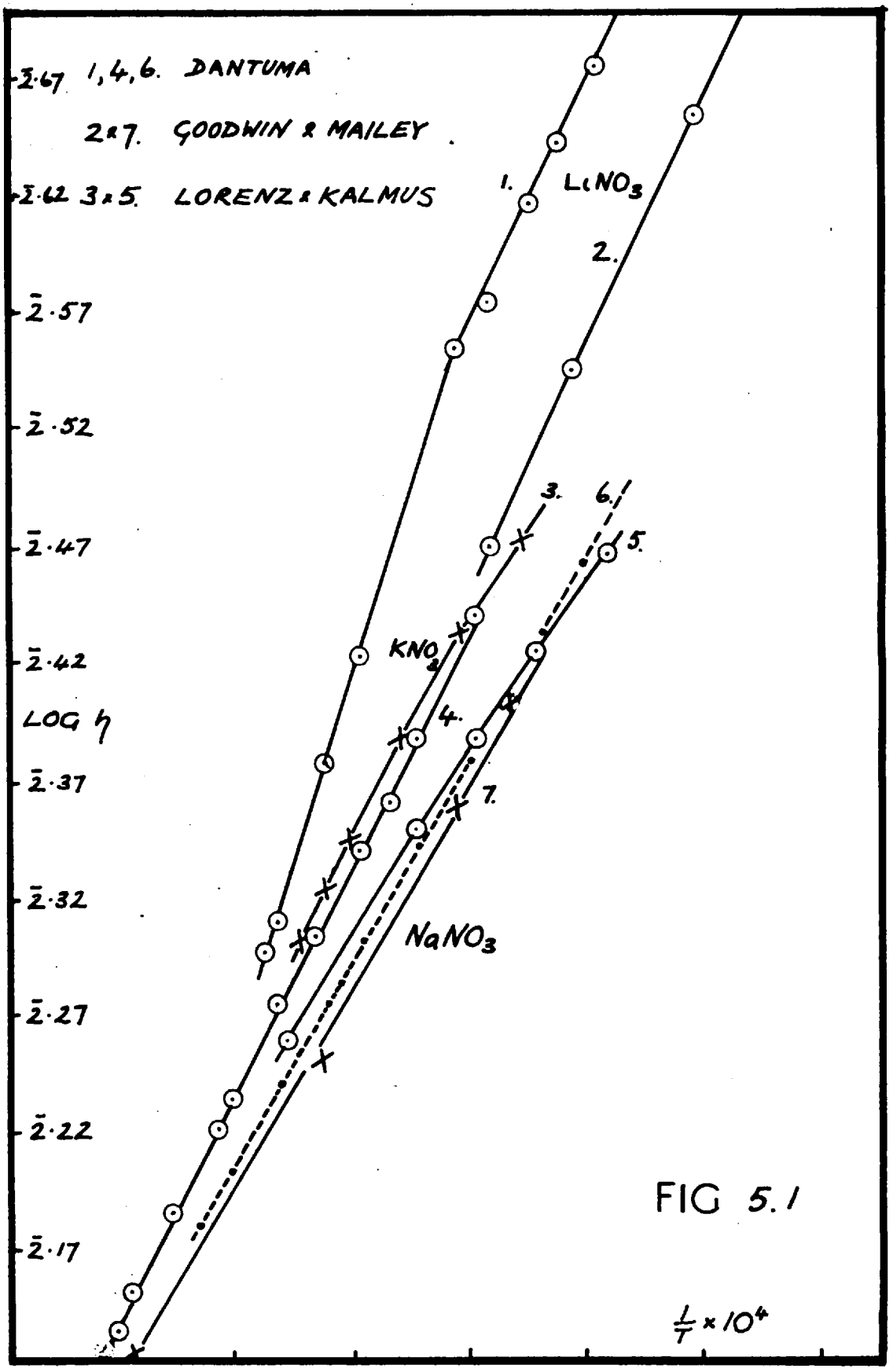
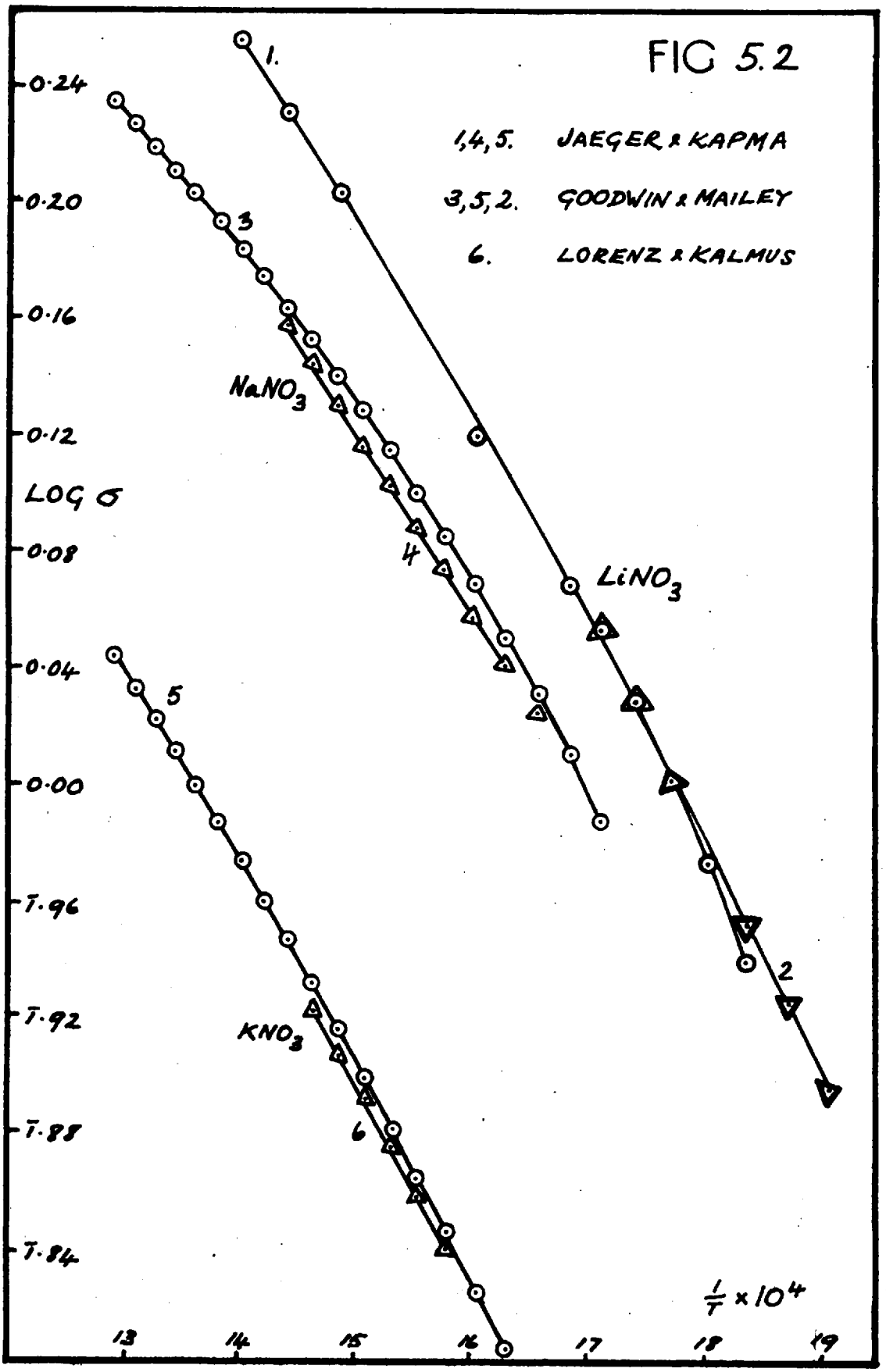

1,4,6. DANTUMA
2&7. GOODWIN & MAILEY
3&5. LORENZ & KALMUS
1. LiNO3
2.
3.
6.
5.
KNO3
4.
7.
NaNO3
LOG η
$\bar{2}\cdot67$
$\bar{2}\cdot62$
$\bar{2}\cdot57$
$\bar{2}\cdot52$
$\bar{2}\cdot47$
$\bar{2}\cdot42$
$\bar{2}\cdot37$
$\bar{2}\cdot32$
$\bar{2}\cdot27$
$\bar{2}\cdot22$
$\bar{2}\cdot17$
$\frac{1}{T}\times10^4$

FIG 5.1


FIG 5.2
1,4,5. JAEGER & KAPMA
3,5,2. GOODWIN & MAILEY
6. LORENZ & KALMUS
LOG σ
0·24
0·20
0·16
0·12
0·08
0·04
0·00
T·96
T·92
T·88
T·84
NaNO3
KNO3
LiNO3
1
2
3
4
5
6
1/T × 10^4
13
14
15
16
17
18
19

5.8 The Electrochemistry of Alkali Nitrates and Nitrites.

Table 5.7 shows the migration parameters for the conductance process in some alkali nitrates. Fig.5.2 gives some sample plots of log σ against $1/_T$. In some cases there appears to be a slight increase in the slope towards the freezing point indicating a slight temperature dependence for the energy of activation.

TABLE 5.7

Electrical Transport Parameters for Alkali Nitrates.

Salt	F.P. °C	E_σ kcal/mole	σ^-	ref
$LiNO_3$	250	4.49	55.4	68
		3.59	24.8	65
$NaNO_3$	306	2.76	10.6	68
		3.42	18.5	65
KNO_3	333	3.49	11.2	65
		3.32	9.6	67
$CsNO_3$	414	2.7	1.82	68
$RbNO_3$	310	3.42	2.09	68

5.9 The Object and Scope of this Research.

The object of this research is

a) to elucidate the structure of the melts of low melting

salts with non-spherical polyatomic anions and to examine the possibility of association in the melt particularly in the freezing point region.

b) to determine, in view of the many 'hole' theories of ionic liquid structure, the character of positional 'holes' and their effect on the physico-chemical properties of pure molten alkali nitrates and binary mixtures of the univaleht alkali cations and divalent alkaline earth cations.

Earlier investigations of the viscosity and electrical conductivity have suggested the occurrence of association in salt melts and have pointed to a relationship between the energies of the two ~~for~~ transport processes. To determine if this association and the connection between the two energy terms can be made a general rule, the measurement of viscosity and electrical conductivity has been extended to new types of low melting salts namely $NaNO_2$ KNO_2 $TlNO_3$ and $K_2Cr_2O_7$. The electrical conductivity of solid $NaNO_2$, KNO_2 and $K_2Cr_2O_7$ have also been measured in order to assess the extent of positional randomisation before the melting point in these salts.

Examination of the role of positional 'holes' in alkali nitrates has been made by studies of the solubility of H_2O in the pure dry alkali nitrates and binary mixtures of alkaline earth nitrates and alkali nitrates in parallel with studies of

electrical conductivity and molar volumes of similar systems. By careful selection of the divalent cation and divalent anion additives, systems can be obtained analogous to those in the solid which show the well known 'Wagner effect' in electrical conductivity. This type of attempt to create additional holes in the melts also makes it possible to study the character of these liquids as solvents and to draw some tentative conclusions on dipole-ion interaction.

References.

1. Whittaker and Lundstrom, U.S.Dept.Agr., Miscellaneous Publ., (1934), 192. Leonhardt and Borchert, Naturwiss (1936), 24,417. Baranov, Lenin Acad.Agr.Sci.Gedroits Inst. Fertilizers and Soil, Sci.Trans.Min.Fertilizers (1935), 3,7. Dabrowska, Uprawa Roslin i Nawozence (1938), 8, 283. Waeser, Chem. Fabrik (1939), 393. Manning, Mineral Ind. (1940), 49, 557. Waeser, Chem.Tech. (1943), 16, 179.

2. Nat. Bur. Stand., Circular 500 (1952).

3. Lehrmann and Breslow, J.A.C.S. (1938), 60, 873.

4. Briscoe, Evans and Robinson, J. Chem. Soc. (1932), 1100.

5. Stern, Z. Phys. Chem. (1909), 65, 667.

6. Kelley, U.S. Dept. of Comm.Bull; Bur.Mines, Washington (1934), 371.

7. Briscoe and Madgin, J. Chem. Soc. (1923), 123, 1608, 2914.

8. Mustajoki, Ann.Acad. Sci. Fennicae A.VI (1957), No.5; No.7.

9. International Critical Tables.

10. Bloom, Knaggs, Molloy and Welch, Trans. Far. Soc. (1953), 49, 1458.

11a. Bureau, Compt. Rend. (1935), 200,395.

b. Dodé, Compt. Rend., (1936), 203, 366.

12. Meneghini, Gazz. chim. ital, (1912), 42 II, 473.
Amadori, Atti. Istit. Veneto (1912/1913), 72 II, 907.

13. Ettinger, Z. anorg. Chem., (1932), 206, 260.

14. Lengyel, Naturwiss (1933), 21, 848.

15. Retgers, Z. Phys. Chem., (1889), 4, 617.

16. Perman and Harrison, J. Chem. Soc. (1924), 125, 709.
Campbell, J.A.C.S. (1942), 64, 2680.

16a. Rhodes and Ubbelohde, Proc. Roy. Soc. (1959), A251, 156.

17. Wyckoff, "Crystal Structures", Interscience, New York, (1957).

18. Elliot, J.A.C.S., (1932), 59, 1380.

19. Tahvonen, Ann.Acad. Sci. Fennicae Series A I, Mathematica Physica (1947), 42, 43, 3.

20. Ketelaar and Strijk, Rec. Trav. Chim. (1945), 64, 174.

21. Palkin, Dokl. Akad. Nauk, S.S.S.R., (1949), 66, 71, 651.

22. Kracek, J.A.C.S., (1931), 53, 2609, 1183.
Kracek, Posnjak and Hendricks, J.A.C.S., (1931), 53,3339.

23. Kornfel'd and Chubinov, J.Expt.Theor. Phys. U.S.S.R., (1957), 33, 33.

Dzialoshinskii and Lifshitz, J. Exptl. Theor. Phys. (1957), 33,299. Miekk - Oja, Ann. Acad. Sci. Fennicae (1941), A I, No.7.

24. Siegel, J. Chem. Phys. (1949), 17, 1146.
25. Hexter, Spectrochimica Acta., (1958), 10,291.
26. Saini and Mercier, Helv. Phys. Acta., (1934), 7, 267.
27. Austin and Pierce, J.A.C.S., (1933), 55, 661.
28. Edwards, Z. Krist., (1931), 80, 154.
29. Kracek, J. Phys. Chem., (1930), 34, 225.
30. Kennedy, Ubbelohde and Woodward, Proc.Roy.Soc., (1953), A219, 303.
31. Lonappan, Proc. Ind. Acad. Sci. (1955), A41., 239.
Fischmeister, J. Nucl. Inorg. Chem., (1956), 3, 182.
32. Finbak and Hassel, Z. Physik (1936), 5, 460; Z. physikal Chem. (1937), 35 B, 25.
33. Korhonen, Ann. Acad. Sci. Fennicae Ser. A I (1951), No.102.
34. Korhonen, Ann. Acad. Sci. Fennicae AI (1953), No. 150.
35. Ferrari, Sabatini and Orioli, Ricera Sci. (1957), 1557.
36. Shunichi Sato, J. Sci. Research Inst., (1954), 48, 59.
37. Rivoir and Abbad, An. Soc. Esp. Fis. Quim, (1943), 39, 306.
38. Struktur Berichte, 5, 83.
39. Ferrari, Cavalco and Tonelli, Gazz, chim. ital, (1950), 80,199.
40. Strijk and Mac Gillavry, Rec. Trav. Chim., (1943), 62, 705; (1946), 65, 127.

41. Truter, Nature (1951), 168, 344; Act. Cryst. (1954), 7, 73. Carpenter, Acta. Cryst. (1952), 5, 132.

42. Zeigler, Z. Krist. (1936), 94A, 491.

43. Ray and Ogg, J. Phys. Chem., (1956), 60, 1599.

44. Kunitomi, J. Chem. Soc. Japan (1944), 65, 74; (1949), 70, 344.

45. Leschewski and Degenhard, Ber. (1939), B72, 1763.

46. Scobai, Z. phys. Chem., (1903), 44, 319.

47. Leschewski and Degenhard, Chem. Fabrik, (1939), 400.

48. Centnerszwer, Roczniki Chem., (1938), 18, 419.

49. Lux and Frey, Z. anorg. Chem., (1948), 257, 86.

50. Leschewski and Degenhard, Z. anorg. allg.Chem., (1938), 239,17.

51. Leschewski and Degenhard, Ber. Ges., Freunden Tech. Hochschule Berlin (1942), 1, 168.

52. Cases - Casanova, Bul. Soc. Chim. de France, (1959), 429, 435.

53. Butkov, Acta. Physico-chem., U.R.S.S., (1936), 5, 137.

54. Oswald, Ann.Chim., (1914), 40, 9.

55. "Encyclopaedia of Chemical Technology" Interscience (1953), 12, 606.

56. Ray, J. Chem. Soc., (1909), 95, 345.

57. Butkov and Tschassowenny, Acta. Physicochem., U.R.S.S.(1936), 5, 146.

58. Mellor, "Treatise on Inorganic Chemistry".

59. Gentele, K. Vet. Ak. Förh (1851), No.4, 123.

60. Gmelin, "Handbuch der Anorganischen chemie", Verslag Chemie (1937).

61. Ray and Ogg, J. Phys. Chem., (1956), 60, 1599.

62. Goodwin and Kalmus, Phys. Rev., (1909), 28, 1.

63. Person, Bull. Bur. Mines, Washington, (1847), (3) 21, 333; (1848), (3) 24 136, 268; (1849), (3) 27, 252.

64. Stern, Z. phys. Chem., (1909), 65, 667.

65. Goodwin and Mailey, Phys. Rev. (1907), 25, 469; (1908), 26, 28.

66. Dantuma, Z. anorg. Chem., (1928), 175, 1.

67. Lorenz and Kalmus, Z. phys. Chem., (1907), 59, 244.

68. Jaeger and Kapma, Z.anorg. Chem., (1920), 113, 27.

EXPERIMENTAL

CHAPTER 6

PRELIMINARY EXPERIMENTAL TECHNIQUES

6.1 Viscosity and Conductivity.

Studies of viscosity and conductivity were made on $NaNO_3$, $NaNO_2$, KNO_2, $TlNO_3$ and $K_2Cr_2O_7$. An attempt was made to measure the viscosity of $Na_2Cr_2O_7$ but was discontinued due to its instability. Thus no correlation of the measurements on $K_2Cr_2O_7$ could be made with a salt of a similar type.

6.2 Materials.

$NaNO_3$	B.D.H. (Analar)
$NaNO_2$	B.D.H. (Analar)
KNO_2	B.D.H.
$TlNO_3$	B.D.H.
$K_2Cr_2O_7$	B.D.H. (Analar)

Table 6.1 shows the specification of these salts as supplied by the manufacturer.

TABLE 6.1

	KNO_2	$NaNO_3$	$NaNO_2$	$K_2Cr_2O_7$ [a]	$TlNO_3$ [b]
Free Acid	-	0.05 ml N/1%	-	-	-
Free Alkali	-	0.05 ml N/1%	-	-	-
Chloride (Cl)	0.03	0.0005%	0.005%	0.0005	0.005
Sulphate (SO_4)	0.3	0.005%	0.01%	0.01	0.02

/Continued..

TABLE 6.1 (Continued..)

	KNO_2	$NaNO_3$	$NaNO_2$	$K_2Cr_2O_7$ [a]	$TlNO_3$ [b]
Nitrite(NO_2)	-	0.0001%	-	-	-
Iodate (IO_3)	-	0.00005%	-	-	-
Phosphate(PO_4)	-	0.001%	-	-	-
Iron (Fe)	-	0.001%	0.001	-	-
Heavy Metals (Pb)	0.001	0.002%	0.002%	-	-
Magnesium(Mg)	-	0.001%	-	-	-
Potassium (K)	-	0.005%	0.005	-	-
Aluminium (Al)	-	-	-	0.003	-
Calcium (Ca)	-	-	-	0.005	-
Sodium (Na)	-	-	-	0.05	-
Moisture	-	-	-	0.05	-
pH	-	-	-	3.7 - 3.9	-

a) Specification after drying, not less than 99.9%.

b) Assay (ex. Tl) not less than 98%.

6.3 Purification.

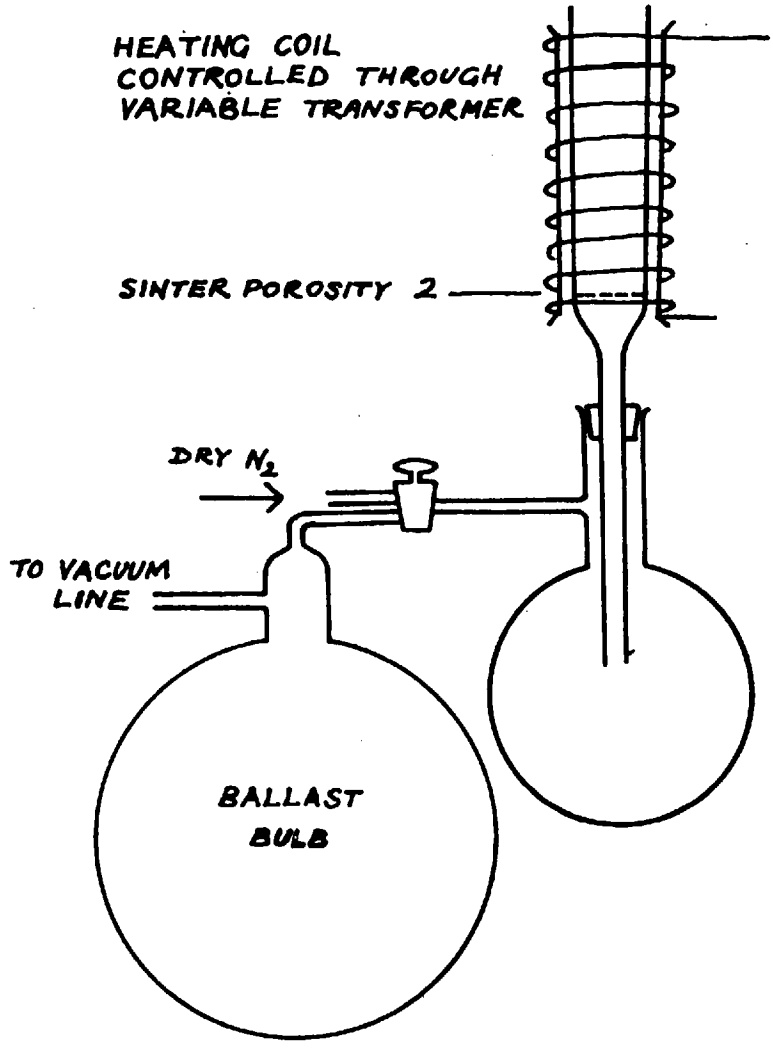
$NaNO_3$, $NaNO_2$ and $K_2Cr_2O_7$ were used in the viscosity and conductivity measurements without further purification. $TlNO_3$ was twice recrystallised from distilled water. KNO_2, because of its very high solubility in water, was recrystallised from the melt. This operation was carried out by heating the salt to just above its melting point (circa 420°C) over a glass sintered disc and

bubbling a slow stream of dry nitrogen up through the sinter disc as the melt slowly cooled. When the melt had begun to crystallise, the nitrogen flow was replaced by a vacuum and the melt drawn rapidly through the sinter disc, leaving the re-crystallised solid. Approximately two thirds of the salt was drawn through. This operation was then repeated with the crystalline fraction. The apparatus is shown in Fig. 6.1. Evidence of the effect of this purification on the properties of KNO_2 is given in Section 8.6.

6.4 Drying.

It is known or suspected that the presence of moisture affects the values of the parameters measured. It is thus necessary that all samples used should be thoroughly dried beforehand. A technique of shock-cooling was employed which was carried out as follows. The samples to be used in the measurements were first oven-dried at 240°C for 4 - 6 days grinding daily until they no longer 'caked'. It was then transferred to a pyrex test tube and the drying continued under vacuum using a wire wound resistance heater controlled by a 'Variac' transformer. In this condition it was heated to a temperature above its solid-transition point but below its melting point. The containing vessel was then immersed in liquid air. The sample was kept under vacuum throughout this process. This procedure was repeated some twelve times. In this way the crystal structure was readily broken up and

FIG. 6.1


HEATING COIL
CONTROLLED THROUGH
VARIABLE TRANSFORMER
SINTER POROSITY 2
DRY N_2
TO VACUUM
LINE
BALLAST
BULB

entrained moisture released.

This shock-cooling operation was based on observations by Kennedy, Ubbelohde and Woodward[1] (1953), who found that water was tenaciously retained in dislocations and co-operative defects in crystals of alkali nitrates. However, when the salt is made to pass through a thermal transformation, the movement of domains and internal boundaries releases this water which can then be quickly pumped off.

6.5 Cleaning of Apparatus.

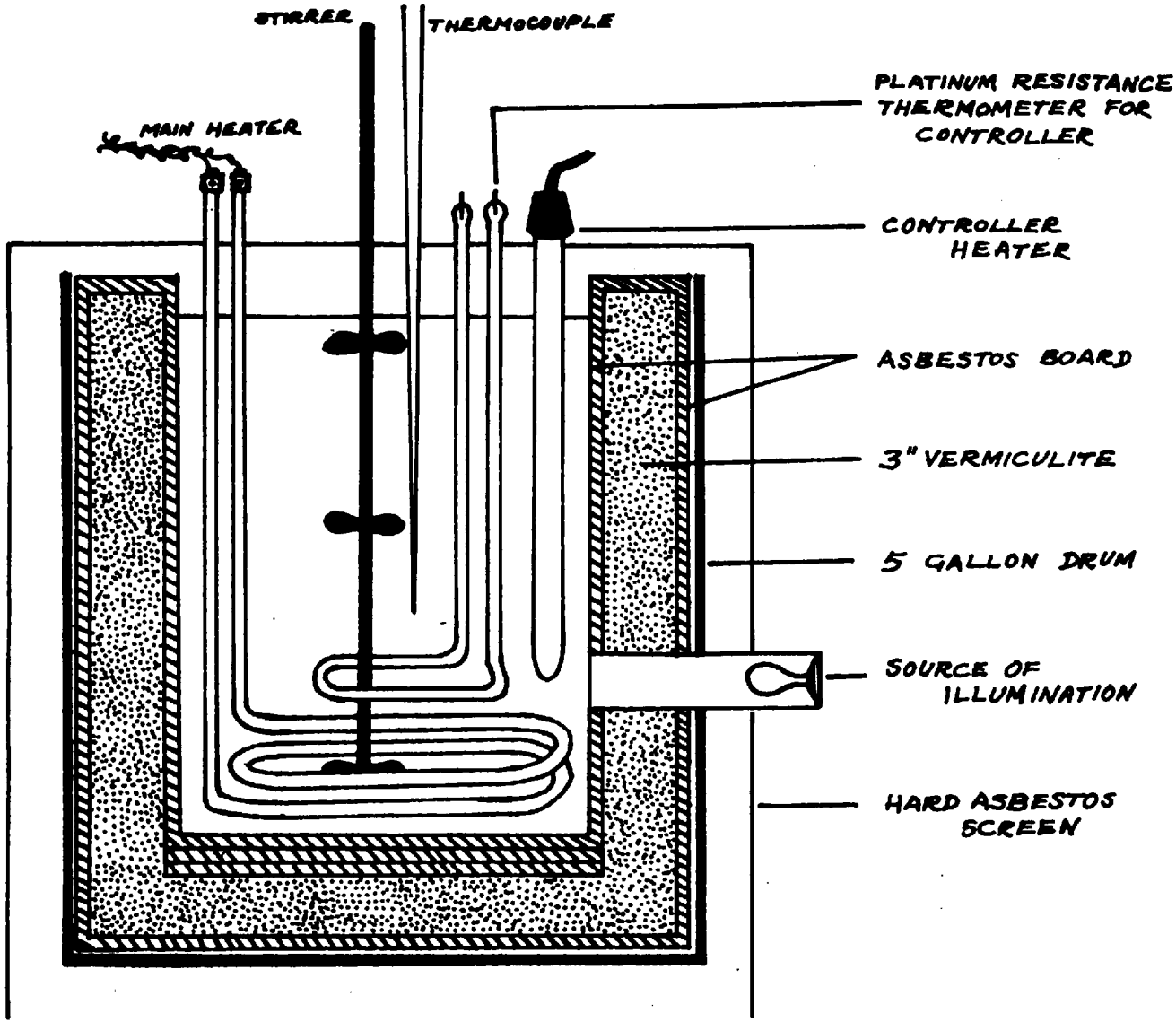
All apparatus was cleaned by hot nitrating mixture, 50% HNO_3: 50% H_2SO_4 rinsed several times with distilled water and dried in air at 200°C.

6.6 Thermostated Bath.

All measurements were carried out in a thermostatically controlled bath (Fig. 6.2). The bath fluid was an eutectic mixture of KNO_3: $NaNO_3$: $NaNO_2$ in the proportions 40:7:53 parts by weight[2]. This allowed a working temperature range of 160°C - 530°C in the present apparatus. The fluid was contained in a 5 litre pyrex beaker surrounded by a layer of asbestos and a 3" layer of vermiculite, held in place by a further layer of asbestos. The whole was further contained in a 5 gallon oil drum. A square screen of hard asbestos surrounded this at a distance of about 3". This was to reduce the effect of radiation from the

FIG. 6.2

THERMOSTATED BATH



bath on surrounding apparatus e.g. the thermocouple ice jacket.

Especially at the higher temperatures this melt gradually etched the pyrex beakers which had eventually to be replaced. Probably the silicon oxide is dissolved out of the pyrex but the nature of the attack has not yet been finally elucidated. The form this attack took is of errosion and embrittlement of the beakers. It has been reported that the bath fluid gradually becomes alkaline[3], but it has not yet been satisfactorily determined whether this was due to decomposition of the melt causing attack on the pyrex or the decomposition products resulting from the reaction.

If necessary it would be possible to attain a higher working temperature by use of an inconel or monel metal container, and quartz apparatus for the measurements.

Heating was by means of a $1\frac{1}{2}$ Kw inconel sheathed heater supplied to our specification by George Bray and Company Limited, Leeds. Inconel is a 79.5 Ni, 13 Cr, 6.5 Fe, 0.08C, 0.2 Cu, 0.25 Mn alloy. This showed no sign of attack after two years continual service in the melt at temperatures often above 400°C and seldom below 250°C. This heater was controlled by a 'Variac' 8 amp. variable transformer. Additional heating and the control of the bath temperature was achieved by the use of a $\frac{1}{4}$ Kw alkali resistant ceramic sheathed heater supplied by Thermal Syndicate Limited, operating through a proportional controller. A 1 Kw

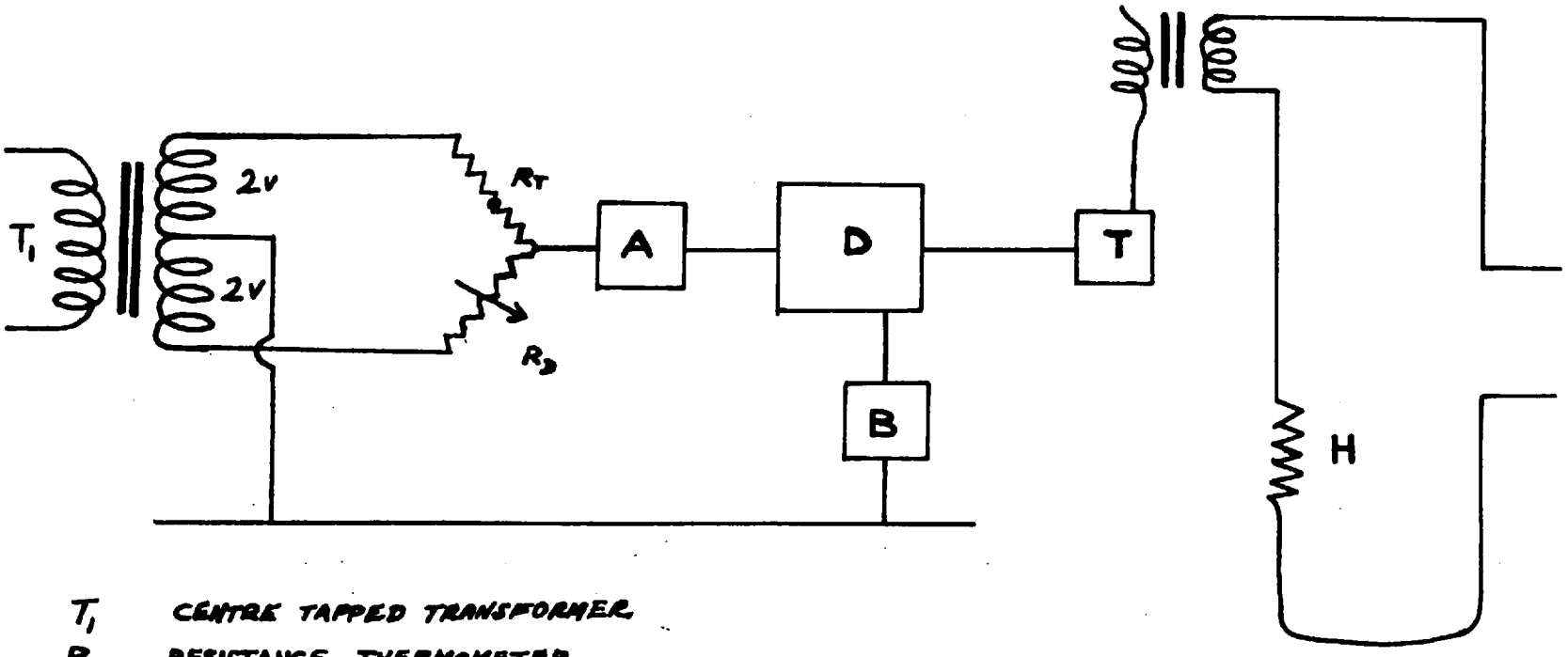
version of this type of heater was used for a short time as a 'main heater' but though resistant to the chemical attack of the melt it was found to have poor mechanical strength. It will function properly when immersed in an already prepared bath but exposure of the part containing the heating element to air during the filling of the bath even for short periods was found sufficient to fracture the sheathing.

Efficient stirring was achieved by means of a three bladed stainless steel propellor driven by a variable speed electric motor. The stainless steel, though darkened in colour after being immersed in the melt bath, showed no other sign of attack. The bath was illuminated by a 100 watt bulb mounted in a can at the side. The inside of the bath was viewed through a slit in the front of the insulation.

6.7 The Temperature Controller.

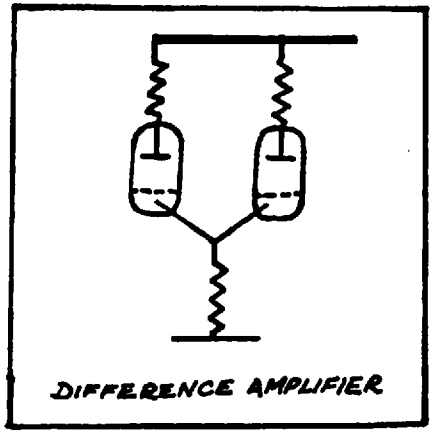
Temperature control was obtained by means of a thyratron bridge circuit Fig.6.3. The bridge consisted of the two output arms of a centre tapped transformer, a platinum resistance thermometer (25Ω) and a series of three decade resistance boxes (0.1 - 100) Ω . The out of phase voltage of the bridge was fed through a high gain A.C. amplifier to a difference amplifier which transmitted the difference voltage between the bridge and a fixed reference, to a thyratron. The thyratron controlled the supply of current to a $\frac{1}{4}$ Kw heater through a transformer. It is possible

CIRCUIT DIAGRAM FOR TEMPERATURE CONTROLS



T_1	CENTRE TAPPED TRANSFORMER
R_T	RESISTANCE THERMOMETER
R_D	VARIABLE RESISTANCE (DECADE BOXES)
A	HIGH GAIN AC AMPLIFIER
B	FIXED REFERENCE
D	DIFFERENCE AMPLIFIER
H	HEATER
V_B	BRIDGE VOLTAGE
V_R	REFERENCE VOLTAGE

FIG 6.3



by calibrating the decade reistances for temperature to set the control to reach a given temperature. In practice, however, the control was put into balance at a temperature approximate to the one desired.

Temperature control was of the order of $\pm 0.05^{\circ}C$.

6.8 Temperature Measurement.

Temperature measurement was by means of a 'pallador' thermocouple. The thermocouple was made of 36 s.w.g. wires of palladium/gold - platinum/iridium alloys. (Johnson-Matthey Pallador thermocouple wire) These materials give an almost linear relationship between temperature and E.M.F. over the range required, with a temperature coefficient of 40 microvolts/degree in the region of room temperature rising to about 60 microvolts/degree in the region of $300^{\circ}C$. This type of thermocouple is claimed to resist oxidation up to $500^{\circ}C$. No change in calibration was detected over several months as shown by checks on the ice point, and the reproducibility of the freezing points of the salts used in cryoscopic studies. The hot junction was gold soldered and sheathed in a thin pyrex tube. The wires were insulated from each other by fine pyrex glass beads and P.V.C. sleeving from the top of this sheath to the cold junctions, which were hard soldered to copper leads and sheathed in thin pyrex tubes containing silicone oil to improve the thermal contact. E.M.F. measurement was by means of:

(i) A Pye Universal potentiometer correct to $\pm$ 1μV up to 340°C and $\pm$ 10μV above this temperature.

and (ii) A Pye Precision Vernier potentiometer reading correct to $\pm$ 1μV at all temperatures.

Both potentiometers were used in conjunction with a Pye Scalamp galvanometer.

6.9 Calibration of Thermocouple.

The thermocouple was standardised as described by Griffiths[4] (see also references 5 and 6), using the melting point of ice (0.00°C), the boiling point of water (100.00°C), the boiling point of Naphthalene (217.4°C) and the boiling point of Sulphur (444.4°C) as the fixed points corrected to 1 atmosphere pressure. Table 6.2 records the temperature and E.M.F. of these fixed points. The order of the calibration by fixed points was;

1. Ice,
2. Steam,
3. Sulphur,
4. Naphthalene,

and 5. Ice.

It is an advantage to anneal the thermocouple at a temperature higher than it is intended to be used. The boiling points were corrected to atmospheric pressure, the barometric pressure being corrected for temperature, latitude and altitude as

described by Griffiths[4].

TABLE 6.2

Calibration of Pallador Thermocouple.

Fixed Point	Temp °C	E.M.F. [1]. mV.
Ice (M.P.)	0.00	0.000 a)
Water (B.P.)	99.415	4.350 b)
Naphthalene(B.P.)	217.04	10.396 c)
Sulphur (B.P.)	444.01	23.390 d)

1. E.M.F. corrected for zero reading of potentiometer.

a) being the corrected mean value of several readings showing no variation;

b) being the corrected mean value of 10 determinations of which the greatest deviation from the mean was 0.002 mV.

c) being the corrected mean value of 12 determinations of which the greatest deviation from the mean was 0.005 mV.

d) being the corrected mean value of 6 determinations of which the greatest deviation from the mean was 0.005 mV.

Throughout the determination of boiling points a small

aluminium 'brolly' was fixed above the tip of the thermocouple. This prevented drops of condensing liquid from running down the thermocouple and condensing on the tip. No significant difference was observed in E.M.F. readings with or without this 'brolly' except in the case of naphthalene where use of the 'brolly' raised the mean value of the E.M.F. by 0.5% and reduced the greatest deviation from the mean from 0.01 mV to the figure quoted with Table 6.2.

The value of the melting point of ice, obtained from the equilibrium mixture of distilled water and crushed ice made from distilled water, was found, by means of a resistance thermometer, to be reproducible and constant within 0.02 - 0.03°C.

The above values of temperature and E.M.F. were used to derive values for the constants in the parabolic equation relating temperature to E.M.F.

$$E = at + bt^2 + ct^3$$

For this thermocouple the equation was:

$$E = (3.9419 \times 10^{-2})t + (4.7618 \times 10^{-5})t^2 - (3.998 \times 10^{-8})t^3$$

A later thermocouple had the equation:

$$E = (3.9098 \times 10^{-2})t + (4.4489 \times 10^{-5})t^2 - (3.1418 \times 10^{-8})t^3$$

Values of E at 5°C intervals of T were calculated and plotted against T over the range (0 - 450)°C. Over 20°C intervals the curve is linear. The accuracy of the plot was such that values

of E.M.F. could be easily read to better than the ± 1μV accuracy of the potentiometer. This high accuracy was particularly valuable in measuring depressions of the freezing points.

References.

1. Kennedy, Ubbelohde and Woodward, Proc. Roy. Soc., (1953), A219, 303.
2. Kirst, Nagle and Castner, Chem. Met. Eng. (1940), 47, 472.
3. Rhodes, PhD. thesis London (1958).
4. Griffiths "Methods of Measuring Temperature" Griffin, London (1947).
5. "Temperature: its Measurement and Control", Am. Inst. Phys. Rheinhold (1956).
6. Calibration of Temperature Measuring Instruments: Notes on Applied Science No.12 Nat. Phys. Lab.

CHAPTER 7

VISCOSITY MEASUREMENTS.

7.1 The Viscometer.

Direct measurement of viscosity requires the determination of the rate of flow of a liquid through a capillary tube of known dimensions. However, very useful results can be obtained by use of various comparative methods, the majority of which are based on flow through a capillary. These and many others are fully described by Barr[1] and Bingham[2].

Various types of viscometer have been used in the determinations of the viscosities of molten salts. Dantuma[3](1928), Karapachev and Stromberg[4] (1935), Berenbilt[5] (1937), and Stretlets, Zhludneva and Reznikov[6](1954), have used various modifications of the oscillating disc. Another method, the falling sphere, has been used by Ogawa [7](1950) and Rogers and Ubbelohde[8] (1953). The capillary method has previously been used by Goodwin and Mailey [9] (1908), Goodwin and Kalmus [10] (1908), Bloom, Harrap and Heymann[11] (1948), Davis, Rogers and Ubbelohde [12] (1953) and Plester, Rogers and Ubbelohde[13] (1956). Objections have been raised to the use of a capillary method for determining the viscosity of molten salts near the freezing point because of the risk of blocking of the capillaries by crystallites and adherance to the walls[8]. Such difficulties were not encountered in the present work nor are they

reported by Goodwin and Mailey or Bloom and Heymann.

For this work the Bingham and Jackson modification[2] of the Ubbelohde viscometer was selected which eliminated the necessity of density determinations and hence removed a principal source of error. The design of this viscometer is illustrated in Fig. 7.1(i) together with the apparatus used for filling, Fig. 7.1 (ii). The capillaries were of Veridia precision bore pyrex glass tubing 8 cms in length, the ends of which were carefully ground out to give square cut ends. In the use of capillary viscometers, the application of a kinetic energy correction is often found necessary which takes the form of an additional term in the viscosity expression:

$$\eta = \frac{\pi g \, p R^4 t}{8 V l} - \frac{m \rho V}{8 \pi l t}$$

η is the viscosity and ρ the density;

g is the acceleration due to gravity;

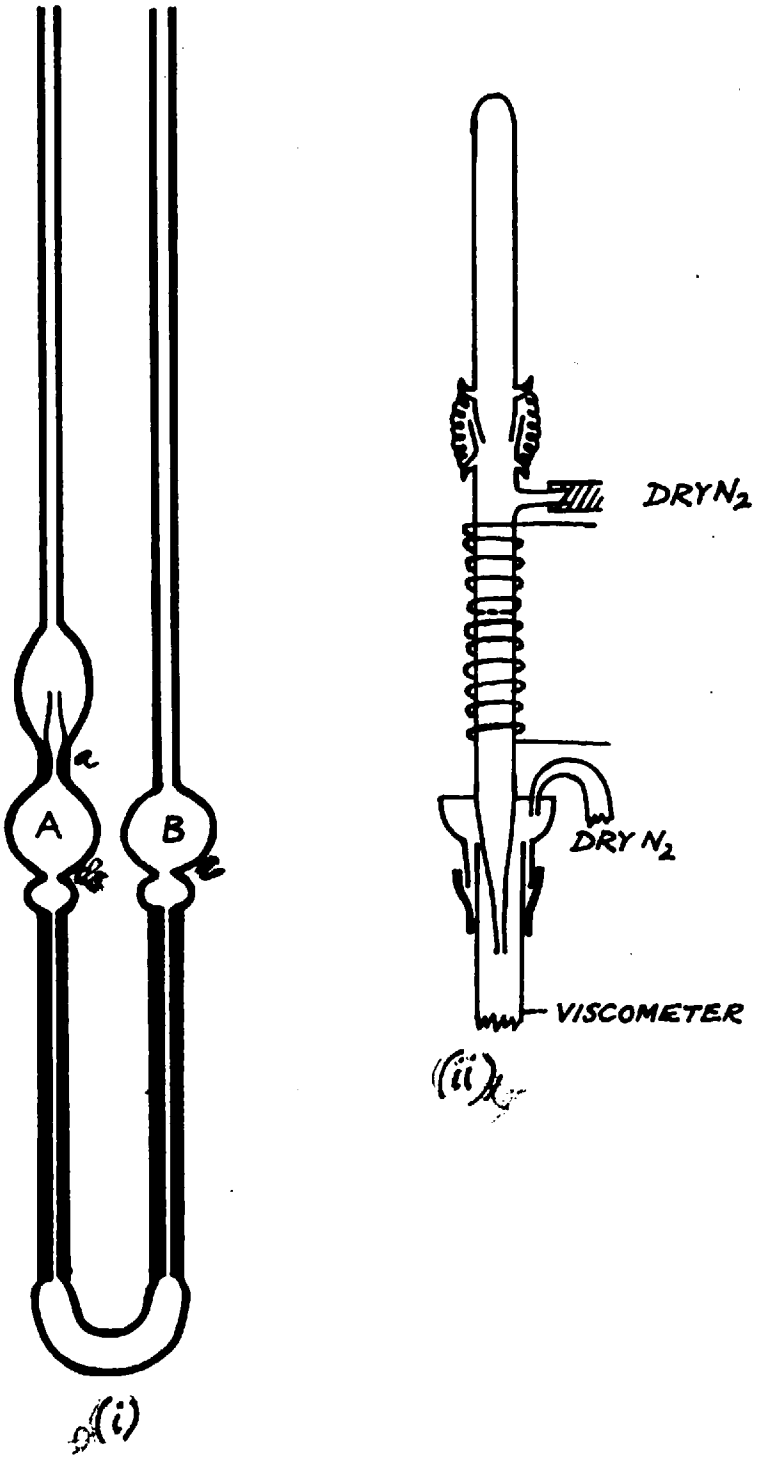
p the pressure;

R is the radius of the capillary and l the length;

V is the volume passing in time t.

It has been suggested that if the ends of the capillaries are 'belled' out no kinetic energy correction need be applied. However, since there has been little definite proof of this Bingham and Jackson[2] have conducted a series of experiments which

FIG 7.1 VISCOMETER



have shown that if the ends of the capillary are ground flat the coefficient m, of the kinetic energy correction can be set equal to 1.24. Further by careful construction of the viscometer and ancillary apparatus the value of the kinetic energy correction can be kept negligible. Thus the chief advantage of this precaution is that it presents one with means of definite evaluation of one of the unknown sources of error in viscosity determination.

The bulbs A and B were of approximately equal volume of 1 cm^3, though a larger volume was found to be necessary in the viscometer used for $K_2Cr_2O_7$ because of its high viscosity. Bulb A had an overflow device to ensure constant volume at each temperature and was constricted at 'a' and 'b' for greater accuracy in reading. At 'b' the large bulb opened out to a smaller bulb immediately above the capillary. B was similar in design to A with a small bulb below 'c' for more accurate reading. The volume of the liquid for any determination filled the viscometer from the tip of the overflow device to mark 'c'. Times of flow were taken for the liquid going from 'a' to 'b' and 'b' to 'a'. A stead rate of flow between the two fixed marks was obtained by the use of a standard constant pressure device.

For $NaNO_3$ and $NaNO_2$ a viscometer having a bore diameter of 0.2 mm. was used.

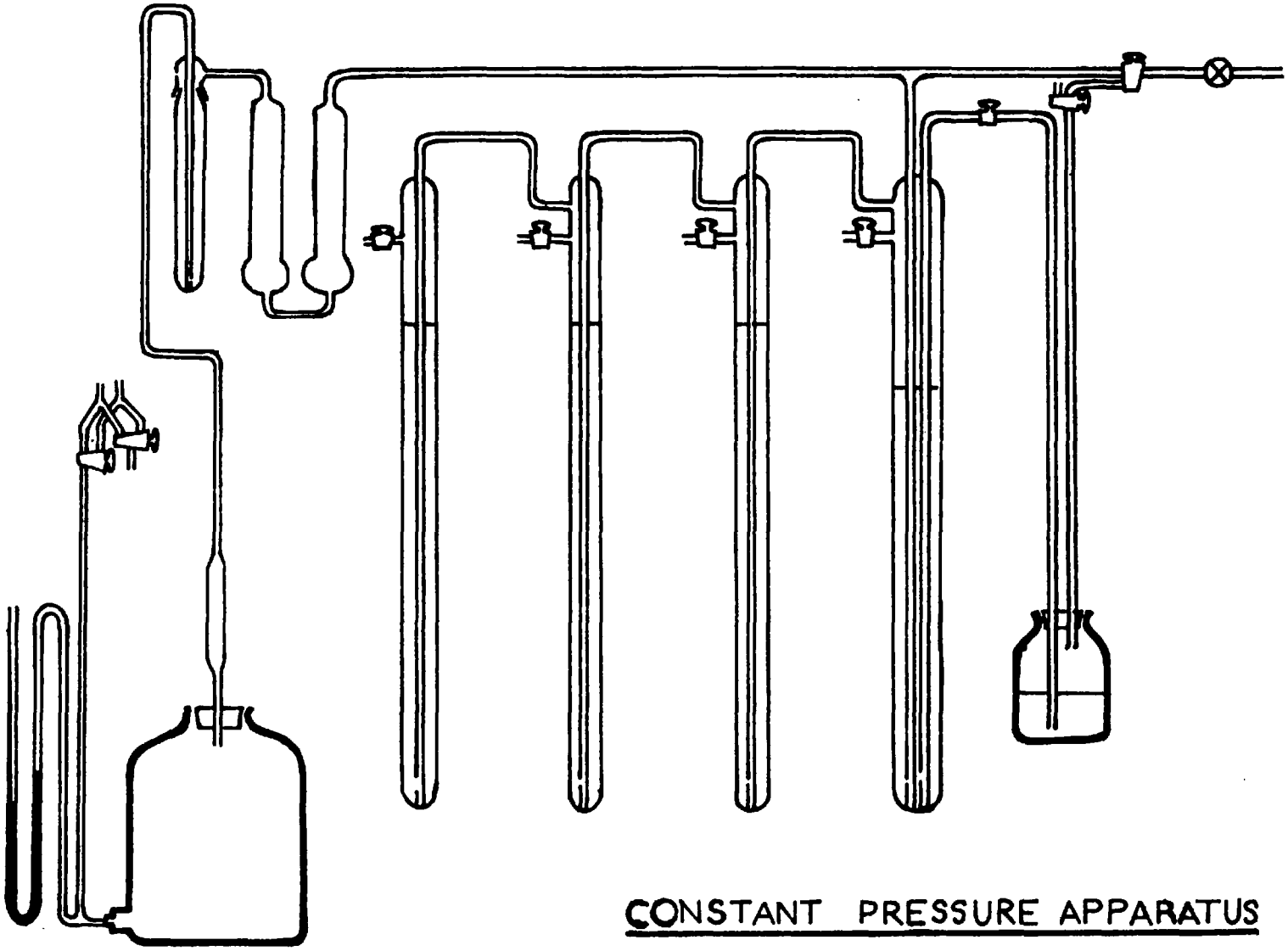
For KNO_2 and $TlNO_3$ a viscometer having a bore diameter of 0.3 mm. was used.

For $\underline{K_2Cr_2O_7}$ a viscometer having a bore diameter of 0.5 mm. was used.

7.2 Constant Pressure Apparatus.

The constant pressure apparatus was of a standard type constructed entirely from pyrex glass. It is illustrated in Fig. 7.2. Each of the four cylinders, 36" length by 1½" diameter, was filled with distilled water, the first being connected by a siphon tube to a water reservoir so that the level of the water contained in it could be varied. The gas used to produce the driving pressure was passed into the system until a pressure determined by the height of the columns was established and the excess bubbled through the water to the atmosphere. One or more columns could be brought into use by closing or opening the taps at the head of each. It was thus possible to obtain exceedingly steady pressures up to the total height of all the columns. Intermediate pressures were obtained by adjusting the level of water in the first column, either by siphoning water from the reservoir or by redirecting the gas pressure to drive the water from the first column back to the reservoir. This was achieved by the use of a two way stopcock.

The gas stream was dried by passing through successive drying columns containing 1. Silica gel, 2. $CaCl_2$, 3. Glass wool in a U-tube immersed in liquid air, before being passed through a cotton wool plug and into a twenty litre aspirator to smooth out



CONSTANT PRESSURE APPARATUS

FIG 7.2

any fluctuations in flow. The aspirator was previously dried by rinsing with alcohol and acetone and passing a slow stream of dry gas through it for two days. From here it was admitted to the viscometer. Reversal of the gas flow to the viscometer was achieved by an arrangement of two two-way stopcocks. Fine control of the gas flow was obtained by the use of a sensitive needle valve placed after the cylinder. The flow was judged to be correct when the gas bubbles were just beginning to rise through the water in a steady stream.

7.3 Calibration of Viscometers.

Five viscometers were used during these investigations. Each viscometer was calibrated with water except that used in the determination of the viscosity of $K_2Cr_2O_7$ where 60% w/w sucrose-water solution was used taking the values of viscosity for this solution as given by Bingham and Jackson[2]. Criticism of the use of water as a calibrating fluid has been made because of the difference between the calibrating temperature and the working temperature. Calibration by $NaNO_3$ has been used by Bloom and Heymann[11] taking the results of Dantuma[3] who used an independent method. However, it can be shown in the present experiments that the error introduced was less than 0.5% with this type of viscometer. The calibration was carried out in a Townson and Mercer water thermostat bath, temperature control $\pm$ 0.01°C.

Pressure measurement was by means of a mercury manometer

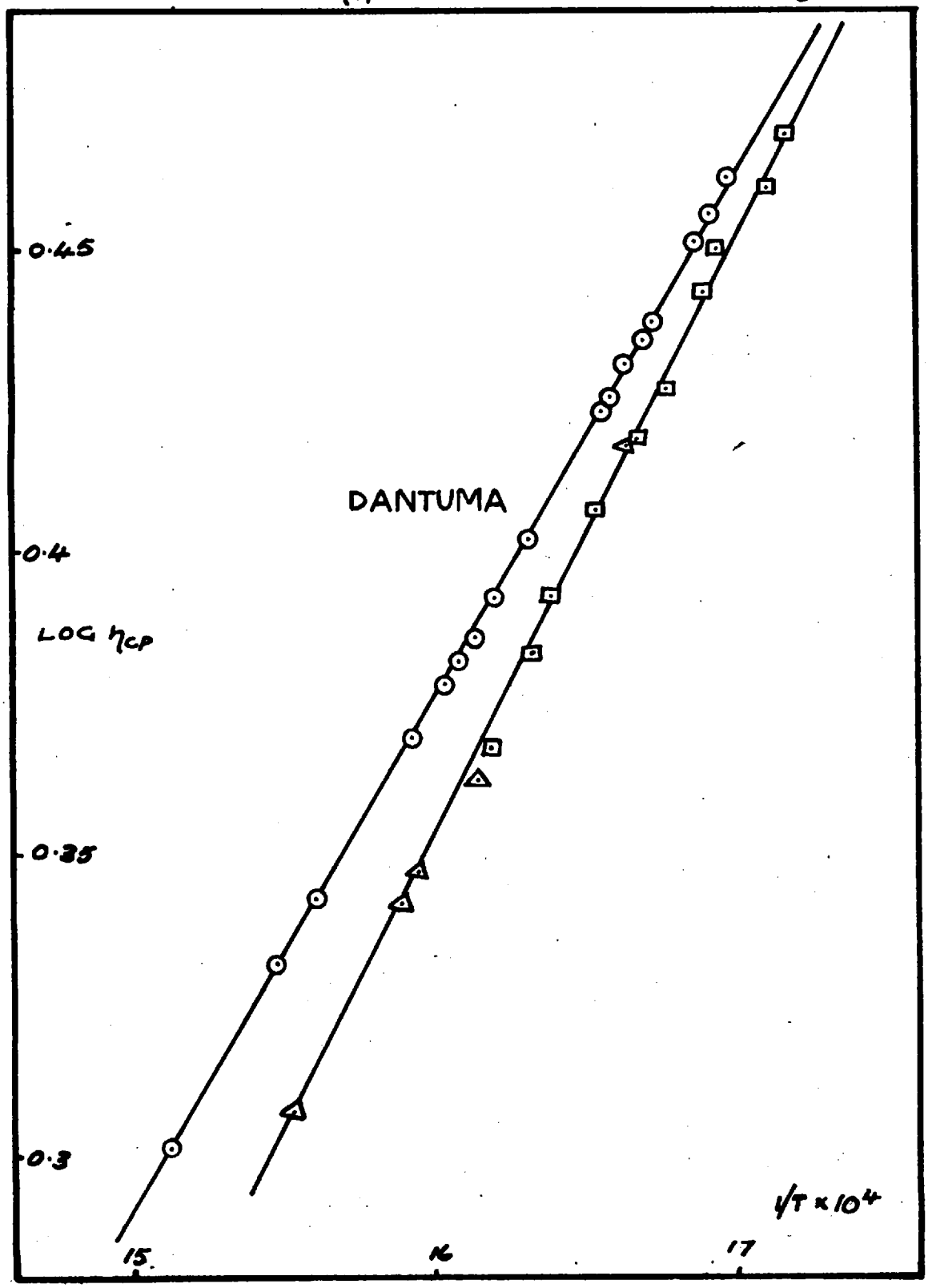
and a Cambridge Instrument Co. cathetometer accurate to ± 0.01 mm. Times of flow were noted on a stop-watch reading to 0.1 sec. A flowtime, the average of at least four times was taken at each pressure. The pressure was varied to four different values at each temperature. Details of the calibrations are noted in Appendix II Tables 1 - 5. The calibration constants for each viscometer are given in Table 7.1.

TABLE 7.1.

Viscometer	Calibration Constant (cp/cm.Hg-sec)
I	2.548×10^{-4}
II	2.163×10^{-4}
III	3.576×10^{-3}
IV	2.661×10^{-3}
V	3.756×10^{-3}

The calibration was repeated in the melt bath previously described using $NaNO_3$ in order to obtain a comparison with the results of previous workers. The values for $NaNO_3$ are shown in Fig. 7.3. together with the results of Dantuma[3]. Good agreement was obtained. Both viscometers I and II were used and the results obtained are plotted together and show a standard deviation of 1% about the line of closest fit. It will be noticed in Fig. 7.3

FIG 7.3 LOG η_{cp} AGAINST 1/T FOR $NaNO_3$ MELT



that though the values of the viscosity are of the same order of magnitude a slight difference in slope is recorded. The reason for this is unknown. The present results were obtained using two different viscometers and two different samples of $NaNO_3$. Differences in the slopes cannot be attributed to the difference between the calibration temperature and the temperature of measurement since such an effect would be very small. Further it would operate through an error in the calibration constant leaving the slope of the line unaltered. Table 7.2 compares the energies of activation for viscous flow of $NaNO_3$ as obtained by different workers.

TABLE 7.2

Activation Energy for Viscous Flow in $NaNO_3$.

$\eta_0 \times 10^4$	$E\eta$	Temperature Range $^0C.$	Reference
10.60	3.85	337 - 495	Goodwin and Mailey [9] (1917)
17.96	3.22	308 - 328	Lorentz & Kalmus [14] (1907)
9.87	3.95	316 - 398	Dantuma [3] (1928)
6.54	4.40	309 - 349	Present Work.

7.4 Filling the Viscometer.

Great care was taken with the filling of the viscometer to ensure that the dried sample was maintained free from moisture.

The procedure was as follows; the dried sample contained in a test tube with a B24 cone was inverted and connected to the B24 socket of the filtering device, Fig.7.1 (ii). It was then brought to a molten state by means of a resistance wire heater wound round the filter. Meanwhile, the viscometer was swept out with a slow stream of dry nitrogen. The molten salt was then driven through the sinter, porosity 3, by means of a positive pressure of dry nitrogen supplied through a side arm. At the same time a flow of dry nitrogen was circulated round the cup enclosing the end of the limb of the viscometer. This procedure was necessary to ensure that no particles of insoluble material entered the viscometer with the subsequent danger of blockage of the capillaries.

The pressure head was established by the use of nitrogen in the case of KNO_2 and $NaNO_2$ and oxygen for $NaNO_3$, $TlNO_3$ and $K_2Cr_2O_7$. This was to minimise the danger of reduction of the nitrates and dichromate and the oxidation of the nitrites at elevated temperatures.

Measurements were made at temperatures rising from the freezing point. Several check points were made during each run with descending temperature to test for hysteresis or possible decomposition. The value of these 'check points' was limited however, since a slight loss in the volume of the liquid in the viscometer occurred with the lowering of the temperature. As can be seen from the description of the viscometer above, Section 7.1,

such a loss is unavoidable. However, in general the absence of decomposition within the temperature range of these experiments was shown by the lack of trend in these results, etc., within the time of study which was, in some cases, up to three days.

7.5 Calculation of Results.

From the Poiseuille equation:

$$V = \frac{\pi P R^4 t}{8\eta L}$$

V is the volume passing in time t;

P is the pressure drop

R and L the radius and length of the capillary respectively.

is derived the following expression which gives the constant for the viscometer;

$$\frac{\Delta P_1 t_1}{\eta_1} = \frac{\Delta P_2 t_2}{\eta_2} = \text{constant}$$

Knowing the constant for the viscometer it can be seen that the slope of the plot ΔP against $1/t$ can be used to derive the viscosity of an unknown liquid. Alternatively, the slope for the line can be determined by a modification of the method of least squares. This employs the limiting factor that the line of the plot passes through the point 0, 0. In general it was found that little difference arose in the value derived by either method.

The viscosites of $NaNO_3$, $TlNO_3$, KNO_2, $NaNO_2$ and $K_2Cr_2O_7$ were determined as described above.

7.6 Results.

The values obtained for the variation of viscosity with temperature of $NaNO_3$, $TlNO_3$, KNO_2, $NaNO_2$ and $K_2Cr_2O_7$ are tabulated, Tables 7.3, 7.4, 7.5, 7.6 and 7.7.

TABLE 7.3

Viscosity of Sodium Nitrate Melt

Temp. (^oK)	$1/T \times 10^4$	η Centipoise	$\log \eta$
584.65	17.103	2.812	0.4490
601.2	16.633	2.616	0.4176
617.7	16.181	2.331	0.3676
619.5	16.142	2.301	0.3617
627.1	15.94	2.226	0.3473
629.3	15.89	2.195	0.3414
646.7	15.46	2.030	0.3075
582.7	17.16	2.944	0.4689
585.1	17.09	2.886	0.4603
590.5	16.93	2.813	0.4492
591.9	16.89	2.773	0.4430
596.4	16.77	2.672	0.4268

/Continued..

TABLE 7.3 (Continued...)

Temp. (^{o}K)	$1/T \times 10^{4}$	η Centipoise	$\log \eta$
599.7	16.67	2.620	0.4183
604.9	16.53	2.553	0.4070
610.2	16.39	2.469	0.3925
612.7	16.32	2.417	0.3832

TABLE 7.4

Viscosity of Sodium Nitrite Melt.

Temp. (^{o}K)	$1/T \times 10^{4}$	η Centipoise	$\log \eta$
556.4	17.97	3.216	0.5079
561.6	17.81	3.080	0.4886
562.2	17.79	3.060	0.4857
567.4	17.62	2.970	0.4728
572.7	17.46	2.871	0.4579
577.0	17.33	2.802	0.4475
583.5	17.14	2.736	0.4356

TABLE 7.5

Viscosity of Potassium Nitrite Melt.

Temp. (^{o}K)	$1/T \times 10^4$	η centipoise	$\log \eta$
686.8	14.56	2.030	0.3075
690.3	14.49	2.002	0.3015
692.0	14.45	1.987	0.2982
694.9	14.39	1.954	0.2909
699.2	14.30	1.933	0.2862
704.3	14.20	1.890	0.2765
708.8	14.11	1.865	0.2707
716.7	13.95	1.830	0.2625
725.4	13.78	1.772	0.2485

TABLE 7.6

Viscosity of Thallium Nitrate Melt.

Temp. (^{o}K)	$1/T \times 10^4$	η centipoise	$\log \eta$
482.0	20.75	3.946	0.5961
485.7	20.59	3.819	0.5819
490.0	20.41	3.681	0.5660
497.7	20.09	3.447	0.5375
504.2	19.83	3.348	0.5248

/Continued....

TABLE 7.6 (Continued...)

Temp. (^{o}K)	1/T x 10^4	η centipoise	log η
512.2	19.52	3.138	0.4967
495.2	20.19	3.407	0.5324
522.5	19.14	2.995	0.4764

TABLE 7.7

Viscosity of Potassium Dichromate Melt.

Temp. (^{o}K)	1/T x 10^4	η centipoise	log η
671.9	14.88	13.806	1.1402
674.3	14.83	13.449	1.1287
679.4	14.72	12.763	1.1058
679.4	14.72	12.776	1.1065
683.6	14.63	12.296	1.0899
688.7	14.52	11.687	1.0678
697.6	14.34	10.798	1.0334
708.4	14.12	9.887	0.9951

Plots of the viscosity of each of the melts gave straight lines in accordance with the equation:

$$\eta = \eta_o \exp (E_\eta / RT)$$

FIG 7.4

LOG η AGAINST 1/T FOR $NaNO_2$ MELT

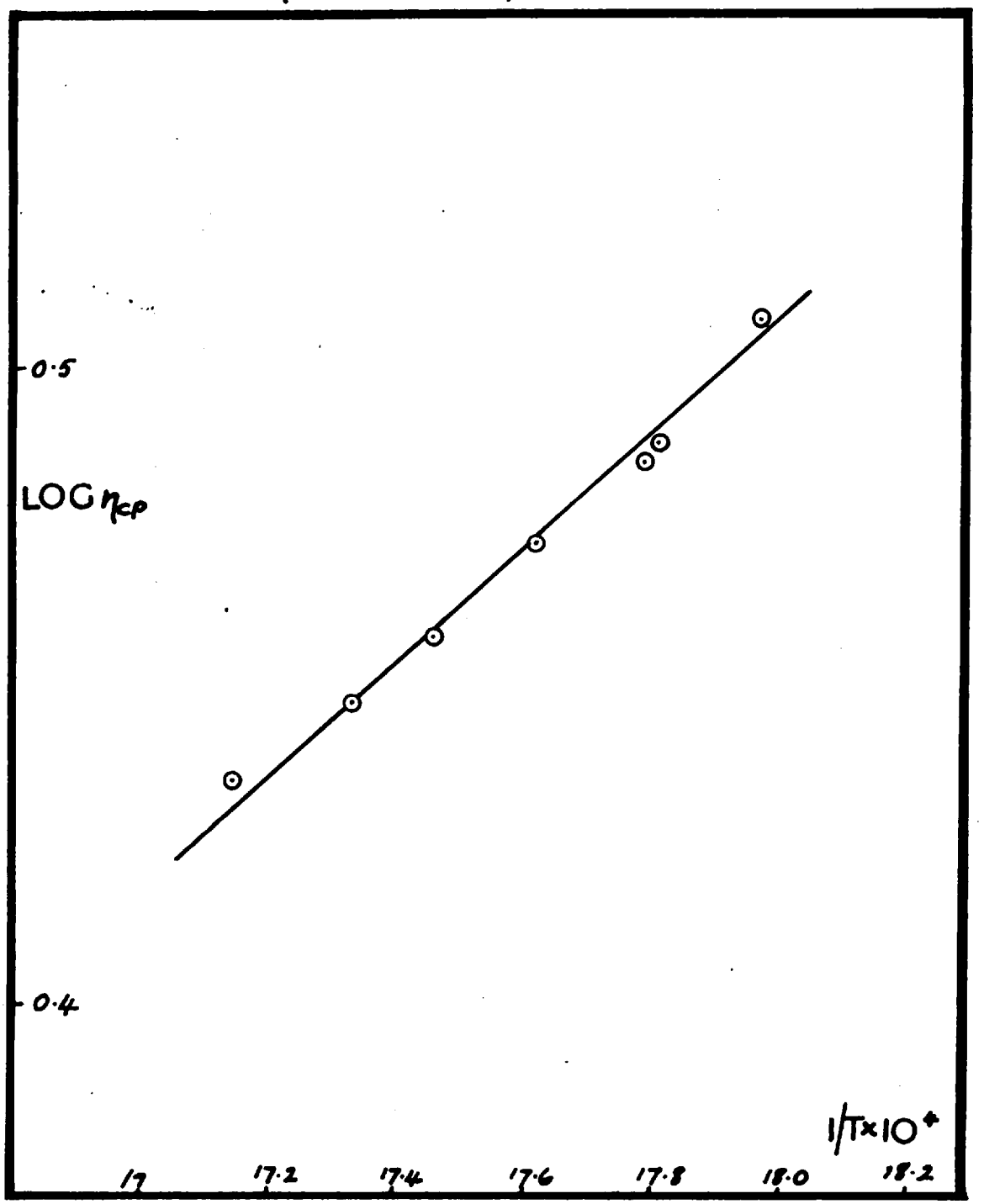


FIG 7.5

LOG η AGAINST 1/T FOR KNO_3 MELT

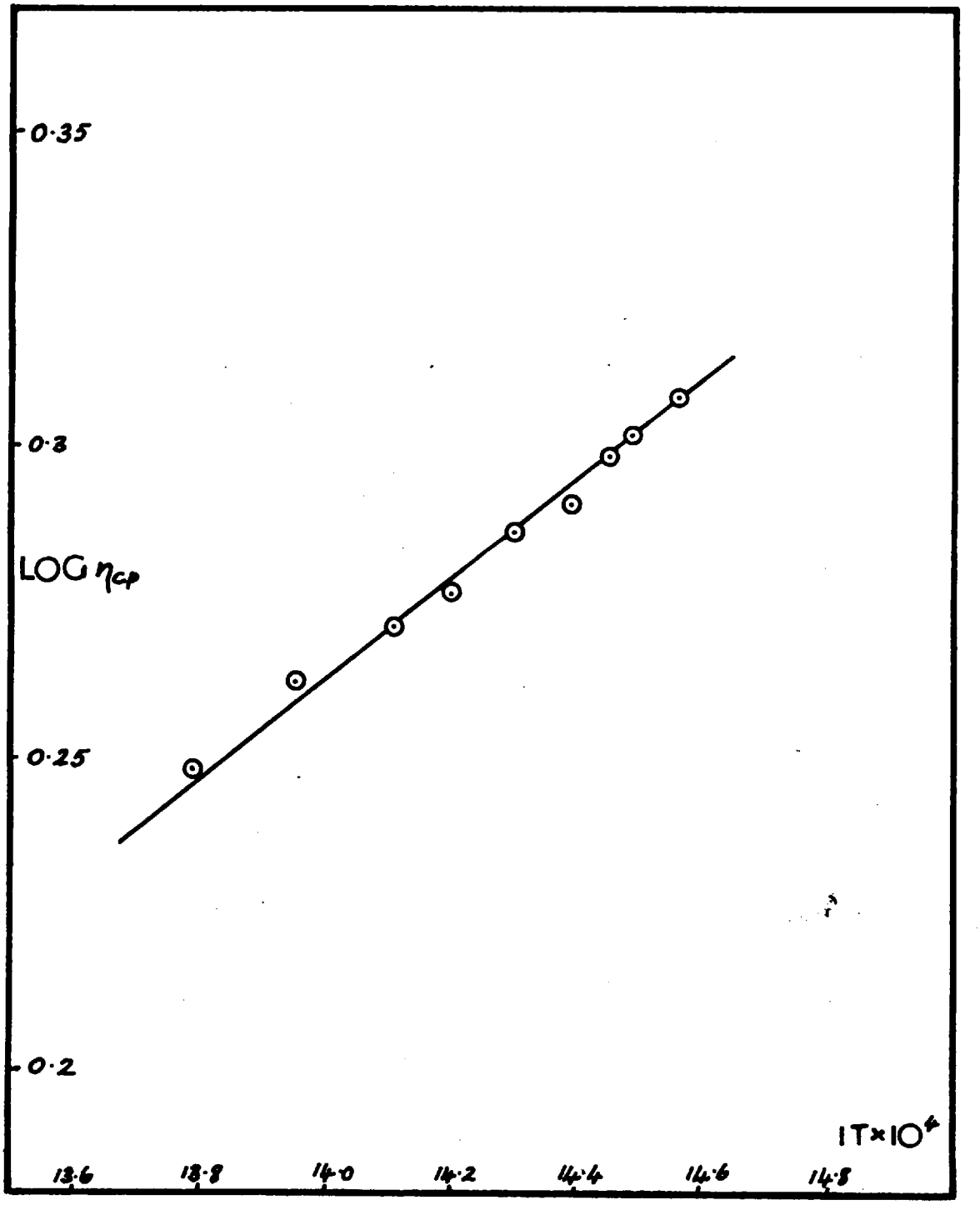


FIG 7.6

LOGη AGAINST 1/T FOR $K_2Cr_2O_7$ MELT

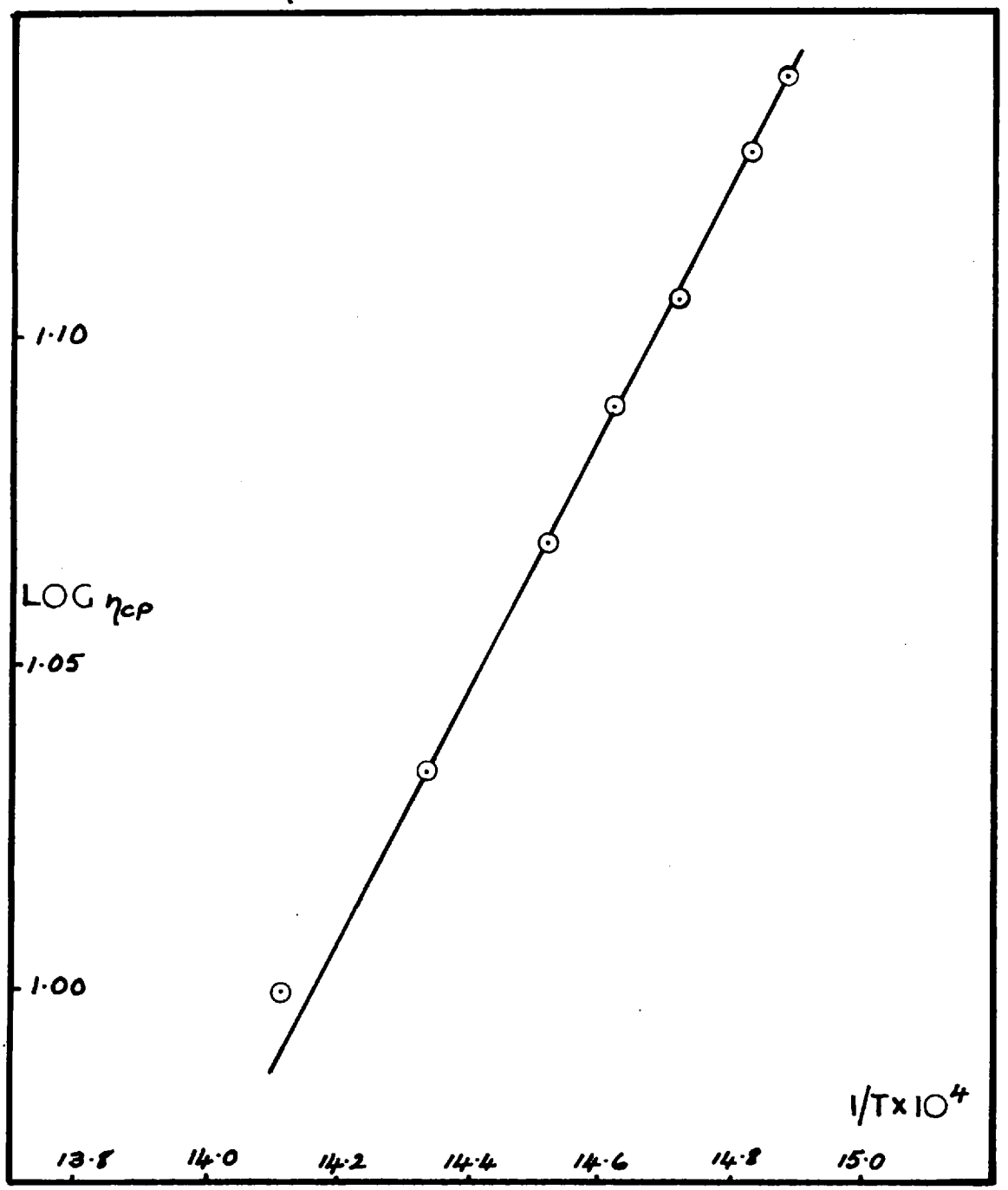
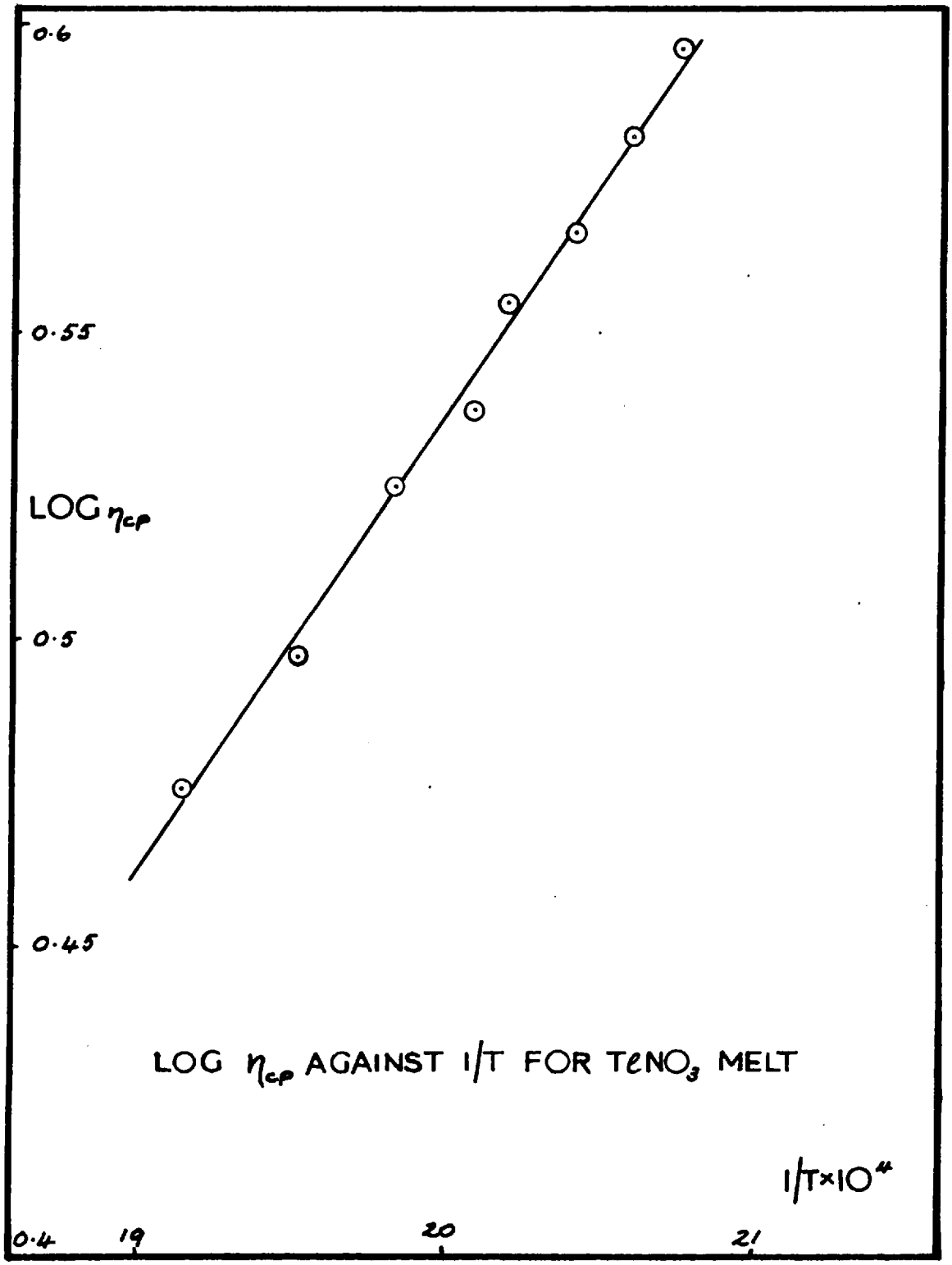


FIG 7.7



LOG η_{cp} AGAINST 1/T FOR $TeNO_3$ MELT

There was no evidence of appreciable departure from linearity on approaching the freezing point, except in the case of $K_2Cr_2O_7$ which showed a slight decrease in slope at 435°C.

The equations of the lines of closest fit for the viscosity results obtained for $NaNO_3$, $NaNO_2$, KNO_2, $TlNO_3$ and $K_2Cr_2O_7$ have been calculated by a method of least squares. These are:

$NaNO_3$ $\eta = 6.54 \times 10^{-4}$ exp.(4.4/RT) range (309 - 347)°C

$NaNO_2$ $\eta = 8.56 \times 10^{-4}$ exp. (4.0/RT) range (282 - 310)°C

KNO_2 $\eta = 13.37 \times 10^{-4}$ exp.(4.23/RT) range (418 - 450)°C

$K_2Cr_2O_7$ $\eta = 1.59 \times 10^{-2}$ exp. (10.5/RT) range (398 - 435)°C

$TlNO_3$ $\eta = 9.04 \times 10^{-4}$ exp. (3.61/RT) range (207 - 250)°C

η_o in poise, E_η in Kcal/mole.

The estimated standard deviations of log η from the correlation line $\log_{10}\eta = \log_{10}\eta_o + E_\eta/2.303\,RT$ together with the standard deviation of E_η, calculated from the variance of the slope, and the correlation coefficient r are given in Table 7.8.

TABLE 7.8

Salt	$S_{(\log_{10}\eta)}$	$S_{(E_\eta)}$ cals.	r
$NaNO_3$	1.42×10^{-3}	34	0.996
$NaNO_2$	2.60×10^{-3}	165	0.996

/Continued...

TABLE 7.8 (Continued..)

Salt	$S_{(\log_{10}\eta)}$	$S_{(E_\eta)}$ cals.	r
KNO_2	1.23×10^{-3}	141.4	0.997
$K_2Cr_2O_7$	2.42×10^{-3}	239.8	0.998
$TlNO_3$	7.90×10^{-3}	249.8	0.968

References

1. Barr, "Monograph of Viscometry" Oxford (1930).
2. Bingham "Fluidity and Plasticity" McGraw-Hill, New York (1922).
3. Dantuma, Z. Anorg. Chem., (1928), 175, 1.
4. Karapachev and Stromberg, J. Gen. Chem., (1935), 5, 625. Karapachev, J. Phys. Chem. (U.S.S.R.) (1935), 6, 1079.
5. Berenbilt, Trans. All-Union Instit. for Aluminium and Magnesium No. 14 (1937).
6. Stretlets, Zhludneva and Reznikov, Consultants Bur., Chem. Collection No.1. Soviet Research in Fused Salts (1949 - 55), Structure and Properties, Quaternary Systems.
7. Ogawa, Japan Inst. Metals B. (1950), 14, 49.
8. Rogers and Ubbelohde, Trans. Far. Soc. (1950), 46, 1051.
9. Goodwin and Mailey, Phys. Rev. (1908), 26, 28.
10. Goodwin and Kalmus, Phys. Rev. (1908), 27, 322.
11. Bloom, Harrap and Heymann, Proc. Roy. Soc. (1948), 194A, 237.
12. Davis, Rogers and Ubbelohde, Proc. Roy. Soc. (1953), 220A, 14.

13. Plester, Rogers and Ubbelohde, Proc. Roy. Soc. (1956), 235A, 469.

14. Lorenz and Kalmus, Z. phys. Chem. (1907), 59, 244

CHAPTER 8.

ELECTROCHEMICAL MEASUREMENTS.

8.1 Choice of Method.

Measurements of conductivity made on $NaNO_2$, KNO_2, $TlNO_3$, and $K_2Cr_2O_7$ are outlined in this chapter.

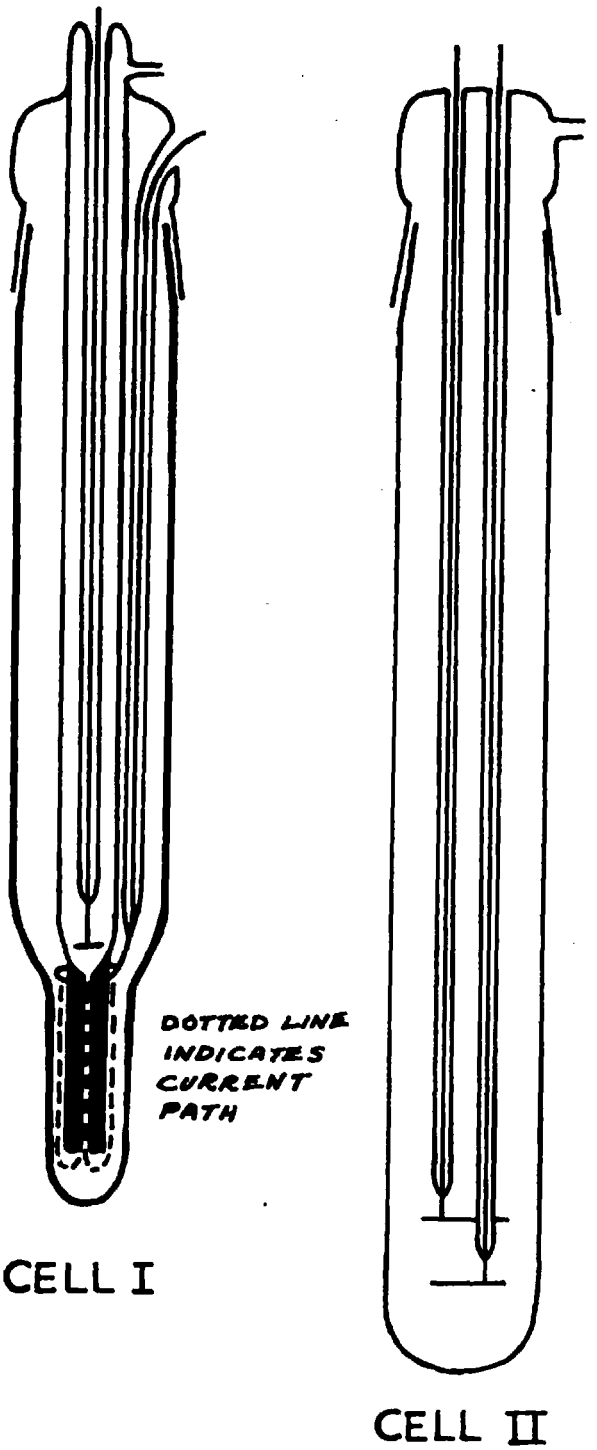
To avoid polarisation difficulties in measurements of electrical conductivity an A.C. method is normally employed. For solid ionic conductors, however, the use of alternating current in an attempt to avoid polarisation can lead to anomalies, attributed to overtones linking with the oscillations of ions in the crystal lattice.[1,2] It was thus considered desirable in the measurement of solid conductances to use a D.C. method. Difficulty was experienced with a normal Wheatstone net due to the time necessary to obtain a reading of resistance, and so a current measuring technique was adopted using a reversing switch in order to minimise polarisation.

8.2 The Cell.

Because of the high conductances a cell with a large cell constant(I) was used for KNO_2 and $NaNO_2$. A cell with a lower cell constant(II) was used for $K_2Cr_2O_7$.

In cell I (Fig.8.1) both electrodes were platinum, one a ring of 30 s.w.g. wire, the other a flat disc 0.4 cm. in diameter. Platinum leads were sealed through the glass and hard soldered onto copper wire. These were separated by a 2 mm. bore capillary

FIG 8.1



tube 4 cms. in length. The current path is shown in Fig. 8.1. Cell II Fig. 8.1 was constructed to give a lower cell constant. Both electrodes were platinum discs 1.35 cms. in diameter and 3 mm. thick. These were gold soldered onto short platinum rods 1 mm. thick which were sealed through glass and hard soldered to copper leads. The glass sleeving of the lower electrode lead passed through a hole in the upper electrode. This improved the rigidity of the construction.

8.3 The Direct Current Circuit.

The circuit illustrated schematically in Fig. 8.2 comprised the conductivity cell in series with a sensitive freely suspended Pye current galvanometer and a reversing switch. Near the melting point where conductivity was high it was found necessary to replace this galvanometer by a less sensitive Pye Scalamp galvanometer. Voltage was supplied across the switch from a series of accumulators through a potential divider. Voltage measurement was by means of a Pye Universal potentiometer in conjunction with a Pye Scalamp galvanometer.

The suspension galvanometer had a sensitivity of

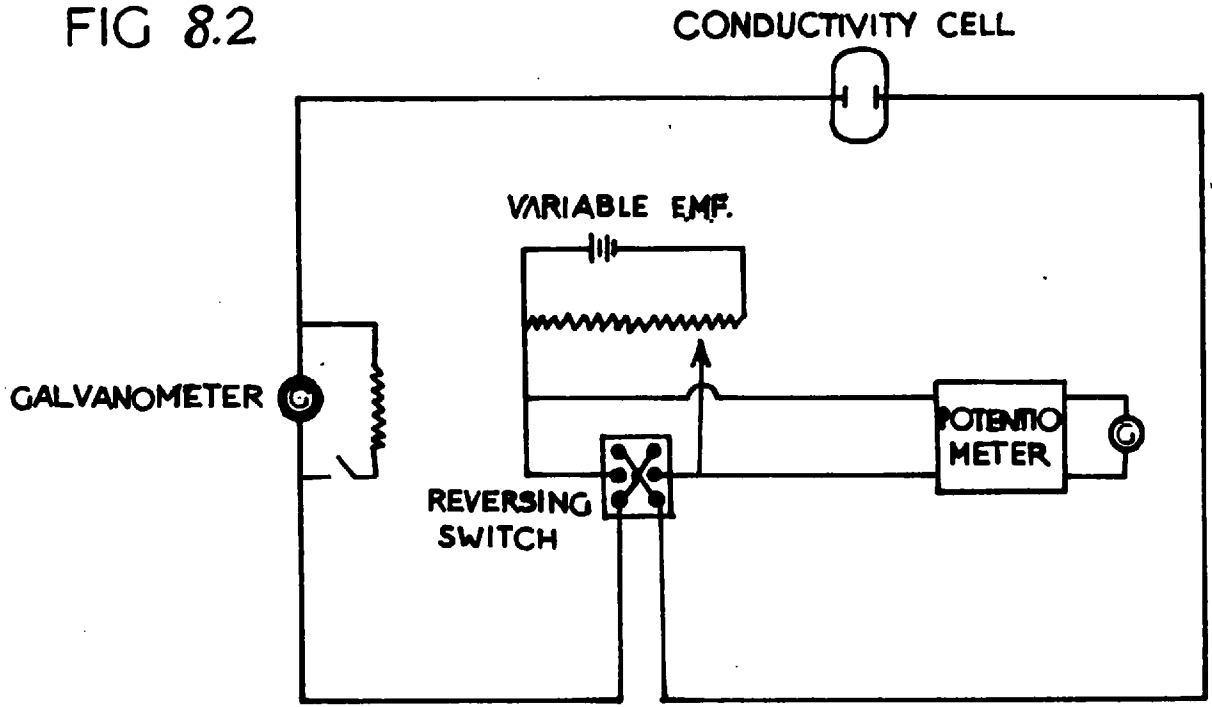
$$4.646 \times 10^{9} \text{ mm/amp.}$$

The Pye Scalamp galvanometer had a sensitivity of approximately

$$5.240 \times 10^{-8} \text{ amp/mm.}$$

Voltage readings by the Pye Universal potentiometer were of the

FIG 8.2



d.c. CIRCUIT DIAGRAM FOR THE MEASUREMENT OF THE ELECTRICAL CONDUCTIVITY IN THE SOLID

accuracy of $\pm$ 1μV up to 340°C.

To reduce the pick up of stray currents, due to the high impedances in the circuit, screened leads were used. Both galvanometers were calibrated by replacing the cell with a standard resistor of 100 KΩ $\pm$ 0.1% and calculating the current passing for each deflection. The calibration constant for the suspension galvanometer was taken as the same for all deflections on the scale at 1 metre. Since it was found that the variation in the sensitivity up to a deflection of 150 mm. was of the order of $\pm$ 0.1%, the value quoted above was used throughout. However, the sensitivity of the Pye Scalamp altered regularly throughout and a value commensurate with the deflection was used. Table 8.1 records the values.

TABLE 8.1

Calibration of Pye Scalamp Galvanometer.

Potential Difference	Deflection	Sensitivity
Volts	mm.	amp/mm x 10^8
0.1410	26.9	5.242
0.2443	46.9	5.209
0.3456	66.75	5.178
0.1661	31.75	5.231
0.0717	13.625	5.262

8.4 Calibration of Conductivity Cell.

The cell constants were obtained by measuring the conductivity of a solution of 0.1N KCl solution with a Wayne-Kerr alternating current bridge (B221) which operates at 1592 c/sec. The results of Jones and Bradshaw [3] (1933) for the conductivity of 0.1N KCl were taken as standard. In the case of Cell II leads' resistance were taken into account. This was of the order of 0.71% of the total measured resistance.

The constants were:

Cell I 124.93 cm^{-1}.

Cell II 0.4741 cm^{-1}.

8.5 Results.

Measurements of the resistance of KNO_2, $NaNO_2$ and $K_2Cr_2O_7$ have been made at temperatures descending from and ascending to the melting point. At each temperature the resistance was measured using five different voltages. At each applied voltage the current was computed from the average of some 10 - 20 galvanometer deflections, the current being reversed at each reading. The point of maximum swing was taken as the most accurate. Variations from Ohm's law at any one temperature, using different voltages, were of the order of $\pm$ 1-2%. From the values of resistance measured the specific conductivity σ was calculated. Tables 8.2, 8.3 and 8.4 record the variation of conductivity with temperature.

Figs. 8.3, 8.4 and 8.5 show plots of log σ against $^1/_T$. A transition is shown in KNO_2 which takes place over a range of 16°C and appears to be continuous. This transition was approached from both sides in order to fix its position as accurately as possible. Table 8.2 records the readings in order.

TABLE 8.2.

Conductivity of KNO_2 solid.

Temp. °K	$1/T \times 10^4$	σ mhos	log σ
680.2	14.70	1.483×10^{-2}	- 1.8288
663.0	15.08	1.092×10^{-2}	- 1.9618
624.0	16.03	5.226×10^{-4}	- 3.2818
578.8	17.28	1.016×10^{-4}	- 3.9931
521.8	19.16	9.156×10^{-6}	- 5.0383
478.1	20.92	1.504×10^{-6}	- 5.8228
674.5	14.83	1.725×10^{-2}	- 1.7632
660.8	15.13	1.233×10^{-2}	- 1.9090
591.7	16.90	1.338×10^{-4}	- 3.8576
538.3	18.58	1.565×10^{-5}	- 4.8055
682.5	14.65	1.756×10^{-2}	- 1.7555
642.6	15.56	2.085×10^{-3}	- 2.6808
653.1	15.31	7.996×10^{-3}	- 2.0972
653.1	15.31	9.384×10^{-3}	- 2.0276

/Continued.....

TABLE 8.2 (Continued..)

Temp. $^{o}K.$	$1/T \times 10^{4}$	σ mhos	$\log \sigma$
638.7	15.65	8.346×10^{-4}	- 3.0785
647.9	15.44	4.038×10^{-3}	- 2.3938
645.8	15.48	3.099×10^{-3}	- 2.5087
640.9	15.61	1.396×10^{-3}	- 2.8551

TABLE 8.3

Conductivity of $K_2Cr_2O_7$ Solid.

Temp. ^{o}K	$1/T \times 10^{4}$	σ mhos	$\log \sigma$
663.0	15.08	6.353×10^{-5}	- 4.197
630.7	15.86	1.103×10^{-6}	- 5.957
604.9	16.53	4.464×10^{-7}	- 6.350
567.7	17.62	1.297×10^{-7}	- 6.887
530.1	18.86	1.709×10^{-8}	- 7.767
479.8	20.84	7.567×10^{-10}	- 9.121

TABLE 8.4

Conductivity of $NaNO_2$ Solid.

Temp. ^{o}K	$1/T \times 10^{4}$	σ mhos	$\log \sigma$
293.2	33.88	3.792×10^{-8}	- 7.4211

/Continued....

TABLE 8.4 (Continued...)

Temp. ^{o}K	$1/T \times 10^{4}$	σ mhos	$\log\sigma$
553.4	18.07	3.547×10^{-1}	- 0.4502
553.5	18.07	2.138×10^{-1}	- 0.6700
518.0	19.31	1.329×10^{-4}	- 3.8765
550.6	18.16	5.898×10^{-4}	- 3.2293
480.2	20.83	7.103×10^{-6}	- 5.1486
468.0	21.37	3.394×10^{-6}	- 5.4693
452.0	22.12	1.470×10^{-6}	- 5.8327
489.8	20.42	9.088×10^{-6}	- 5.0415
509.4	19.63	2.784×10^{-5}	- 4.555
519.6	19.25	4.736×10^{-5}	- 4.3246

Plots of the conductivity of $NaNO_2$ and $K_2Cr_2O_7$ are taken through the solid liquid transition. However, too much stress cannot be laid on the accuracy of these points since temperature measurements were made in the melt bath and assumed to be the same for the sample. While this is a reasonable assumption for measurements in a pure solid or pure liquid, it introduces difficulties at a transition point since the contribution of the latent heat of fusion is unknown. Difficulty was encountered in reproducing these values.

It will be seen that the variation of conductivity with

temperature can be represented by the expression

$$\sigma = \sigma_0 \quad \exp\ (-E_\sigma/RT)$$

The equations of closest fit for the linear portions of the plots are (σ mhos cm^{-1} E_σ Kcal/mole)

	Range ^oC
$NaNO_2$ $\sigma = 2.94 \times 10^5$ exp. (-23.8/RT)	175 - 261.5
KNO_2 below melting point $\sigma = 9.33 \times 10^4 \exp(-21.0/RT)$	380.5 - 415.5
KNO_2 below transition $\sigma = 1.40 \times 10^5$ exp. (-24.2/RT)	203 - 364
$K_2Cr_2O_7$ $\sigma = 1.55 \times 10^4$ exp. (-29.1/RT)	203 - 364

The estimated standard deviation of $\log_{10}\sigma$ from the correlation

$$\log_{10}\sigma = \log_{10}\sigma_0 + E_\sigma/2.303RT$$

together with the correlation coefficient r and the standard deviation of E_σ, calculated from the variance of the slope are shown in Table 8.5.

TABLE 8.5

Salt	$S(\log_{10}\sigma) \times 10^2$	$S\ E_\sigma$(cals) $\times 10^{-2}$	r
$NaNO_2$	4.58	8.74	0.997
KNO_2 below MPt.	5.86	45.5	0.919
KNO_2 below Transition	8.44	8.42	0.997
$K_2Cr_2O_7$	9.18	10.62	0.996

FIG 8.3 LOG σ AGAINST 1/T FOR $NaNO_2$

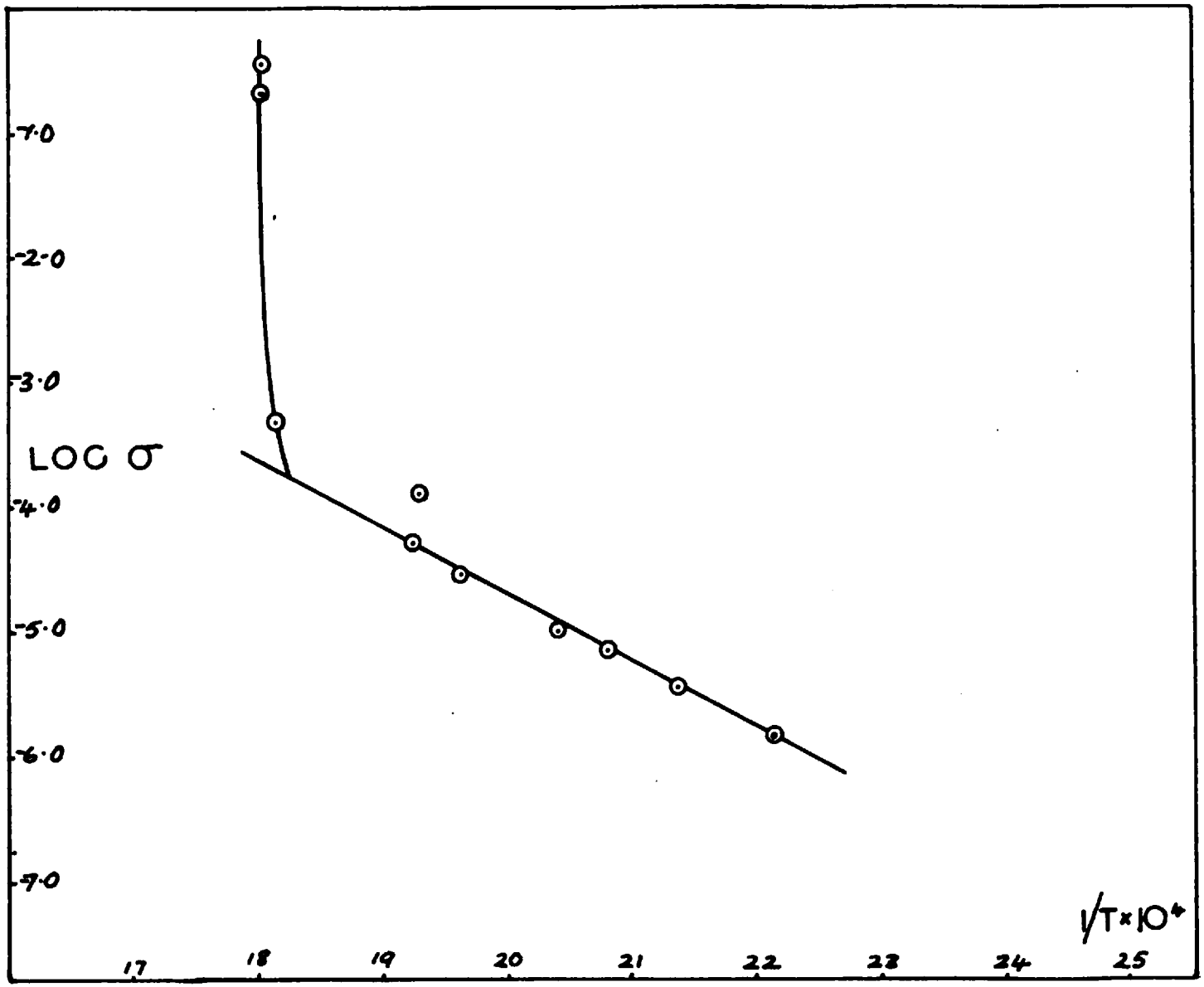


FIG 8.4 LOG σ AGAINST 1/T FOR KNO_2 SOLID

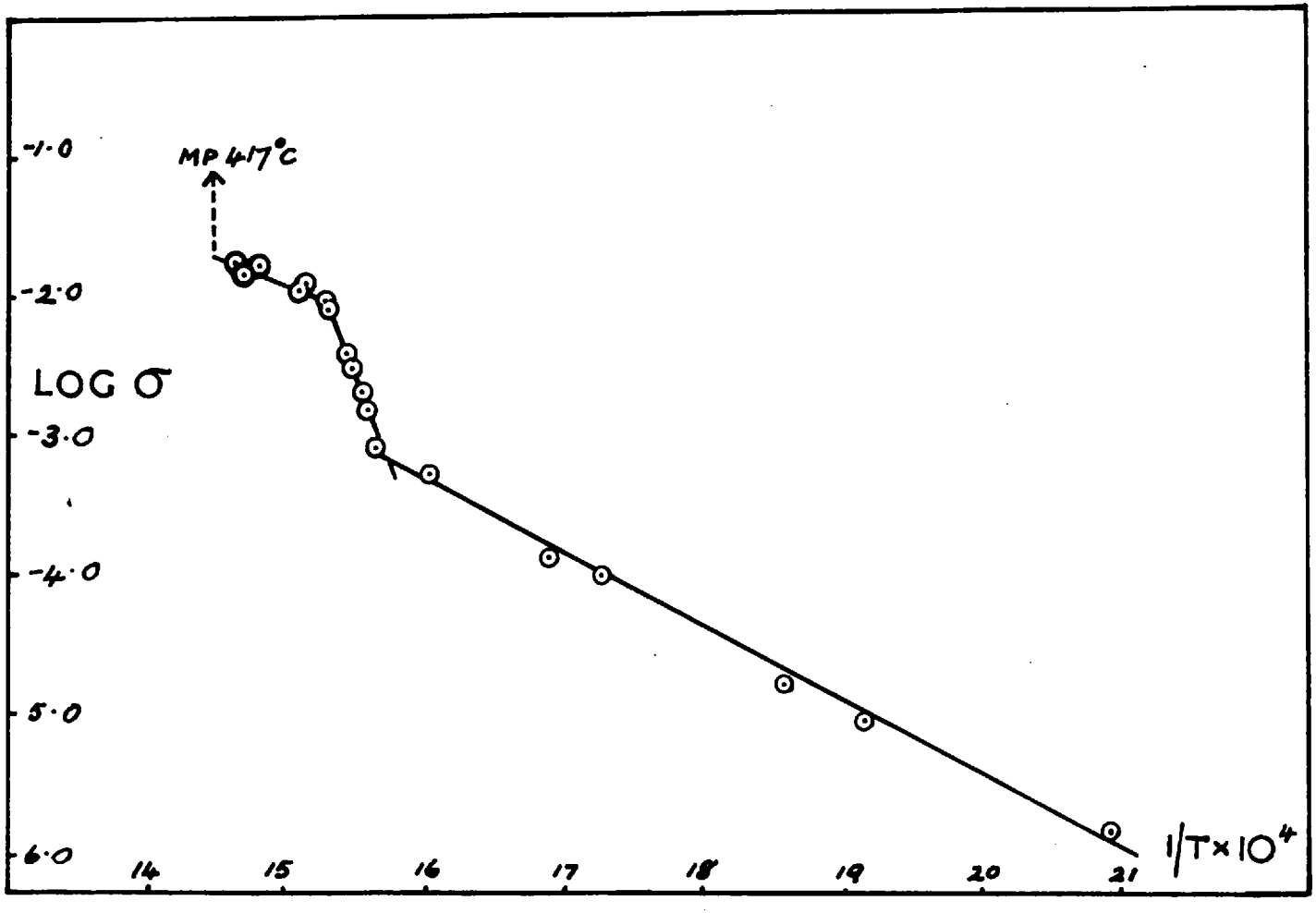
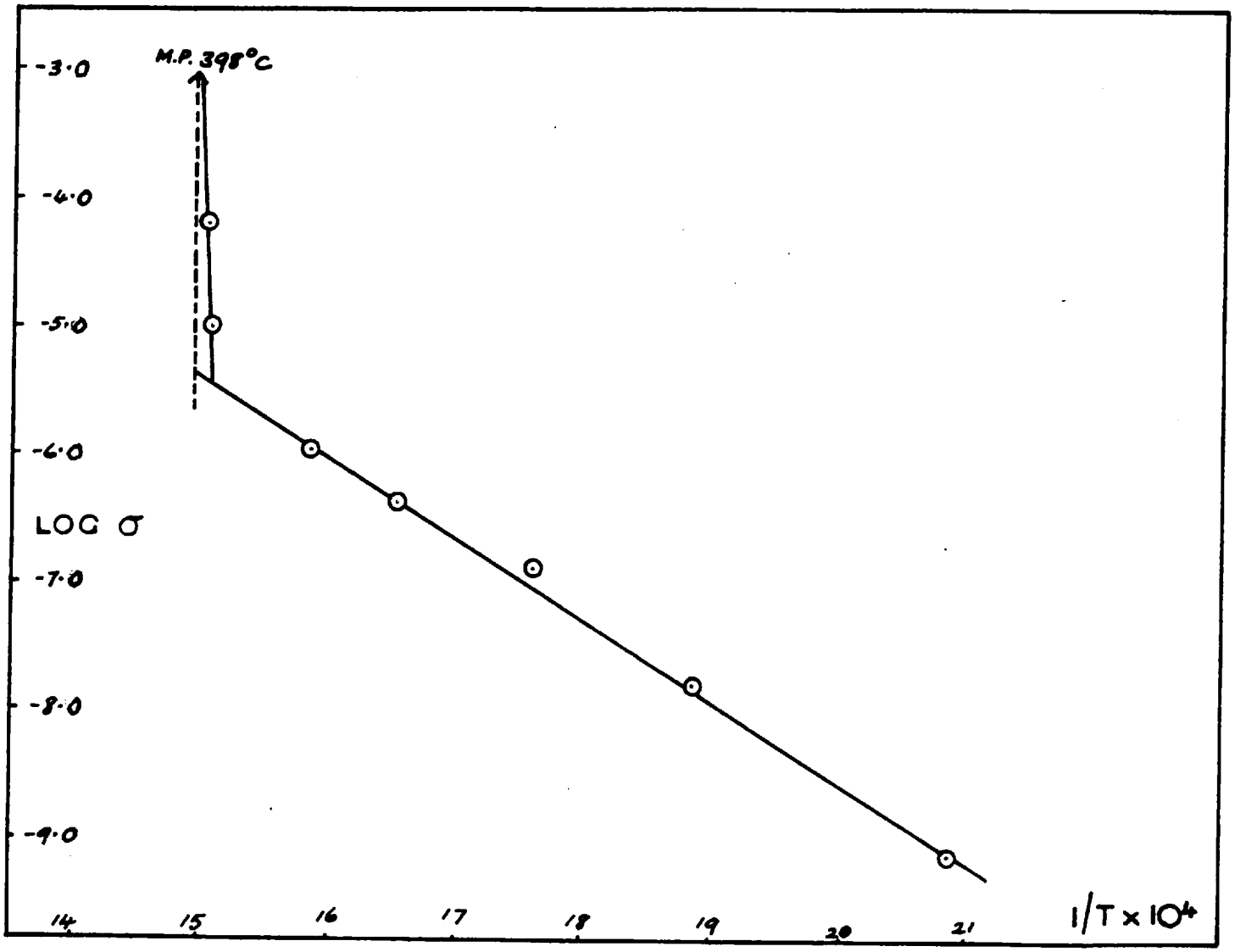


FIG 8.5 LOG σ AGAINST 1/T FOR $K_2Cr_2O_7$



8.6 Conductivity Measurements on Ionic Melts.

For the measurement of conductivity in molten KNO_2, $NaNO_2$, $TlNO_3$ and $K_2Cr_2O_7$ polarisation was avoided by the use of an alternating current bridge. This was a Wayne-Kerr alternating current bridge (B221) operating at 1592 cycles/second. This is a direct reading conductance bridge. Balance is obtained by magic eye focussing.

The cell used in all measurements of electrical conductivity in the molten state was that described as Cell I in Section 8.2. Calibration was as previously described in Section 8.4. Measurements were made at temperatures descending to and ascending from the freezing point. This was done to check for hysteresis or possible decomposition.

The sample to be used was dried as described in Section 6.4, using the test tube of the cell throughout the whole operation. The dried sample was then brought to a molten state under vacuum. Dry nitrogen was then admitted and the capillary section lowered into place whilst being swept out with a slow stream of dry nitrogen. Readings of conductivity were made at some twenty different temperatures.

8.7 Results.

Tables 8.6, 8.7, 8.8 and 8.9 show the variation of electrical conductivity with temperature. Plots of log σ against

1/T have been made Figs. 8.6, 8.7, 8.8 and 8.9. Two sets of data are shown for KNO_2.

1. The results obtained on a sample recrystallised from water and held molten for some days.

2. A sample recrystallised twice from the melt as previously described in Section 6.3.

The latter was taken as the most accurate and results quoted are for this sample. Sample 1. gave off bubbles slowly throughout the time that measurements were being conducted on it. This could have been due to (a) release of H_2O trapped in the melt, (b) decomposition of KNO_2 or (c) decomposition of KNO_3 impurity; (b) and (c) were thought the most likely. A similar difficulty was experienced when attempts were made to measure the viscosity of KNO_2 but due to the nature of the technique used it was impossible to obtain any results. However, subsequent measurements of viscosity using sample 2. above were satisfactory.

The variation of conductivity with temperature could in all cases be represented by:

$$\sigma = \sigma_o \text{ exp. } (-E_\sigma/RT)$$

The equations derived for the best straight lines on the basis of the above expression are:

	Range ^oC
$NaNO_2$, σ = 10.9 exp. (-2.98/RT)	280.5 - 311
KNO_2, σ = 9.64 exp.(-2.97/RT)	416 - 450

		Range °C
$K_2Cr_2O_7$ σ =	73 exp. (-7.8/RT)	399 - 434
$TlNO_3$ σ =	10.64 exp.(-3.26/RT)	207 - 253

TABLE 8.6

Conductivity of KNO_2 Melt (1).

Temp °K.	$1/T \times 10^4$	σ Mhos	log σ
732.2	13.66	1.264	0.10173
727.2	13.75	1.206	0.08131
718.2	13.92	1.209	0.08237
715.7	13.97	1.218	0.08563
711.7	14.05	1.195	0.07740
707.9	14.13	1.183	0.07299
704.5	14.19	1.170	0.06819
698.2	14.32	1.148	0.05999
696.4	14.36	1.138	0.05617
691.5	14.46	1.117	0.04802
689.1	14.51	1.107	0.04309
686.7	14.56	0.8536	- 0.06874
689.1	14.51	0.8945	- 0.04842

Conductivity of KNO_2 Melt (2).

Temp ^oK	$1/T \times 10^4$	σ Mhos	$\log\sigma$
691.4	14.46	1.109	0.04487
701.9	14.25	1.147	0.0616
703.6	14.21	1.143	0.0638
701.6	14.25	1.133	0.0641
701.2	14.26	1.138	0.0654
699.4	14.30	1.137	0.0657
698.2	14.32	1.133	0.05424
697.6	14.33	1.129	0.05270
696.8	14.35	1.127	0.05190
696.1	14.37	1.125	0.05115
695.1	14.39	1.120	0.04922
692.5	14.44	1.110	0.04532
691.6	14.46	1.107	0.04409
689.1	14.51	1.097	0.04026
705.3	14.18	1.145	0.05883
712.7	13.03	1.169	0.06779
721.5	13.86	1.213	0.08385
722.2	13.85	1.218	0.08563
723.4	13.82	1.221	0.08672
719.1	13.91	1.209	0.08237
701.9	14.25	1.133	0.05424

TABLE 8.7

Conductivity $TlNO_3$ Melt.

Temp. ^oK	$1/T \times 10^4$	σ_s mhos	$-\log\sigma$
525.4	19.4	0.4695	0.3369
522.8	19.13	0.4603	0.3369
522.2	19.15	0.4588	0.3383
521.2	19.19	0.4555	0.3415
518.4	19.29	0.4478	0.3489
518.2	19.30	0.4471	0.3496
513.2	19.49	0.4337	0.3628
512.8	19.50	0.4330	0.3635
505.8	19.77	0.4134	0.3836
499.4	20.02	0.3973	0.4007
499.6	20.02	0.3978	0.4003
493.1	20.27	0.3818	0.4182
492.7	20.30	0.3803	0.4199
486.8	20.54	0.3636	0.4394
488.0	20.49	0.3676	0.4346
484.6	20.64	0.3589	0.4450
483.7	20.67	0.3569	0.4475
483.0	20.70	0.3547	0.4501
481.4	20.77	0.3516	0.4540
481.2	20.78	0.3509	0.4548
486.2	20.57	0.3633	0.4397
483.0	20.70	0.3533	0.4494
481.4	20.77	0.3510	0.4547

TABLE 8.8

Conductivity of $K_2Cr_2O_7$ Melt.

Temp. ^oK	$1/T \times 10^4$	σ_s mhos	$-\log \sigma$
706.3	14.16	0.2833	0.5477
705.1	14.18	0.2774	0.5569
702.3	14.24	0.2706	0.5677
701.1	14.26	0.2666	0.5741
699.2	14.30	0.2624	0.5810
696.7	14.35	0.2559	0.5920
694.5	14.40	0.2519	0.5988
692.6	14.44	0.2479	0.6057
686.9	14.56	0.2356	0.6275
684.8	14.60	0.2316	0.6353
683.8	14.62	0.2269	0.6442
676.8	14.78	0.2163	0.6649
675.6	14.80	0.2140	0.6696
675.3	14.81	0.2133	0.6710
675.0	14.815	0.2126	0.6725
674.7	14.82	0.2118	0.6741
674.4	14.83	0.2110	0.6756
673.9	14.84	0.2101	0.6776
673.4	14.85	0.2093	0.6793
672.9	14.86	0.2079	0.6821
672.7	14.87	0.2055	0.6871
682.9	14.64	0.2265	0.6449
679.9	14.71	0.2194	0.6588

TABLE 8.9

Conductivity of $NaNO_2$ Melt.

Temp ^oK	$1/T \times 10^4$	σ_s mhos	$\log \sigma$
583.6	11.13	1.3901	0.1430
579.4	10.93	1.3652	0.1351
577.6	10.86	1.3564	0.1322
577.8	10.86	1.3564	0.1322
575.2	10.70	1.3364	0.1258
572.2	10.56	1.3189	0.1202
571.8	10.55	1.3177	0.1199
570.8	10.50	1.3114	0.1176
569.2	10.43	1.3027	0.1149
567.8	10.36	1.2910	0.1120
566.0	10.26	1.2815	0.1076
564.0	10.16	1.2690	0.1034
561.7	10.05	1.2552	0.0986
558.5	9.889	1.2351	0.09168
556.6	9.795	1.2240	0.0878
555.8	9.762	1.2193	0.0860
555.2	9.730	1.2153	0.0846
553.8	9.640	1.2048	0.0810
553.7	9.630	1.2028	0.0802
568.8	10.44	1.3040	0.1153
575.0	10.68	1.3339	0.1252
574.3	10.65	1.3302	0.1239

FIG 8.6

LOG σ AGAINST $1/T$ FOR $NaNO_2$

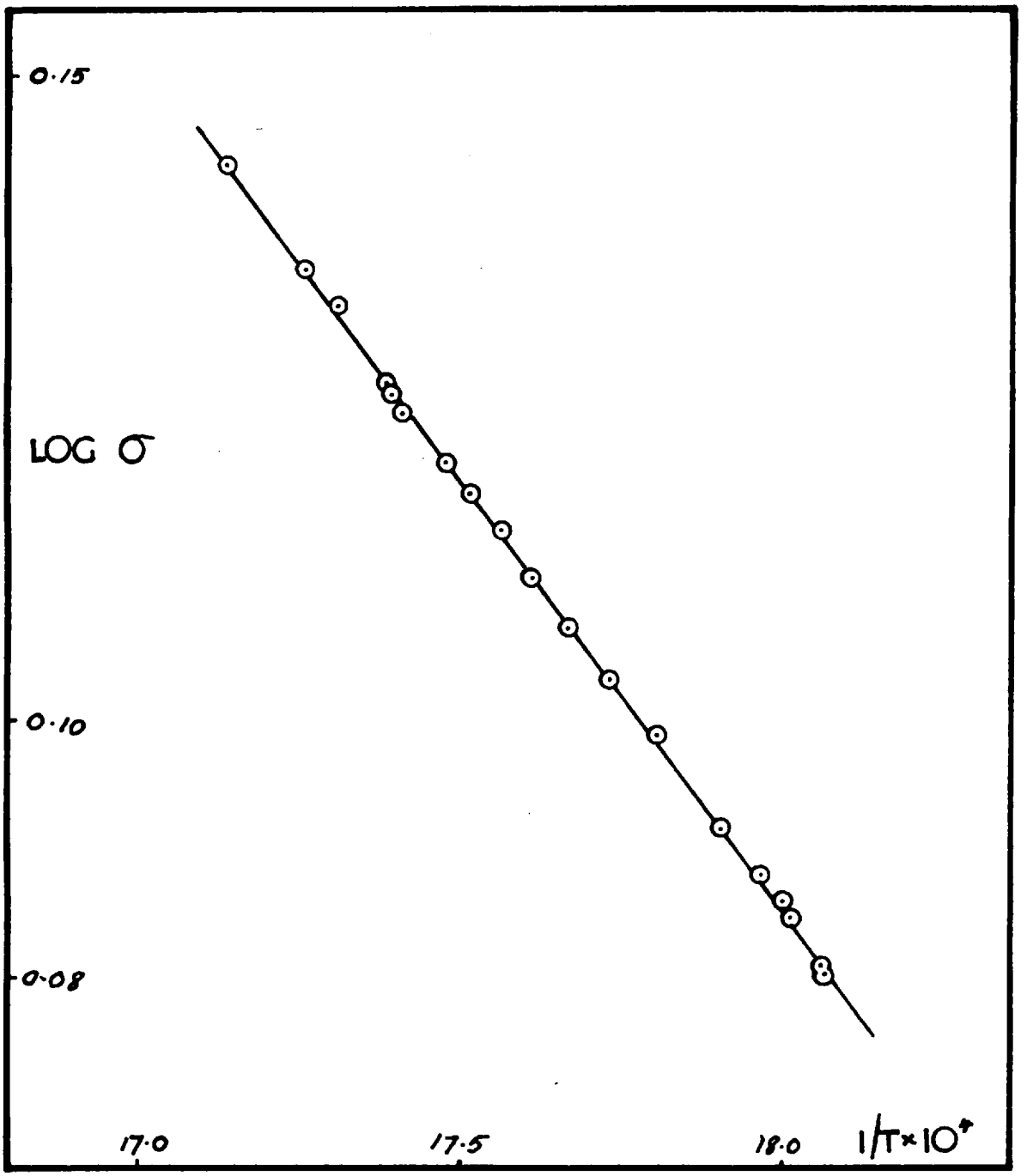


FIG. 8.7

LOG σ_s AGAINST 1/T FOR KNO_2 MELT

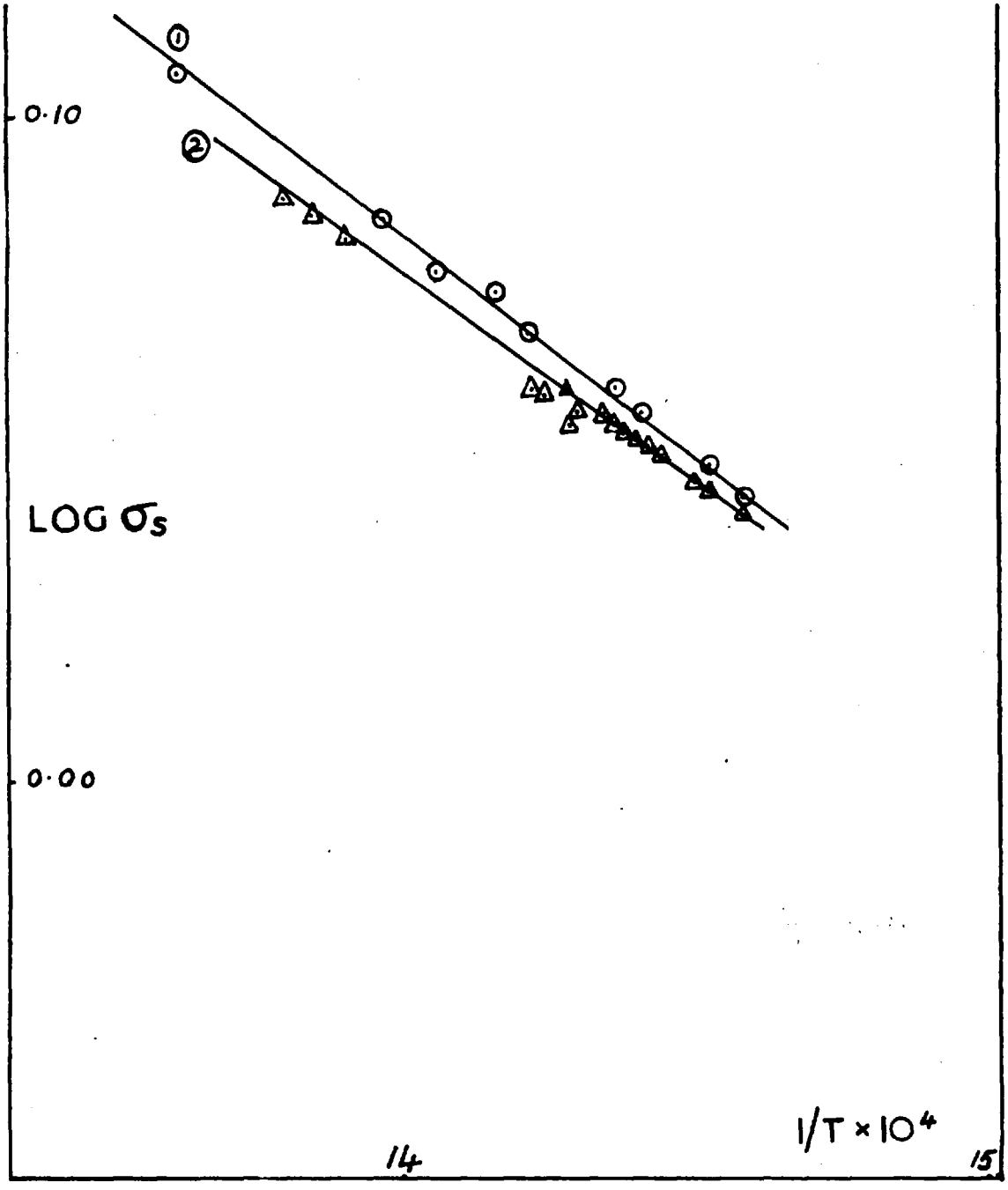


FIG. 8.8

LOG σ_s AGAINST 1/T FOR $K_2Cr_2O_7$ MELT

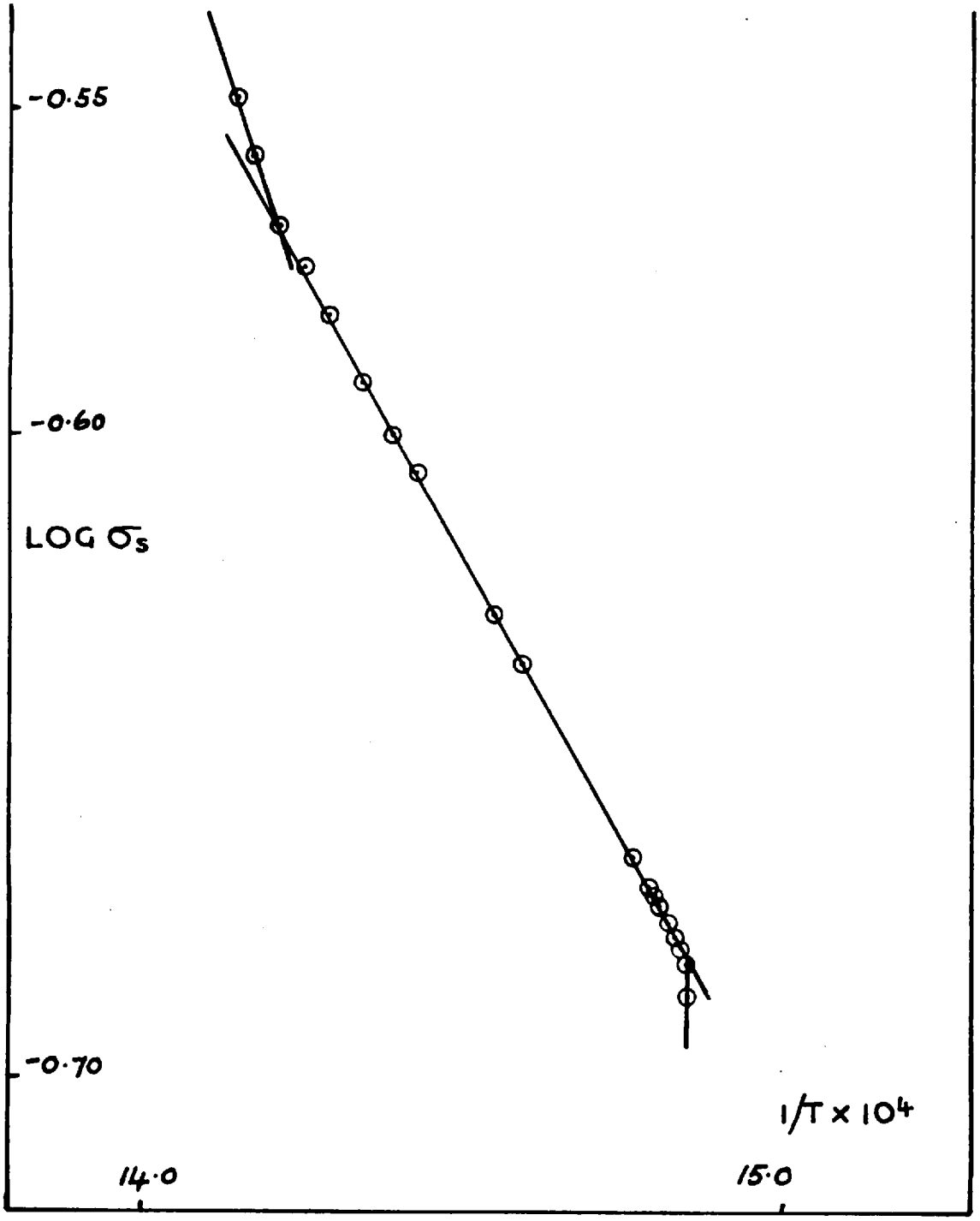
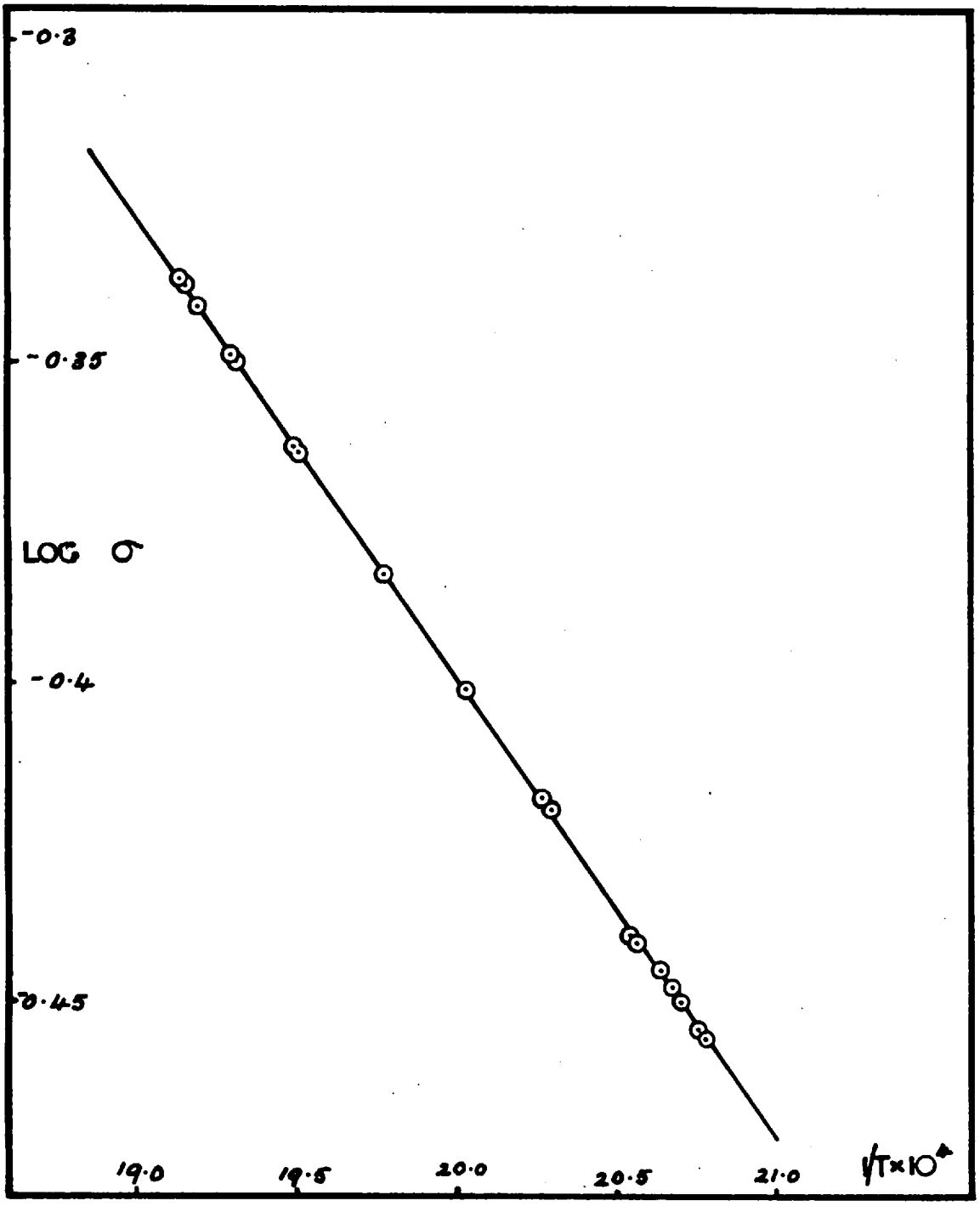


FIG 8.9

LOG σ AGAINST 1/T FOR $TlNO_3$ MELT



The estimated standard deviations of $\log_{10}\sigma$ from the correlation, $\log_{10}\sigma = \log_{10}\sigma_0 + E_\sigma \theta/2.303RT$, together with the correlation coefficient r, and the standard deviation of E_σ, calculated from the variance of the slope, are shown in Table 8.10.

TABLE 8.10

Salt	$S(\log_{10}\sigma)$	$S(E_\sigma)$ cal.	r
$NaNO_2$	6.69×10^{-4}	23.61	0.999
KNO_2	1.14×10^{-3}	5.63×10^{2}	0.97
$K_2Cr_2O_7$	1.50×10^{-3}	79.16	0.999
$TlNO_3$	3.76×10^{-4}	5.995	0.9999

References.

1. Phipps and Partridge, J.A.C.S., (1929), 51, 1331.
2. Moss, M.Sc. Thesis Queen's University, Belfast (1954).
3. Jones and Bradshaw, J.A.C.S. (1933), 55, 1780.

CHAPTER 9.

Gas Solubility in Ionic Melts.

9.1 Selection of Systems.

As discussed earlier, Section 1.4.3, the addition of a divalent cation to a salt having a monovalent cation and common anion, providing it forms a solid solution, will create a vacant cation site for each divalent cation added. This is the basis of the well known "Wagner" effect for the electrical conductivity in the solid. Similarly, the addition of a salt with a common cation and a divalent anion will produce a vacant anion site. Though no evidence has been found in the literature it might be expected to exhibit similar behaviour to that containing a vacant cation site. In extending this to the liquid state the careful selection of the divalent additives is essential. In this study of sodium, potassium and caesium nitrate, in order to ensure that the effect of the additive was one of charge divalent cations were selected which were close to the monovalent cation in ionic radius. This led to the selection of $Ba(NO_3)_2$ as the additive in the study of KNO_3 and to $Ca(NO_3)_2$ as the additive in the study of $NaNO_3$. Table 1.2 shows the relative sizes of divalent and univalent cations. These divalent cations were selected on the assumption that if the liquid quasi crystalline lattice is controlled primarily by the

anion, then the addition of a divalent cation much smaller or larger than the cation already there would introduce a spatial effect by distorting the lattice.

The solubility of H_2O in the systems $NaNO_3$, KNO_3, $CsNO_3$, $NaNO_3$ - $Ca(NO_3)_2$, KNO_3 - $Ba(NO_3)_2$, KNO_3 - K_2SO_4, KNO_3 - $K_2Cr_2O_7$ and $CsNO_3$ - $Ba(NO_3)_2$ has been examined by a cryoscopic technique.

9.2 Materials.

$NaNO_3$	B.D.H. A.R. grade
$NaNO_3$	Judactan W.A.B.A.
KNO_3	B.D.H. A.R. grade
KNO_3	Judactan W.A.B.A.
$CsNO_3$	Judex
$Ba(NO_3)_2$	Judex A.R. grade
$Ca(NO_3)_2$	B.D.H. anhydrous
K_2SO_4	B.D.H. A.R. grade
$K_2Cr_2O_7$	B.D.H. A.R. grade
H_2SO_4	Hopkins and Williams A.R. grade

Table 9.1 shows the manufacturers specification for these materials.

TABLE 9.1

Specification of Chemical Materials.

	$NaNO_3$	KNO_3	$Ba(NO_3)_2$	K_2SO_4	$Ca(NO_3)_2$	$CsNO_3$ b)	$K_2Cr_2O_7$	KNO_3 a)
Chloride (Cl)	0.0004	0.0005	<0.0005	0.0005	0.005	-		0.0005
Alkali free(NaOH)	0.0C2	-	-	-	-	-		
Iodate (IO_3)	No reaction	No reaction	-	-	-	-		0.00005
Iron (Fe)	0.0001	0.00006	<0.0005	0.0005	0.001	-		0.0002
Lead (Pb)	0.0002	0.0002	<0.001	0.001	0.001			0.0004
Nitrite (NO_2)	No reaction	No reaction	-	-	-			0.0001
Phosphate (PO_4)	No reaction	0.0004	-	-	-			0.001
Sulphate (SO_4)	0.0001	0.0005	-	-	0.02			0.005
Reaction 10% soln.	-	pH 7.0	-	-	-			
Not ppt. by H_2SO_4	-	-	< 0.1%	-	-			
Reaction 5% soln.	-	-	pH 6.0-7.0	-	-			
Free acid	-	-	-	0.1ml N/1	-			0.05ml N/1
Free alkali	-	-	-	0.1ml N/1	-			0.05ml N/1
Calcium and Magnesium(Ca+Mg)	-	-	-	0.01	-			
Sodium (Na)	-	-	-	0.05	-			0.02
Total Nitrogen (N)	-	-	-	0.001	-			
Magnesium					0.05			0.001

See Table 6.1

a) - BDH

b) - No assay available but overall purity quoted by manufacturers as 99.8% (Manufacturers:- General Chemicals and Pharmaceuticals Limited)

9.3 Preliminary Treatments.

The ancillary apparatus, thermostat bath and controller, thermocouples etc., and their use have been previously described in Chapter 6.

The drying of the principal compounds, $NaNO_3$, KNO_3 and $CsNO_3$ was by the same technique as described in Section 6.4. Other salts were dried in air at 280°C over several days - usually not less than 1 - 2 weeks. $Ca(NO_3)_2$ was dried in air at 280°C for several weeks. Further drying of samples was achieved in the cryoscopic apparatus by passing **dry nitrogen for 24 hours before** any determination of the freezing point was made.

9.4 Cryoscopic Apparatus.

The apparatus, Fig. 9.1, was designed to allow arrests of a reasonable length on the temperature time plot. It consisted of an inner pyrex tube 3.5 cms. in diameter surrounded by an outer pyrex jacket 5.5 cms. in diameter. The inner tube was fitted into the outer jacket through a B40 standard joint. The B.34 coned cap carried a standardised thermocouple in a sheath fitted through a B.10 standard joint, an entry for a spiral oscillating stirrer, and a fine glass tube used as the gas inlet. Later a further inlet tube was provided for the insertion of a platinum nucleating device or water injection syringe. The stirrer was a long glass rod coiled at its lower end. Several short lengths of soft iron wire were sealed into a pocket at its upper end. The stirrer was

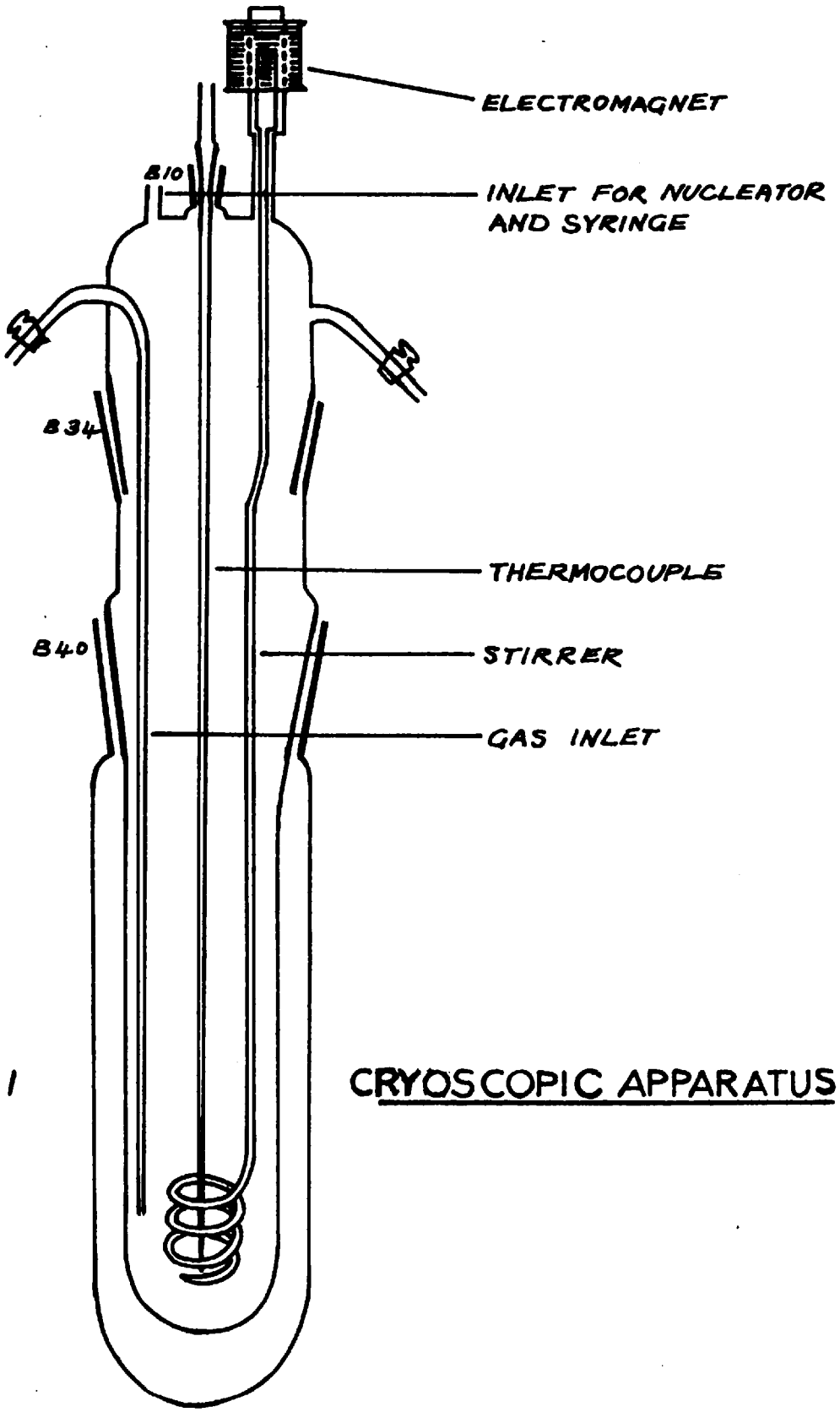


FIG 9.1 CRYOSCOPIC APPARATUS

driven magnetically at a speed of 120 oscillations per minute by means of a solenoid of copper wire 3,000 ohms resistance, working through a make and break control from a D.C. mains supply of 230 V.

The make and break device consisted of a synchronous motor driving a 10 or 20 toothed wheel at 6 r.p.m. This toothed wheel closed two electrical contacts supplying current to the solenoid as each tooth came in contact with them. The 10 and 20 toothed wheel provided for stirrer speeds of 60 and 120 oscillations/min. respectively, the latter being the most frequently used.

The thermocouple sheath served to protect the thermocouple from the melt and also acted as a guide for the stirrer. The gas flow to the apparatus was controlled after it had issued from the cylinder by a fine needle valve (supplied by Edwards), and again just before entry to the apparatus by a glass stopcock. The gas inlet extended to within 3 mm. of the bottom of the inner tube and was drawn out at its tip to a diameter of 1 mm. A tap was fitted on a side arm coming from the B.34 cone cap. This was designed to be used as an exit for the gas or as a point for the evacuation of the apparatus. Both this tap and the tap on the gas inlet tube were lubricated with Edwards high temperature Apiezon T. grease. The gas inlet and outlet arms were sloped downwards to prevent any grease from the taps running into the cell at high temperatures.

P.T.F.E. sleeves (Loughborough Glass Co.) were used on the B.10 and B.34 standard joints because the close proximity of these joints to the bath precluded the use of grease.

The salts to be studied were weighed in the cell after having been air dried as previously described and further dried by the thermal shock technique in situ (Section 6.4). This was carried out over a period of 24 hours. The sample was then brought to a molten state under vacuum, left in this way for 24 hours then covered with an atmosphere of dry nitrogen before putting the B.34 cap in place. A typical sample weighed approximately 40 - 50 gms.

9.5 Measurement of the Freezing Point.

To measure the freezing point the temperature of the sample was first taken to approximately 5° above its freezing point. The sample was then slowly cooled, readings of temperature being taken at regular intervals until it remained steady at the arrest. This is the freezing point. Normally the process was accomplished by setting the bath to control to approximately 2° below the expected freezing point of the sample and taking temperature readings at minute intervals. This allowed a cooling rate of approximately 0.2 - 0.3^{o} per minute. However, for reasons that will be explained, this was reduced in some cases to rates of 0.1^{o} per minute. Throughout this process the stirrer was kept in motion.

At one stage a nucleating device was introduced when it was thought that erratic freezing points of $NaNO_3$ were due to the formation of a metastable phase. This consisted of a long pyrex glass rod with a platinum wire sealed into the end on which a small quantity of the pure $NaNO_3$ was allowed to crystallise. This was kept above the surface of the melt by means of a crocodile clip on its shank, and was lowered into the melt when it came near to the freezing point by releasing this clip. Sufficient pure solid was kept on the tip to maintain a centre of nucleation during the separation of solid from the molten sample.

With the pure samples it was possible to obtain long arrests (ca 10 mins) and so it was unnecessary to make any deduction of the true freezing point by extrapolation of the slope after the arrest through the supercooling zone to its intersection with the slope above the arrest, as has been proposed by Keenan[1] (1956). When large quantities of solute had been added the length of the arrests were greatly reduced - in some cases as short as 3 mins. No extrapolations were made here since any such extrapolation is uncertain, and the peak of the arrest showed such good reproducibility (better than $\pm$ 0.05°C) that it was considered more reliable.

9.6 Tests on Rates of Cooling.

Before determining the solubilities of gases in molten salts it was found necessary to examine the effect of the cooling

rate. Two possible precautions might be necessary.

If the starting temperature of the cooling process is high the melt may contain a non equilibrium concentration of gas at the freezing point. If the solubility increases with temperature this will lead to a high value for the solubility as determined at the freezing point. If on the other hand the solubility decreases with rise of temperature a value of the gas solubility at the freezing point will be determined which is lower than the equilibrium value. Two precautions are indicated:

(i) A starting temperature very close to the freezing point must be used to ensure that the solubility at this temperature is not far removed from the equilibrium value at the freezing point.

(ii) A very slow rate of cooling is desirable to enable the equilibrium to be maintained throughout the fall in temperature.

To check this the freezing point of KNO_3 under moist nitrogen was determined using cooling rates of $0.3^{\circ}C$ per min. and $0.1^{\circ}C$ per min. starting from temperatures $2^{\circ}C$ and $5^{\circ}C$ above the freezing point. Similar values were obtained in each case to within $\pm 0.05^{\circ}C$.

9.7 Purity of Solute and Solvent.

The solvents used were purer than analytical reagent grade.

A criterion of solvent purity is normally taken to be the freezing point, the higher the freezing point the purer the sample. In the present investigation it was found that an added criterion was the reproducibility found in successive runs where different samples approximated to the same freezing point.

TABLE 9.2

Freezing Points ^{o}C of Different Samples of KNO_3

Judactan (W.A.B.A.)	B.D.H. Analar.
334.95	334.15
335.00	334.30
334.93	334.40

9.8 Drying of the Gas.

The gases used were N_2, O_2 free (British Oxygen Company) O_2 (British Oxygen Company) and CO_2.

Both O_2 and N_2 were fed from the cylinder through a needle valve for fine control and then passed through a glass wool filled drying tube immersed in liquid air before being admitted to the cell. The necessity of taking the greatest precautions with drying the gases before admittance to the cell is exemplified by the following, showing the difference in results obtained using $CaCl_2$ as a drying agent and drying by freezing out H_2O in a cold trap. Passing the

gas (N_2) through a 4 ft. drying column containing $CaCl_2$ before admitting to the cell gave a freezing point for KNO_3 of 334.85 ± 0.05°C, using the glass wool filled trap immersed in liquid air gave 334.95 ± 0.05°C. These values were obtained by determining the freezing point using a trap immersed in liquid air and then repeating having replaced this by a drying column containing $CaCl_2$ and again with a trap in liquid air. The values for the freezing point noted above were obtained.

During examination of the solubility of H_2O in these melts the H_2O was admitted to the melt entrained in a stream of N_2. The H_2O vapour pressures were controlled by either saturating the nitrogen stream at different temperatures by bubbling through water or by bubbling through H_2SO_4 containing various proportions of added water at a fixed temperature.

The temperature control was achieved by immersion of the saturating apparatus in a Townson and Mercer water filled thermostat bath. This gave temperature control of ± 0.03°C. 0°C was obtained by immersing the saturators in an equilibrium mixture of distilled water and crushed ice formed from distilled water.

9.9 The Saturators.

The nitrogen was saturated with water vapour by passing through a series of water filled tubes. The first was a 12" long pyrex tube filled to a depth of 7" with water over a sintered glass disc porosity 1. This was followed by passing through three water

filled bubblers and finally through a tube, similar to the first, containing glass wool.

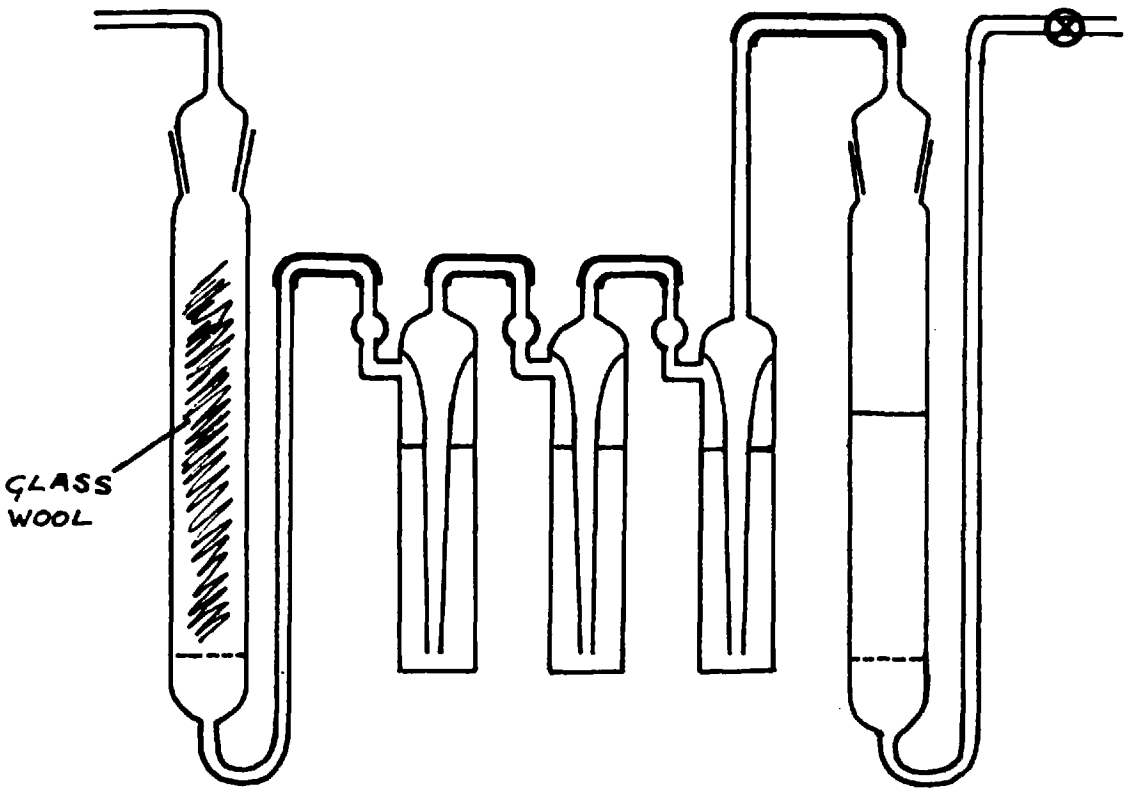
Preliminary determinations of the freezing point of $NaNO_3$ using variations of the above system but without the tube containing glass wool were unsatisfactory due to their erratic nature. This was thought to be due to excess water in the form of fine droplets in the nitrogen stream. Regularity of results was subsequently obtained by the addition of the tube containing glass wool. Fig. 9.2 shows the arrangement of saturators finally used. All connections were made with P.V.C. tubing and kept as short as possible.

With H_2O in the saturators control temperatures of 0, 15 and 20°C were used. 70, 60, 40 and 30% w/w solutions of H_2SO_4 in water were used at temperatures of 0 and 15°C. This made available partial pressures of H_2O of 0.154, 0.205, 0.506, 0.686, 2.55, 3.43, 4.579, 7.27, 9.65, 12.788, and 17.535 mm Hg. The vapour pressure above the H_2SO_4 solutions was taken to be due entirely to H_2O, cf. Table 9.3 which shows the contribution of H_2SO_4 to the vapour pressure at high concentrations[2].

TABLE 9.3

% H_2SO_4	Temp. °C	Partial Pressure mm.Hg.
89.25	183	0.5
91.26	191	0.6
95.06	180	2.1

FIG 9.2 SATURATORS



9.10 Solid Solutes.

Solid solutes were introduced into the cell by means of a long thistle funnel so placed that its end was about 1 cm. above the surface of the molten sample. A weighed quantity of the solid solute was added to the solvent by means of this funnel. To ensure accurate weight determination the funnel was weighed before and after use; a correction could then be applied for any solute which had lodged in the funnel.

To ensure thorough mixing the melt was stirred for some time before determining the freezing point, normally about half an hour. The weight of solute was determined to $\pm$ 0.0001g. The magnitude of the additions will be indicated in the relevant sections, but in general it did not exceed a total of 5 mole %. Approximately 40 - 50 g. of solvent were used. This allowed greater accuracy in the additions since a small percentage addition became a weight of reasonable proportion. Solvent weights were known to $\pm$ 0.01 g.

9.11 The Systematic Study of Nitrate Systems.

From depression of the freezing point measurements, it was concluded that in all the nitrate melts the solubility of the gases N_2 and O_2, and CO_2 in $NaNO_3$ melt was less than the minimum detectable which was approximately 10^{-4} moles H_2O/mole melt.

In subsequent work the freezing point of the dry melt was determined in an atmosphere of dry nitrogen followed by

determination in an atmosphere of nitrogen containing a known moisture content in order to determine the solubility of H_2O at this known partial pressure of H_2O. The freezing point as determined in an atmosphere of dry nitrogen was regarded as the absolute freezing point and subsequent depressions were attributed to the solubility of H_2O in the melt. The freezing point was then redetermined in an atmosphere of dry nitrogen after sweeping out dissolved water with dry nitrogen. This was used as a test for decomposition. In calculating the solubility from the depression of the freezing point, two assumptions were made:

i) H_2O dissolved in the melt without dissociation.

ii) H_2O did not dissolve in the separating solid i.e. there was no solid solution of H_2O in the solid salt.

Table 9.4 summarises the solubility of H_2O in pure alkali nitrate melts and in alkali nitrate melts containing a divalent cation or anion.

TABLE 9.4

Salt Melt	Solubility H_2O moles H_2O/mole melt x 10^4
$CsNO_3$	9.23
$CsNO_3$ + 4.33 Mole % $Ba(NO_3)_2$	6.28
KNO_3	3.86
KNO_3 + 0.94 Mole % $Ba(NO_3)_2$	5.97
KNO_3 + 4.17 mole % $Ba(NO_3)_2$	4.21
KNO_3 + 1.91 mole % $K_2Cr_2O_7$	5.97
$NaNO_3$	1.41
$NaNO_3$ + 4.02 mole % $Ca(NO_3)_2$	2.04

9.12 Results

An outline of the procedure adopted in the measurement of H_2O solubility in each system is given here with fuller details in Appendix III.

9.12:1 Systems Based on $CsNO_3$.

The H_2O solubility in molten $CsNO_3$ and $CsNO_3$ + 4.33 mole % $Ba(NO_3)_2$ was measured. Little difficulty was experienced in this system. The absence of any significant solid solution of $Ba(NO_3)_2$ in $CsNO_3$ was shown by comparing the depression of the freezing point of $CsNO_3$ produced by 4.33 mole % $Ba(NO_3)_2$ with that calculated from the independently determined value for the heat of fusion of Mustajoki [3] (1957). This value of H_f = 3.37 Kcal/mole has been used throughout in the calculation of the H_2O solubilities:

$$\Delta T_{f_{expt.}} = 14.75^{\circ}C \quad \Delta T_{f_{calc.}} = 12.0^{\circ}C.$$

Figs. 9.3 and 9.4 show typical cooling curves for these systems.

9.12:2 Systems Based on KNO_3.

The solubility of H_2O in pure KNO_3 was determined. Because of the extremely low value for the freezing point depression recorded it was decided to confirm this depression by approaching the equilibrium value from the supersaturated side. To do this a long fine glass tube was let in at the top of the cell and the tip lowered below the surface of the melt. To this was connected a syringe filled with distilled water. About 0.55 ccs. were injected into the melt in this way. This was repeated.

After the first injection of H_2O the freezing point of the KNO_3 was measured at intervals while sweeping the melt with dry N_2. After the second injection the freezing point was determined at intervals while sweeping the melt with N_2 containing H_2O of 18.4 mm. Hg partial pressure. The greater part of the H_2O added in this way was immediately expelled, though a large quantity was retained for a reasonable length of time. Flushing out with N_2 rapidly removed most of the dissolved H_2O but the last traces were most tenaciously held. Typical cooling curves are shown in Fig. 9.5.

As a first step in the measurement of the solubility of H_2O in KNO_3 containing $Ba(NO_3)_2$ the freezing point of KNO_3 containing varying quantities of $Ba(NO_3)_2$ was determined. Fig. 9.6 shows

FIG. 9.3

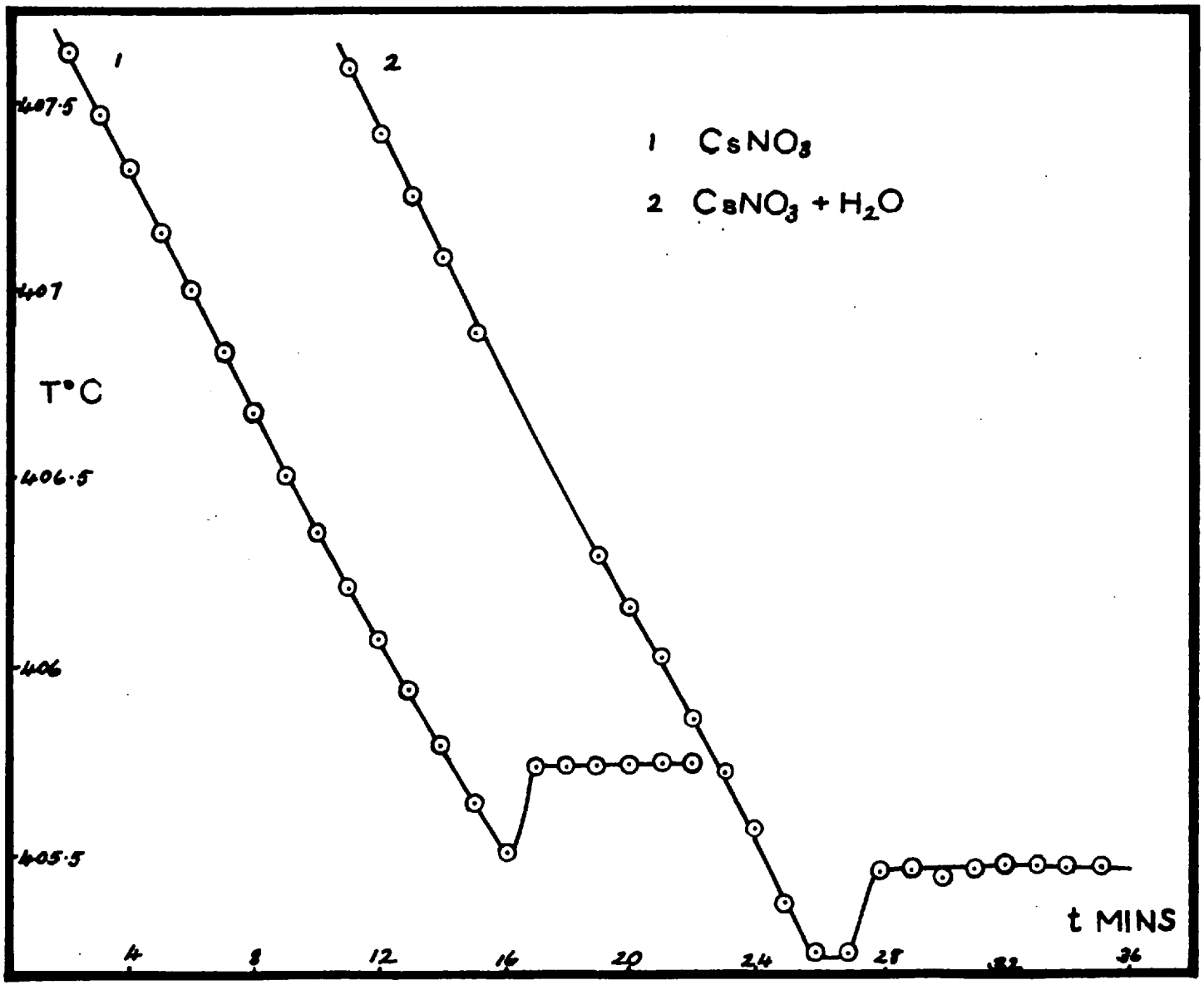

1
2
407·5
407
T°C
406·5
406
405·5
1 CsNO3
2 CsNO3 + H2O
4
8
12
16
20
24
28
36
t MINS

FIG. 9.4

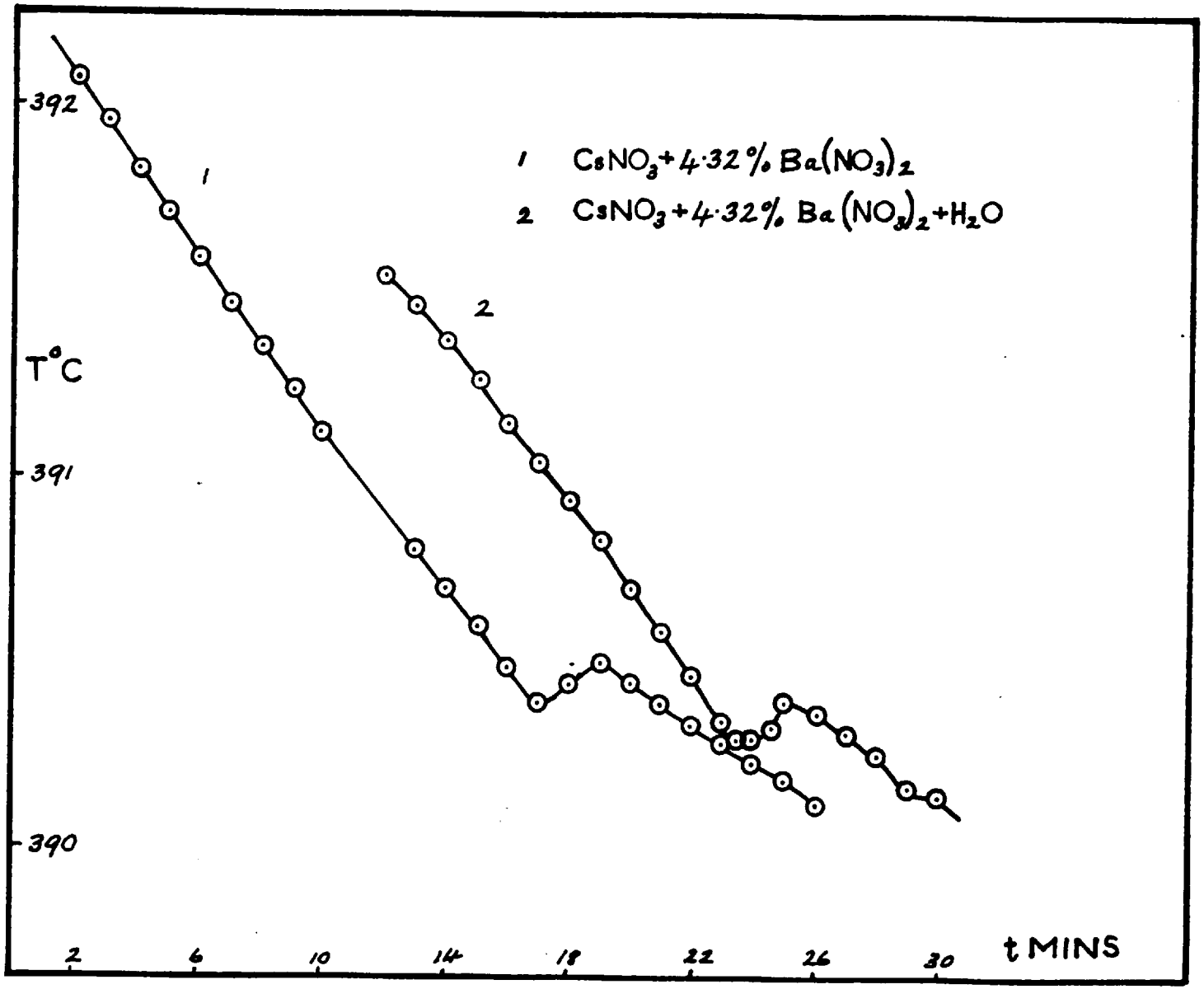

392
391
390
T°C
1
2
1 $CsNO_3$+4·32% $Ba(NO_3)_2$
2 $CsNO_3$+4·32% $Ba(NO_3)_2$+H_2O
2
6
10
14
18
22
26
30
t MINS

FIG. 9.5

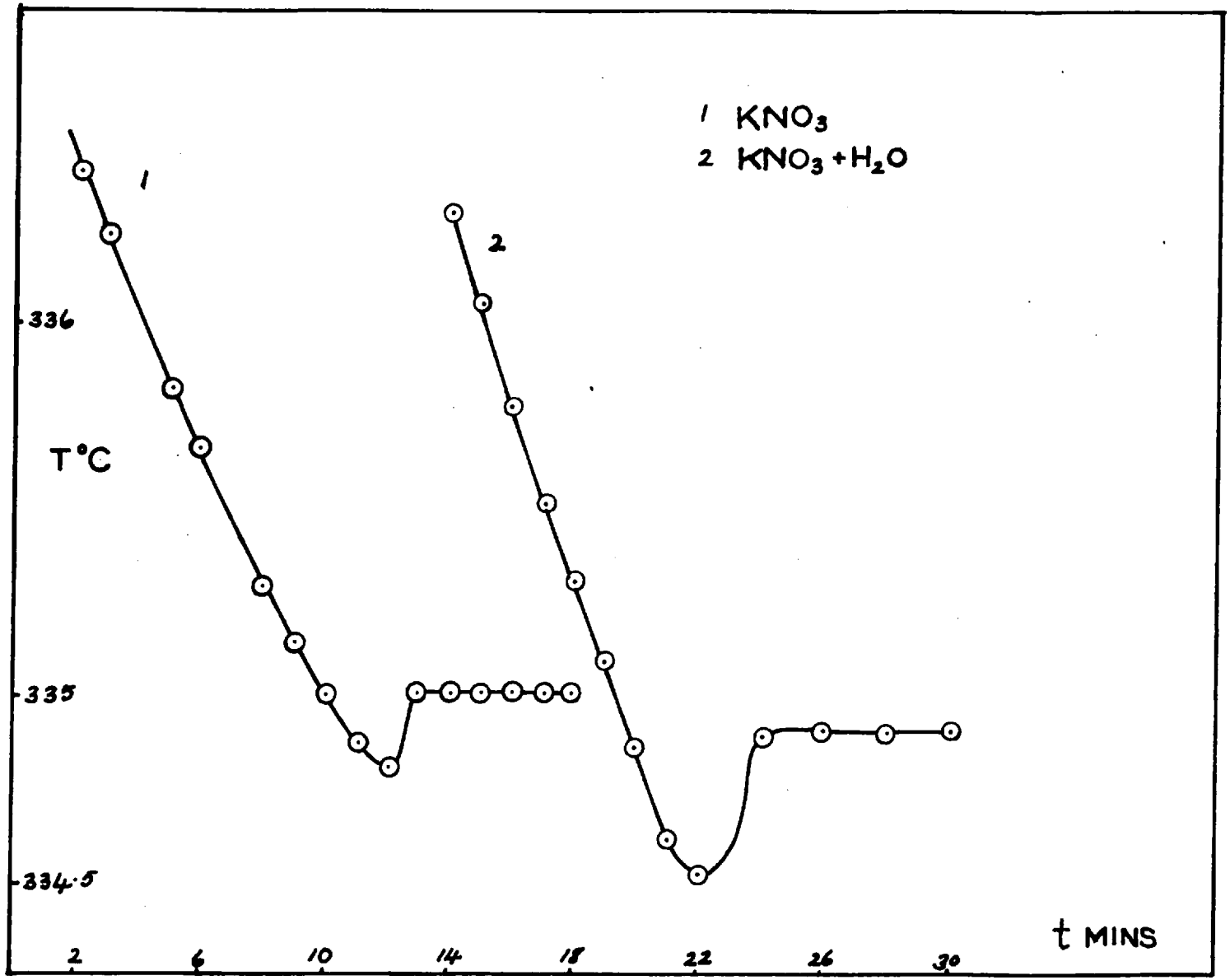
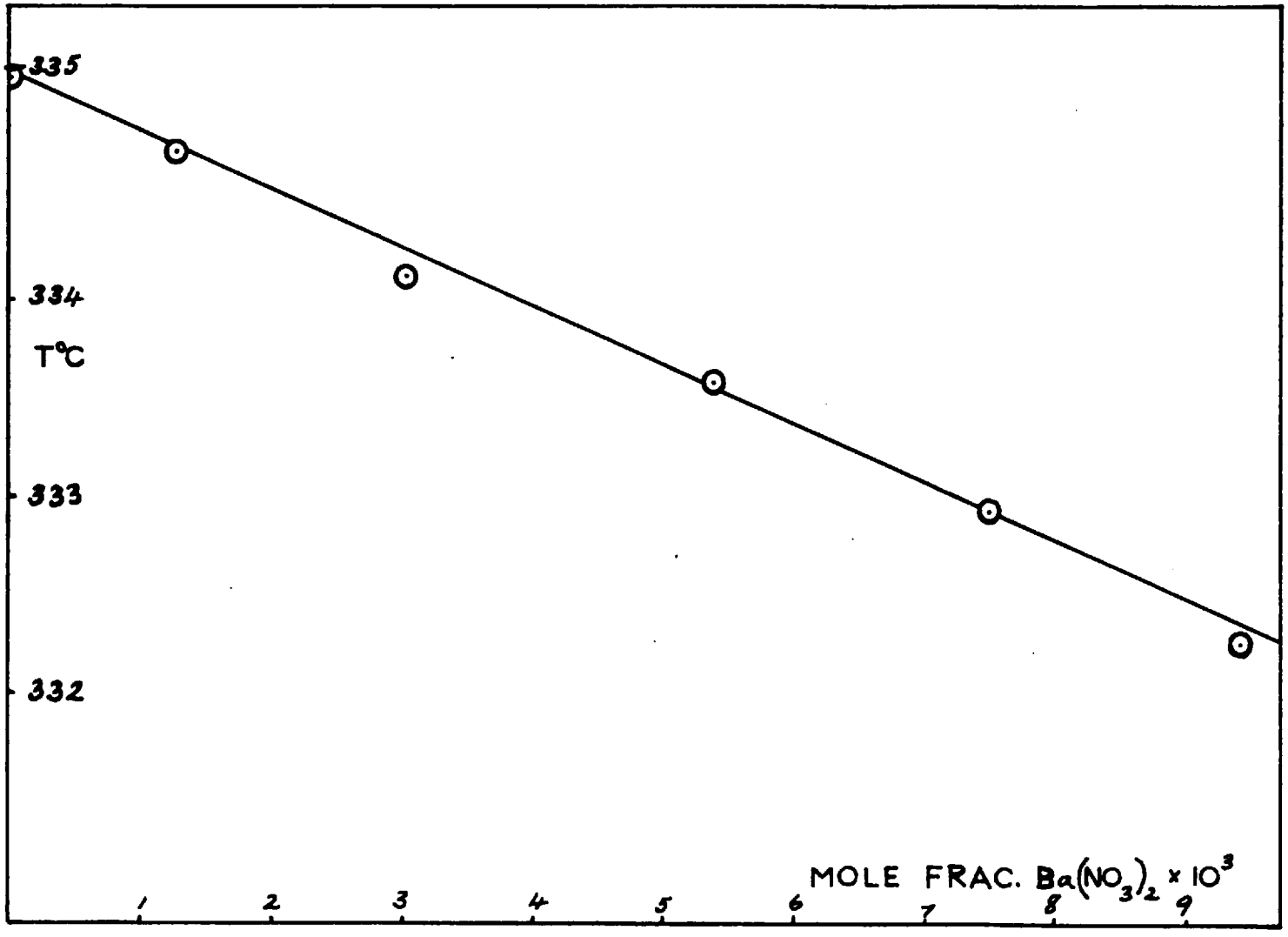


FIG. 9.6 $KNO_3 - Ba(NO_3)_2$



% mole concentration of $Ba(NO_3)_2$ plotted against freezing point. The heat of fusion H_f, derived in this way was 2.57 Kcal/mole (cf. H_f = 2.57 Kcal/mole reported by Goodwin and Mailey [4] 1908 from calorimetric measurements). This indicated absence of solid solution of $Ba(NO_3)_2$ in KNO_3. This value of H_f was used in all calculations of solubility of H_2O in KNO_3 systems.

The solubility of H_2O in KNO_3 containing 0.94 mole % $Ba(NO_3)_2$ and 4.17 mole % $Ba(NO_3)_2$ was determined. In the former N_2 containing H_2O of 4.6 and 18 mm Hg partial pressure was used. No significant difference was observed in the water solubility with the change in partial pressure of H_2O.

The freezing point of KNO_3 was determined after the addition of 2.35 mole % K_2SO_4. The appearance of the melt suggested only partial solution of K_2SO_4. This was confirmed from the value of the freezing point depression of 2.75°C which can be compared with the theoretical value of 6.69°C calculated using a value of 2.57 Kcal/mole for H_f. No further examination of this system was made.

The effect of the presence of a divalent anion on the solubility of H_2O in KNO_3 was therefore studied using $K_2Cr_2O_7$. The freezing point of dry KNO_3 containing 1.91 mole $K_2Cr_2O_7$ was determined. Comparison of the experimental and theoretical values for the depression of the freezing point depression showed the absence of solid solution:

$$\Delta T_{f_{expt.}} = 6.00^{\circ}C \quad . \quad \Delta T_{f_{calc.}} = 5.45^{\circ}C$$

The solubility of H_2O in this system showed no increase over that in pure KNO_3.

9.12:3 Systems Based on $NaNO_3$.

Determination of the solubility of H_2O in fused $NaNO_3$ systems presented the greatest difficulties both experimentally and from the point of view of interpretation. The main conclusion is that solubilities in this melt are much larger.

Pure $NaNO_3$ crystallised in transparent crystals which adhered to the stirrer and the walls of the cryoscopic cell. The strength of this adherance was such that even a stirring rate of 120 strokes/min. was insufficient to dislodge those on the stirrer. The cause of this was not clear but three points were noted:

i) All samples of pure $NaNO_3$ examined behaved in this way.

ii) The addition of even small amounts of impurity reduced this adhesion - $Ca(NO_3)_2$ entirely and $NaNO_2$ partly.

iii) It was not affected by the presence of moisture.

It might be thought that this adhesion was due to the absence of a centre of nucleation but the frequency with which it occurred would seem to preclude this. An alternative suggestion is that $NaNO_3$ can separate as a rather disordered crystal, but since the freezing point determination was accompanied by reasonably long arrests and no marked supercooling, this disorder cannot be as

extensive as that found in a glass.

The solubility of H_2O in pure $NaNO_3$, $NaNO_3$ + $Ca(NO_3)_2$, $NaNO_3$ + $NaNO_2$, $NaNO_3$ + $NaNO_2$ + $Ca(NO_3)_2$ was determined.

The observed depression of the freezing point of $NaNO_3$ containing 4.02 mole % $Ca(NO_3)_2$ can be compared with that calculated using Mustajoki's [3] (1957) value for the heat of fusion of 3.49 Kcal/mole.

$$\Delta T_{f_{expt.}} = 8.13^{\circ}C \qquad \Delta T_{f_{calc.}} = 7.77^{\circ}C$$

In all calculations of H_2O solubility in molten $NaNO_3$ systems this value of H_f, has been used. This showed the absence of appreciable solid solution of $Ca(NO_3)_2$ in $NaNO_3$.

The solubility of H_2O of 21 mm.Hg partial pressure in $NaNO_3$ containing 4.02 mole % $Ca(NO_3)_2$ and 0.089 mole % $Ca(NO_3)_2$ exhibited no significant increase over that in pure $NaNO_3$. However, with moist N_2 the system containing 0.089 mole % $Ca(NO_3)_2$ was marked by a gradual decrease in the apparent freezing point depression over several days, although the freezing point of the system in the presence of dry N_2 remained substantially the same. This suggests a decrease in the H_2O solubility with age of the melt. Analysis of an aged melt showed the presence of slight traces of NO_2^-. A knowledge of the chemistry of nitrates indicates that this is consistent with the decomposition of NO_3^-. This led to an examination of the solubility of H_2O in $NaNO_3$ containing known quantities of

$NaNO_2$ and subsequently to the determination of the solubility of H_2O in $NaNO_3$ containing known quantities of $NaNO_2$ and $Ca(NO_3)_2$. As a first step the formation of solid solutions of $NaNO_2$ in $NaNO_3$ was examined. In Fig. 9.9 the plot of freezing point against $NaNO_2$ concentration shows that marked solid solution takes place.

Thus the systems examined for water solubility were:

(i) Pure $NaNO_3$.

(ii) $NaNO_3$ + 4.02 mole % $Ca(NO_3)_2$.

(iii) $NaNO_3$ + 0.089 mole % $Ca(NO_3)_2$.

(iv) system (iii) with time.

(v) $NaNO_3$ + 1.24 mole % $NaNO_2$.

(vi) $NaNO_3$ + 0.11 mole % $NaNO_2$.

(vii) $NaNO_3$ + 0.11 mole % $NaNO_2$ + 0.046 mole % $Ca(NO_3)_2$.

This systematic examination demonstrated that systems containing $NaNO_2$ had an apparent solubility of H_2O which was less than that found for melts of pure $NaNO_3$ and of $NaNO_3$ containing only $Ca(NO_3)_2$. Details of these results and those in the preceeding sections are collected in Appendix III and discussed in Chapter 11. Typical cooling curves for the systems examined are shown in Figs. 9.7 and 9.8.

FIG. 9.7

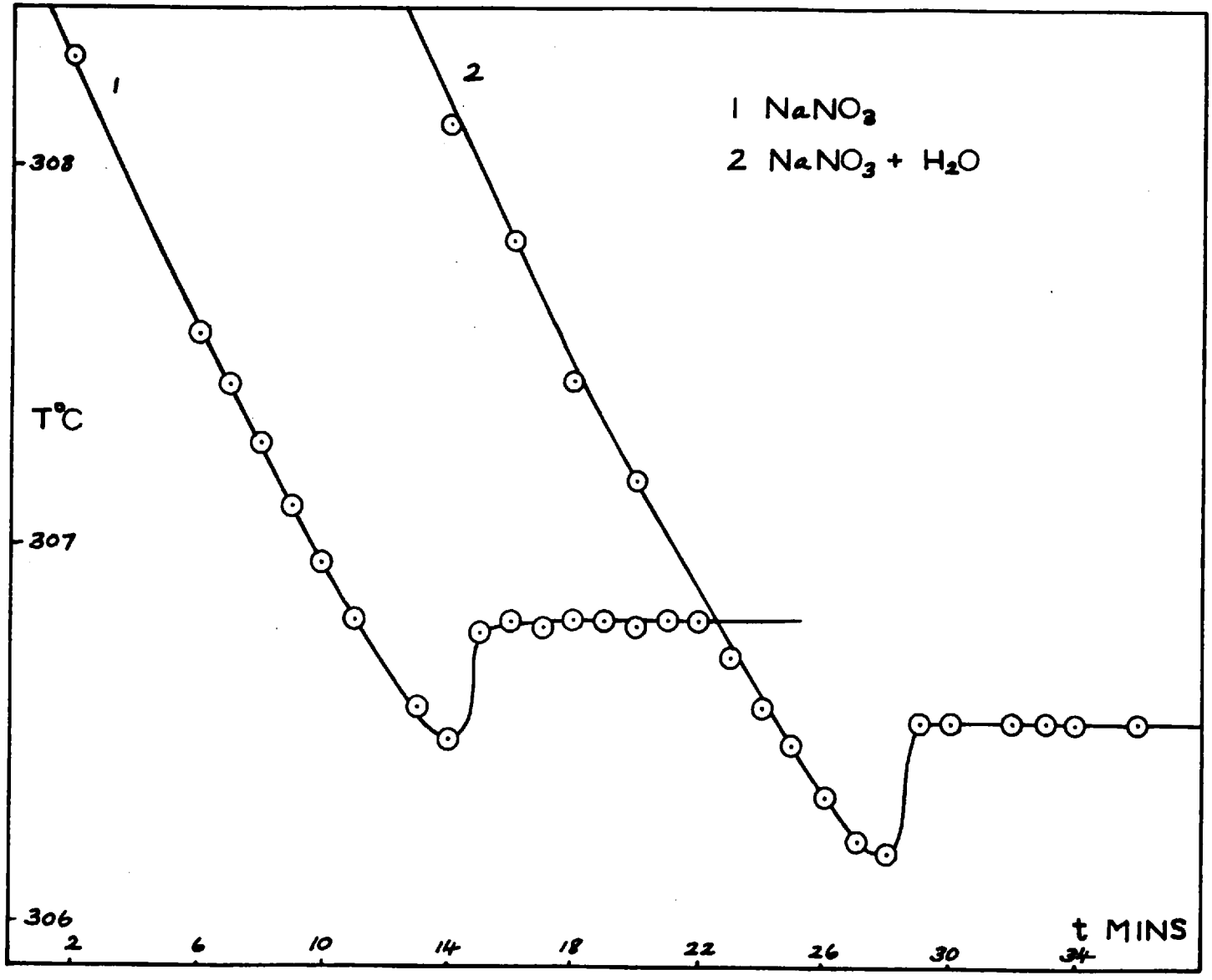


FIG. 9.8

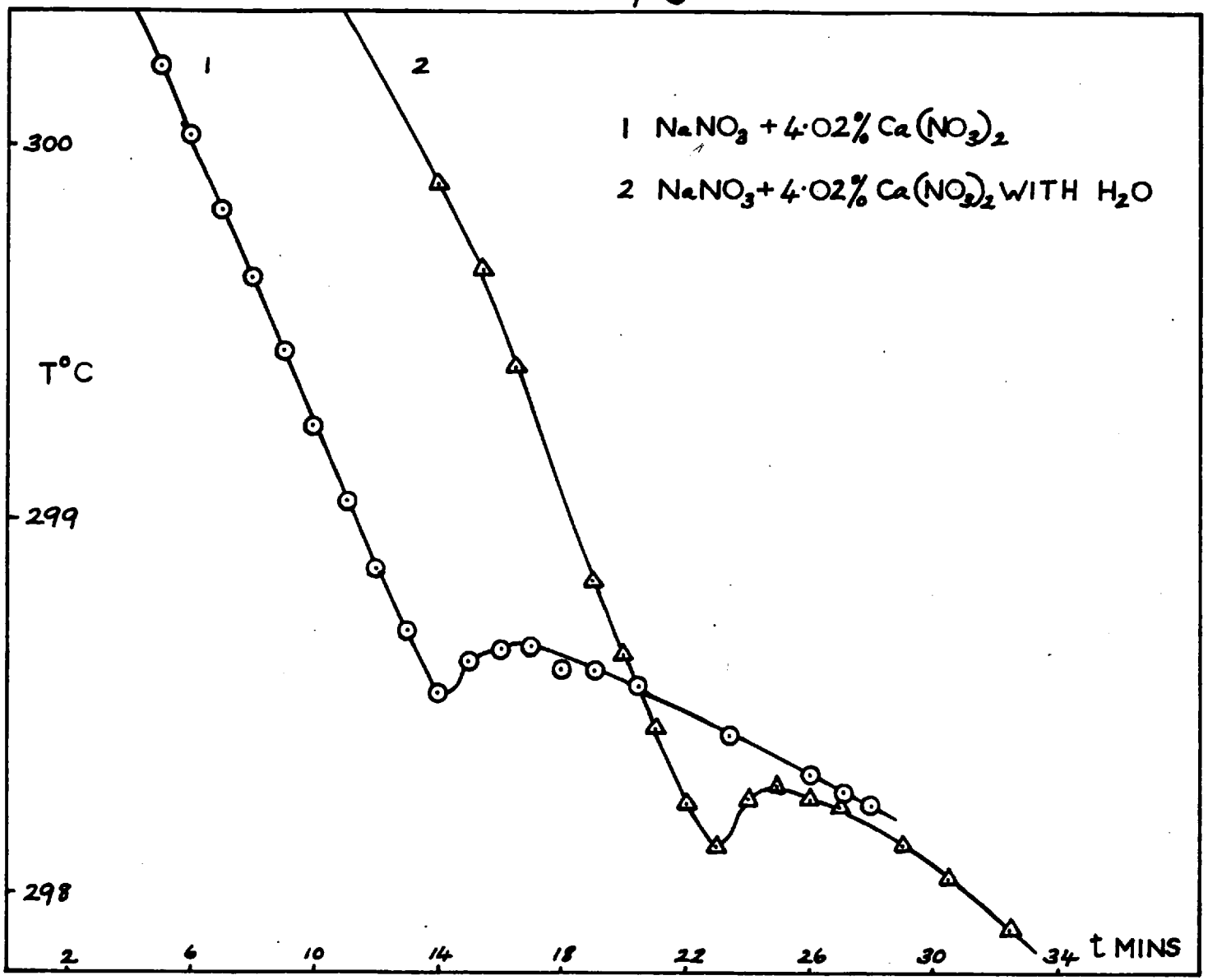
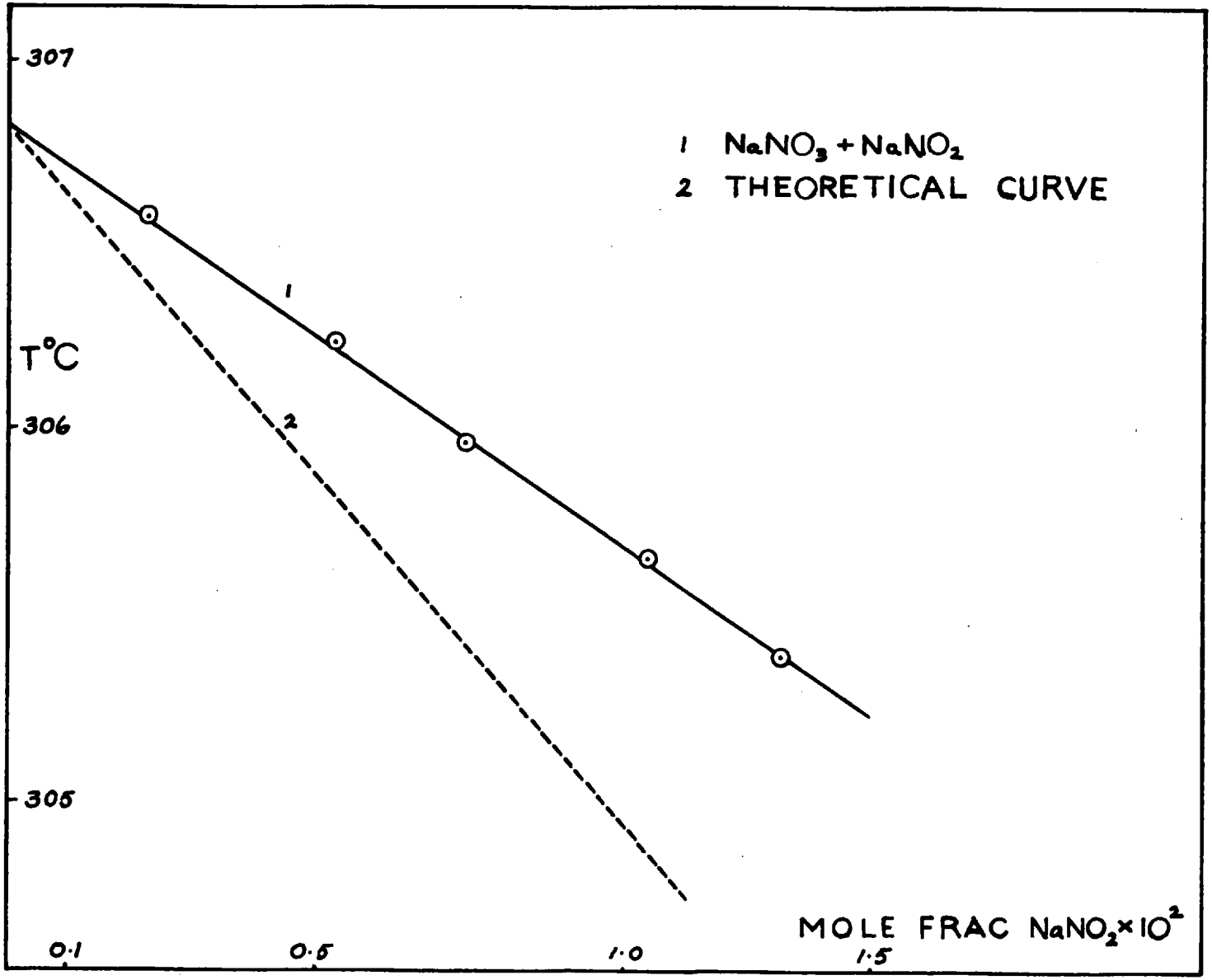

1
2
1 $NaNO_3$ + 4·02% $Ca(NO_3)_2$
2 $NaNO_3$ + 4·02% $Ca(NO_3)_2$ WITH H_2O
300
299
298
T°C
2
6
10
14
18
22
26
30
34
t MINS

FIG. 9.9


307
306
305
T°C
1 NaNO3 + NaNO2
2 THEORETICAL CURVE
1
2
0·1
0·5
1·0
1·5
MOLE FRAC NaNO2 × 10²

9.13 Accuracy of Solubility Determinations.

The accuracy of the solubility determinations depends in the first instance, upon the accuracy of the measurement of the freezing point; in most cases this was of the order of ± 0.03°C, but was found in a few cases to be of the order of ± 0.05°C. This led to accuracies of ± 0.06°C and ±0.10°C in the reproducibility of the actual value of the depression. The final accuracy of the solubility depends also on the actual magnitude of ΔT_f the freezing point depression and on the value of H_f, the heat of fusion.

9.14 Other Results of Interest.

Other work of particular interest in the investigation of gas solubility has been carried out in this department. This includes measurement of the electrical conductivity of pure solid KNO_3 and of the system KNO_3 + $Ca(NO_3)_2$ and the density and electrical conductivity of molten KNO_3 and the system KNO_3 + $Ba(NO_3)_2$.

9.14:1 The Electrical Conductivity of Solid KNO_3.

The conductivity of pure solid KNO_3 has been measured by E. Rhodes [5], using a cell and D.C. method similar to that described in Chapter 8. This was repeated for a sample containing a small amount of $Ca(NO_3)_2$. It was verified from cryoscopic measurements that small quantities of $Ca(NO_3)_2$ of the order of 0.43 mole % form solid solutions with KNO_3.

The plot of log σ against $1/_T$ for pure KNO_3 and KNO_3 +0.43 mole % $Ca(NO_3)_2$ are shown in Fig. 9.10.

There was a rise in the conductivity with the addition of $Ca(NO_3)_2$.

9.14:2 The Electrical Conductivity of Molten KNO_3.

The electrical conductivity of pure molten KNO_3 and KNO_3 containing various quantities of $Ba(NO_3)_2$ has been measured by B. Cleaver [5], using a Wayne Kerr alternating current bridge and a capillary cell similar to that described in Chapter 8. Fig.9.11 shows plots of log σ against 1/T for KNO_3 containing 0, 5, 10 and 22 mole % $Ba(NO_3)_2$. That for $(KNO_3)_2$ containing 22 mole % $Ba(NO_3)_2$ has been extended in Fig. 9.12 to show that part of the log σ against 1/T plot below the freezing point of pure KNO_3.

The energies of activation for temperature ranges close to and well above the freezing point are recorded in Table 9.5

TABLE 9.5

The Activation Energies of Electrical Conductance for KNO_3 + $Ba(NO_3)_2$.

Mole % $Ba(NO_3)_2$	Activation Energy, E_σ, Kcal/mole	
	388-434°C	332-388°C
0	3.38	3.61
5	3.49	3.72
10	3.64	3.80
22	-	3.92

9.14:3 The Specific Volume of KNO_3 - $Ba(NO_3)_2$.

The densities of KNO_3 - $Ba(NO_3)_2$ have been measured by B. Cleaver. Isotherms of density against concentration of $Ba(NO_3)_2$ are shown in Fig. 9.13.

Mean molar volumes have been calculated from these values using the expression $V_m = \frac{M_1 x_1 + M_2 x_2}{d}$.

M_1 and M_2 are the molecular weights; x_1 and x_2 are percentage molar concentration and d is the density.
KNO_3 has been taken as $(KNO_3)_2$. Plots of V_m against % mole composition are given in Fig. 9.14. In both Figs. 9.13 and 9.14 each plot has been represented by a straight line.

References.

1. Keenan, J. Phys. Chem., (1956).
2. Perry, "Chemical Engineers' Handbook" McGraw-Hill N.Y. (1950).
3. Mustajoki, Ann. Acad. Sci. Fennicae, AVI (1957) No.5, No.7.
4. Goodwin and Mailey, Phys. Rev. (1908), 26, 28.
5. Cleaver, Rhodes and Ubbelohde, In Course of Publication.

FIG. 9.10

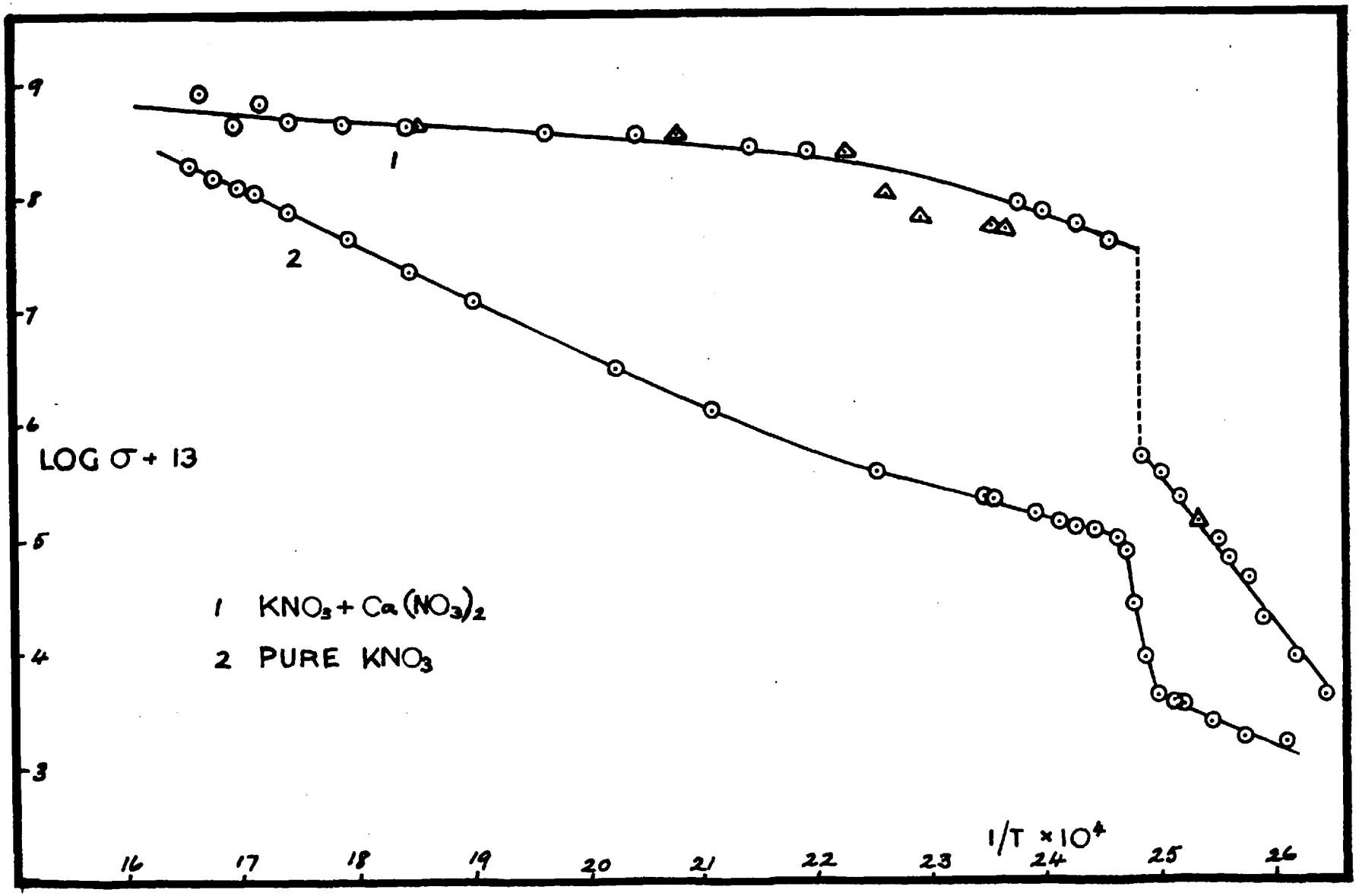

9
8
7
6
5
4
3
LOG σ + 13
1
2
1 KNO3 + Ca(NO3)2
2 PURE KNO3
16
17
18
19
20
21
22
23
24
25
26
1/T x 10⁴

FIG 9.11

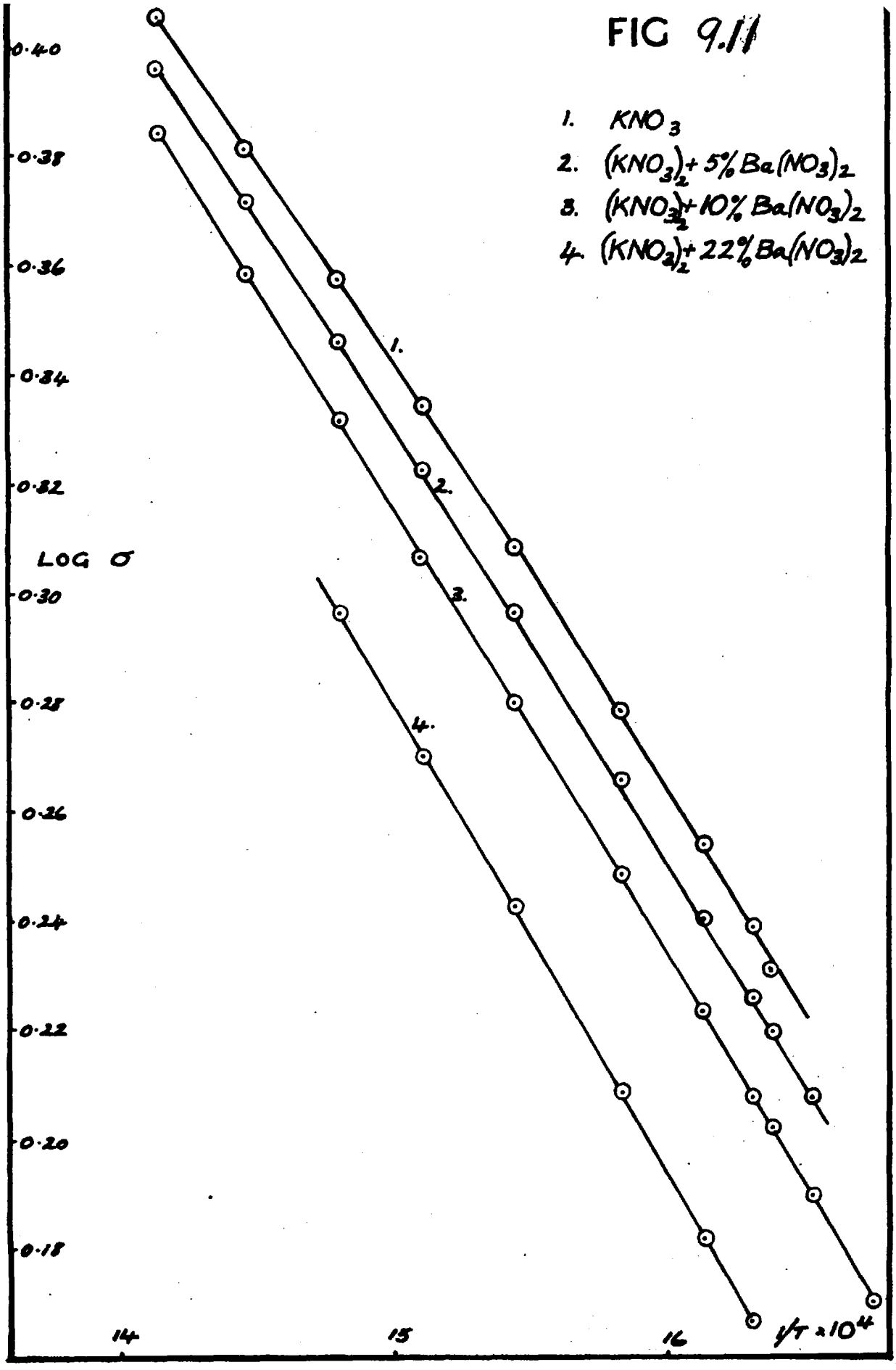

1. KNO_3
2. $(KNO_3)_2$ + 5% $Ba(NO_3)_2$
3. $(KNO_3)_2$ + 10% $Ba(NO_3)_2$
4. $(KNO_3)_2$ + 22% $Ba(NO_3)_2$
LOG σ
0·40
0·38
0·36
0·34
0·32
0·30
0·28
0·26
0·24
0·22
0·20
0·18
1.
2.
3.
4.
14
15
16
1/T ×10⁴

FIG. 9.12

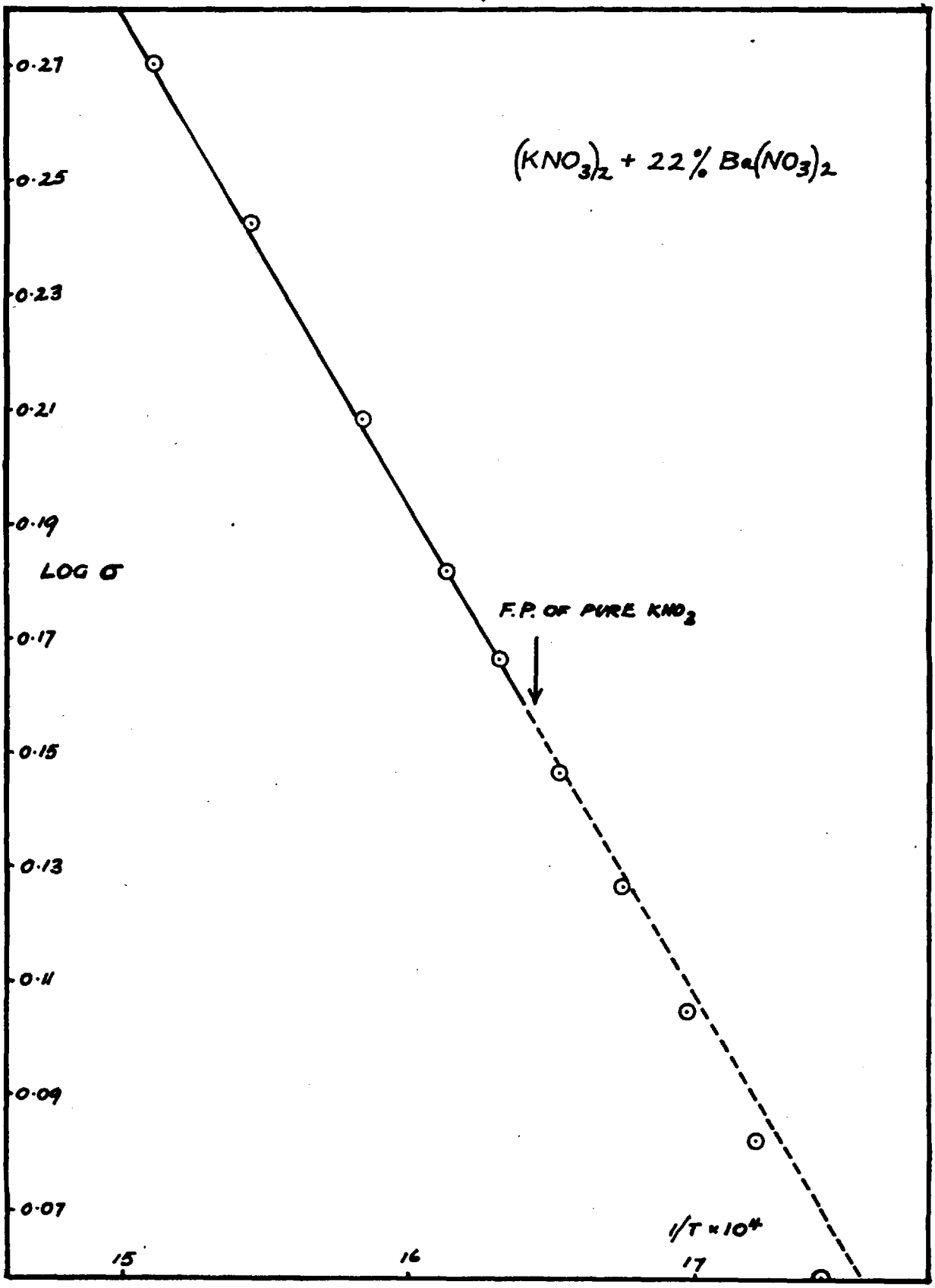

0·27
0·25
0·23
0·21
0·19
LOG σ
0·17
0·15
0·13
0·11
0·09
0·07
$(KNO_3)_2$ + 22% $Ba(NO_3)_2$
F.P. OF PURE KNO_3
1/T × 10^4
15
16
17

FIG. 9.13

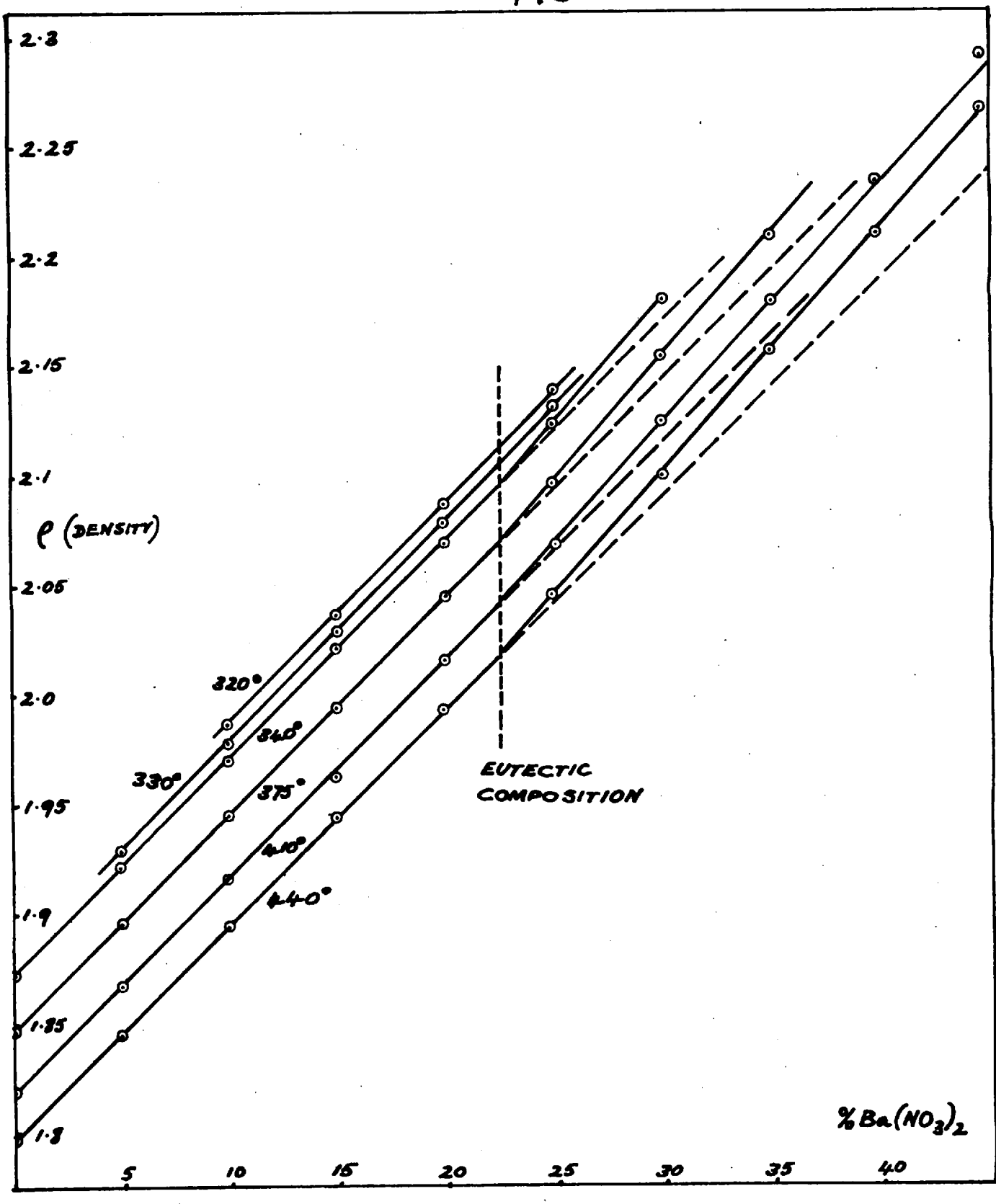
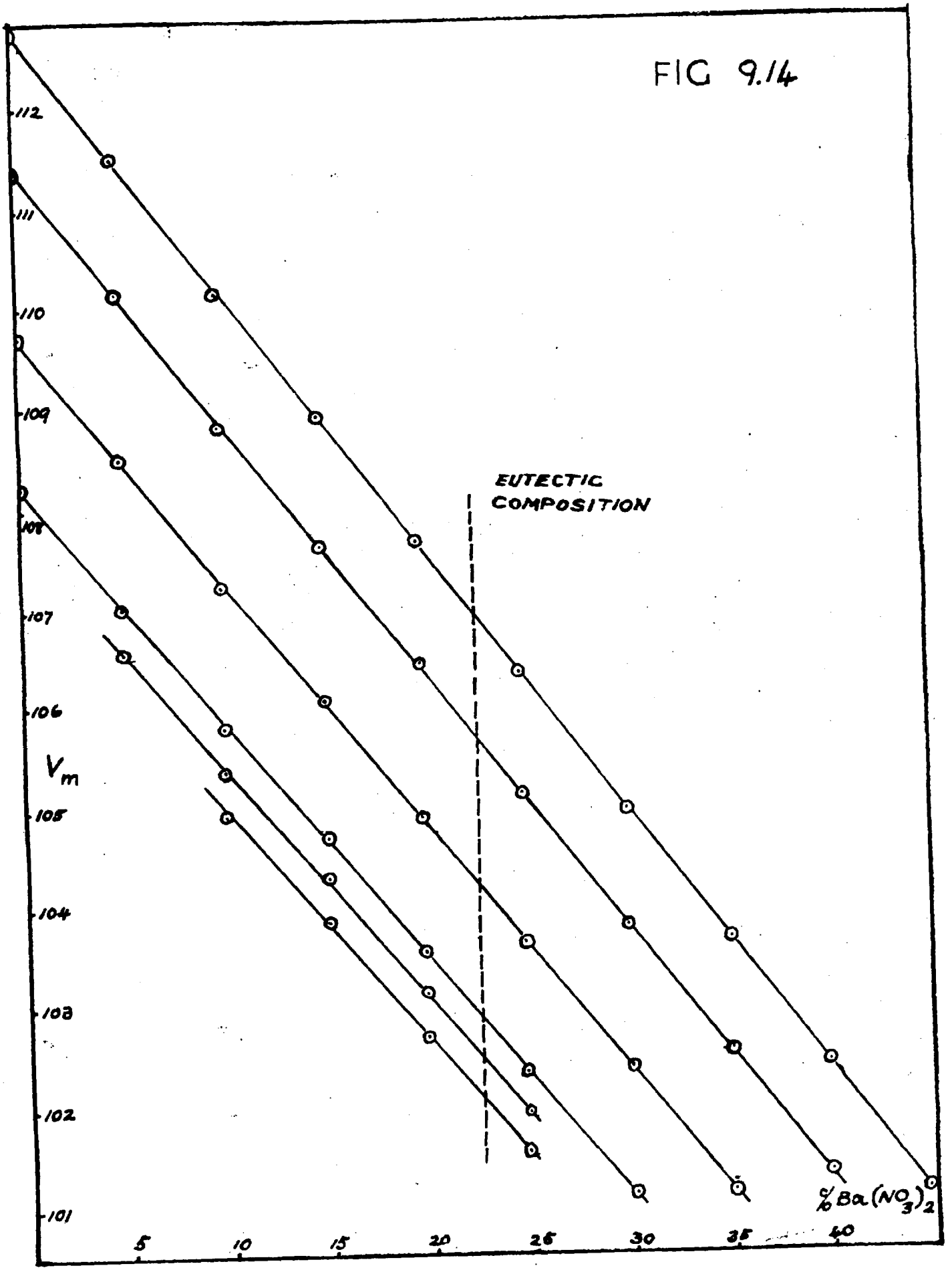

2·3
2·25
2·2
2·15
2·1
ρ (DENSITY)
2·05
2·0
1·95
1·9
1·85
1·8
320°
330°
340°
375°
410°
440°
EUTECTIC
COMPOSITION
% Ba(NO3)2
5
10
15
20
25
30
35
40

FIG 9.14


112
111
110
109
108
107
106
V_m
105
104
103
102
101
EUTECTIC
COMPOSITION
5
10
15
20
25
30
35
40
% $Ba(NO_3)_2$

D I S C U S S I O N

CHAPTER 10

THE STRUCTURAL INTERPRETATION OF ELECTROCHEMICAL AND VISCOSITY MEASUREMENTS.

10.1 Electrical Conductivity of Molten Salts.

The electrical conductivities of KNO_2, $NaNO_2$, $TlNO_3$ and $K_2Cr_2O_7$ in the molten state can be represented by a simple Arrhenius type plot of the form $\sigma = \sigma_0 e^{-E/RT}$ Details of the equation for each salt are given in Chapter 8 with fuller details in Appendix II. The conductances of these salts are similar to those of the alkali halides though slightly lower. $NaNO_2$ and KNO_2 have values of conductance intermediate between those of KBr and RbBr; $TlNO_3$ and $K_2Cr_2O_7$ have values somewhat lower. Table 10.1 compares values for the electrical conductances of different salts near their freezing points. The last column in Table 10.1 shows something of the temperature effect.

TABLE 10.1

Melt	FP°C	T°C close to F.P.	σ ohms^{-1} cms^{-1}	$\frac{\sigma}{T} \times 10^3$
$NaNO_2$	281	282	1.2153	2.19
KNO_2	419	419.3	1.110	1.6
$TlNO_3$	206	208.2	0.3516	0.728
$K_2Cr_2O_7$	398	399.7	0.2079	0.309
NaBr	745	744.0	2.8720	2.82
NaI	659	663	2.2452	2.42
KBr	735	737.8	1.6108	1.59
RbCl	722	729.8	1.5250	1.52

Comparison of the absolute magnitudes of the conductances of fused salts should be made at corresponding temperatures. However, the definition of a corresponding temperature scale is not obvious. Isothermal comparison is not useful since the log σ vs. $1/T$ curve of one salt frequently intersects that of another and such a comparison would thus depend on the temperature selected. Commonly used corresponding temperatures are often based on equal fractions of the critical temperature or at temperatures corresponding to equal vapour pressures. However, neither of these is useful in comparisons in ionic melts since in the case of the alkali halides they are not known with sufficient precision, and in the case of the lower melting alkali nitrates and nitrites decomposition sets in long before the critical temperature. The melting points of these salts are known with a reasonable degree of accuracy and thus these have been used as corresponding temperatures. Yaffe and Van Artsdalen [1] (1956) have defined $\Theta = \frac{T^{o}K}{T_{m}^{o}K}$ (T_m is the melting point) as a corresponding temperature. An example of the use of this form of the corresponding temperature is given above, where the specific conductances have been compared close to the freezing point i.e. at $\Theta = 1$.

Again useful comparison can be made of the pre-exponential term for different salts.

TABLE 10.2

Salt	M.P.^{o}C	σ_o Ω^{-1} cm $^{-1}$	E_σ Kcal/mole.
$NaNO_2$	281	10.9	2.98
KNO_2	419	9.64	2.97
$TlNO_3$	206	10.64	3.26
$K_2Cr_2O_7$	398	73	7.8
$NaNO_3$	307	10.6	2.76
KNO_3	333	11.2	3.49
$RbNO_3$	310	2.09	3.42
$CsNO_3$	414	1.82	2.7
LiCl	613	11.5	1.15
NaCl	801	7.3	1.54
KCl	776	6.5	2.30
RbCl	715	6.5	2.83
CsCl	646	6.6	3.33

Table 10.2 shows that low melting salts with polyatomic anions generally have higher values for σ_o and E_σ than the corresponding salts with inert gas like anions. It would seem that the explanation for this lies in the collapsed structure of the nitrate melts. This collapsed structure would arise from the non spherical nature of the anions which allows them to interlock and draw their corresponding cations closer. Independent evidence for this is offered by the volume change on melting and free volume

in the liquid. The free volume is considered to be largely 'hole' volume. It will be observed from the limited data available for these parameters (Table 10.3) that the salts with polyatomic anions have low volume changes on freezing and small 'hole' volumes. However, no general relationship between the change of volume on melting and the free volume is apparent. This is not surprising since, apart from other considerations, the volume change on fusion of KNO_3 is uncertain and further the data for the free volume, which is claimed could be as much as 50% in error, is well above the melting point.

TABLE 10.3

Comparison of Free Volume and Volume Change on Fusion of Some Ionic Melts.

Salt	M.Pt. °C	$\Delta V/V_s$ %	Ref.	T°C	Free Vol. V_f'	Free Vol. V_f'' (ml.mole^{-1})	$\frac{\Delta V}{V_s V_f'}$	$\frac{\Delta V}{V_s V_f''}$
LiCl	613	26.2	a	700	1.01	0.49	0.259	0.535
NaCl	801	25.0	a	800	0.75	0.42	0.333	0.595
KCl	776	17.3	a	800	0.85	0.51	0.203	0.339
LiBr	547	24.3	a	700	1.05	0.78	0.231	0.312
NaBr	755	22.4	a	800	1.15	0.74	0.195	0.303
KBr	730	16.6	a	800	1.02	0.68	0.163	0.244
$LiNO_3$	255	28.2	b	300	0.16	0.25	1.76	1.125
$NaNO_3$	306	11		307	0.18	0.13	0.611	0.845
KNO_3	333	1	b	333	0.10	0.13	0.10	0.077

a) Sauerwald and Schinke [2] (1956)

b) Derived from the crystal expansion data of Fischmeister (1957) and the volume expansion of the liquid of Jaeger[4] (1917). Free volumes data from Bockris and Richards (1957). (See Section 3).

10.1.1 Calculation of Free Volume

According to the sound velocity method of Kincaid and Eyring (1938) for determining the free volume of a liquid,

$$V_f = \frac{(U_G)^3}{(U_L)} V \quad \ldots\ldots\ldots 10.1$$

U_G is the velocity of sound in the gas phase and U_L that measured in the liquid. This is based on two assumptions,

i) that the sound is transmitted with infinite velocity through a solid particle in the liquid,

and

ii) that the observed finite velocity is due to the time necessary for one ion to travel after impact until it strikes a neighbouring ion. Bockris and Richards[5] (1957) regard the ions as simple harmonic oscillators, so that at maximum velocity, when all the energy is kinetic $\frac{1}{2} mu^2_{max.} = kT$

$$\text{and therefore } u_{mean} = \tfrac{1}{2} u_{max.} = \left(\frac{RT}{2M_i}\right)^{\frac{1}{2}} \quad \ldots\ldots 10.2$$

Thus for a pure molten salt AX, with an effective value of

$M_i = (M_A M_X)^{\frac{1}{2}}$ (10.1) becomes:

$$V_f = \left\{ \frac{1}{U_L} \left\{ \frac{RT}{2(M_A M_X)^{\frac{1}{2}}} \right\}^{\frac{1}{2}} \right\}^3 \quad \ldots\ldots\ldots 10.3$$

This is the V_f'' of Table 10.3

The second measurement of free volume is given by the expression:

$$V_f' = \frac{4\pi a^3}{3v} \left(v^{\frac{1}{3}} - v_o^{\frac{1}{3}} \right)^3 \quad \ldots\ldots 10.4$$

This equation was derived and developed by Collins and Navadi [8] (1954) and Buehler, Wentorf, Hirschfelder and Curtiss[9] (1951).

v_o is the incompressible volume per ion;
a the interionic distance and v the mean volume of an ion. v_o can be calculated from the equation of state proposed by Buehler et al.,

$$P_{tot}\ V \left\{ 1 - (v_o/v)^{\frac{1}{3}} \right\} = RT \quad \ldots\ldots\ldots 10.5$$

P_{tot} is given by $P_{atm} + T\alpha/\beta$ ($T\alpha/\beta$ is the internal pressure). In table 10.3 V_f' was computed using values of 'a', the interionic distance measured at room temperature. The values of free volume obtained using this latter expression are probably preferable to those derived from 10.3 because of the more exact method of deduction used.

10.1.2 Activation Energy and Cation Radius.

Yaffe and Van Artsdalen[1] have found with careful measurement

of the specific conductances of alkali halides that the dependence of σ on temperature is given by $\sigma = \exp\left(A + \frac{B}{T} + CT\right)$ and thus the energy of activation as calculated from the Arrhenius plot will not be constant. The energy of activation will depend on at least two opposing factors

(i) As the melt expands with rising temperature the total coulombic forces among the constituent ions will be reduced and thus the activation energy should decrease.

(ii) As the liquid expands the average number of nearest neighbours is likely to decrease due to the increase in the number of holes and as a result the attractive force per nearest neighbour will rise causing a rise in the activation energy.

This latter effect might be expected to predominate where there is a difference in anion and cation sizes and the former the smaller the disparity. Basically these same conditions should apply to molten nitrates and nitrites. However, no change in E_σ with temperature has been detected. This can be readily understood if it is considered that the anions are close together and that it is the anion-anion contact which dictates the mechanism of the conductance process. That is, whereas in inert gas type ions E_σ might be expected to remain constant when there is a large difference in size between anion and cation, the small cation being

able to move relatively freely because of its size, with polyatomic ions a similar effect will be produced by this interlocking action of the anions. This effect will be supplemented by the much smaller hole volume which will tend to reduce both these mechanisms. Thus it might be expected that a series of alkali salts with polyatomic anions would have relatively high activation energies of similar magnitude, which is in fact the case.

Plots of σ_0 and E_σ against $\frac{r_a}{r_c}$, anion to cation radius ratio, for the chlorides and bromides and the nitrates and nitrites have been made, Figs. 10.1 and 10.2. The anionic radius for the nitrite has been taken as 1.95 $\mathring{A}$ which is larger than NO_3^- (1.89$\mathring{A}$) but of the same size as SCN^-. With the halides it is seen that the energy of activation decreases with cation size but with the polyatomic ions no such regular change is observable. However, one striking feature of the nitrates and nitrites is that their energies of activation are all fairly close to one another (with the exception of $LiNO_3$) which lends support to the suggestion that it is the anion which controls the conductance. The value of E_σ for $LiNO_3$ recorded in Fig. 10.1 is that of Jaeger and Kapma [10] (1920). This is the value found close to the freezing point. Above this E_σ becomes 2.83 Kcal/mole which can be compared with 3.59 Kcal/mole given by Goodwin and Mailey [11] (1908) over the entire temperature range. Either of these values would fall into

FIG 10.1

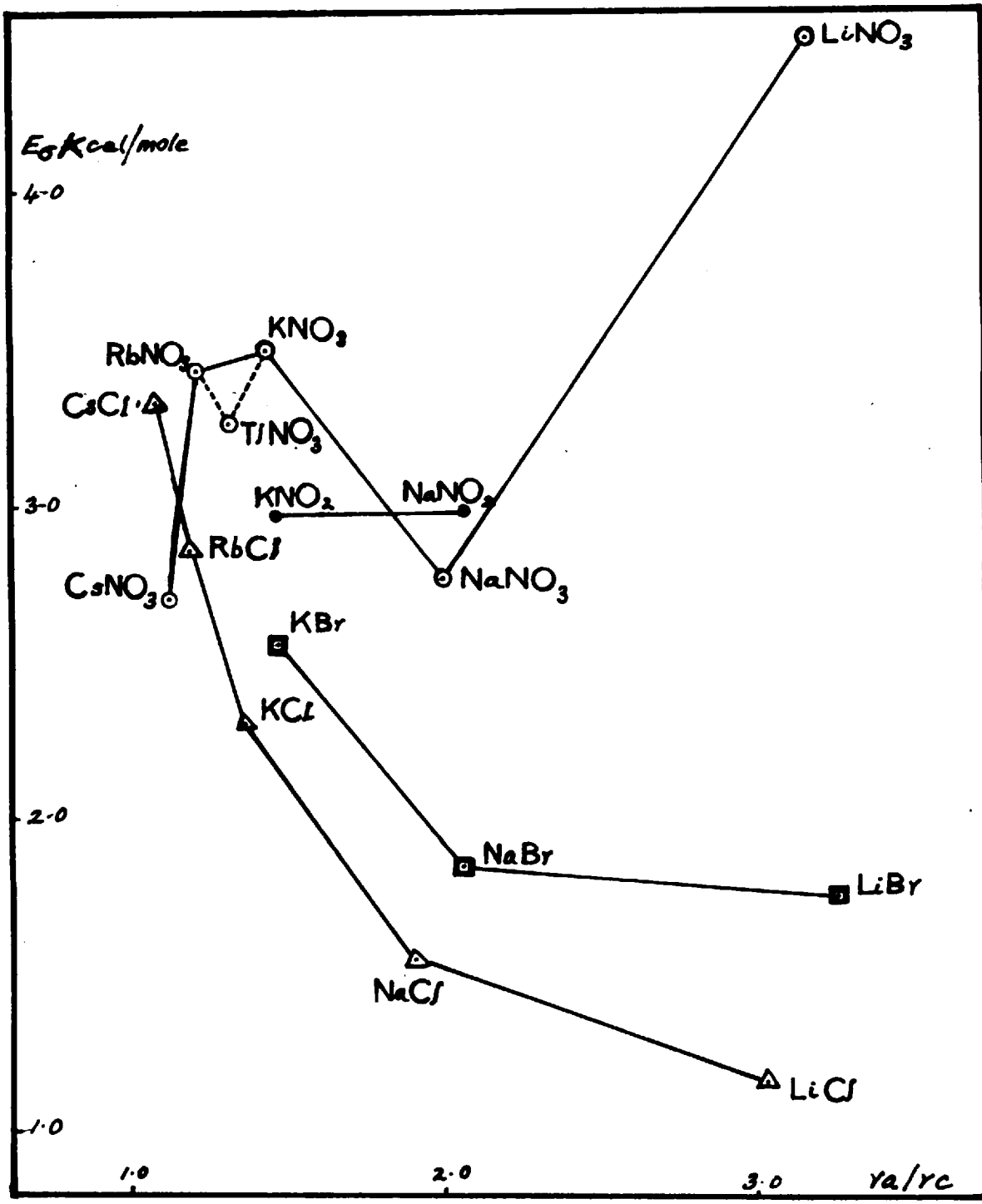
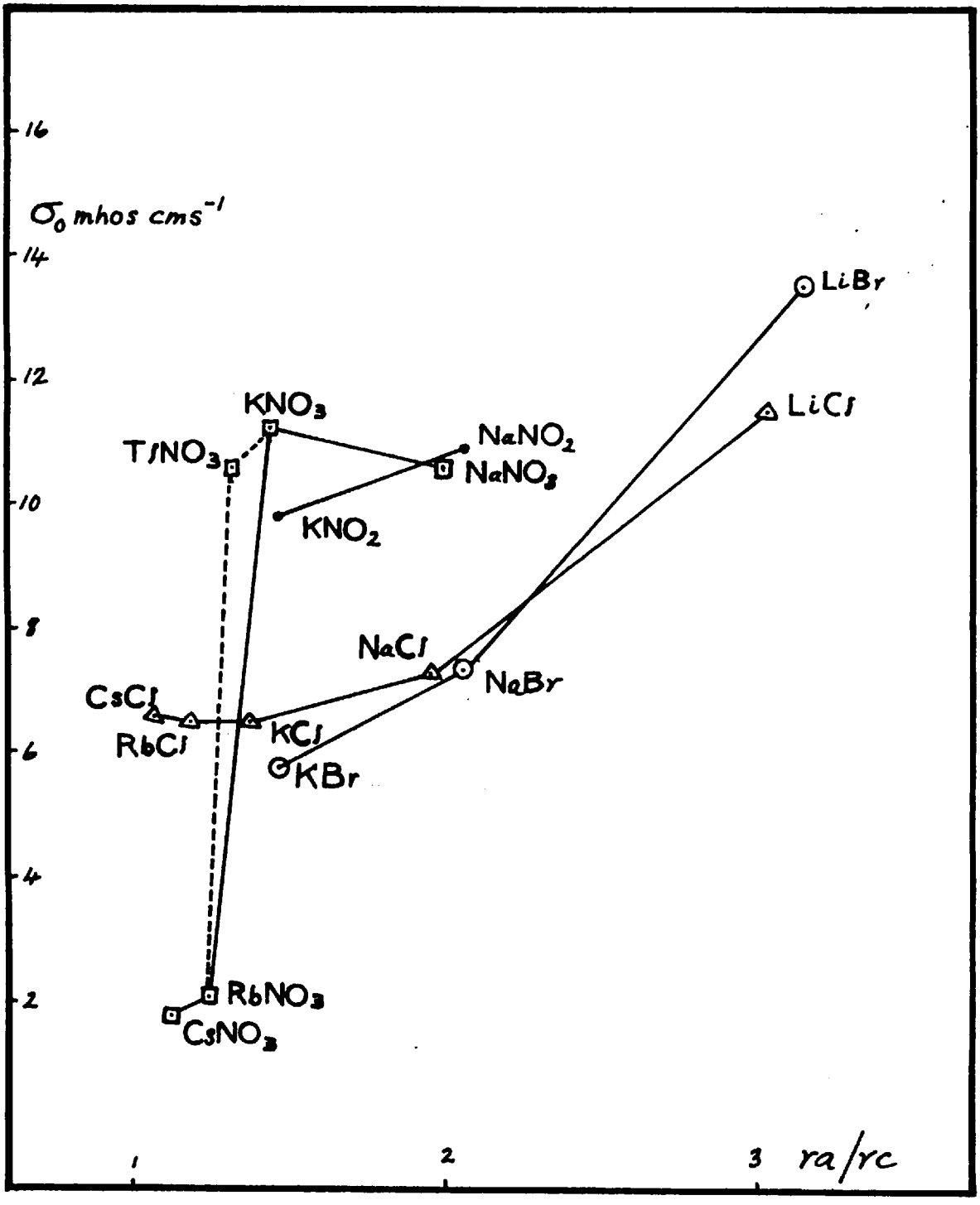

E_s Kcal/mole
4·0
3·0
2·0
1·0
1·0
2·0
3·0
r_a/r_c
$LiNO_3$
KNO_3
$RbNO_3$
$CsCl$
$TlNO_3$
KNO_2
$NaNO_2$
$RbCl$
$CsNO_3$
$NaNO_3$
KBr
KCl
NaBr
LiBr
NaCl
LiCl

FIG 10.2


16
σ_0 mhos cms^{-1}
14
12
10
8
6
4
2
1
2
3
ra/rc
LiBr
LiCl
NaCl
NaBr
KCl
KBr
RbCl
CsCl
KNO_3
$TlNO_3$
$NaNO_2$
$NaNO_3$
KNO_2
$RbNO_3$
$CsNO_3$

what would appear to be an average value for E_σ for nitrites and nitrates 3.1± 0.4 Kcal/mole.

10.1.3 Activation Energy and Free Volume.

It is interesting to note in connection with studies of conductance that where the energy for the process is high the free, or 'hole' volume tends to be low. This general relationship can be seen by comparing the values given for V_f in Table 10.3 with the values of E_σ in Table 10.2. This tends to indicate that the movement of ions in the conductance process may be dependent on the juxtaposition of a hole and emphasises that the relative movement of the ions is most important.

Further evidence of the shrinkage in KNO_3 and $NaNO_3$ melts has been given by Rhodes and Ubbelohde [6] (1959). Their measuremant of the ultra violet absorption spectra of these salts through the melting point show that there is little or no difference and a decrease in the cation-anion distance in the melt is even possible.

10.2 Electrical Conductivity of Solid Salts.

The electrical conductances in the solid salts have been found to fit an Arrhenius type relationship which has been given in Section 8.5.

The energies of activation for the conductance process in KNO_2, $NaNO_2$ and $K_2Cr_2O_7$ have been calculated and are tabulated in Table 10.4 where they are compared with similar values for alkali halides.

TABLE 10.4

Salt	Temp. range °C	E_σ Kcal/mole	$\sigma_o\ \Omega^{-1}\ cm^{-1}$	Ref.
$NaNO_2$	175 - 261	23.8	2.94×10^5	Present work
KNO_2 (a)	380 - 415	21.0	9.33×10^4	"
KNO_2 (b)	203 - 364	24.2	1.40×10^5	"
$K_2Cr_2O_7$	203 - 398	29.1	1.55×10^4	"
CsCl	below 469	22.9	50	cf. Moss
	above 469	22.9	1	(1954)
CsBr	340 - 623	26.1	1×10^3	"
CsI	530 - 600	31.6	3×10^4	"
NaCl	-	40.8	10^4	"
KCl	-	46.6	10^6	"
RbCl	-	48.9	10^6	"

The low values for the activation energies for electrical conductance in these solids might be taken as evidence of electronic rather than ionic conduction. CsCl, CsBr and CsI also show anomalous values for E_σ. In the case of the Cs salts additional evidence of the electronic character of the conductance process has been provided by transport number measurements (See Harpur, Moss and Ubbelohde [12] 1955). The magnitude of the values of E_σ for the other alkali chlorides are those normally found.

A transition was observed in solid KNO_2. The conductivity data suggest that it is spread over about 16°C and is continuous.

No previous report of this transition has been found.

10.2.1 The Relation of Electrical Conductance in Solid and Molten Salts.

The jump in electrical conductivity in passing from the solid to the liquid can throw some light on the increase of positional disorder on melting. Low values for this jump can be interpreted as evidence of premelting i.e. where premelting occurs some positional disordering takes place in the solid below the melting point and the subsequent jump in electrical conductivity on passing through the melting point is reduced. In the present investigation only KNO_2 shows evidence of premelting, the other salts seem normal. Table 10.5 shows the jump in conductivity on melting of some ionic salts.

TABLE 10.5

Jump in Conductivity on Melting.

Substance	$\sigma_{liq.}/\sigma_{solid}$	Ref.
NaCl	3,000	13
KCl	10,000	13
KBr	7,000	13
AgCl	30	13
AgBr	20	13
$NaNO_3$	1,000	13
$NaNO_2$	3,000	Present Work.
KNO_3	3,000	13

/Continued...

TABLE 10.5 (Continued..)

Substance	$\sigma_{liq.}/\sigma_{solid}$	Ref.
(1) KNO_2	40	Present Work.
$AgNO_3$	500	13
$K_2Cr_2O_7$	6,000	Present Work.
KCNS	3,000	14
$KHSO_4$	70,000	14

(1) 1,000 if referred to σ below the transition in the solid.

The values of the jump for KNO_2, $NaNO_2$ and $K_2Cr_2O_7$ can be compared with AgCl and AgBr which both show marked premelting.

10.3 The Viscosity of Molten Salts.

As has been demonstrated earlier the viscosity of $NaNO_2$, KNO_2, $TlNO_3$ and $K_2Cr_2O_7$ are related to temperature by an Arrhenius type of expression, $\eta = \eta_o \exp.(E_\eta/RT)$.

The values of E_η and the pre-exponential term have been calculated and are given in Table 10.6 together with those of some other low melting salts with polyatomic anions and the higher melting alkali halides.

Table 10.6 shows that for the high melting salts E_η is consistently higher than for the low melting alkali nitrates and nitrites, with the exception of NaCNS, KCNS and $KHSO_4$. As can be

seen with these salts there is a noticeable increase in the activation energy for viscous flow near the melting point. This has been ascribed to the formation of association complexes which dissociate at the higher temperatures.

TABLE 10.6

Salt	M.P. °C	$\eta_0 \times 10^4$ poise	E_η Kcal/mole	Ref.
LiCl	613	-	8.8	Bloom and Heymann[15]
NaCl	801	1.95	9.4	" "
KCl	776	3.55	7.8	" "
LiBr	547	-	6.0	" "
NaBr	755	8.13	10.63	" "
KBr	730	2.95	7.96	" "
$LiNO_3$	255	11.9	4.23	Dantuma[16]
$NaNO_3$	306.8	9.87	3.95	"
KNO_3	333.1	14.12	3.66	Lorenz and Kalmus[17]
NH_4NO_3	169.6	1.59	4.6	Shirai and Nishikawa[18]
$TlNO_3$	206	9.04	3.61	Present Work.
$NaNO_2$	281	8.5	4.0	" "
KNO_2	419	13.37	4.23	" "
$K_2Cr_2O_7$	398	159.8	10.5	" "
NaCNS	287	190	5.8	(a) Plester, Rogers.
		480	4.7	(b) and Ubbelohde[14]
KCNS	173.2	15.3	8.00	(a) "
		178	5.72	(b) "
$KHSO_4$	207	6.5×10^{-3}	3.89	(a) Rogers and
		2.3×10^{-2}	11.95	(b) Ubbelohde[19]

(a) Just above the freezing point.

(b) Well above the freezing point.

In the comparison of the viscosities of salts with widely different melting points the problem of corresponding states again arises. One procedure though not entirely satisfactory, is to use entropies, ΔS_η calculated from the formal absolute rate expression for viscosity of Glasstone, Laidler and Eyring [21] (1948).

$$\Delta S_\eta = R \ln (h N / v \eta_0)$$

In this expression the values for the specific volume v , for $K_2Cr_2O_7$ and $TlNO_3$ were taken from Jaeger [4] and for $NaNO_2$ from Husband [24] (1958). v was calculated from the volume of the crystal for KNO_2 assuming only 1% expansion on melting i.e. of the same order as that for KNO_3.

It will be seen that salts with non spherical anions frequently have large negative entropies of activation for viscous flow. This would conform with the predominance of highly selective activation processes of comparatively low activation energy. However, the entropies for melts of the sulphocyanides (unless considered for that portion of the log η against 1/T plot 20^oC above the melting point) show that this suggestion cannot be made wholly general for salts of low melting points. Positive entropies of activation imply non selective activation. This can be compared with the melts of the polyphenyls.[22] Here ΔS_η is negative for

the planar hydrbcarbons and linear polyphenyls but for the branched molecules it is large and positive. This is attributable to cybotactic group formation or molecular interlocking. The process of flow involves extensive disordering.

TABLE 10.7

Entropies of Viscous Flow Based on the Rate Equation.

Salt	M.P.°C	ΔS_η (eu)	Ref.
$LiNO_3$	255	- 4.86	Davis et al[20]
$NaNO_3$	306.8	- 5.95	"
KNO_3	333	- 5.75	"
$AgNO_3$	212	- 5.36	"
$TlNO_3$	206.4	- 4.34	Present Work.
$NaNO_2$	281	- 4.18	" "
KNO_2	419	- 5.45	" "
$K_2Cr_2O_7$	398	- 3.06	" "
KCNS	173.2	+ 2.91	Plester et al[14]
NaCNS	287	- 1.65	" "
NaCl	801	- 1.28	cf. Plester et al
NaBr	755	- 4.38	" "
KCl	776	- 3.05	" "

For KCNS the above positive value of entropy is found from η_o calculated from the slope of the line given by a plot of $\log\eta$ against 1/T for the temperature range (175 - 195)°C. However, if

η_o is calculated from the plot of this line in the region (200 - 230)°C, a value of - 4.28 is found. Similarly the value of ΔS_η = - 1.65 for NaCNS is found for the range (305 - 325)°C, whereas in the range (325 - 350)°C ΔS_η = - 3.52.

10.3.1 Methods of Relaxation of Shear.

There are three possible mechanisms by which an ionic melt could relax shear and transfer momentum.

(a) The first can be referred to as convective. A convective mechanism would require that the ions taking part in this process move into 'holes' at adjacent sites. This type of mechanism would be expected to be the predominant one in a diffusion process. Comparison of the free volumes listed in Table 10.3 with the energies of activation for the viscous process for various salts, Table 10.6, shows that where the 'hole' volumes are large the energies of activation for the process are also large. This is contrary to what one might expect if a convective mechanism played an important role. However, it is in line with what has been suggested by Longuet - Higgins [23], namely that the contribution of a convective mechanism would be small, possibly of the order of 10% in a viscous process. It must be borne in mind, however, that this conclusion relates primarily to non ionic liquids where it would be expected that the interaction would be smaller. In the case of an ionic liquid it is possible that the contribution of a convective mechanism might be even less.

(b) The second method of momentum transfer is by a collisional mechanism. In this method the particles of the system transfer their momentum by collision with their nearest neighbours. In an ionic melt where the electrostatic forces hold the ions firmly in place such a mechanism would be more likely. Examination of the energies of activation for the viscous process and free volume show that where the free volume is large, as in the halides, the energies are also large. This is what would be expected if this mechanism played a large part.

(c) Inherent in the structure of low melting salts with non spherical polyatomic anions is the ability to relax shearing stress by the mutual turning over of non spherical ions without large relative movements of centres of positive and negative charge. This would lead to a lowering of the activation energy for the viscous process in these compounds. Reference to Table 10.6 shows that ionic melts such as those of the alkali nitrates and nitrites have a lower activation energy for viscous flow than the alkali halides with their inert gas type anions. It thus seems that this latter mechanism plays a part in the viscous process.

It appears therefore, that both collisional and rotational factors contribute to the relaxation of shearing stress in low melting salts with non-spherical polyatomic anions. The participation of both would account for the quite significant

differences in the energies of the two types of melt.

10.3.2 Relation of Energy of Activation for Viscosity with the Cation Radius.

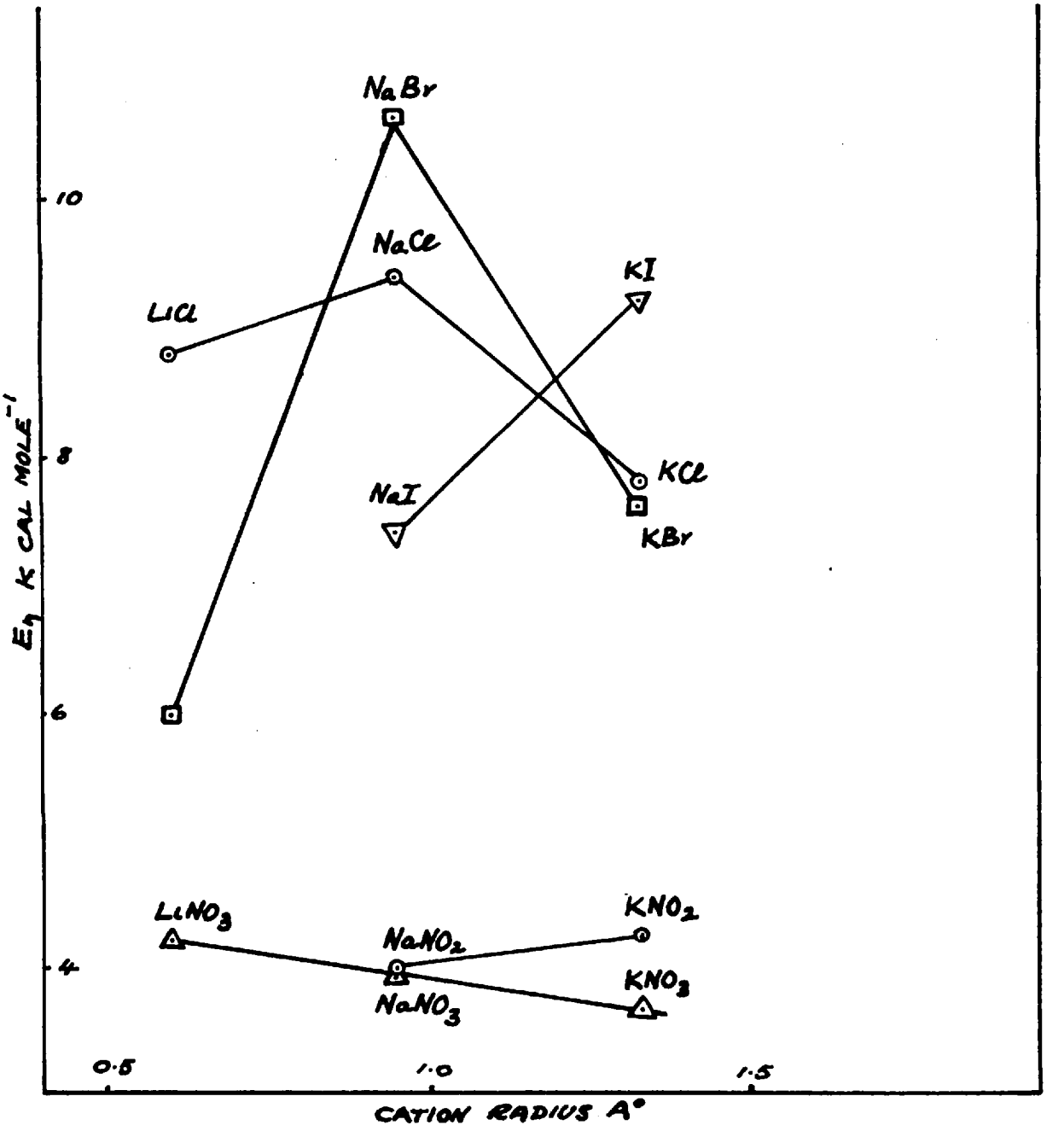
Fig. 10.3 shows the energies of activation for the viscous process plotted against the cation radius for the alkali nitrates and nitrites together with those for the alkali halides. No relationship appears to exist for alkali halides but a definite trend exists for the alkali nitrates in which the energy decreases with increasing cation size. Insufficient data exist for any conclusion to be drawn for the nitrites. Because of their dependence on the slope of the log η against 1/T plot too great importance cannot be drawn from this gradation in activation energy. However, one very noticeable point does emerge and that is the close similarity in magnitude of the energy of activation for low melting salts with polyatomic anions. This suggests that the viscous process in these salts depends overwhelmingly on one ion and that the influence of the other ion is of much less significance. The ion playing this major role would therefore appear to be the anion. This would fit in with the relaxation of shearing stress by the turning over of the non spherical anions, and as would be expected on this basis the energies of activation for nitrites and nitrates are closely similar.

10.4 Comparison of Viscosity and Conductivity.

If $E_\eta / E_\sigma = m$, then applying the modified Walden rule:

FIG 10.3

E_η AGAINST CATION RADIUS FOR SOME IONIC MELTS



$$\sigma^m \eta = \text{a constant}$$

i.e. $m \log \sigma + \log \eta = \text{a constant.}$

It follows that a plot of log σ against log η should be linear with a slope of m. Such plots are shown for $NaNO_2$, KNO_2, $TlNO_3$ and $K_2Cr_2O_7$, in Figs. 10.4, 10.5, 10.6 and 10.7. The abnormally low values for m have been suggested as being indicative of ionic association. Stress was earlier laid on the higher values for the activation energy in the conductance process which were taken as being indicative of a larger unit than the cation being involved.[14,19,20] The correspondingly low values for the energy of activation for the viscous process in low melting salts with non spherical polyatomic anions was largely overlooked. This would appear to be a correct conclusion for such salts as KSCN, NaSCN and $KHSO_4$ where a decrease in the energy of activation for viscous flow is observed with increasing temperature; suggestive of the presence of polymeric units just above the freezing point which dissociate at higher temperatures (Table 10.6). However, there does not seem to be a parallel case for the alkali nitrates where such changes in slope in the plot of log η against 1/T that have been reported (Section 5.7) suggest a decrease in the energy of activation energy above the freezing point. In the case of the alkali nitrates and nitrites some other form of association would seem to be indicated. It has been said[15] that the conductance process is controlled by the smaller cation while

viscous flow which involves a configurational change is dependent on the larger anion. This is illustrated in the case of the alkali halides where the energies of the two processes are quite different but cannot be taken as being the case for the low melting salts examined here. All available evidence for the nitrates and nitrites point to some mechanism of association, due to an interlocking of the anions because of their non symmetrical character or of an overlapping of the bond orbitals of the nitrate ions. This leads to;

(a) a closer knit structure for these liquids as shown by their small volume change on fusion and small free volume (Table 10.3);

(b) a higher energy of activation for the conductance process, since though the smaller cation remains the principal conducting ion, the close interlacing of the nitrate ions inhibits its movement and ultimately increases the energy of the process to nearer that of the viscous process;

and (c) a decrease in the activation energy for the viscous process since as well as bringing the lattice closer together to allow the transfer of momentum to operate more efficiently through a collision mechanism, it allows rotation of a non spherical anion to have a significant effect. In view of this last effect therefore it would not be surprising if the energy of activation of viscous flow for such salts as $LiNO_3$ and $NaNO_3$ proved to be lower near the

melting point, since it would be in this region that a relaxation of shearing stress by rotation of the anion would have its greatest effect. An effect that would be reduced with increased temperature due to the expansion of the liquid lattice. It is not surprising to find that $LiNO_3$ has quite a large volume change on fusion relative to that of other nitrates.

This view of the liquid structure of the alkali nitrates and nitrites is underlined by the findings from the electrical conductivity and viscosity of $K_2Cr_2O_7$. In this salt the energy of activation for the viscous process is high, as might be expected for a salt with such a large anion. However, because of the ability of these large non spherical anions to overlap or associate the ratio of E_η / E_σ is of the same order as that for the nitrates and nitrites. Thus the large energy of activation for conductance of this salt is brought about by the restriction in movement of the cations by the interlacing of the anions.

It can be noted also, that the surface tensions of the alkali nitrates (Section 3.7) show no gradation with increasing cation size unlike the alkali halides. This could be attributed to anion-anion contact, with any moderating effect of cation size being nullified by the ability of the non spherical anions to rotate.

FIG 10.4

CONDUCTIVITY RELATED TO VISCOSITY $NaNO_2$

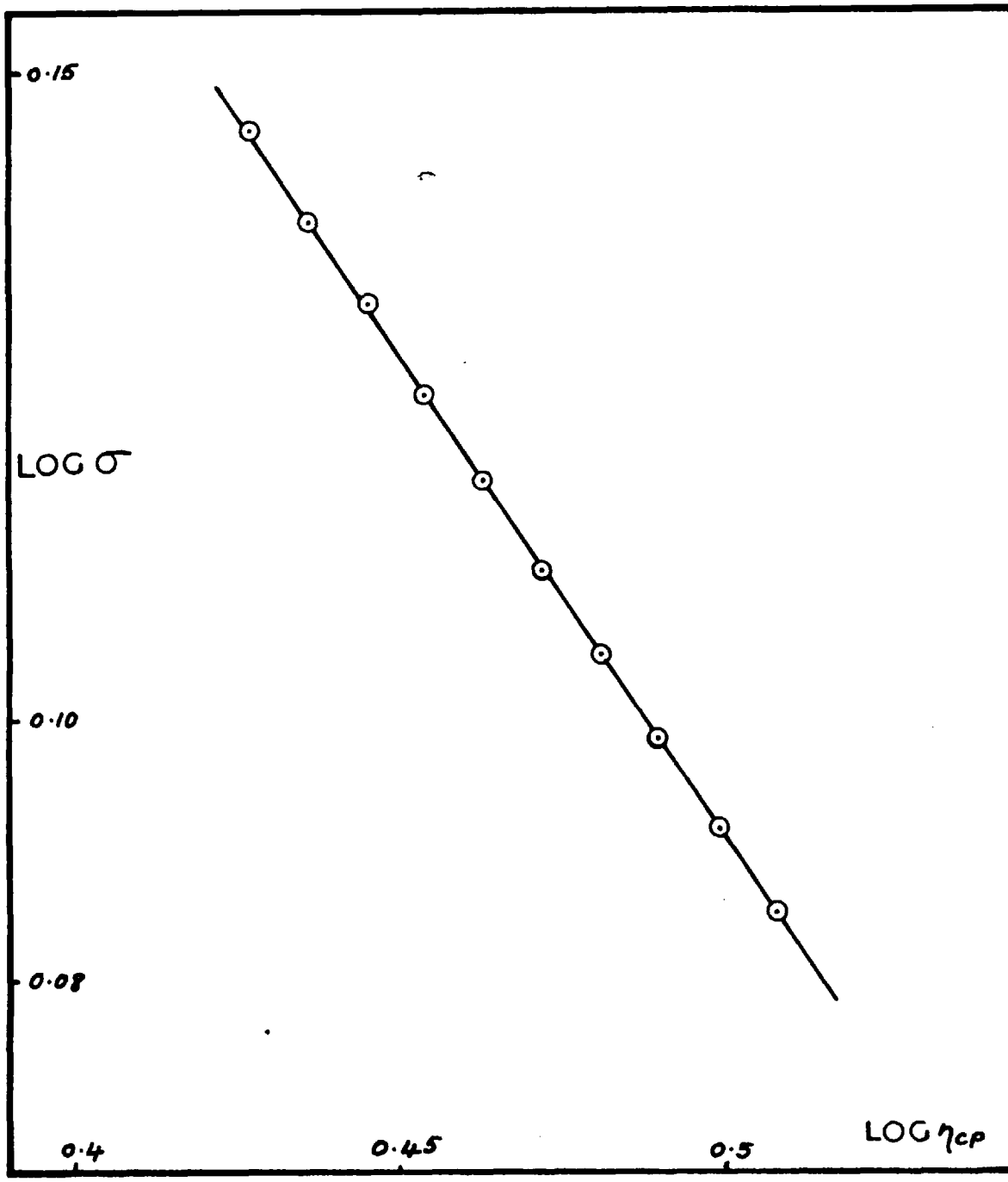


FIG 10.5

CONDUCTIVITY RELATED TO VISCOSITY KNO_2

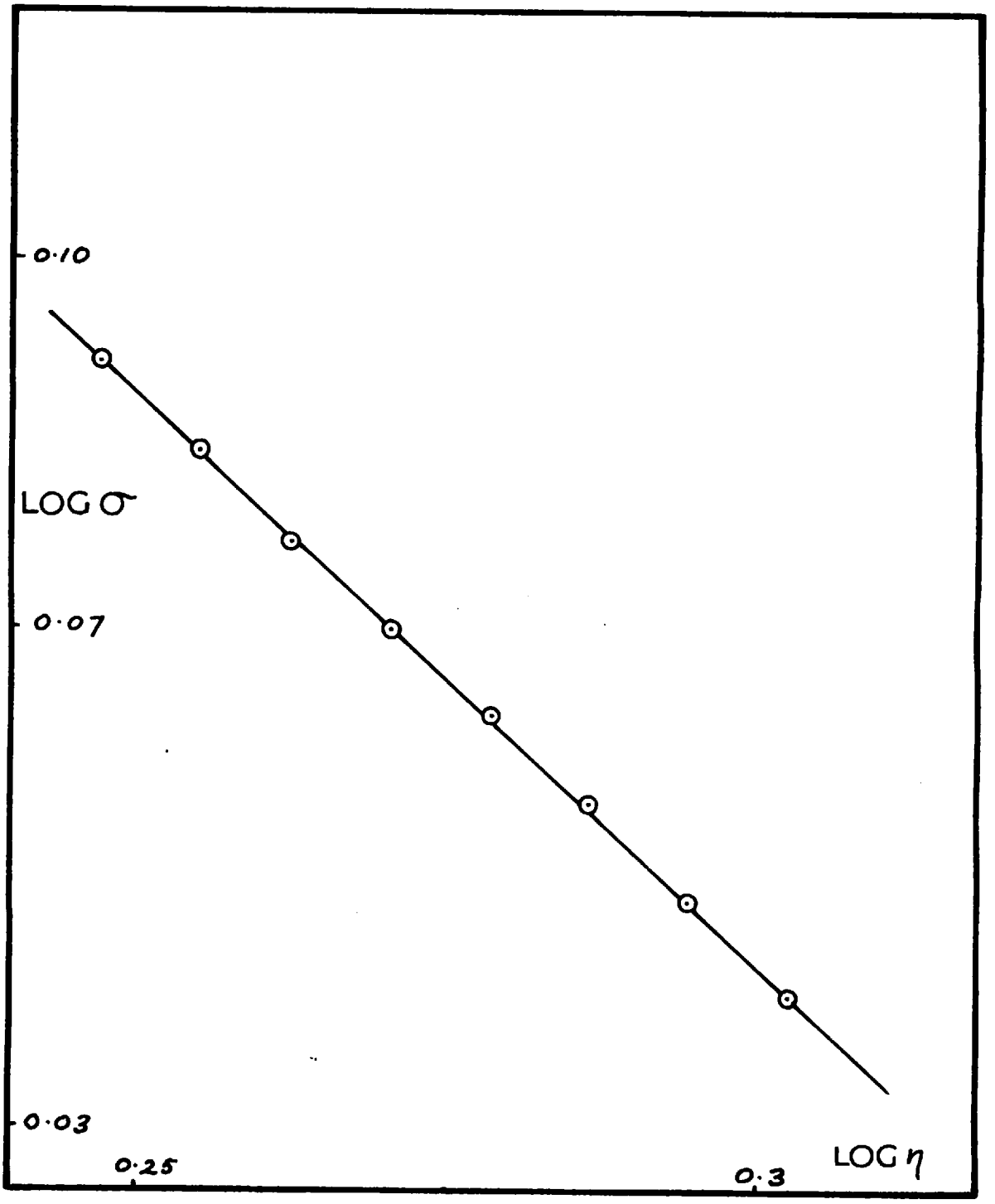


FIG 10.6

CONDUCTIVITY RELATED TO VISCOSITY FOR $TlNO_3$

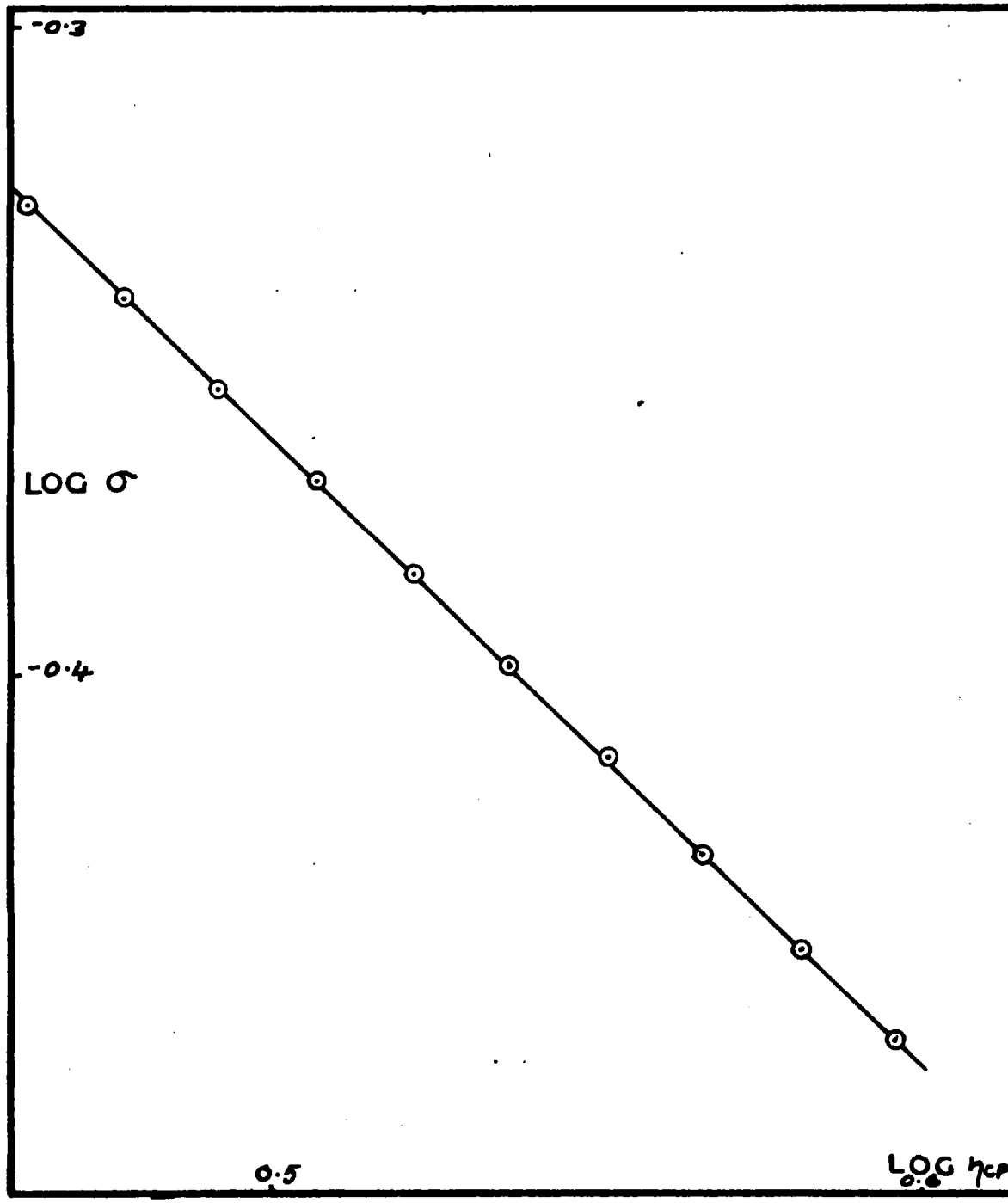
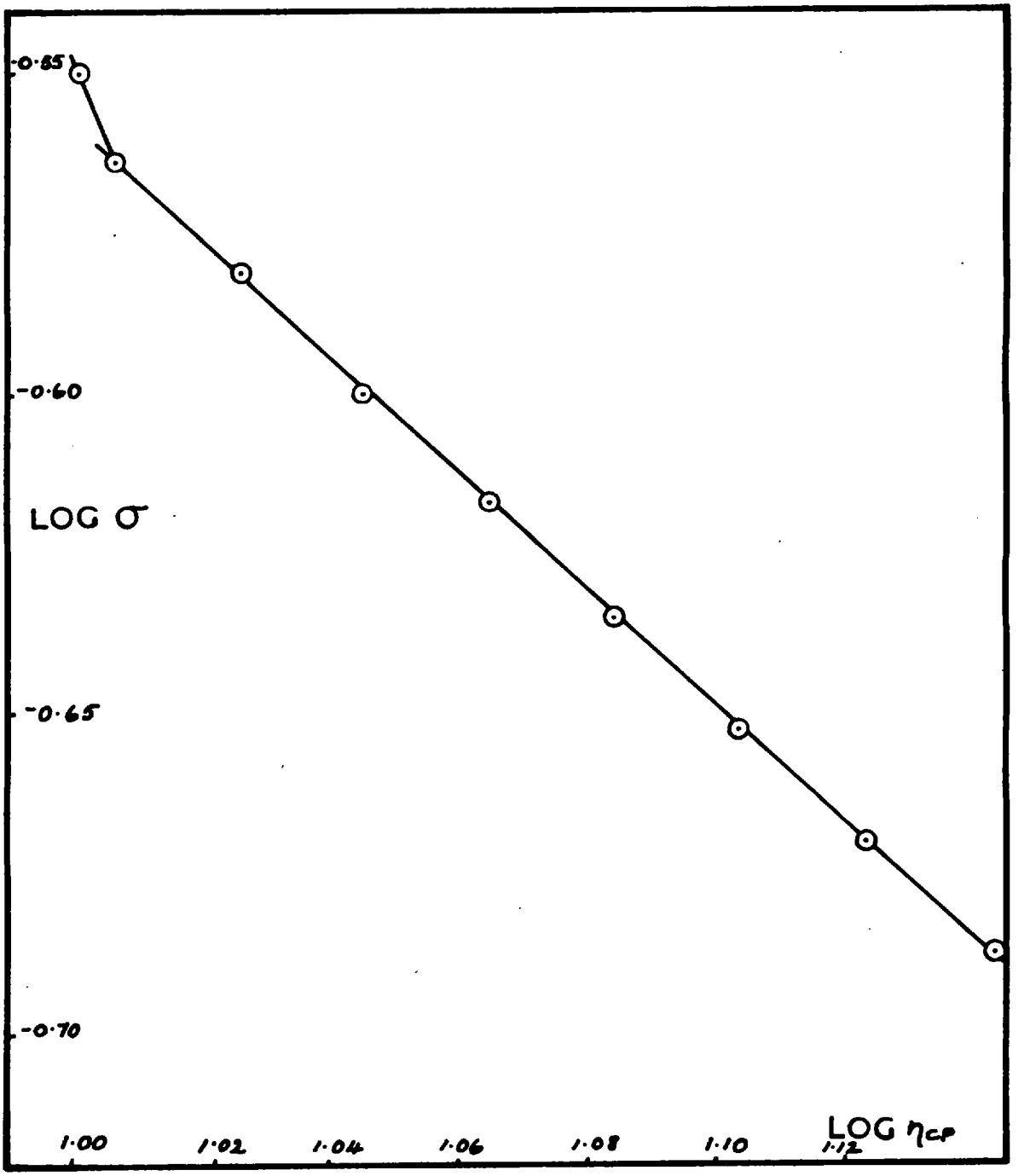


FIG 10.7

CONDUCTIVITY RELATED TO VISCOSITY $K_2Cr_2O_7$



References.

1. Yaffe and Van Artsdalen. J. Phys. Chem. (1956), 60, 1125.
2. Sauerwald and Schinke, Z. anorg. Chem. (1956), 287, 21.
3. Fischmeister, J. Inorg. Nuc. Chem., (1956), 3, 182.
4. Jaeger, Z. anorg. Chem. (1917), 101, 16.
5. Bockris and Richards, Proc. Roy. Soc. (1957), 241A, 44.
6. Rhodes and Ubbelohde, Proc. Roy. Soc. (1959), 251A, 156.
7. Kincaid and Eyring, J. Chem. Phys. (1938), 6, 620.
8. Collins and Navidi, J. Chem. Phys. (1954), 22, 1954.
9. Buehler, Wentorf, Hirschfelder and Curtiss, J. Chem. Phys. (1951), 19, 61.
10. Jaeger and Kapma, Z. anorg. Chem. (1920), 113, 27.
11. Goodwin and Mailey, Phys. Rev. (1908), 26, 28.
12. Harpur, Moss and Ubbelohde, Proc. Roy. Soc. (1955), 232A, 196. Harpur and Ubbelohde, Proc. Roy. Soc. (1955), 232A, 310.
13. Ubbelohde, Quart. Rev. (1950), 4, 356.
14. Plester, Rogers and Ubbelohde, Proc. Roy. Soc. (1956), 235A, 469.
15. Bloom and Heymann, Proc. Roy. Soc., (1947), 188A, 392.
16. Dantuma, Z. anorg. Chem., (1928), 175, 1.
17. Lorenz and Kalmus, Z. physik. Chem. (1907), 59, 17.
18. Shirai and Nishikawa, Sci. Pap. Col. Gen. Educ. Tokyō, (1958), 8, 61.
19. Rogers and Ubbelohde, Trans. Far. Soc. (1950), 46, 1051.

20. Davis, Rogers and Ubbelohde, Proc. Roy. Soc. (1953), A220, 14.

21. Glasstone, Laidler and Eyring, "Theory of Rate Processes" McGraw-Hill, N.Y. (1941), p. 480.

22. Andrews and Ubbelohde, Proc. Roy. Soc. (1955), 228A, 435.
McLaughlin and Ubbelohde, Trans. Far. Soc. (1957), 53,628.
Magill and Ubbelohde, Trans. Far. Soc. (1958), 54, 1811.

23. Longuet-Higgins and Pople, J. Chem. Phys. (1956), 25, 384.

24. Husband, J. Sci. Instr. (1958), 35, 300.

CHAPTER 11.

THE STRUCTURAL SIGNIFICANCE OF H_2O SOLUBILITY IN MOLTEN SALTS.

The solubility of H_2O in pure molten salts has been shown to persist to high temperatures (Section 4) and not unexpectedly the magnitude of the H_2O solubility was found to be greater than that for the inert gases.

In the present work on alkali nitrates this trend has been confirmed. What is most remarkable is the quite large difference in magnitude for the H_2O solubility from that reported for the inert gases (Chapter 4). This should allow a greater accuracy to be obtained in further work on the solubility of H_2O in alkali nitrates using a more refined technique.

11.1 The Order of Magnitude of H_2O Solubility in Molten Nitrates.

The results for the solubility of H_2O in molten nitrates are given in Table 9.3, Section 9.12. Comparison with the results reported for the solubility of inert gases (Chapter 4) showsthat there is a considerable increase in the solubility of H_2O over that for inert gases. The cause of this difference is discussed in Section 11.7. A complete comparison of actual values for the two types of gas cannot be made since strictly, corresponding temperatures should be used. Evidence in the literature suggests a positive temperature coefficient of solubility

for solution of inert gases, but a negative coefficient for the solution of H_2O. However, in the present investigation owing to the nature of the technique values for the solubility were only obtained at the freezing point and consequently the sign of the temperature coefficient could not be confirmed.

11.2 The Effect of Positional Holes in the Melt on Gas Solubility.

If it is possible to create holes in a molten ionic system similar to those in a solid ionic system it would seem likely that an enhancement of the gas solubility would result. The solubility of H_2O in molten alkali nitrates could be increased by the addition of an alkaline earth nitrate in two ways:

(a) As will be pointed out in Section 11.7 the charge of an ion is of prime importance in the interaction energy between H_2O and a cation, which in the case of ions with a double charge will lead to a greater solubility of H_2O.

(b) The replacement of two monovalent cations by one divalent cation will lead to a vacant site and hence a greater number of holes. The extent to which this will enhance the gas solubility will be determined by the rigidity of the liquid lattice and the size of the holes. The determination, therefore, of the role of positional holes depends on whether the introduction of a cation with a higher charge will create a hole, thus suggesting that the liquid structure is dependent on anion-anion contact, or whether the anticipated increase in hole volume is compensated by the

greater charge drawing the lattice closer together. Either or both of these effects could occur. The latter effect may introduce a rigidity to the lattice while still preserving holes though smaller than ion size.

The solubility of H_2O in $NaNO_3 + Ca(NO_3)_2$, $KNO_3 + Ba(NO_3)_2$, $CsNO_3 + Ba(NO_3)_2$ and $KNO_3 + K_2Cr_2O_7$ has been shown to be similar to that of the pure molten nitrates. In the case of $KNO_3 + Ba(NO_3)_2$ and $NaNO_3 + Ca(NO_3)_2$ a slight increase was observed, and though the anomalous nature of the results obtained for $NaNO_3$ throws some doubt on its magnitude, it is clear that any increase is significantly small. With $CsNO_3 + Ba(NO_3)_2$ a slight decrease was detected but the magnitude was again relatively small. The solubility of H_2O in $KNO_3 + K_2Cr_2O_7$ showed no change over that for pure KNO_3. The selection of the quoted value for H_2O solubility in $NaNO_3$ is discussed in Section 11.8.

This leads to the conclusion that the formation of holes if it occurs, does not cause any marked increase solubility, possibly because of some compensating structural change. If the part played by the holes was significant in increasing the solubility, the introduction of the large anion, $Cr_2O_7^{--}$ would seem to afford the best opportunity of accomplishing this. However, it is of importance to note that the difference in size of $Cr_2O_7^{--}$ and NO_3^- may produce a change in the co-ordination number. The systems that have shown an increase have been those which contained a divalent cation. This together with the magnitude of the change

in solubility tends to suggest that this increase was due to the increased interaction between H_2O and the divalent cation rather than any remarkable increase in hole volume. In the systems where increasing additions of divalent ion were made no significant change in the solubility was observed. Whether the increase was due to the added interaction of the divalent cation or to the creation of holes, it would be expected to rise with the divalent ion content. However, it is likely that any such effect would be masked by the insensitivity of the technique. It might have been possible to confirm this by measurements of the solubility of H_2O in the pure divalent cation salt or systems containing a very high proportion of divalent cation. The present technique would, however, be unsuitable for such a determination due to its dependence on the stability of the salt. The highly polarising cations would make the systems vulnerable to decomposition according to reactions such as:

$$2M(NO_3)_2 \longrightarrow 2MO + 4NO_2 + O_2$$

Furthermore such a system would be of no relevance for the present studies of the role of positional holes since the basic structure would be that of a molten alkaline earth nitrate which is likely to have a different co-ordination number.

The salient conclusion that arises from this is that the formation of holes is compensated by some structural change. It seems likely therefore, that though the replacement of two monovalent ions by one divalent ion could cause a hole to form, a

compensating structural change takes place. There are two possible forms that this structural change could take, both depending on the greater charge of the added ion.

(i) The divalent ion exerting its greater attractive power on neighbouring anions draws them closer about itself.

(ii) The greater charge could cause the anions to lock more tightly. This can be qualitatively understood if the structure proposed in the previous chapter is envisaged. The overlapping anions could be likened to meshing cogwheels which can rotate against one another. This would cause them to lock even more firmly and perhaps reduce the rotation. It is possible that the activation energy for viscous flow of such a mixed system might be higher than in the simple salt. This would in effect be a test of the contribution of rotation to the relaxation of shear (See Chapter 10) and indeed the evidence available for similar mixed systems suggest this to be so.[1]

Both (i) and (ii) should have this effect of reducing the rotation but if the anions are already in very close contact the introduction of a divalent cation would create positional holes since the structure of the liquid would be dictated by the anion-anion contact which would not easily be decreased. However, this rigidifying effect would make a larger energy necessary for the creation of a hole to accept the gas molecule, whether this cavity creation was dependent on work against the surface tension, or removal of an ion from a quasi-crystalline lattice point. Further

mention of this is made in Section 11.5.

In addition it is possible that some slight decrease in hole volume could occur through the greater polarising power of the divalent cation acting on the readily polarisable anion.

If marked structural changes take place on the addition of divalent cations they might be expected to affect other parameters (see Section 11.5).

11.3 The Solubility of H_2O and Free Volume.

The solubility of H_2O in the pure nitrates was found to decrease in going from $NaNO_3$ to KNO_3 but a slight increase was observed in the solubility in $CsNO_3$ over that of KNO_3. This trend in solubility can be usefully compared with the free volume found in these salts (Table 10.3).

$$\frac{V_f\ NaNO_3}{V_f\ KNO_3} = \frac{0.18}{0.10} = 1.8 \text{ (Near the freezing point).}$$

$$\frac{\text{Solubility of } H_2O \text{ in } NaNO_3}{\text{Solubility of } H_2O \text{ in } KNO_3} = \frac{1.41 \times 10^{-3}}{3.86 \times 10^{-4}} = 3.6$$

The free volume in $CsNO_3$ is unknown. To an order of magnitude therefore, the ratios of the solubility of H_2O to free volume for $NaNO_3$ and KNO_3 are similar. Comparison with the volume change on fusion of these salts is less rewarding (See Table 10.3). However, this is not surprising since much of the volume change in KNO_3 has probably taken place at solid-solid transitions before the melting

point.

$$\frac{\Delta V_f/V_s \ NaNO_3}{\Delta V_f/V_s \ KNO_3} = 11$$

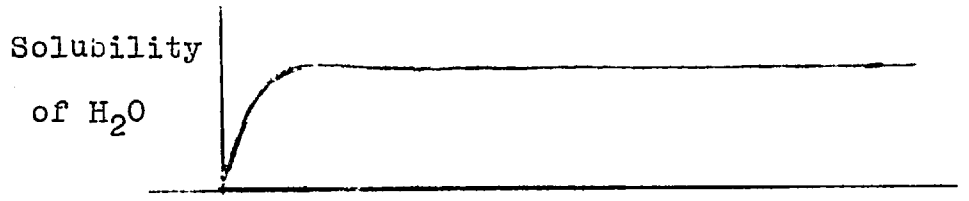
This suggests a relationship between the free volume and the solubility of H_2O in $NaNO_3$ and KNO_3, which might be taken as an indication of a larger free volume in $CsNO_3$ than in KNO_3. However, since the H_2O solubilities calculated are dependent on the measurement of the heats of fusion of individual salts made by other workers too much stress cannot be laid on the difference in solubility of H_2O in $CsNO_3$ and KNO_3.

11.4 The Form of the Solubility Curve for H_2O in Alkali Melts.

No apparent change in solubility of H_2O was observed with different partial pressures of H_2O. The reason for this is not clear. It would seem to indicate that the saturation is achieved at low partial pressures of H_2O and remains constant at higher partial pressures. The technique did not allow partial pressures of H_2O much in excess of 20 mmHg to be used. This, coupled with the insensitivity of the technique, prevents any definite conclusion being drawn from this aspect of the results. Further investigation of the change of solubility with H_2O pressures awaits a method which would allow a more extensive range of partial pressures of H_2O to be studied.

Superficially at any rate the solubility of H_2O in alkali nitrates would appear to follow a scheme such as shown in Fig. 11.1.

Fig. 11.1



This form of solubility curve is already familiar in the adsorption of H_2O on silica gel or N_2 on carbon at low temperatures.[2]

11.5 The Role of Positional Holes in the Structure of Molten Nitrates and their Influence on Physical Properties.

11.5.1 Positional Holes in Solid Nitrates.

The enhancement of the electrical conductivity in solids by the creation of positional holes through the addition of cations possessing a higher charge is well known for ionic salts. Indeed this was the basis of the mechanism of electrical conductance in solid ionic halides proposed by Wagner and discussed in Section 1.5. However, the literature seems to be devoid of any information on similar investigations on mixed nitrates.

Results showing the enhancement of the electrical conductivity of solid KNO_3 by the addition of $Ca(NO_3)_2$ are given in Section 9.14.1. This demonstrates that alkali nitrates behave similarly to alkali halides, i.e.

(a) Addition of a divalent ion which forms a solid solution

will create positional holes.

(b) The holes so created will enhance the electrical conductivity which in turn is evidence of the presence of vacant sites in the solids.

This information is useful since it emphasises the regular nature of solid alkali nitrates in as much as it shows that these solids can be compared with the simpler alkali halides. Further it allows comparison to be made between the structure of the solid crystalline salt and the so called quasi-crystalline liquid.

11.5.2 The Effect of Positional Holes on the Density and Molar Volume of Mixed Nitrate Systems.

If the structure of a molten alkali nitrate collapsed on the addition of a divalent cation, some indication of this might be detected in measurements of density and molar volume.

The results given in Section 9 show that the isotherms of density against composition of the system KNO_3 - $Ba(NO_3)_2$ exhibit a slight negative deviation[2] Fig. 9.13. However, the values recorded in Fig. 9.13 could be represented by a straight line up to the eutectic composition, and even beyond the deviation is only slight and represents differences in the fourth figure of the density i.e. 1 in 1,000. This suggests that the partial molar density is virtually constant up to and beyond the eutectic composition, but different in value for the two parts of the curve.

A plot of the mean molar volume, which is perhaps more

important, calculated like the densities on the basis of $(KNO_3)_2$ - $Ba(NO_3)_2$, shows no marked deviation. Any detectable deviation is again of the order of 1 in 1000. Thus this system appears to behave ideally. It is, however, interesting to note that the coefficient of expansion of the system $(KNO_3)_2$ - $Ba(NO_3)_2$ decreases with increasing $Ba(NO_3)_2$ content. This can probably be attributed to an increase in 'lattice energy' with increasing $Ba(NO_3)_2$ content.

11.5.3 The Role of Positional Holes in the Electrical Conductivity of Molten Salts.

The effect of vacant cation sites on the electrical conductivity in the solid has been discussed. The addition of $Ba(NO_3)_2$ to KNO_3 in the molten state lowers the conductivity, and what is more striking, the energy for the process increases while the pre-exponential term remains substantially the same. This has also been shown to be the case for the addition of $Ca(NO_3)_2$ to KNO_3. Moreover, below the freezing point of pure KNO_3 the conductivity no longer obeys the simple Arrhenius expression. Thus as can be seen from Fig. 9.12, the plot of log σ against 1/T gives a straight line to the freezing point for pure KNO_3 and thereafter deviates from a straight line.

The mechanism suggested by this behaviour can best be explained by the same argument as that put forward for the H_2O solubility in molten alkali nitrates. The addition of an ion

carrying an extra charge acts so as to limit the mobility of the current carrying ion which can be presumed to be chiefly K^+.

Considering the model for the structure and the mechanism put forward in Chapter 10 for the electrical conductivity (that is accepting that the controlling factor in determining the mobility of the ions is the anion-anion contact), it follows that the increase in the energy of activation for the conductance process in the system KNO_3 - $Ba(NO_3)_2$ must be due to some increase in the anion-anion interaction presumably brought about by the added interaction between Ba^{++} and NO_3^-. This additional interaction of the barium ion with the nitrate ions surrounding it could lead to some form of cluster formation of anions with the Ba^{++} at the centre. A qualitative picture can be taken of the conductance process as being one in which the positive ion threads its way between the 'arms' of the non-spherical anions under the influence of the electric field, aided perhaps by the rotation of the anions. If the liquid now contains clusters due to the Ba^{++}- NO_3^- interaction a lowering of the electrical conductivity and an increase in the energy of activation for the process can arise in two ways:

(i) Since these clusters could be fairly large units their contribution to the conductance process will be very small. As a result there will be a lowering in the total number of the conducting species i.e. the addition of one Ba^{++} would remove $2K^+$ without giving any adoquate conducting replacement.

(ii) These clusters will offer an obstruction to the movement of the K^+.

This is in essence what has been suggested in the discussion on the solubility data, i.e. an intensification of the NO_3^- - NO_3^- interaction through the Ba^{++} - NO_3^- interaction. This same behaviour is exhibited by the KNO_3 - $Ca(NO_3)_2$ system in the molten state.

In general therefore, measurements of gas solubility and electrical conductivity in molten nitrates to which a divalent cation has been added, show no analogous change in physical properties to those exhibited in the solid. This would seem to indicate that cation and anion vacancies as found in the solid are not present in the liquid. It does not however, preclude the formation of some sort of positional hole, but does show that if this occurs a compensating structural change, or over compensating structural change, nullifies, or even reverses the likelihood of changes in physical properties that might be produced in the solid. This appears to be primarily due to two things.

(i) In the liquid the mobility of the ions is such that when an ion is removed the surrounding ions can, to a large extent, close the gap, whilst still adhering to the conditions necessary for electrical neutrality.

(ii) The structure of the non-spherical anions, which could lead to interlocking and extensive anion-anion overlap, lends itself

through the greater polarising power of those cations with a greater charge than the alkali nitrates to intensification, of this effect.

The results for the density and molar volumes of these systems given in Chapter 9 in no way contradict this general conclusion.

11.6 Comparison of the Results of H_2O Solubility with some Solubility Measurements of Other Workers.

The results of two groups of workers are worthy of comment. These are the results of Duke and Doan[3] who have studied the solubility of H_2O in molten systems containing $LiNO_3$, and Keenan[4] who has measured the solubility of H_2O in NH_4NO_3 (See Section 4.4)

Duke and Doan reported no H_2O solubility except in melts containing Li^+. From the magnitude of the solubilities found in the present work it seems surprising that they did not detect H_2O solubility in either $NaNO_3$ or KNO_3. The present experiments, however, were conducted at the freezing point where the solubility might be expected to be at its greatest. The technique of drying adopted by Duke and Doan casts some doubt on the dryness of their melt. This consisted of pumping the molten salt until no change in pressure was observed on isolating the pump. In view of the tenacity with which water is retained in these melts this would not seem to be the best method.

Keenan in his work on the solubility of H_2O in NH_4NO_3 found

very high solubilities, (Section 4.4) much higher than any of the solubilities found in the present work. Although this may well be due to NH_4NO_3 exhibiting different solvent characteristics from those of the alkali nitrates, one point in his experimental technique deserves mention. Water was added to NH_4NO_3 at room temperature, allowed to equilibrate for an hour and its freezing point determined. The H_2O content was found by removing some of the melt when the first solid had just appeared and analysing with Karl Fischer reagent. In view of the fact that, at least in KNO_3, large quantities of excess H_2O can be retained in solution for some time, it is possible that these determinations of solubility represent non equilibrium values, which are not really relevant to the present discussion.

11.7 The Mechanism of Gas Solubility in Ionic Melts.

The existing data for the solubility of gases in ionic melts have been set out in Section 4.4. One striking feature that emerges from a general review of this material is that H_2O dissolves in ionic melts with liberation of heat as instanced by the work of Burkhard and Corbett[5] and Duke and Doan, while the solution of an inert gas requires the absorption of heat as shown by the work of Grimes et al[6]. It is of interest to note that the solubility of the dipolar HF in molten fluorides is also accompanied by a liberation of heat. In this case, however, it may be necessary to consider chemical combination.

Three main models can be considered in any discussion on the mechanism of solution.

1. The gas molecule displaces an ion from its site in the quasi-crystalline melt. This would involve a relatively large energy.

2a. The gas molecule enters a cavity already present in the liquid.

2b. The gas molecule creates a hole by entering the liquid interstitially, expands the hole to accommodate itself or enters an already vacant site or positional hole and expands it to molecular dimensions.

Eley[7] (1939) has considered a model for the solubility of an inert gas in H_2O in which the gas molecule enters a cage of H_2O molecules. A similar approach to the formation of clathrate compounds between H_2O and the inert gases and quinol and different gases has been made by van der Waals[8] (1956,1958). The process of creating a hole or expanding a hole will involve a positive internal energy change. This will be covered in part by the negative change in internal energy produced by the interaction of the gas molecules with the ions surrounding the hole. The total internal energy change can therefore be represented in all cases by

$$\Delta E = \Delta E_h + \Delta E_a$$

ΔE_h is the internal energy change due to the formation of a hole, and $-\Delta E_a$ is the internal energy change produced by the presence

of the gas molecule in the hole.

If $\triangle E_h > - \triangle E_a$ the temperature coefficient of solubility will be positive. If $- \triangle E_a > \triangle E_h$ the temperature coefficient of solubility will be negative. For the reason already given model 1 is not likely to be of much significance since the energy required to remove an ion from its site and replace it with a gas molecule will be large. Lange and Watzel[9] (1938) have calculated the energy required to make a hole on a quasi-lattice point of water to be of the order of 10 Kcal. This would suggest that the energy of solution would always be positive since it is unlikely that the energy that would be regained from solvent-solute interaction would exceed this value. This would lead to a positive energy change throughout since only a very strong solute-solvent interaction would produce the negative enthalpy change reported for H_2O in ionic melts [3,5]. Again model 2a would suggest a negative coefficient of solubility for all gases since the positive energy change introduced in the creation of the hole would be near to zero. It is with model 2b that the greatest interest lies, since the balance between the energy required to create a hole and that regained by solvent-solute interaction is such that the sign of the total energy change is altered by the polar character of the gas. It is with this last model that this discussion will primarily be concerned.

The internal energy of solution is regarded as being approximately equal to the enthalpy of solution, ~~i.e. the entropy of~~

~~of solution is presumed to be small. In the absence of any means of making an estimation of entropy of solution this appears to be reasonable approximation.~~

An approach to the calculation of the interaction between gas molecules and ions can be made through electrostatics.

If as a first approximation the H_2O is considered as a point dipole the interaction energy between H_2O and an ion can be calculated. The following expression has been derived for the work done in bringing an H_2O molecule from infinity to contact with an ion[10].

$$W = -\frac{e\bar{m}^x}{S^3}\,\bar{S} - \frac{3}{S^5}(\bar{m}_o\,\bar{S})(\bar{m}^x S) + \frac{\bar{m}_o\,\bar{m}^x}{S^3} + \frac{m_o^2}{2\alpha_1} + \frac{\bar{m}^x}{2\alpha_1} + \frac{\bar{m}^x - \bar{m}}{2\alpha_2} \quad \ldots 11.1$$

S is the distance between the centre of the particle charge 'e' and polarisability α_1 and the dipole m, of polarisability α_2. m_o and m_1 are the induced dipoles in the charged particle and the dipole respectively. The bar indicates a vector quantity, The general solution is very intricate but it is possible to carry out a simple calculation for the particular case in which the permanent dipole has the same or opposite direction of the vector S. This leads to maximum or minimum values. The minimum value for this interaction will be,

$$W = \frac{-\left\{\frac{em}{S^2} + \frac{\alpha_2 e^2}{2S^4} + \frac{2\alpha_1}{S^6} m^2\right\}}{1 - \frac{4\alpha_1\alpha_2}{S^6}} \quad \ldots\ldots 11.2$$

Considering this interaction i.e. the interaction of the negative end of the H_2O dipole with the positive ion it can be shown that only the terms $\frac{em}{S^2}$ and $\frac{\alpha_2 e^2}{2S^4}$ are significant. Specimen values for the interaction of H_2O with Na^+ are given in Table 11.1. S has been taken as being equal to the radius of the H_2O plus the radius of the Na ion. Fig. 11.2 demonstrates the dependence of both these terms on the distance of separation of Na^+ and H_2O.

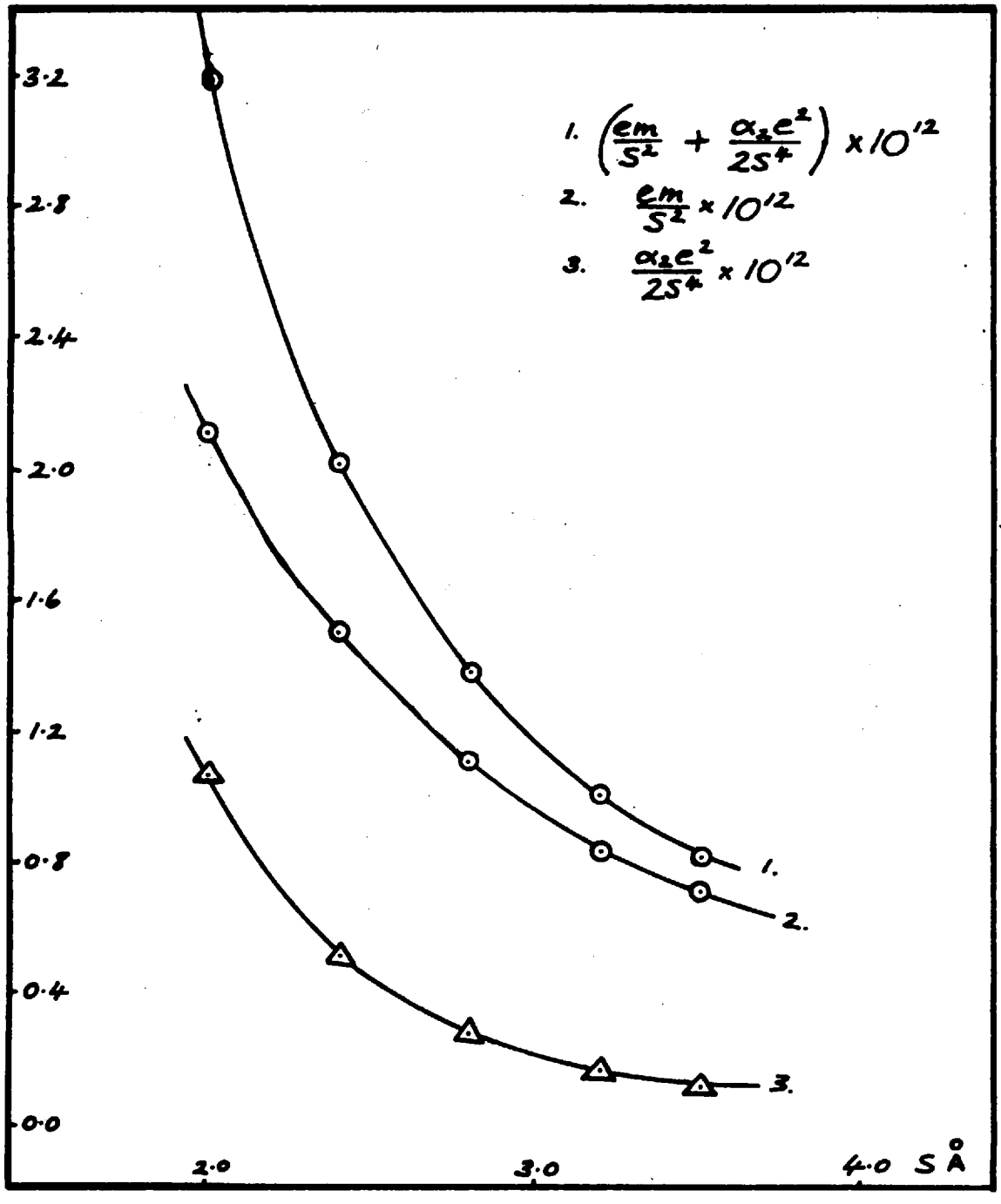
TABLE 11.1

The Interaction of Na^+ with H_2O.

Term	Energy(ergs)
$\frac{em}{S^2}$	1.44×10^{-12}
$\frac{\alpha_2 e^2}{2S^4}$	4.8×10^{-13}
$\frac{2\alpha_1 m^2}{S^6}$	5.7×10^{-16}
$\frac{4\alpha_1\alpha_2}{S^6}$	5.236×10^{-3}

It is of interest to note that Duke and Doan[3] discuss only the S^{-4} term in their consideration of the solubility of H_2O in

FIG 11.1


3·2
2·8
2·4
2·0
1·6
1·2
0·8
0·4
0·0
2·0
3·0
4·0 S Å
1. $\left(\frac{em}{S^2} + \frac{\alpha_2 e^2}{2S^4}\right) \times 10^{12}$
2. $\frac{em}{S^2} \times 10^{12}$
3. $\frac{\alpha_2 e^2}{2S^4} \times 10^{12}$
1.
2.
3.

melts containing $LiNO_3$, neglecting any mention of the S^{-2} term. Values of W calculated for the interaction of H_2O with different cations are given in Table 11.2.

TABLE 11.2

ion	$-W_{H_2O} \times 10^{12}$ ergs.
Na	1.92
K	1.35
Cs	1.02

The energies in Table 11.2 are based on the first two terms only of Equation 11.2.

For the calculation of the energy of interaction between an ion and a particle not possessing a permanent dipole moment an expression similar to 11.2 can be derived, but since m = ɔ it reduces to

$$W = \frac{\alpha_2 e^2}{2S^4} \quad \frac{1}{1 - \frac{4\alpha_1\alpha_2}{S^6}} \qquad \ldots\ldots\ldots 11.3$$

When the interaction energy for an ion and an inert gas is calculated on the basis of equation 11.3 it is found that this is lower than that for the interaction of an ion and H_2O. Table 11.3 shows values for this interaction calculated for Na^+ and K^+ with different inert gases.

TABLE 11.3

Interaction Energies for Na^+ and K^+ with Inert Gases.

Gas	$-W \times 10^{13}$ ergs.	
	Na^+	K^+
He	1.04	0.55
Ne	1.24	0.70
A	3.02	1.83

The values calculated in Tables 11.2 and 11.3 are based on the contact of ion and dipole and so:

$S = r_1 + r_2$ (r_1 is the radius of the ion
r_2 is the collision radius of a gas atom or molecule.)

It can be seen that the important factors in the interaction of an ion and a dipole are e, m, α_2 and S. The effect of increasing ion charge will be discussed in a subsequent section.

An additional interaction energy will also arise from the interaction of the positive end of the dipole with an anion. Calculation of this interaction can be made by the same method as that described for cation-dipole interaction.

The above calculations are inaccurate when the distance of separation between the particles is of the same order as their radii. A correction factor must be applied. The correction

factor is largely independent of the dielectric constant. Table 11.4 shows values of some correction factors calculated by Böttcher[10] on the basis of a sphere of radius 'a' and dielectric constant ε, separated from a point charge by distance S.

TABLE 11.4

Correction Factors.

$\frac{s}{a}$	$\varepsilon = 2$	$\varepsilon = 4$	$\varepsilon = 6$
1.5	1.94	1.88	1.86
2	1.38	1.36	1.36
4	1.07	1.07	1.07
10	1.01	1.01	1.01

This means that the interaction energies can be 50 - 100% higher than those calculated by the simple formula.

The data show that a higher solubility of H_2O than of the inert gases can be expected from a consideration of this interaction.

Table 11.5 illustrates the strength of the interaction energy between the divalent ions Ca^{++} and Ba^{++} and H_2O. As in the previous calculations the species are assumed to behave as charges particle and point dipole.

TABLE 11.5

The Interaction Energy of H_2O and M^{++}

ion	$\frac{em}{s^2} \times 10^{12}$	$\frac{\alpha_2 e^2}{2s^4} \times 10^{12}$	$-W \times 10^{12}$
Ca^{++}	2.79	1.79	4.58
Ba^{++}	2.13	1.04	3.17

This interaction would lead to the same sign for the energy of interaction whether the gas in solution was H_2O or an inert gas. However, as has been pointed out above the evidence suggests a change of sign when a dipolar gas is considered as the solute. This repulsive term which appears to be greatest with H_2O will be larger than the energy of hole creation. Some indication therefore, can be gauged of its size. It is found that the interaction of H_2O with an ion depends principally on $\frac{em}{s^2} + \frac{\alpha_2 e^2}{2s^4}$

In general $$\frac{em}{s^2} > \frac{\alpha_2 e^2}{2s^4}$$

In the case of the inert gas atom the $\frac{em}{s^2}$ term is zero. Hence the additional term producing a net repulsion must lie between $\frac{em}{s^2}$ and $\frac{\alpha_2 e^2}{2s^4}$, if its source is common to both H_2O and an inert gas atom. If this term is called A,

$$\left| \frac{\alpha_2 e^2}{2s^4} \right| + \left| \frac{em}{s^2} \right| > \left| A \right| > \frac{\alpha_2 e^2}{2s^4}$$

A being of opposite sign to the other two terms.

One simple approach is to regard this energy as the energy required to create a hole in a molten ionic salt. Following Uhlig[11] (1937) and Grimes et al.[6] this can be considered as work against the surface tension of the liquid, thus

$$W_e = W_\gamma - W_{el}$$

W_{el} is the energy due to the electrostatic interaction, W_γ is the surface energy of a hole the size of a gas molecule.

$$W_e = 4\pi r^2 \gamma \qquad (\gamma \text{ is a microscopic surface tension.})$$

For this purpose it is assumed that $\gamma_{mic} = \gamma_{mac}$. This is not strictly true since a real liquid could not be regarded as a continuous fluid.

Table 11.6 compares the energies required to create a hole in an ionic liquid of the size of a gas molecule in this way. H_2O has been regarded as a sphere radius 3A° in diameter. If there are holes already present in the liquid then the work done against the surface tension will be less than this work of creating a hole.

$$W'_\gamma = 4\pi r^2 \gamma - 4\pi r_1^2 \gamma$$
$$= 4\pi\gamma (r^2 - r_1^2)$$

r_1 is the radius of the hole already present.

TABLE 11.6

Melt	W_γ ergs x 10^{13} for different gases					
	H_2O	He	Ne	A	Kr	Xe
$LiNO_3$	3.31	2.48	2.88	4.25	4.76	5.88
$NaNO_3$	3.39	2.55	2.95	4.36	4.88	6.03
KNO_3	3.19	2.40	2.78	4.10	4.60	5.68
$RbNO_3$	3.08	2.30	2.68	3.96	4.44	5.48
$CsNO_3$	3.11	2.35	2.71	3.99	4.48	5.53

The values for W_γ are shown in Table 11.6 and can be compared with the values for the interaction energy W_{el}. It will be observed from this that $W_\gamma > W_{el}$ for the solution of inert gas molecules whereas $W_{el} > W_\gamma$ for the solution of an inert gas atom in an ionic melt. This could account for the difference in sign in the enthalpy of solution between H_2O and inert gas solutes. This consideration that the energy to form a hole is only derived from the work done against the surface tensions appears to produce a value of the correct order of magnitude though this is clearly an over simplification and further energy terms would be required. It would seem, however, to indicate that the energy involved in hole formation is lower than a mechanism involving the displacement of an ion from a quasi-crystalline lattice site. A more extensive

treatment of the theory of gas solubility in ionic melts awaits more detailed and systematic results.

11.8 The Anomalous Behaviour of Solutions of H_2O in Molten $NaNO_3$.

H_2O showed a high solubility in $NaNO_3$ (Chapter 9) which within any one series of determinations over a short period of time was reproducible. However it was not always reproducible from one series to another and was shown to exhibit an ageing effect which manifests itself as an apparent decrease in the solubility. There are two possible explanations for this:

(i) The melt ages and the solubility is in fact reduced - due to some structural change in the melt which is time dependent.

(ii) The solubility in the melt does not alter but under certain conditions H_2O can form a solid solution with the precipitating $NaNO_3$, leading to an apparently low value for the freezing point depression.

The latter explanation would seem the most reasonable and can be attributed to two causes:

(a) The decomposition of nitrate to nitrite and the subsequent solution of H_2O in the solid solution of $NaNO_2$ in $NaNO_3$.

(b) The spontaneous crystallisation of another $NaNO_3$

crystal type which is more amenable to the formation of solid solutions of H_2O.

In favour of (a) was the fact that in one case a small trace of NO_2^- was detected in $NaNO_3$ after an anomalously low freezing point depression had been found. However, though it was verified that $NaNO_2$ formed a solid solution with $NaNO_3$ the slope of the temperature against mole fraction $NaNO_2$ plot was such that continual decomposition would have shown itself in the gradual lowering of the freezing point in the presence of dry N_2. This was not observed. Though the depression of the freezing point in the presence of water vapour gradually reduced; the freezing point with dry N_2 remained substantially the same over several days.

In favour of (b) is the fact that $NaNO_3$ exhibits a solid-solid transition at 275°C which is continuous. If the solid recrystallising from the melt contained a proportion of the crystal form which occurs below the transition and further, if this crystal form readily dissolves H_2O, the unpredictability of the apparent solubility would be explained.

It was noted during the course of experiments on $NaNO_3$, that when crystallising from the melt in the pure state the crystals adhered to the walls of the solubility cell and stirrer. This effect disappeared with the addition of $Ca(NO_3)_2$ even in small quantities, and was reduced with the addition of small quantities of $NaNO_2$. This suggest that $NaNO_3$ can crystallise in a relatively

disordered state and it is possible that two different types of crystal can be precipitated from the melt; it being purely fortuitous which one predominates. Such behaviour has been noted in KSCN, where two heats of fusion have been reported. Both of these are correct since each depends on different forms of the solid with different heats of fusion separating from the melt [12]. Against this suggestion, however, it must be noted that the second order transition in $NaNO_3$, although spread over a considerable temperature range below 275°C, appears to terminate quite sharply at the upper temperature. Further, unlike KSCN no anomalous heats of fusion have been reported for $NaNO_3$. Thus without further investigation, which would have to include X-ray crystallographic studies near the melting point, it is impossible to know precisely the cause of the anomalous values for the solubility of H_2O in $NaNO_3$ which can occur even in the presence of $Ca(NO_3)_2$. The results summarised in Chapter 9 for $NaNO_3$ have been derived on the basis of the highest value obtained, i.e. mechanism (ii) is considered to be the most likely.

References.

1. Consultants Bureau Inc., Chem. Coll. No.I "Soviet Research in Fused Salts (1949-1955)".

2. Glasstone "Textbook of Physical Chemistry" Van Nostrand, N.Y. (1946).

3. Duke and Doan, Iowa State College, J. of Sci. (1958), 32, 451.

4. Keenan, J. Phys. Chem. (1957), 61, 780.

5. Burkhard and Corbett, J.A.C.S. (1957), 79, 6361.

6. Grimes, Smith and Watson, J. Phys. Chem. (1958), 62, 862.
Blander, Grimes, Smith and Watson, J. Phys. Chem. (1959), 63, 1164. Shaffer, Grimes and Watson, J. Phys. Chem. (1959), 63, 1999.

7. Eley, Trans. Far. Soc. (1939), 35, 1281, 1421.

8. van der Waals, Trans. Far. Soc. (1956), 52, 184.
van der Waals and Platteeuw, Molec. Phys. (1958), 1, 91.

9. Lange and Watzel, Z. physikal Chem. A. (1938), 182, 1.

10. Böttcher, "The Theory of Electric Polarisation" Elsevier, Amsterdam (1952).

11. Uhlig, J. Phys. Chem., (1937), 41, 1215.

12. Rhodes, PhD. Thesis, London 1958.

CHAPTER 12.

GENERAL CONCLUSIONS.

The study of the electrical conductance and viscosity of molten $NaNO_2$, KNO_2, $TlNO_3$ and $K_2Cr_2O_7$ has shown that the ratio of E_η / E_σ is close to 1. This demonstrates that the species controlling the mechanism in both these processes is the same. Comparison of the results for these salts with those for other salts with polyatomic anions leads to the conclusion that this can now be regarded as a general rule for such salts. This conception of the non spherical anion as the controlling ion is supported by the evidence of surface tension. This anion-anion interaction can be regarded as a form of complex formation. It must be pointed out however, that there is no evidence that these "complexes" are of a chemical nature, rather must they be regarded as physical interlocking of non spherical anions or the overlapping of the bond orbitals of non spherical anions.

This picture of a lattice controlled by anion-anion interaction is not contradicted by the results for H_2O solubility in $NaNO_3$, KNO_3 and $CsNO_3$. These results show that the solubility is large compared with what might be expected for an inert gas. This relatively large solubility can be accounted for in terms of interaction between dipole and ion. Some dependence of gas solubility on the presence of cavities in the liquid, as has been suggested

for the solubility of inert gases, can not be overlooked and indeed it seems that the solubility is related to the free volume in alkali nitrates though its role is smaller than that of electrostatic interaction.

The creation of positional holes in solid alkali nitrates has been demonstrated by the change in the electrical conductance in the solid when small quantities of a salt having a common anion but a divalent cation are added to form a solid solution. The addition of similar divalent cations to the melt and their small effect on gas solubility shows that the concept of vacant lattice sites as interpreted for solid structures does not have a parallel in the liquid. This is not to say that molten alkali nitrates containing a small amount of alkaline earth nitrate are not quasi-crystalline in character but rather that their structure changes with the addition of divalent cations and forms a modified alkali nitrate structure.

APPENDIX I.

Derivation of the Relation between Gas Solubility and Surface Tension (cf. Uhlig[1] 1937)

Assume a spherical gas molecule radius r, and further assume that when a molecule of gas dissolves in a non reacting solvent it produces a hole of the same radius in the solvent. Then the work required to create a hole is:

$4\pi r^2\gamma$ γ= surface tension.

If E is the interaction energy between molecules involved and W is the change in energy in transferring a molecule from the solvent phase to the low temperature gas phase, then the work required to remove a gas molecule from a hole

$$\Delta W = E - 4\pi r^2\gamma$$

This neglects the interaction energy between solvent and solute molecules in the gas phase.

From the Maxwell-Boltzman distribution theorem:

$\frac{c'}{c} = e^{-\Delta W/kt}$ c' is the concentration of gas in solvent.

c is the concentration of gas in the gas phase.

W is the work required to transfer a molecule from the solvent phase to the gas phase. If Henry's law is obeyed $\frac{c'}{c}$ is independen

of pressure.

$$\text{Thus} \quad \ln \frac{c'}{c} = \frac{-4\pi r^2\gamma + E}{kT}$$

If the gas interacts but little with the solvent and does not tend to solvate then the major part of the solubility will depend on $4\pi r^2\gamma$ since E would be small. Thus $\frac{c'}{c}$ plotted against will result in a straight line whose slope is proportional to the square of the gas molecule radius and whose intercept will provide E.

If $4\pi r^2\gamma > E$ the solubility will increase with temperature.

If $4\pi r^2\gamma > E$ the solubility will increase with temperature.

In this work terms have been inserted. To separate between internal energy and entropy terms one has to make assumptions about vibrational entropy similar to those discussed in Mott and Gurney[2] for the creation of holes in lattices q.v.

~~If any change of entropy can be neglected then ΔU can be equated with ΔH the heat change (See Chapter 11).~~

References.

1. Uhlig, J. Phys. Chem. (1937), 41, 1215.

2. Mott and Gurney, "Electronic processes in Ionic Crystals" O.U.P. 1940.

APPENDIX II

Calibration of Viscometers.

Viscometer I. Bore 0.2 mm.

Temp. °C	Flow Time secs. 'a'-'b'	'b'-'a'	ΔP cms.Hg.	ΔP.t. cm-secs.	$\frac{\eta}{\Delta P.t.} \times 10^4$
36.2	701	691	3.935	2737.186	2.578
	699.4	691			
	303.3	302.1	9.135	1764.479	2.553
	303.0	302.1			
	185.4	185.2	15.044	2786.901	2.532
	185.0	185.4			
	135.9	136.0	20.642	2806.796	2.514
	135.9	136.1			
53.0	518.0	512.0	3.937	2027.555	2.579
	518.0	512.0			
	228.0	226.2	9.103	2064.105	2.533
	226.5	226.3			
	138.8	139.5	15.009	2088.502	2.504
	139.0	139.3			
	102.2	102.8	20.620	2114.581	2.473
	102.2	103.0			

Viscometer II. Bore = 0.2 mm.

Temp. ^{o}C	Flow Time Secs. 'a'-'b'	'b'-'a'	ΔP cms.Hg.	$\Delta P.t.$ cm-secs.	$\frac{\eta}{\Delta P.t.} \times 10^4$
33.8	665.6	646.3	4.735	3112.000	2.378
	667.5	648.5			
	666.5	649.0			
	358.2	352.8	9.660	3433.647	2.155
	357.7	353.0			
	357.8	353.2			
	242.9	236.0	14.500	3456.981	2.141
	237.8	236.9			
	238.5	237.5			
	239.2	238.5			
	174.7	173.9	19.958	3482.338	2.125
	174.7	174.3			
	175.2	174.1			
33.3	674.2	657.6	5.167	3437.347	2.175
	673.5	657.6			
	671.5	657.1			

/Continued.....

Viscometer II (Continued...)

Temp. °C	Flow Time secs. 'a'-'b'	'b'-a'	ΔP cms.Hg.	ΔP.t. cm-secs.	$\frac{\eta}{\Delta P.t.}$ x 10^4
	314.6	311.2	11.047	3456.974	2.163
	314.2	311.6			
	314.2	311.8			
	210.3	208.1	14.569	3039.458	2.460
	209.1	207.7			
	209.2	207.7			
	209.2	207.7			
	155.8	155.2	22.260	3447.9	2.169
	155.5	155.2			
	155.5	155.2			
36.2	630.2	616.5	5.213	3249.35	2.172
	630.2	616.0			
	630.5	616.5			
	302.1	298.9	10.793	3242.49	2.176
	301.9	298.8			
	197.2	196.8	16.559	3263.36	2.162
	197.7	196.6			
	147.6	147.0	22.266	3278.11	2.153
	147.4	146.9			

/Continued.....

Viscometer II (Continued..)

Temp. °C	Flow Time secs. 'a'-'b'	'b' -'a'	ΔP. cms.Hg.	ΔP.t. cm-secs.	$\frac{\eta}{\Delta P.t.} \times 10^4$
38.2	605.7	591.6	5.167	3091.29	2.196
	605.2	590.6			
	289.8	287.1	10.797	3115.47	2.179
	290.3	287.0			
	141.8	141.1	22.244	3145.3	2.158
	141.6	141.1			
	189.2	188.8	16.569	3137.8	2.163
	189.8	188.8			

Viscometer III. Bore = 0.3 mm.

Temp. °C	Flow Time secs. 'a'-'b'	'b'-'a'	ΔP. cms.Hg.	ΔP.t. cm-secs.	$\frac{\eta}{\Delta P.t.} \times 10^3$
41.6	39.7	39.5	4.505	177.59	3.586
	39.7	39.1			
	39.2	39.5			
	39.5	39.4			
	39.5	39.1			

/Continued.....

Viscometer III (Continued...)

Temp. °C	Flow Time secs. 'a'-'b'	'b'-'a'	ΔP. cms.Hg.	ΔP.t. cm-secs.	$\frac{\eta}{\Delta P.t.} \times 10^3$
	64.9	64.6	2.715	175.86	3.621
	65.0	64.4			
	65.1	64.7			
	65.0	64.5			
	24.5	24.4	7.290	178.24	3.573
	24.4	24.5			
59.0	18.9	18.8	7.335	138.63	3.433
	18.9	18.9			
	28.2	28.3	4.790	135.32	3.517
	28.2	28.3			
	51.8	51.9	2.560	132.86	3.582
	51.9	52.0			

Viscometer IV Bore = 0.3 mm.

Temp. ^{o}C	Flow Time secs. 'a'-'b'	'b'-'a'	ΔP. cm.Hg.	$\Delta P.t.$ cm-secs.	$\frac{\eta}{\Delta P.t.} \times 10^{3}$
24.9	62.5	62.6	5.276	330.54	2.710
	62.8	62.8			
	62.7	62.5			
	85.6	85.4	4.025	344.12	2.603
	85.6	85.4			
	85.6	85.4			
	127.6	130.8	2.627	338.81	2.744
	126.4	132.1			
	127.0	131.0			
	125.5	131.5			
	127.6	131.2			
	201.5	212.5	1.668	345.28	2.594
	201.5	212.5			
	86.6	88.4	3.869	337.47	2.654
	86.4	87.5			

Viscometer V. Bore = 0.5 mm.

Calibrated using 60% w/w sucrose-water solution.

Temp. °C	Flow Time secs. 'a'-'b'	'b'-'a'	ΔP. cm.Hg.	Δp.t. cm-secs.	$\frac{\eta}{\Delta p.t.} \times 10^3$
50.0	223.7 223.8	224.3 224.1	16.605	3719.10	3.766
	168.2 168.2	167.7 168.7	22.230	3739.10	3.746
	659.6	662.2	5.681	3754.57	3.730
	321.1 321.2	322.3 322.2	11.597	3730.75	3.754
	213.3 211.1	212.2 212.1	17.619	3738.3	3.747
	160.4 160.4	160.3 160.3	23.256	3729.10	3.756

Solid Conductivity

$NaNO_2$

Temp. °C	Average deflection mms.	Number of results on which based.	Volts	Resistance ohms.
22	116 ± 6.0	14	8.7	3.35×10^9
	107 ± 2.0	10	78	3.33×10^9
	70.3 ± 2.0	12	52	3.30×10^9
	59 ± 2.0	16	43.5	3.29×10^9
	47,5 ± 3.0	14	35	3.31×10^9
207	200 ± 1.0	8	0.757	1.757×10^7
	138 ± 1.0	12	0.524	1.762×10^7
	86.5 ± 1.0	12	0.329	1.767×10^7
	63.7 ± 1.0	10	0.240	1.749×10^7
194.8	218 ± 1.0	12	1.707	3.641×10^7
	178.2 ± 1.0	12	1.408	3.662×10^7
	132 ± 2.0	12	1.047	3.685×10^7
	99.1 ± 1.0	12	0.793	3.715×10^7
	70.3 ± 1.5	12	0.559	3.695×10^7
	39.5 ± 1.0	12	0.314	3.689×10^7

/Continued.....

$NaNO_2$ (Continued...)

Temp. °C	Average deflection mms.	Number of results on which based.	Volts	Resistance ohms
178.8	71.3 ± 1.0	12	1.319	8.601×10^7
	89.5 ± 1.0	12	1.641	8.517×10^7
	55.8 ± 1.0	12	1.015	8.459×10^7
	34.0 ± 0.5	12	0.619	8.468×10^7
	17.1 ± 0.3	12	0.311	8.432×10^7
216.6	104.5 ± 1.0	12	0.311	1.384×10^7
	55.6 ± 1.0	10	0.165	1.375×10^7
	185.2 ± 1.0	10	0.544	1.364×10^7
236.2	185.4 ± 1.0	12	0.178	4.460×10^6
	120.3 ± 2.0	14	0.117	4.522×10^6
	144.1 ± 1.0	14	0.138	4.459×10^6
	93.6 ± 0.5	12	0.091	4.502×10^6
246.4	148 ± 2.0	12	0.0907	2.847×10^6
	61 ± 1.0	12	0.0347	2.643×10^6
	163.9 ± 2.0	12	0.0928	2.630×10^6

$K_2Cr_2O_7$

389.8	7.88 ± 0.5	8	0.003	7.229×10^3
	36.75 ± 0.0	10	0.0144	7.496×10^3
	11.0 ± 0.0	10	0.0044	7.596×10^3

/Continued....

$K_2Cr_2O_7$ (Continued..)

Temp. °C	Average deflection mms.	Number of results on which based.	Volts	Resistance ohms.
389.8 (Contd.)	62.0 ± 0.0	10	0.0241	7.496×10^3
	25.75 ± 0.25	12	0.0101	7.481×10^3
357.5	9.25 ± 0.00	10	0.2078	4.263×10^5
	20.3 ± 0.00	10	0.4607	4.322×10^5
	29.5 ± 0.25	10	0.6653	4.303×10^5
	47.4 ± 0.25	12	1.0606	4.294×10^5
	26.1 ± 0.1	12	0.590	4.316×10^5
	13.5 ± 0.0	10	0.3048	4.291×10^5
332.8	5.25 ± 0.25	10	0.3050	1.101×10^6
	20.0 ± 0.0	10	1.124	1.070×10^6
	27.25 ± 0.0	10	1.514	1.060×10^6
	27.0 ± 0.0	10	1.492	1.055×10^6
	29.6 ± 0.1	10	1.645	1.062×10^6
	13.0 ± 0.0	10	0.7276	1.063×10^6
294.5	8.0 ± 0.0	10	1.562	3.703×10^6
	9.0 ± 0.0	10	1.747	3.683×10^6
	9.0 ± 0.1	10	1.698	3.560×10^6
256.9	29.1 ± 0.5	10	0.1740	2.783×10^7
	93.25 ± 0.25	10	0.558	2.780×10^7
	169.75 ± 0.5	10	1.004	2.747×10^7

/Continued.....

$K_2Cr_2O_7$ (Continued)

Temp. °C	Average deflection mms.	Number of results on which based.	Volts	Resistance ohms.
256.9 (Contd.)	53.0 ± 1.0	10	0.320	2.799×10^7
	170.0 ± 0.5	10	1.009	2.760×10^7
206.6	26 ± 0.0	10	3.6	6.435×10^8
	28.5 ± 0.2	10	3.94	6.425×10^8
	37.5 ± 0.5	10	5.0	6.195×10^8
	44.25 ± 0.25	10	5.9	6.194×10^8
	60.75 ± 0.25	10	7.95	6.081×10^8

KNO_2

407.1	60 ± 1.0	22	0.2514	8.076×10^3
	28 ± 1.0	20	0.1332	9.078×10^3
	18.0 ± 0.0	20	0.0756	7.992×10^3
	37.0 ± 1.0	22	0.1652	8.550×10^3
	17.50 ± 1.0	18	0.0864	8.57×10^3
389.8	48.8 ± 1.0	24	0.290	1.142×10^4
	32.5 ± 2.0	24	0.1980	1.162×10^4
	12.7 ± 0.0	24	0.0751	1.124×10^4
	33.2 ± 2.0	24	0.1982	1.140×10^4
	20.3 ± 0.0	24	0.1228	1.151×10^4

/Continued.....

KNO_2 (Continued...)

Temp. °C	Average deflection mms.	Number of results on which based	Volts	Resistance ohms.
350.8	44.9 ± 0.5	20	0.5593	2.392×10^5
	55 ± 0.0	20	0.6835	2.392×10^5
	68.45 ± 0.5	20	0.8436	2.382×10^5
	34.5 ± 0.0	26	0.4291	2.379×10^5
	17.6 ± 0.5	20	0.2224	2.404×10^5
305.6	24.85 ± 0.0	20	1.5879	1.219×10^6
	22.35 ± 0.0	20	1.4234	1.230×10^6
	26.1 ± 0.0	20	1.6775	1.227×10^6
	24.5 ± 0.0	16	1.5855	1.234×10^6
	20.85 ± 0.0	14	1.3499	1.236×10^6
248.6	223.75 ± 1.0	10	1.3502	0.6503×10^7
	98.3 ± 1.0	12	0.2910	1.375×10^7
	179.8 ± 1.5	12	0.5258	1.359×10^7
	125.9 ± 1.0	12	0.3717	1.372×10^7
204.9	65.7 ± 1.0	18	1.1365	8.040×10^7
	79.4 ± 1.0	20	1.4065	8.230×10^7
	97.9 ± 1.5	20	1.741	8.262×10^7
	60.4 ± 0.5	18	1.1035	8.488×10^7
	78.0 ± 0.5	18	1.4302	8.519×10^7

/Continued.....

KNO_2 (Continued...)

Temp. °C	Average Deflection mms.	Number of results on which based	Volts	Resistance ohms.
401.3	36.8 ± 0.2	28	0.1475	7.671×10^3
	61.0 ± 1.0	26	0.2212	6.991×10^3
	73.7 ± 1.0	24	0.2676	7.136×10^3
	20. ± 0.0	15	0.855	8.144×10^3
	44.5 ± 0.5	16	0.1660	7.169×10^3
387.6	29.5 ± 0.2	20	0.1662	1.075×10^4
	68.8 ± 0.5	18	0.3330	0.935×10^4
	28.8 ± 0.3	18	0.1260	0.835×10^4
	58.5 ± 0.0	10	0.2854	0.940×10^4
	22.0 ± 0.0	10	0.1272	1.101×10^4
319	31.0 ± 0.0	10	1.4534	8.807×10^5
	36.0 ± 0.0	10	1.6958	9.014×10^5
	19.0 ± 0.0	10	0.8996	9.005×10^5
	27.35 ± 0.2	10	1.3091	9.135×10^5
266	59.85 ± 0.5	10	0.1048	8.098×10^6
	173 ± 1.0	14	0.2972	7.982×10^6
	99.96 ± 1.5	12	0.1729	8.034×10^6
	41.96 ± 0.5	12	0.7060	7.817×10^6
	151.6 ± 0.75	12	0.2465	7.554×10^6
409.3	74.5 ± 0.0	12	0.2452	6.366×10^3
	50.5 ± 0.0	10	0.1802	6.857×10^3

/Continued.....

KNO_2 (Continued...)

Temp. °C	Average Deflection mms.	Number of results on which based.	Volts	Resistance ohms
409.3 (Contd.)	23.0 ± 0.0	10	0.0950	7.872×10^3
	59.0 ± 0.0	10	0.2054	6.721×10^3
	20.5 ± 0.0	10	0.0867	8.061×10^3
369.4	56.8 ± 0.0	16	0.1770	6.000×10^4
	23.4 ± 0.0	16	0.0747	6.082×10^4
	51.4 ± 0.0	16	0.1604	5.997×10^4
	34.5 ± 0.0	12	0.1083	6.004×10^4
	56.8 ± 0.0	22	0.1735	5.880×10^4
381	35.5 ± 0.0	10	0.0289	1.557×10^4
	61.5 ± 0.0	10	0.0504	1.580×10^4
	28.0 ± 0.0	7	0.0227	1.549×10^4
	69.5 ± 0.5	12	0.4678	1.3002×10^4
	41.5 ± 0.0	10	0.2941	1.3622×10^4
365.5	47.0 ± 0.0	4	0.3660	1.495×10^5
	65.0 ± 0.0	4	0.5061	1.503×10^5
	39.3 ± 0.0	4	0.3057	1.490×10^5
	19.0 ± 0.0	4	0.1488	1.500×10^5
	58.5 ± 0.0	4	0.4525	1.490×10^5
374.7	49 ± 0.0	4	0.07997	3.135×10^4
	29.25 ± 0.0	4	0.04778	3.119×10^4

/Continued.....

KNO_2(Continued..)

Temp. °C	Average Deflection mms.	Number of results on which based	Volts	Resistance ohms.
374.7 (Contd.)	66.5 ± 0.0	6	0.10645	3.092×10^4
	17.5 ± 0.0	6	0.02784	3.027×10^4
327.6	12.75 ± 0.0	4	0.2698	4.017×10^4
	50.0 ± 0.0	4	0.10629	4.083×10^4
	47.5 ± 0.0	4	0.09983	4.035×10^4
	18.0 ± 0.0	4	0.03788	4.005×10^4
	65.0 ± 0.0	4	0.1350	4.009×10^4
367.7	29.0 ± 0.0	4	1.3509	8.893×10^4
	54.0 ± 0.0	4	0.2513	8.953×10^4
	36.0 ± 0.0	4	0.1685	8.953×10^4
	48.0 ± 0.0	4	0.2252	9.008×10^4
	29.5 ± 0.0	4	0.1380	8.932×10^4

APPENDIX III

Details of Solubility Results.

TABLE 1.

Solubility of H_2O in $CsNO_3$.

No.	Atmosphere	T_f °C	ΔT_f °C	Solubility moles H_2O/mole melt
1	dry N_2	405.74	0.00	-
2	" "	405.75	0.00	-
3	" "	405.74	0.00	-
4	N_2 + H_2O of	405.49	0.25	9.23×10^{-4}
5	19.1 mm.Hg. p.p.	405.48	0.26	9.60×10^{-4}
6	dry N_2	405.58	0.16	5.91×10^{-4}
7	" "	405.66	0.11	4.06×10^{-4}
8	" "	405.67	0.11	4.06×10^{-4}
9	N_2 + H_2O of	405.49	0.25	9.23×10^{-4}
10	19.1 mm.Hg. p.p.	405.49	0.25	9.23×10^{-4}
11	dry N_2	405.67	0.11	2.95×10^{-4}

6, 7, 8 and 11 appear to be residual moisture.

TABLE 2.

Solubility of H_2O in $CsNO_3$ containing 4.33 mole % $Ba(NO_3)_2$

No.	Atmosphere	T_f °C	ΔT_f °C	Solubility moles H_2O/mole melt
1	dry N_2	391.00	0.00	-
2	" "	391.00	0.00	-
3	N_2 + H_2O of	390.83	0.17	6.28×10^{-4}
4	17.8 mm.Hg.p.p.	390.83	0.17	6.28×10^{-4}
5	dry N_2	390.99	0.00	-
6	" "	391.00	0.00	-
7	N_2 + H_2O of	390.83	0.17	6.28×10^{-4}
8	17.8 mm.Hg.p.p.	390.83	0.17	6.28×10^{-4}
9	dry N_2	390.97	0.03	1.11×10^{-4}

TABLE 3.

Solubility of H_2O in KNO_3.

No.	Atmosphere	T_f °C	ΔT_f °C	Solubility moles H_2O/mole melt
1	dry N_2	335.06	0.00	-
2	" "	335.03	0.00	-
3	" "	335.06	0.00	-
4	N_2 + H_2O of	334.83	0.23	8.07×10^{-4}
5	2.1 mm.Hg.p.p.	334.80	0.26	9.12×10^{-4}
6	" "	334.95	0.11	3.86×10^{-4}
7	" "	334.95	0.11	3.86×10^{-4}

/Continued.....

TABLE 3 (Continued..)

No.	Atmosphere	T_f °C	ΔT_f °C	Solubility moles H_2O/mole melt
8	N_2 + H_2O (p.p. 9.4 mm.Hg.)	334.95	0.11	3.86×10^{-4}
9	N_2 + H_2O (p.p.	334.95	0.11	3.86×10^{-4}
10	20.4 mm.Hg.)	334.95	0.11	3.86×10^{-4}

TABLE 4

Injecting KNO_3 with H_2O.

No.	Atmosphere	Approx. time(hrs.)	ΔT_f °C	Solubility moles H_2O/mole melt
1	No gas flow	0	1.53	5.37×10^{-3}
2	" " "	2.5	1.00	3.51×10^{-3}
3	" " "	18	0.63	2.21×10^{-3}
4	dry N_2	20	0.45	1.58×10^{-3}
5	" "	23	0.11	3.86×10^{-4}
6	" "	30	0.00	-

TABLE 5

Injecting KNO_3 with H_2O.

No.	Atmosphere	ΔT_f °C	Solubility moles H_2O/mole melt
1	No gas flow	2.5	8.8×10^{-3}
2	" " "	1.7	5.97×10^{-3}

/Continued.....

TABLE 5 (Continued..)

No.	Atmosphere	ΔT_f °C	Solubility moles H_2O/mole melt
3	N_2 + H_2O (p.p.=	0.33	1.16×10^{-3}
4	18.4 mm.Hg.)	0.33	1.16×10^{-3}
5	" "	0.50	1.76×10^{-3}
6	" "	0.38	1.34×10^{-3}
7	" "	0.30	1.05×10^{-3}
8	" "	0.18	6.30×10^{-4}

TABLE 6

KNO_3 + $Ba(NO_3)_2$.

No.	$Ba(NO_3)_2$. mole %	T_f °C	ΔT_f °C
1	0.132	334.61	0.45
2	0.306	334.00	1.06
3	0.540	333.46	1.60
4	0.752	332.83	2.23
5	0.943	332.11	2.95

TABLE 7.

Solubility of H_2O in KNO_3 containing 0.94 mole % $Ba(NO_3)_2$.

No.	Atmosphere	T_f °C	ΔT_f °C	Solubility moles H_2O/mole melt
1	dry N_2	332.13	0.00	-

/Continued.....

TABLE 7 (Continued..)

No.	Atmosphere	T_f °C	ΔT_f °C	Solubility moles H_2O/mole melt
2	dry N_2	332.13	0.00	-
3	N_2 + H_2O (p.p.	331.96	0.17	5.97×10^{-4}
4	4.6 mm.Hg.)	331.96	0.17	5.97×10^{-4}
5	dry N_2	332.13	0.00	-
a) 6	N_2 + H_2O (p.p. 18.0 mm.Hg.)	331.91	0.22	7.72×10^{-4}
7	dry N_2	332.08	0.05	1.75×10^{-4}

a), reproducibility of the order of ± 0.05°C.

TABLE 8

Solubility of H_2O in KNO_3 containing 4.17 mole% $Ba(NO_3)_2$

No.	Atmosphere	T_f °C	ΔT_f °C	Solubility moles H_2O/mole melt
1	dry N_2	321.64	0.00	-
2	" "	321.64	0.00	-
3	N_2 + H_2O (p.p. 21 mm.Hg.)	321.51	0.13	4.21×10^{-4}

TABLE 9.

Solubility of H_2O in KNO_3 containing 1.91 mole % $K_2Cr_2O_7$

Atmosphere	T_f °C	ΔT_f °C	Solubility Moles H_2O/mole melt
dry N_2	329.06	0.00 ± 0.03	-
N_2 + H_2O(p.p.=17.8 mm.Hg.)	328.89	0.17 ± 0.03	5.97×10^{-4}

TABLE 10.

Solubility of H_2O in $NaNO_3$.

No.	Atmosphere	T_f °C	ΔT_f °C	Solubility mole H_2O/mole melt
1	dry N_2	306.80	-	-
2	" "	306.82	-	-
3	N_2 + H_2O (p.p.	306.53	0.28	1.41×10^{-3}
4	16.5 mm.Hg.)	306.52	0.28	1.41×10^{-3}
5	dry N_2	306.80	-	-
6	" "	306.80	-	-

TABLE 11.

Solubility of H_2O in $NaNO_3$ containing 4.02 mole % $Ca(NO_3)_2$.

No.	Atmosphere	T_f °C	ΔT_f °C	Solubility mole H_2O/mole melt
1	dry N_2	298.67	-	-
2	" "	298.66	-	-
3	" "	298.68	-	-
4	N_2 + H_2O (p.p.	298.30	0.37	1.94×10^{-3}
5	21 mm.Hg.)	298.29	0.38	1.99×10^{-3}
6	dry N_2	298.53	0.12	6.29×10^{-4}
7	" "	298.57	0.10	5.24×10^{-4}

6 and 7 appear to represent residual moisture.

TABLE 12.

Change in Solubility of H_2O in $NaNO_3$ containing 0.089 mole % $Ca(NO_3)_2$ over eight days.

No.	Atmosphere	T_f °C	ΔT_f °C	Solubility moles H_2O/mole melt
1	N_2 + H_2O (p.p.20mm.Hg.)	306.29	0.33	1.73×10^{-3}
2	" " " " "	306.22	0.40	2.1×10^{-3}
3	" " " " "	306.24	0.38	1.99×10^{-3}
4	dry N_2	306.54	0.083	4.35×10^{-4}
5	" "	306.54	0.083	4.35×10^{-4}
6	N_2 + H_2O (p.p.20mm.Hg.)	306.42	0.20	1.05×10^{-3}
7	" " " " "	306.42	0.20	1.05×10^{-3}
8	" " " " "	306.47	0.15	7.86×10^{-4}
9	dry N_2	306.62	0.00	-
10	" "	306.57	0.05	2.62×10^{-4}
11	N_2 + H_2O (p.p.20mm.Hg.)	306.49	0.13	6.81×10^{-4}
12	" " " " "	306.49	0.13	6.81×10^{-4}
13	dry N_2	306.59	0.03	1.57×10^{-4}
14	" "	306.62	0.00	-

Table 12 shows that though the apparent solubility of H_2O decreases with time there is no change in the freezing point in the presence of dry N_2 indicating the absence of decomposition in the melt.

TABLE 13.

$NaNO_3$ + $NaNO_2$

No.	Concentration $NaNO_2$ % mole fraction	T_f °C	ΔT_f °C
1	0.227	306.57	0.23
2	0.527	306.24	0.56
3	0.744	305.97	0.83
4	1.044	305.62	1.18
5	1.240	305.39	1.41

Table 13 shows the extent of solid solution of $NaNO_2$ in $NaNO_3$. The heat of fusion H_f calculated from these results is 5.66 Kcals/mole cf. 3.49 Kcal/mole (Mustajoki 1957).

TABLE 14.

Solubility of H_2O in $NaNO_3$ containing 1.24 mole % $NaNO_2$.

No.	Atmosphere	T_f °C	ΔT_f °C	Solubility moles H_2O/mole melt
1	N_2 + H_2O(p.p.17.7mm.Hg.)	305.35	0.18	9.43×10^{-4}
2	" " " " "	305.35	0.18	9.43×10^{-4}
3	" " " " "	305.35	0.18	9.43×10^{-4}
4	dry N_2	305.53	-	-
5	N_2 + H_2O(p.p.17.7mm.Hg.)	305.32	0.21	1.10×10^{-3}

TABLE 15.

Solubility of H_2O in $NaNO_3$ containing both $Ca(NO_3)_2$ and $NaNO_2$.

No.	System addns. mole %	Atmosphere	ΔT_{f_1} °C	ΔT_{f_2} °C	Solubility moles H_2O/ mole melt.
1	$NaNO_3$	dry N_2	0.00	0.00	-
2	$NaNO_3$	$N_2 + H_2O$ (p.p. 17.7mm.Hg.)	0.07	0.07	3.67×10^{-4}
3	$NaNO_3$	" " "	0.07	0.07	3.67×10^{-4}
4	$NaNO_3$ + (0.11)$NaNO_2$	" " "	0.28	0.13	6.81×10^{-4}
5	$NaNO_3$ + (0.11)$NaNO_2$	dry N_2	0.21	0.07	3.67×10^{-4}
6	$NaNO_3$ + (0.11)$NaNO_2$	" "	0.15	0.00	-
7	$NaNO_3$ + (0.11)$NaNO_2$	" "	0.15	0.00	-
8	$NaNO_3$ + (0.11)$NaNO_2$	" "	0.25	0.00	-
9	+ (0.046)$Ca(NO_3)_2$	$N_2 + H_2O$ (p.p. 17.7 mm.Hg.)	0.45	0.20	1.05×10^{-3}
10	" "	dry N_2	0.25	0.00	-
11	" "	$N_2 + H_2O$ (p.p. 17.7 mm.Hg.)	0.45	0.20	1.05×10^{-3}

ΔT_{f_1} is the total depression of the freezing point, ΔT_{f_2} is the depression due to H_2O. From this table the solubility of H_2O appears to increase slightly in the presence of $NaNO_2$ and to increase further with the addition of $Ca(NO_3)_2$. This emphasises

the unpredictable nature of the solubility of H_2O in $NaNO_3$ especially with NO_3^- present.

Offprinted from the *Transactions of the Faraday Society*,
No. 444, Vol. 55, Part 12, December, 1959

MELTING AND CRYSTAL STRUCTURE

TESTS OF THE ASSOCIATION COMPLEX THEORY FOR SOME LOW-MELTING SALTS

MELTING AND CRYSTAL STRUCTURE

TESTS OF THE ASSOCIATION COMPLEX THEORY FOR SOME LOW-MELTING SALTS

BY J. P. FRAME, ELIZABETH RHODES AND A. R. UBBELOHDE *
Dept. of Chemical Engineering, Imperial College of Science and Technology, London S.W.7

Received 30*th July*, 1959

Measurements have been made of electrical conductance of solid and molten sodium and potassium nitrites and potassium dichromate, and on molten thallium nitrate. Viscosities of melts of these salts have also been determined. Like other low-melting salts previously studied, these melts have low ratios of the activation energies E_η/E_σ for viscosity and ion conductance, pointing to the presence of association complexes. Entropies of activation for viscous flow have also been evaluated on the basis of absolute-reaction-rate equations. Though high negative entropies indicating highly selective relaxation mechanisms are found for some of the nitrates, no general correlation between selective processes and low melting points can be postulated.

From the ratio of electrical conductances $\sigma_{liquid}/\sigma_{solid}$ for these salts, premelting in the crystals appears to be much less prominent than in the silver halides, except for KNO_2. However, the low activation energies for conductance in some of these salts suggests some electronic conductance in the solids, which may obscure homophase premelting. Conductivity data reveal a hitherto unknown transformation in solid KNO_2. This appears to be continuous, with onset temperature of about 365°C.

Measurements of surface energies have been made on $NaNO_2$, KCNS, $K_2Cr_2O_7$ and $KClO_3$, near the freezing points of their melts.

Salts with simple inert-gas-type ions generally have high melting points. For these substances, melting involves primarily positional disordering of the ions with respect to an ideal crystal lattice. Salts with polyatomic anions such as the nitrates [1] and the sulphocyanides [2] generally show much lower melting points. This has been explained on the assumption that other mechanisms of melting are operative, in addition to positional disordering. In particular, association complexes appear to be formed in the melts. Various tests of this explanation have been developed. For example, when complex formation is at all extensive,

(i) the volume change on melting tends to be small,
(ii) the ratio of activation energies E_η and E_σ for viscosity and ionic conductance tends to be low.

The present paper extends this second criterion to new types of low-melting salts, including KNO_2, $NaNO_2$, $TlNO_3$ and $K_2Cr_2O_7$. Results discussed below confirm that low values of E_η/E_σ are indeed found for all these low melting salts. However, this does not establish whether the association complexes whose formation is postulated involve wholly electrostatic binding forces, or whether definite rearrangement of the quantum-mechanical bonding is involved. It might be expected that if complex formation involves such rearrangement this would have an appreciable effect on the surface energy of the melts. Such complexes might lower the surface energy and would then be absorbed preferentially in the surface. To test this, measurements of surface tension over a range of temperatures have been made for various low melting salts, including KCNS, $NaNO_2$, $K_2Cr_2O_7$ and $KClO_3$. Various correlations between surface energies and structure of the melts are discussed below.

* experimental work on surface tensions by the late L. J. B. Husband.

EXPERIMENTAL

For experiments on transport processes, each of the salts $NaNO_2$, KNO_2, $TlNO_3$ (B.D.H., A.R.) and $K_2Cr_2O_7$ (Hopkins and Williams, A.R.) were twice recrystallized. Water was used as solvent for recrystallization except with KNO_2, which was twice recrystallized from the melt, in view of its exceedingly high solubility in water.

Prior to use, the recrystallized materials were air-dried at 180°C for 48 h, followed by thermal shock drying.[3] All transport measurements were made in a bath of mixed molten salts thermostatically controlled by a thyratron bridge circuit to $\pm$ 0·05°C.

Viscosities were determined by means of a modified Ubbelohde viscometer, which was calibrated with water at 25°, 35° and 40°C. This calibration was checked with molten $NaNO_3$; present results gave agreement within experimental error, which has a standard deviation of $\pm$ 1 % about the line of closest fit (see below). Melts were filtered into this viscometer through a sintered-glass disc (porosity 3) taking care to exclude atmospheric moisture. Flow times under steady pressures of gas were determined by conventional procedures; for the nitrites, nitrogen was used, and for $K_2Cr_2O_7$ and $TlNO_3$, oxygen was used as the driving gas. It was verified that calculated viscosities for all these melts were independent of flow rates within the range of these experiments. Chemical stability of the melts during the experiments was verified from lack of trend in the results with time of study, up to about 2 days.

Conductivities of both solids and melts were measured in a design of cell based on one previously described.[4] The cell constant was obtained using 0·1 N KCl solution, as standard calibrating fluid.[5] For solid ionic conductors the use of alternating current in the attempt to avoid polarization can lead to anomalies attributed to overtones linking with oscillations of ions in the crystal lattices.[6] Since only approximate values of conductivity of the solids were required, in order to evaluate the ratios of specific resistances $\sigma_{solid}/\sigma_{liquid}$ that can help to characterize the melting process, a direct current method was used to measure σ_{solid}. This comprised the conductivity cell in series with a sensitive calibrated galvanometer and a reversing switch. Voltage was supplied across the switch from a series of accumulators through a potential divider. Voltage measurement was by potentiometer. To reduce the pick-up of stray currents, due to the high impedances in the circuit, screened leads were used. For the melts, polarization was avoided by making measurements with a Wayne-Kerr alternating current bridge (B221) operating at 1592 c/sec. Measurements of conductivity were made at temperatures descending to and ascending from the melting point in the melt and were reproducible to $\pm$ 0·5 %. Because of the influence of past history on the absolute resistance of polycrystalline solids, measurements were made at temperatures descending from the melting point for the solid. At each temperature the voltage was varied to six different values and the average of 12 current galvanometer readings at maximum deflection taken. To reduce the effect of any polarization the current was reversed with each galvanometer reading.

Plots of the viscosities of each of the melts gave straight lines in accordance with the equation

$$\eta = \eta_0 \exp (E_\eta/RT).$$

There was no evidence of appreciable departure from linearity on approaching the freezing point of any of these substances, indicating the absence of marked prefreezing in these melts.

Equations of lines of closest fit for the viscosity results obtained for the salts in the present investigation are (η in poises):

$$NaNO_2,\ \eta = 8{\cdot}56 \times 10^{-4} \exp (4{\cdot}0/RT),\ \text{range (282-310)°C};$$
$$KNO_2,\ \eta = 13{\cdot}37 \times 10^{-4} \exp (4{\cdot}23/RT),\ \text{range (418-450)°C};$$
$$K_2Cr_2O_7,\ \eta = 1{\cdot}59 \times 10^{-2} \exp (10{\cdot}5/RT),\ \text{range (398-435)°C};$$
$$TlNO_3,\ \eta = 2{\cdot}86 \times 10^{-4} \exp (3{\cdot}61/RT),\ \text{range (207-250)°C}.$$

Equations of lines of closest fit for conductances of molten salts in the present investigations are (σ in mhos cm^{-1}):

$$NaNO_2,\ \sigma = 10{\cdot}9 \exp (-2{\cdot}98)RT);$$
$$KNO_2,\ \sigma = 9{\cdot}64 \exp (-2{\cdot}97/RT);$$
$$K_2Cr_2O_7,\ \sigma = 73 \exp (-7{\cdot}8/RT);$$
$$TlNO_3,\ \sigma = 10{\cdot}64 \exp (-3{\cdot}26/RT).$$

Fig. 1 records the approximate conductivities found for the solids.

For experiments on surface tension, a maximum bubble-pressure method was used, with two jets of unequal diameters immersed to the same depth. Following Sugden,[7] calculations of the surface tension do not involve the hydrostatic pressure, provided that

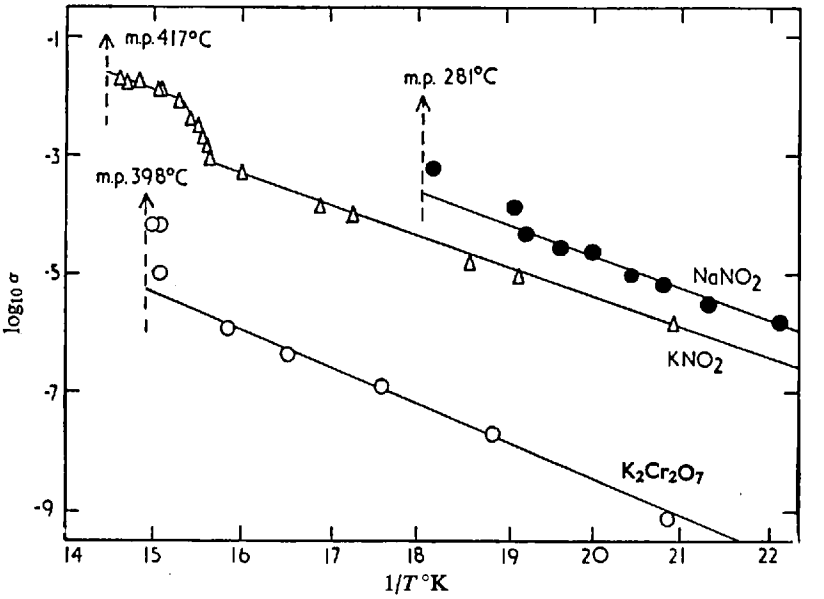


FIG. 1.—Conductivity (σ in mhos cm^{-1}).
Conductivity in the solid state for $NaNO_2$ ●, KNO_2 △, and $K_2Cr_2O_7$ ○.

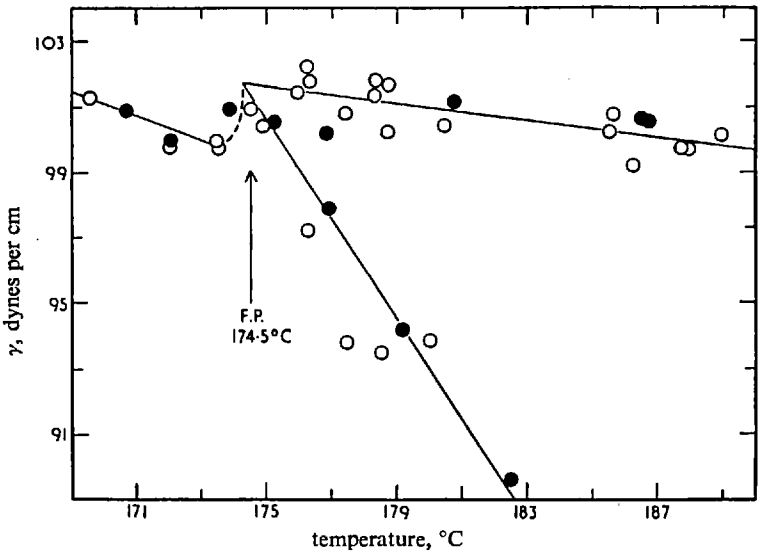


FIG. 2.—Surface tension γ of KCNS.
Experimental results from run A shown by ○, and run B by ●.

the depth of immersion is greater than 2 mm which ensures proper bubble formation.[8] In the present experiments, depths of immersion ranging from 1 to 2 cm were used. Jaeger [9] used immersions of only 0·1 to 0·3 mm which seems too low.

Two Pyrex jets were used, with internal diameters of 0·22 and 2·64 mm, respectively. Careful hand-grinding was applied to obtain external bevels of $\tan^{-1}(1/3)$ at the tips. The larger jet was also internally bevelled to achieve a truly circular bore to $\pm$ 0·5 %. Examination showed that the smaller jet was circular to $\pm$ 3 %. Both jets were ground flat transversely.

For these experiments KCNS and $KClO_3$ of A.R. grade were used without further purification. $K_2Cr_2O_7$ and $NaNO_2$ were twice recrystallized from water. All these salts were dried before use as described above. The melts proved to be quite stable under the conditions of use, except $KClO_3$ which produced up to 2 % of KCl on being kept molten for 4 days. Nitrogen (O_2 content < 1 p.p.m.; B.O.C. "white spot"), dried in a liquid oxygen trap was used for blowing bubbles in KCNS. With $K_2Cr_2O_7$, $NaNO_2$ and $KClO_3$ oxygen (B.O.C. cylinder gas) was dried in a similar manner. An overflow bubbler preceded the bottles and by its means the pressure in the system beyond the bottles could be kept steady to $\pm$ 3 dynes cm^{-2}. Pressures up to 5×10^4 dynes cm^{-2} could be established and were measured by a manometer containing dibutyl phthalate.

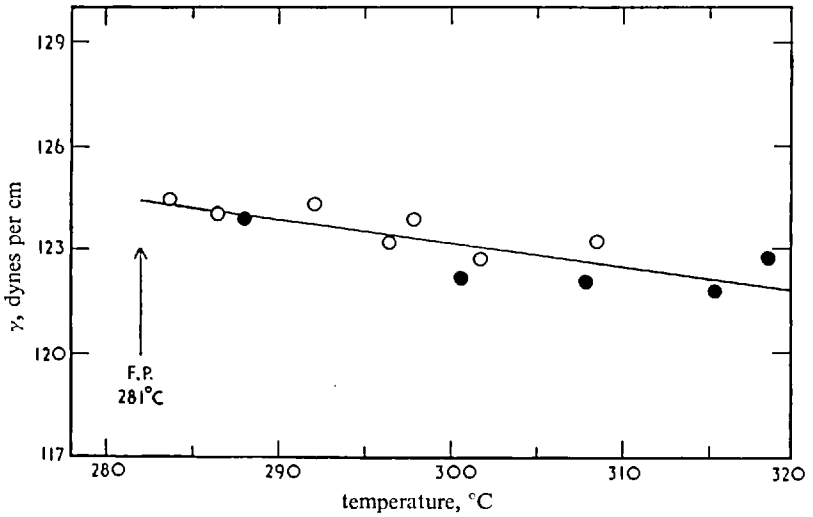


FIG. 3.—Surface tension γ of $NaNO_2$.
Experimental results from run A shown by ○, and run B by ●.

When the apparatus was in use the whole system including the jets could be flushed out without bubbling through the melt. This procedure was desirable as the surface tension of the melts was found to be higher if they were not subjected to violent turbulence. Bubble growth times were of the order of 2-8 min. This is even slower than rates used by Duke and Dahl.[10] The temperature of the gas and melt was equilibrated by passing the gas through a pre-heater immersed in the thermostat which was a mixed nitrate + nitrite melt bath which could be used between 160°C and 480°C. The electronic temperature control was $\pm$ 0·05°C.

Densities of the melts measured by means of a manometric densitometer [11] were as follows (ρ in g per ml, t_f is the temperature of fusion).

$$NaNO_2 \text{ melt, } \rho = 1{\cdot}8202 \pm 0{\cdot}0004 - 0{\cdot}00069\ (t - t_f),\ t_f = 281°C;$$
$$KCNS \text{ melt, } \rho = 1{\cdot}6005 \pm 0{\cdot}0007 - 0{\cdot}00080\ (t - t_f),\ t_f = 174°C;$$
$$KClO_3 \text{ melt, } \rho = 1{\cdot}9550 \pm 0{\cdot}0004 - 0{\cdot}00067\ (t - t_f),\ t_f = 356°C;$$
$$K_2Cr_2O_7 \text{ melt, } \rho = 2{\cdot}286 \pm 0{\cdot}0005 - 0{\cdot}00069\ (t - t_f),\ t_f = 398°C.$$

$NaNO_2$ was the only instance where values of the surface tension γ were found to be reproducible independent of the age of the melt. With KCNS, the freshly prepared melt showed a much steeper temperature dependence ($d\gamma/dT$). This was about $-$ 1·36 dyne cm^{-1}/deg. initially and after some stay in the apparatus fell to the more normal value of about 0·14 dyne cm^{-1}/deg. Fig. 2 illustrates the course of this behaviour. Results for $NaNO_2$ (fig. 3) are given to mark the contrast.

For the other two salts studied, variations of γ with temperature and age of melt showed rather greater spread, almost certainly due to incipient decomposition leading to sorption of some impurities at the melt surface; these affect the surface tension and moreover prolonged bubbling appeared to influence their migration to the surface. In spite of these uncertainties, and because the temperature coefficient is in any case small, values of γ_f at the freezing points could be obtained with considerable certainty. These are recorded in table 4. It may be noted that Jaeger [9] reports a somewhat higher value for $K_2Cr_2O_7$; extrapolated to the freezing point his results would give 140 dyne/cm.

DISCUSSION

From the new experimental findings, recorded above, the previous conclusion that salts with low melting points exhibit low ratios of the activation energies, E_η/E_σ, can be made even more general. For convenience, table 1 records all the values now available.

TABLE 1.—TRANSPORT PARAMETERS OF IONIC MELTS

salt	m.p. °C	viscosity			electrical conductance			E_η/E_σ
		ref.	E_η	$\eta_0\times10^4$	ref.	E_σ	σ_0	
LiCl	613	12	8·8	—	12	1·15	11·5	7·6
NaCl	801	12	9·4	1·95	12	1·54	7·3	6·1
KCl	776	12	7·8	3·55	12	2·30	6·5	3·4
RbCl	715	12	—	—	12	2·83	6·5	—
CsCl	646	12	—	—	12	3·33	6·6	—
LiBr	547	12	6·0	—	12	1·75	13·5	3·4
NaBr	755	12	10·63	8·13	12	1·84	7·4	5·8
KBr	730	12	7·96	2·95	12	2·55	5·8	3·1
NaI	651	12	7·4	—	12	1·25	4·8	5·9
KI	723	12	9·2	—	12	2·75	5·5	3·4
AgCl	455	12	2·9	—	12	0·99	7·4	2·9
AgBr	434	12	5·4	8·51	12	0·7-1·0	—	6·4
AgI	552	12	5·8	10·96	12	0·8	4·0	7·3
CuCl	422	12	4·23	11·9	12	0·85	6·2	5·0
$MgCl_2$	708	—	—	—	12	3·56	6·4	—
$CaCl_2$	772	12	9·5	—	12	4·1	13·5	2·3
$SrCl_2$	873	—	—	—	12	4·0	11·0	—
$BaCl_2$	962	—	—	—	12	4·15	10·5	—
$CdCl_2$	568	12	4·5	—	12	2·30	7·3	2·0
$CdBr_2$	567	—	—	—	12	2·75	5·4	—
$PbCl_2$	501	12	6·6	—	12	3·3-4·5	—	1·8
$PbBr_2$	373	12	9·2	—	12	4·35	16·0	2·1
$LiNO_3$	255	13	4·23	11·9	15	4·49	55·4	0·94
$NaNO_3$	306·8	13	3·95	9·87	15	2·76	10·6	1·4
$NaNO_2$	281	*	4·0	8·5	*	2·98	10·9	1·34
KNO_3	333·1	14	3·66	14·12	16	3·49	11·2	1·05
KNO_2	419	*	4·23	13·37	*	2·97	9·64	1·42
$RbNO_3$	310	—	—	—	15	3·42	2·09	—
$CsNO_3$	414	—	—	—	15	2·7	1·82	—
NH_4NO_3	169·6	17	4·6	1·59	—	—	—	—
$TlNO_3$	206	*	3·61	~~2·86~~ 9.24	*	3·26	10·64	1·11
$AgNO_3$	212	1	3·08	13·87	1	4·57	74·5	0·70
$K_2Cr_2O_7$	398	*	10·5	159·8	*	7·8	73	1·35
NaCNS	287	2	5·8	1·90	2	4·7	43	1·21
KCNS	173·2	2	8	0·153	2	5·8	100	1·38
$NaHSO_4$	~~240~~ 175	—	—	—	18	5·7	38	—
$KHSO_4$	210	18	12·0	$2·3\times10^{-6}$	18	6·2	33	1·94
NH_4HSO_4	136	—	—	—	18	5·3	43	—
NaOH	318·4	19	5·47	4·79	—	—	—	—
KOH	360·4	19	6·13	2·46	—	—	—	—

Units of E_η and E_σ are in kcal/mole, η_0 is in poises and σ_0 in mhos cm^{-1}.

* Results of present work. To make trends in the above results easier to follow plots are given in fig. 4 and 5.

In a previous publication,[2] the low value of this ratio was attributed to the fact that the structure of the melts containing non-spherical ions tends to hinder any relative movement of positive and negative charges in a velocity gradient. If complex ions are present, such relative movement would involve a high activation energy. Melts containing these complex ions can, however, relax shearing stresses by another mechanism. Mutual turning-over of non-spherical ions can take place, without large relative movements of centres of positive and negative charge. Inspection of table 1 shows that E_η is in fact strikingly low for ionic melts such as nitrates and nitrites. It is suggested that these low values refer to relaxation of shear by turning over of non-spherical ions. As would be expected on this basis, the viscosity parameters for nitrates and nitrites are closely similar.

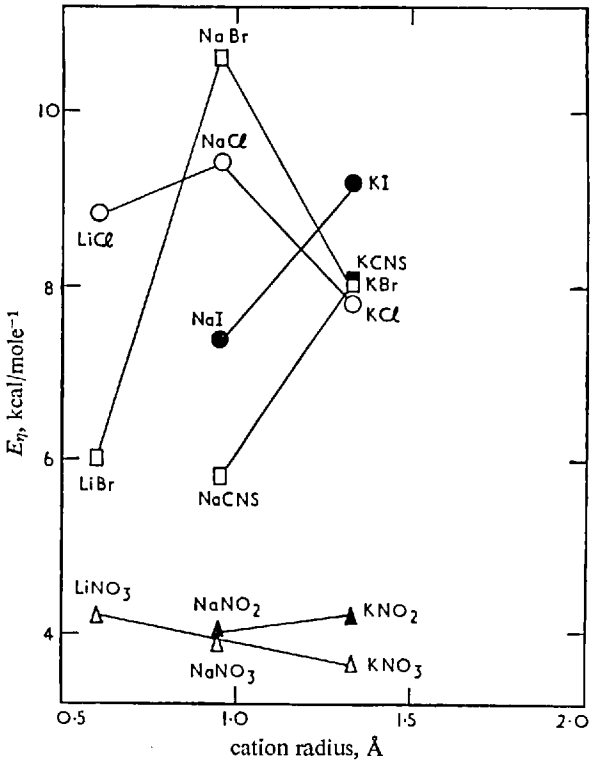


FIG. 4.—Activation energy for viscous flow E_η.

On the other hand, ion-transport activation energies of low melting salts tend to be higher than for high-melting salts. Transport of ions must involve relative movement of positive and negative charges and the complexed structure postulated for the melts makes such movement more difficult.

In order to relate this postulated difference in structure between melts of non-spherical and spherical ions more completely with differences in transport mechanisms, information is required on transport numbers in the melts, and also on ion diffusion. Though these data are not yet available, other methods of study[3] confirm the presence of some kind of association complex in the melts of non-spherical ions.

More detailed discussion of individual transport parameters already available is hampered by the problem of selecting suitable corresponding temperatures in comparing melts that have very different melting points. One procedure, though

not fully satisfactory, is to use entropies ΔS_η calculated from the formal absolute rate expression for viscosity of Glasstone, Laidler and Eyring [20]

$$\Delta S_\eta = R \ln (hN/V\eta_0).$$

In this expression, values of the specific volume V for $K_2Cr_2O_7$ and $TlNO_3$ were taken from Jaeger,[9] and for $NaNO_2$ from Husband.[11] V was calculated from the volume of the crystals for KNO_2 assuming only 5 % expansion on melting.

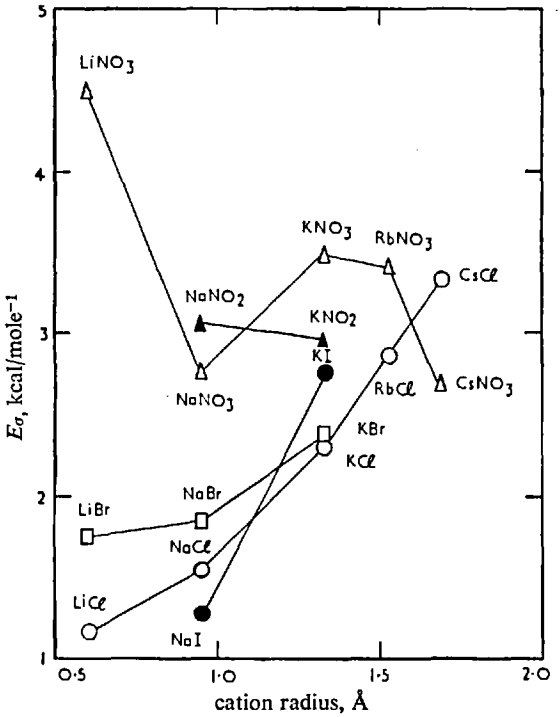


FIG. 5.—Activation energy for electrical conductance E_η.

It will be seen from table 2 that the salts with non-spherical anions frequently have large negative entropies of activation, for viscous flow. This would conform with the predominance of highly selective activation processes, of comparatively low activation energy. However, the entropies for melts of the sulphocyanides

TABLE 2.—ENTROPIES OF VISCOUS FLOW BASED ON THE RATE EQUATON

salt	m.p., °C	ΔS_η (eV)	ref.
$LiNO_3$	255	− 4·86	Davis *et al.*[1]
$NaNO_3$	306·8	− 5·95	,, ,,
KNO_3	333	− 5·75	,, ,,
$AgNO_3$	212	− 5·36	,, ,,
$TlNO_3$	206·4	− ~~2·48~~ −4.34	present work
$NaNO_2$	281	− 4·18	,, ,,
KNO_2	419	− 5·45	,, ,,
$K_2Cr_2O_7$	398	− 3·06	,, ,,
KCNS	173·2	+ 2·91	Plester *et al.*[2]
NaCNS	287	− 1·65	,, ,,
NaCl	801	− 1·28	cf. Plester *et al.*[2]
NaBr	755	− 4·38	,, ,,
KCl	776	− 3·05	,, ,,

show that this suggestion cannot be made wholly general for salts of low melting points. Positive entropies of activation imply non-selective activation (cf. melts of the polyphenyls [21]).

Although the results for the electrical conductances of the polycrystalline solids are somewhat approximate, they give some additional information about the melting mechanisms.

Plots of transport measurements show that except in KNO_2 premelting does not appear to be exceptionally prominent in the low-melting crystals now investigated (fig. 1). Equations of closest fit for the linear portions are (σ in mhos cm^{-1}):

	range, °C
$NaNO_2$, $\sigma = 2{\cdot}94 \times 10^5 \exp(-23{\cdot}8/RT)$,	175-261·5;
KNO_2 below melting point, $\sigma = 9{\cdot}33 \times 10^4 \exp(-21{\cdot}0/RT)$,	380·5-415·5;
KNO_2 below transition, $\sigma = 1{\cdot}40 \times 10^5 \exp(-24{\cdot}2/RT)$,	203-364;
$K_2Cr_2O_7$, $\sigma = 1{\cdot}55 \times 10^4 \exp(-29{\cdot}1/RT)$,	203-364.

Table 3 records the jump in electrical conductivity which can throw light on the increase of positional disorder on melting. There appears to be considerable premelting in KNO_2, which also exhibits a transition in the solid. Values of $\sigma_{liquid}/\sigma_{solid}$ for the other salts studied seem normal. However, the low activation energies for electrical conductance of the solids recorded in fig. 1 could refer to electronic conduction rather than ion migration in these solids.[24] Further evidence seems desirable, but whichever mechanism applies, the present findings indicate structural changes in solid KNO_2 near the melting point.

TABLE 3.—JUMP IN CONDUCTIVITY ON MELTING

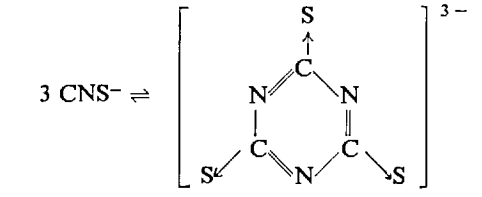
substance	$\sigma_{liquid}/\sigma_{solid}$	ref.
NaCl	3,000	22
KCl	10,000	22
KBr	7,000	22
AgCl	30	22
AgBr	20	22
$NaNO_3$	1,000	22
$NaNO_2$	3,000	*
KNO_3	3,000	22
KNO_2†	40	*
$AgNO_3$	500	22
$K_2Cr_2O_7$	6,000	*
KCNS	3,000	2
$KHSO_4$	70,000	2

* present work.

† 1000 if referred to σ below the transition in the solid.

The transition in solid KNO_2 is of interest since the conductivity data suggest it is spread over about 16°C, and is probably continuous.[23]

Conclusions from measurements on the surface energies of these melts can be summarized quite briefly. As has been stated, temperature coefficients of surface tension of some of the low melting salts showed an unexpectedly high variability. This would normally be attributed to the presence of surface-active impurities that are difficult to eliminate. However, the finding that quite uniform results could be obtained for molten sodium nitrite suggests that such "surface-active impurities" may be derived from the salts themselves by some kind of bond rearrangement. For example, in the sulphocyanides a suggested polymerization would be to chain ions, or to rings such as



in the melt. As this would involve rearrangement of bonds a rate of change comparable with the time of observation on surface tensions does not seem out of the question. Table 4 gives values of γ_f and $d\gamma/dT$ for the present salts.

TABLE 4.—SURFACE TENSIONS AT THE MELTING POINTS

salt	f.p., °C	γ_f dynes/cm	$d\gamma/dT$ dynes cm^{-1} $deg.^{-1}$	temp. range
$NaNO_2$	281	$124{\cdot}5 \pm 0{\cdot}2$	$-0{\cdot}07$	281 to 320°C
KCNS	175	$101{\cdot}5 \pm 0{\cdot}5$	$-1{\cdot}36$	fresh melt, 175 to 185°C
			$-0{\cdot}14$	aged melt, 175° to 200°C
$KClO_3$	368	$81{\cdot}0 \pm 0{\cdot}2$	$-0{\cdot}4$	368 to 378°C
			$-0{\cdot}05$	in supercooled region
$K_2Cr_2O_7$	397	$129{\cdot}0 \pm 0{\cdot}5$	$-0{\cdot}27$	400 to 440°C

In order to appreciate the significance of these findings for interpreting the structure of the melts, surface tensions γ_f for various salts of alkali-metals have been calculated at their melting points from Jaeger's results.[9] These are recorded in table 5. For simple spherical ions, it will be seen that a marked trend is observed in γ_f, with change of cation, only when the anion is small, as for the fluorides.

TABLE 5.—EXTRAPOLATED VALUE OF SURFACE TENSION AT THE MELTING POINT γf DYNES/CM; ALKALI SALTS

	Li^+	Na^+	K^+	Rb^+	Cs^+
F^-	251	201	142	133	107
Cl^-	138	114	97	98	91
Br^-		106	89	91	82
I^-		87	81	82	75
NO_3^-	117	120	113	109	110

For the iodides, the trend is much smaller and it is practically absent for the nitrates. This suggests that the surface of the low-melting salts tends to be determined by the anions packing in contact, with cations in crevices where they exert no perceptible van der Waals' repulsions. New findings on low-melting salts other than the nitrates fit in with this general picture.

1 Davis, Rogers and Ubbelohde, *Proc. Roy. Soc. A*, 1953, **220**, 14.
2 Plester, Rogers and Ubbelohde, *Proc. Roy. Soc. A*, 1956, **235**, 469.
3 Rhodes and Ubbelohde, *Proc. Roy. Soc. A*, 1959, **251**, 156.
4 Biltz and Klemm, *Z. anorg. Chem.*, 1926, **152**, 267.
5 Jones and Bradshaw, *J. Amer. Chem. Soc.*, 1933, **55**, 1780.
6 Phipps and Partridge, *J. Amer. Chem. Soc.*, 1929, **51**, 1331.
7 Sugden, *J. Chem. Soc.*, 1922, **121**, 858.
8 Drath and Sauerwald, *Z. anorg. Chem.*, 1927, **162**, 301.
9 Jaeger, *Z. anorg. Chem.*, 1917, **101**, 1.
10 Dahl and Duke, *U.S. Atomic Energy Comm. ISC.* 923, 1957.
11 Husband, *J. Sci. Instr.*, 1958, **35**, 300.
12 Bloom and Heymann, *Proc. Roy. Soc. A*, 1947, **188**, 392.
13 Dantuma, *Z. anorg. Chem.*, 1928, **175**, 1.
14 Lorenz and Kalmus, *Z. physik. Chem.*, 1907, **59**, 17.
15 Jaeger and Kapma, *Z. anorg. Chem.*, 1920, **113**, 27.
16 Goodwin and Mailey, *Physic. Rev.*, 1907, **25**, 469; 1908, **26**, 28.
17 Shirai and Nishikawa, *Sci. Pap. Col. Gen. Educ. Tokyo*, 1958, **8**, 61.
18 Rogers and Ubbelohde, *Trans. Faraday Soc.*, 1950, **46**, 1051.
19 Barrer, *Trans. Faraday Soc.*, 1943, **39**, 48.
20 Glasstone, Laidler and Eyring, *Theory of Rate Processes* (McGraw-Hill, New York, 1941), p. 480.
21 Andrews and Ubbelohde, *Proc. Roy. Soc. A*, 1955, **228**, 435.
22 Ubbelohde, *Quart. Rev.*, 1950, **4**, 356.
23 Ubbelohde and Woodward, *Proc. Roy. Soc. A*, 1947, **188**, 357.
24 Harpur, Moss and Ubbelohde, *Proc. Roy. Soc. A*, 1955, **232**, 196.